Rapid optimization of photoredox reactions for continuous flow systems using microscale batch technology

María González-Esguevillas[†], David F. Fernández[†], Juan A. Rincón[‡], Mario Barberis[‡], Oscar de Frutos[‡], Carlos Mateos[‡], Susana García-Cerrada[‡], Javier Agejas[‡] & David W. C. MacMillan[†]*

[†] *Merck Center for Catalysis at Princeton University, Princeton, New Jersey 08544, United States*

[‡] *Centro de Investigación Eli Lilly, S. A., Avda. de la Industria 30, 28108, Alcobendas, Madrid, Spain*

*Corresponding Author email: dmacmill@princeton.edu

Supporting Information

Table of Contents

1. General information

Commercial reagents were purified prior to use following the guidelines of Perrin and Armarego.[1] Solvents were purified by passage through columns of activated alumina, or according to the method of Grubbs.[2] Organic solutions were concentrated under reduced pressure on a Büchi rotary evaporator using a water bath. Chromatographic purification of products was accomplished using forced-flow column chromatography on ICN 60 32-64 mesh silica gel 63 according to the method of Still.[3] Thin-layer chromatography (TLC) was performed on Silicycle 0.25 mm silica gel F-254 plates. Visualization of the developed chromatogram was performed by fluorescence quenching or by ceric ammonium molybdate, iodine, *p*-anisaldehyde or $KMnO_4$ stain. ^1H NMR spectra were recorded on a Bruker UltraShield Plus 500 MHz unless otherwise noted and are internally referenced to residual protio solvent signals: $CDCl_3$ (7.26 ppm), $(CD_3)_2CO$ (2.05 ppm), or $(CD_3)_2SO$ (2.50 ppm), multiplicity (s = singlet, d = doublet, t = triplet, q = quartet, m = multiplet, dd = doublet of doublet, dt = doublet of triplet, ddd = doublet of doublet of doublet, br = broad), coupling constant (Hz), integration. ^{13}C NMR spectra were recorded on a Bruker UltraShield Plus 500 (200, 125 MHz respectively) and data are reported in terms of chemical shift relative to $CDCl_3$ (77.0 ppm), $(CD_3)_2CO$ (29.84 ppm), or $(CD_3)_2SO$ (39.5 ppm). ^{19}F NMR spectra were recorded on a Bruker NanoBay 300 MHz (282 MHz). IR spectra were recorded on a Perkin Elmer Paragon 1000 spectrometer and are reported in wavenumbers (cm^{-1}). High Resolution Mass spectra were obtained from the Princeton University Mass Spectral Facility. Liquid chromatography (LC) analysis was performed on an Agilent 1290 Infinity II LC system (ultra-high-performance LC, UPLC).

The photobox used for our experiments called FLOSIM was built using acrylic mirrors (Glossy Gallery Square Shatterproof acrylic safety mirror, 8inx8in), a AC Infinity Axial 1238 fan in combination with a fan speed controller (AC Infinity, Fan Speed Controller for 100 to 125V AC Axial Muffin Cooling Fans, Single Connector, for DIY Cooling Ventilation Exhaust Projects). Plano concave lens from ThorLabs (F = –150 and D = 50.8mm, BK7A coated plano concave lens (LC1611-A)) were used to disperse the light inside of the box.

The reactions were performed using one Kessil LEDs (PR160-390nm, 427nm, 440nm, 456nm, 467nm) for batch reaction and two or four lights for the FLOSIM device. For the optimization/simulation photoredox reaction process were used the glass reactor microplates by

Zinsser Analytic (96-well plate, part number 3600500) and transparent sealing films PCR by BrandTech (781390 or 781391ES). The 1 mL-Nunc 96-well plate by VWR (73520-122) has been used for the UPLC analysis. All liquid handling operations, both reaction setup and quenching for UPLC analysis, were performed via multichannel pipetting, since the glass plate has the standard dimensions from the SBS (SLAS/ANSI) format.

The reactions in continuous flow were accomplished using a Vapourtec E-Series (60W; 385nm, 420nm, 450nm Gen-1) or a PhotoSyn instrument from Uniqsis (700W, 455 nm LEDs) in combination with a water cooler by Thermo Fisher Scientific (R-740 Unit) and a Rainin HPXL solvent delivery system pump.

Safety Statement: During the course of all the experimentation no unexpected or unusually high safety hazards were encountered.

2. Device building process

To build a home-made FLOSIM device is necessary the above material:

- (4) 8"x8" acrylic mirrors
- Copper wire (or hinges)
- Mylar tape
- AC Infinity Axial 1238 fan in combination with a fan speed controller
- Velcro straps
- PR 160 Kessil LEDs
- Kessil Rig Mounting System

Box assembly: Two of the acrylic mirrors are cut in half (4" H x 8" W) and small holes are made at 0.5 cm away of the corners. For the bottom of the FLOSIM device: using a Dremel tool two holes (6.4 cm diameter) were made away from each other 2.2 cm, alongside with small holes on the corners of the mirror. In the same way a big hole in the center of the last acrylic mirror is made to place the fan on the top of the box. The bottom mirror is joined with the copper wire to the side mirror walls (mirror with 4" H x 8" W size). All the edges are cover with mylar tape to prevent light leakage. Finally, the lid (the fan-equipped acrylic mirror) is closing the box with Velcro straps or with hinges.

Glass plate stand: Four glass fragments (2 of 3 x 13.7 cm and 2 of 2 x 17 cm) were cut, cover with mylar tape and fused forming a rectangle (see below). To this structure were attached four 4-mL vials (Thermo Fisher, C4015-88) with hot glue gun (Fig. S1, part 1, right and part 3C).

Note: This platform was built to set the glass-plate at a distance of about 4 cm which allow a better light dispersion and air flowing.

FLOSIM device assembly: Using a Kessil Rig Mounting System the LEDs were clamped on the way show above, focusing the lights in vertical position. The distance between the lights are 2.2 cm (2.5 cm gave us also good results). We place 2 lenses (F = –150 and D = 50.8mm) over the Kessil LEDs due to helps with the dispersion of the light along the box (Fig. S1, 2D and 2E).

The box is positioned over the lights. The rack is set on the center of the box and the glass 96-well plate over it (Fig. S1, 2F–H). Next the top mirror is able to close the box and fixed with Velcro straps. The fan is activated at medium speed and the reaction starts to run.

NOTES:

1. The FLOSIM device is able to work also using the whole acrylic mirrors, building a square 8”x8” box (20.3 cm x 20.3 cm). Better temperature control and homogeneity were observed using the described 4” height box (10.15 cm).

2. The distance between the plate and the bottom mirror of the box is 5 cm, but the lights are placed between 0.8-1.0 cm inside of the box.

3. The use a box with 2.5 cm between the lights instead 2.2 cm works similarly in terms of homogeneity. It is also acceptable to use a box with only one light on the center or 4 lights with 2.5 cm between each one and from the center of the mirror. The election of one box or the others is done based on the number of wells are needed to use it in the optimization and/or the power we will need to use in flow.

4. The use of lens with F = –100 and D = 50.8mm instead of F = –150 provide similar results, whereas using lens with F = –75 shows a decrease in the homogeneity of the results across the plate.

5. The FLOSIM device was used with the glass reactor microplates by Zinsser Analytic that has the standard dimensions from the SBS (SLAS/ANSI) format. One of the key advantages of these high purity, temperature resistant borosilicate glass plates is the possibility to reuse them hundreds of times without any detrimental effect in the reaction outcome.

6. Knowing the benefits of having a 96-well plate, we decided to design the FLOSIM platform, which allows to increase the actual output of the light by simply moving to the worldwide used Kessil light sources, that they are already characterized by total output power and also by an intensity map of two Kessil lamps with exactly the same configuration as ours (https://www.kessil.com/science/pdf/PR160L_Intensity_Map_3.pdf).

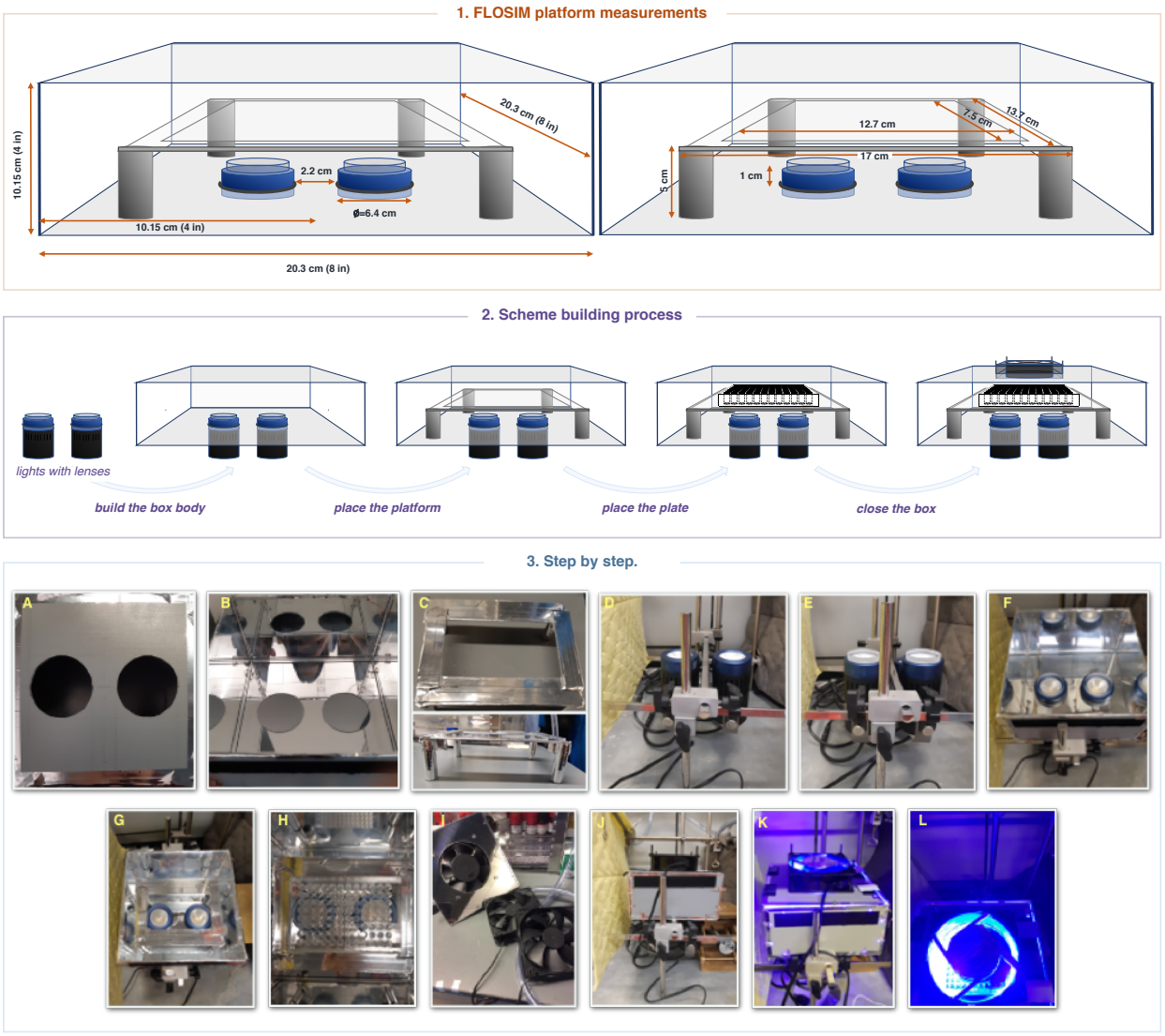

Fig. S1. Part 1. Mesasurements of the elements to built the FLOSIM platform. Left scheme: height and width of the box, distance between the holes for the Kessil and hole diameter for Kessil LEDs; Right scheme: measurements of the glass plate stand and distance with the lights. Part 2. Building process scheme. Part 3. Sequence pictures showing the building process step by step: a) bottom mirror, b) box with mirror walls, c) stand for plate, d) lights with the Kessil Rig Mounting System, e) lens, f) box over the lights, g) placing the stand inside of the box, h) plate inside of the box, i) top mirror with a fan on the center, j) box closed, k and l) FLOSIM device on.

2. 1. Homogeneity analysis between different boxes and parameters.

To this purpose we chose the following procedure for the decarboxylative arylation as a test reaction: a round-bottom flask equipped with a Teflon septum and magnetic stir bar was charged with the 1-bromo-4-(trifluoromethyl)-benzene (1.0 equiv), N-Boc-Proline (Boc-Pro-OH) (1.5

equiv), 1,3,5-trimethoxybenzene as internal standard, [Ir(dF(CF$_3$ppy)$_2$dtbbpy]PF$_6$ (1 mol%), NiCl$_2$·dme (5 mol%), 4,4′-ditertbutyl-pyridine (5 mol%) and 1,1,3,3-tetramethylguanidine (TMG) (1.5 equiv) in DMA (0.2 M). The resulting solution was then sparged with N_2 for 15 minutes. The reaction flask was sealed with parafilm and transferred to the inert atmosphere glove box (nitrogen glove box). Next, inside of the box, under positive nitrogen atmosphere, 60 μL of the reaction solution was dispensed to each well of the glass 96-well plate. The plate was sealed with a sealing film (PCR) and moved to the HTE FLOSIM device at the bench to run the reaction for 15 minutes. Upon completion, the reaction mixture was diluted with 100 μL of acetonitrile. Then, an aliquot (20 – 45 μL) was transferred to a plastic 96-well plate (Nunc 96-well plate by VWR (73520-122)), diluted with 950 μL of acetonitrile and analyzed by UPLC.

Different variables during the device building were tested to achieve the best environment to obtain homogeneity in the plate and enable a reliable optimization. First, using an 8”x8” mirrors for the FLOSIM device and the fan with medium speed, we have evaluated the use of different plano concave lens (50.8 mm of diameter, –75 mm, –100 mm or –150 mm of focal length which correspond to –13.3, –10.0 or –6.7 diopter respectively) which are able to disperse the light to different angles. Also, the distance between the lights (from 1.5 cm to 3 cm) and the space between the lights and the fan were analyzed as a variable. Both extreme settings, very close or far away, gave no homogeneous results due to the dispersion of the light. We also noticed that the temperature is not equally distributed inside of the device. However, we can see using a 2.2 cm or 2.5 cm of distance between the lights the distribution in the plate is more appropriate (Fig. S2). Although in all these cases the results are very similar in the whole plate, we can see a slightly better distribution when lens with F= –100 or –150 are used in combination with a 2.2 cm of distance between lights.

The position and the number of used fans were also evaluated. Fans could be placed on the lateral mirrors or on the top of the box. Even using two fans on the lateral mirror are able to facilitate the circulation of the air inside of the device, we established that the use of one big fan instead of two small fans on the top of the device allow better results.

Fig. S2. HTE FLOSIM optimization to check the homogeneity across the plate using the 8"x8" setup.

Next, we evaluated the height of the FLOSIM platform. Using a 8"x8" FLOSIM device we obtained good results, but owing to the plate is situated 4 cm away from the lights (~5 cm from the bottom of the box), the fan is 15 cm away from the plate, resulting in a more challenging temperature control (this fact is more pronounced for longer reaction times). Accordingly, we built a device with 4" of height which allows a similar distance between the lights and plate, and the plate with the fan. As shown Figure S3, the use of this FLOSIM platform provided greater results.

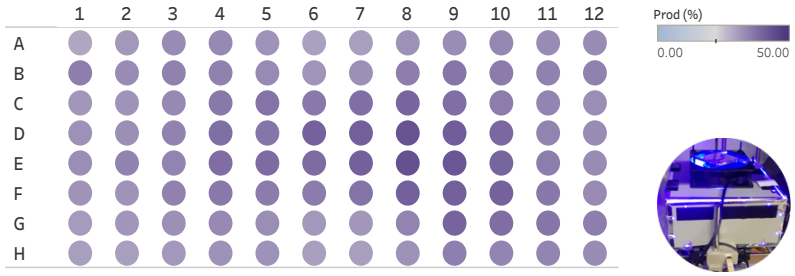

Fig. S3. Homogeneity across the plate using the 4"x8" FLOSIM device.

To allow a high level of reproducibility between plates and flow, we need to be sure all the well positions we used during the optimization offer the same level of the reactivity (same light penetration and temperature). We observed some positions (the wells on the edges of the plate) in which the results are not perfectly matched with the others. *We decided to use this FLOSIM device for our optimization only using the center positions (C1-12 to F1-12 rows or B3-10 to G3-10 (48 positions)) to explore our hypothesis with different reactions and on the other hand we have continued with the box optimization*.

In addition, we could observe using a box with 4 lights help with the homogeneity in the whole plate as well as it opens the opportunity to use different light intensity (different output power) which enables the use of different flow systems.

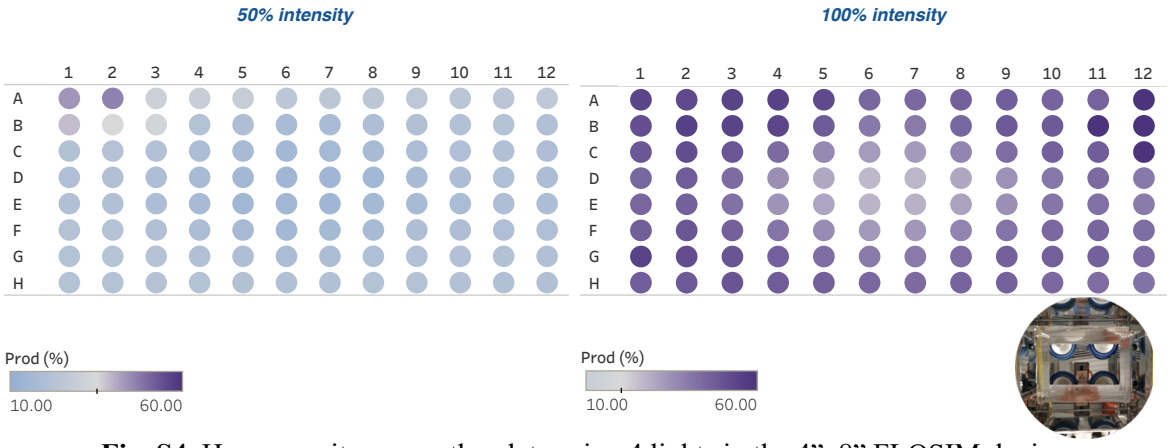

Fig. S4. Homogeneity across the plate using 4 lights in the 4"x8" FLOSIM device.

NOTE: *For the purpose of the optimization studies described in the main text we have utilized a 2-light FLOSIM device, that allows for better temperature control using the cooling system described in section 2. The 48 central positions of the plate were used to maintain higher levels of homogeneity across the plate during the photoredox reaction optimization campaigns.*

2. 2. Calculation of the required reaction volume.

Based on our hypothesis, matching the light penetration pathway in both setups, flow reactor systems and 96-well plates, we could recreate the flow environment using a high-throughput experimentation platform. Thus, if both parameters, the inner diameter of the reactor coil tubing

(i.d.) and the diameter of one individual well on the plate are known, we can obtain the needed volume to simulate flow conditions in a micro-scale vessel.

We can consider each well as a cylinder, so if our hypothesis is right, we could reproduce the flow conditions in the plate assuming the i.d. of the reactor-coil tubing is the same than the height of the solution in the plate. Considering these parameters, we are able to calculate the needed reaction volume in plates. For example, the i.d. in the regular reactor-coils from Vapourtec Ltc. is 1.3 mm, and the diameter of each well in the plate is 7.5 mm. With this in hand and with the mathematical equation of the volume of cylinder we can obtain easily the needed reaction volume.

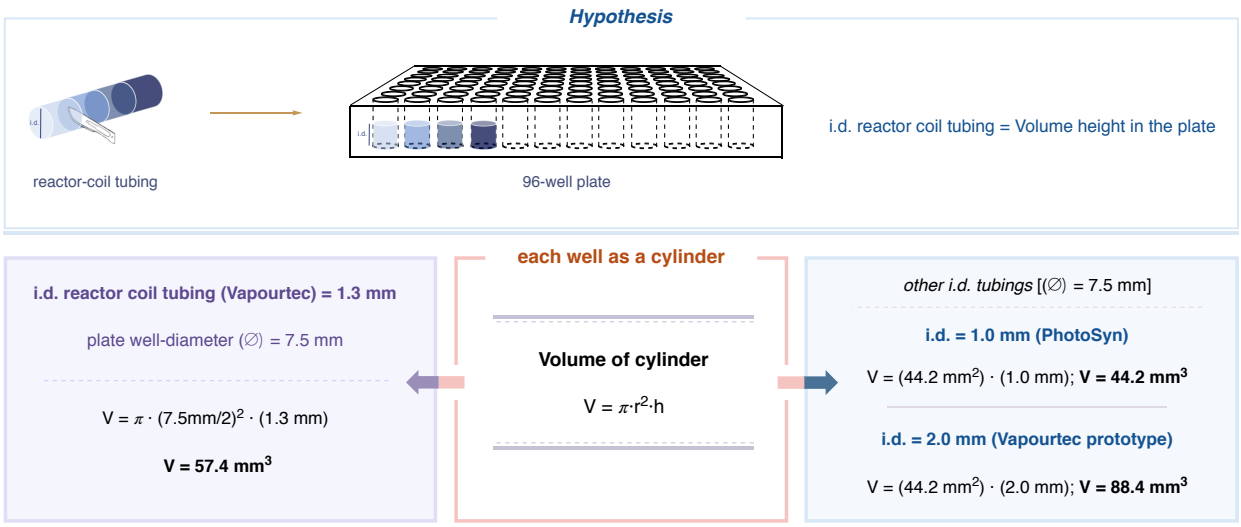

Fig. S5. Mathematical calculation of the required volume based on our hypothesis.

Taking this in account, we could calculate the required volume to run reactions in plates to compare with different flow system. So, we found the needed volume in plates for the regular tubing using the Vapourtec system (i.d. = 1.3 mm) is 57.4 µL. In the same way, we obtain the needed volume for different tubings, such as PhotoSyn reactor tubing (i.d. = 1.0 mm) or a prototype reactor-coil from Vapourtec (i.d. = 2.0 mm) with higher diameter which can help with the use of heterogeneous solutions (44.2 µL and 88.4 µL respectively) (Figure S5).

Next, to facilitate the experimental section in plates we would like to bring close the calculated volume to a higher round number. For example in the first case where we need a 57.4 µL of volume, we would like to use a near volume (60 µL). To verify this assumption, we performed a comparative study using the following homogeneous conditions for the decarboxylative arylation:

a 40 mL-vial equipped with a Teflon septum and magnetic stir bar was charged with the 1-bromo-4-(trifluoromethyl)-benzene (56 µL, 0.4 mmol, 1.0 equiv), *N*-Boc-Proline (Boc-Pro-OH) (129.2 mg, 0.6 mmol, 1.5 equiv), 1,3,5-trimethoxybenzene (67.2 mg, 0.4 mmol, 1.0 equiv) as internal standard, [Ir(dF(CF_3ppy)$_2$dtbbpy]PF_6 (4.4 mg, $4{\cdot}10^3$ mmol, 1 mol%), $NiCl_2{\cdot}$dme (4.4 mg, 0.02 mmol, 5 mol%), 4,4´-ditertbutyl-pyridine (5.4 mg, 0.02 mmol, 5 mol%) and 1,1,3,3-tetramethylguanidine (TMG) (75.2 µL, 0.6 mmol, 1.5 equiv) in a mixture of DMSO:DMF 1:1 (0.1 M). This solution was then sparged with N_2 for 15 minutes, sealed with parafilm and transferred to the nitrogen glove box. Next, inside of the box, under nitrogen atmosphere, we were dispensed both volumes, 57.4 µL and 60 µL of the reaction solution on different wells of the glass 96-well plate. The plate was sealed with a sealing film (PCR) and moved to the FLOSIM platform outside the glove box to run the reaction for 15 minutes.

We were pleased to find both volumes present similar results and allow to use 60 µL to run the optimization reactions (Figure S6).

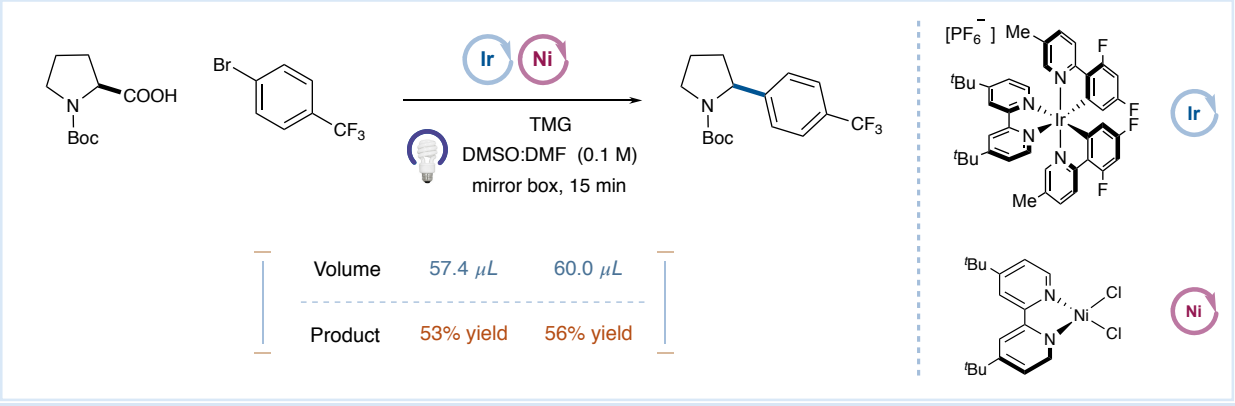

Fig. S6. Testing the calculated volume vs experimental volume. Each data is an average of 6 examples. Yields determined by UPLC using 1,3,5-trimethoxybenzene as internal standard.

2.3. Temperature distribution as function of the reaction time

Along with the wavelength of the lights, one of the most important parameters which allow a perfect match between both setups, HTE screening and the flow system, is the temperature factor. To recreate the same environment in both setups we have to use similar conditions, such as similar lights (power and wavelength) and temperature. The temperature can be modulated easily in the

flow systems; thus, we examined the solution temperature inside of the plate at different positions for different reaction times. After that, we are able to use this data to transfer the optimized conditions from plates to flow taking account the corresponding temperature for the related reaction time (shown on the Figure S7).

time	1 min	2 min	4 min	5 min	6 min	8 min	10 min	12 min	15 min	20 min	25 min	30 min	35 min	40 min	45 min
temperature	25°C	27°C	28°C	29°C	29°C	30°C	31°C	32°C	33°C	34°C	35°C	36°C	37°C	38°C	40°C

Fig. S7. Temperature vs reaction time. Each data is an average of 6 examples.

2.4. Use of other commercially available HTE platform.

At the outset of this project, we analyzed the standardize aluminum reaction blocks “Para-dox” operating with glass inserts in conjunction with the Lumidox LED Arrays commercially available from Analytical Sales.

As shown in the Section 2.2. we need to calculate the required volume to simulate a flow system in a multi-reaction system. In this case, we used the standard glass inserts from Analytical Sales (1mL) with 6 mm of internal diameter. With this in hand and considering the Vapourtec parameters as the standard flow system (i.d. = 1.3 mm), we found the needed volume for this plates is 36.8 µL. As happens in the previous section, to facilitate the experimental part, we dispensed a near volume to the calculated volume (40 µL).

Several HTE campaigns using this platform showed that the LED arrays were not powerful enough to induce the photoredox reaction in the requires short reaction times for a flow simulation. Under the same reaction conditions shown in Section 2.1 no product formation was observed in 15 and 30 minutes of reaction time. After 24 hours we are able to observe some product formation (about 10% yield), although the result is very homogeneous along the plate the poor power of this LEDs, the simulation is not feasible, and we decided to continue with our FLOSIM platform.

Very recently, we were able to access to the second generation of blue LED Arrays from Analytical Sales: the Lumidox II (420 nm, 445 nm and 470 nm with solid or cooling base). To our delight, we could see that these LED plate offers vast more intensity than the previous generation,

allowing to see good reactivity in the minute-hour time frame which could be beneficial for this purpose.

First, we evaluated the 470 nm LED (lens mat and active cooling base) to compare with the first generation of Lumidox and check if the new radiant power is efficiently enough for this purpose. In this case using the maximum power, we observed better results regarding the first generation (30% average yield of product formation with a 3.46 stdv.). Next, we examinate the 445 nm LED setup (disperse lens and solid base) obtaining 39% average yield (with 2.41 of stdv.). The system was overheated during the running and the Lumidox Controller stops, switching off the LED arrays. Finally, we analyzed the 420 nm LEDs (lens mat and active cooling base) which offer a better comparison with our system. In this case we found a 42% average yield of product formation with a 2.97 stdv. All these experiments were run entirely in a glovebox, so to have a fair comparation with our FLOSIM system we prepare everything as shown in section 2.2 and run the reaction out of the glove box for 15 minutes. Here we observed a reasonable product yield formation though the homogeneity along the plate is diminished (39% average yield of product formation with a 7.84 stdv.) so we consider that using these aluminum plates require to perform the whole process in a glove box (see Section 8.2).

As we pointed out, through the course of our studies we observed a major drawback with Lumidox II system. This is due to the Gen II arrays contain a resettable fuse. If the internal temperature surpasses this fuse the unit temporarily turns off (see Analytical Sales website, FAQ). The high temperature reached by the system likely due to the proximity between the LEDs and the plate also could help some reactions to take place not only by light but also by heat transfer.

Notwithstanding of the good results in terms of homogeneity, this suggests the use of this system is not a good candidate yet to do this simulation flow process.

3. General Procedures.

3.1. Batch reaction setup.

An oven-dried 8 mL screw cap septum vial equipped with a magnetic stirring bar was charged with substrate A, (hetero)aryl substrate B and photocatalyst. The base, additives and anhydrous solvent were added sequentially. 4,4′-Di-tert-butyl-2,2′-dipyridyl and nickel(II) chloride were added as a stock solution prepared in a separated vial in the corresponding solvent (sonicated for 10 minutes before addition). The mixture contained in the vial was degassed by sparging with nitrogen while stirring for 10-15 minutes before sealing the vessel with Parafilm. The reaction was stirred and irradiated using the blue Kessil LED lamp of the appropriate wavelength (2-7 cm away, with cooling fan varying the position to keep the reaction at the required temperature) for the needed time.

The reaction mixture was removed from the light and cooled to ambient temperature. An aqueous workup and a flash column chromatography on silica gel afforded the desired product.
Note: In the C–N coupling reaction, the copper catalyst ($Cu(acac)_2$) was added as a single portion before the solvent loading. After that the reaction mixture was sonicated for 3 minutes.

3.2. Reaction using the FLOSIM platform.

Stock solutions of common reactants and reagents were prepared in a volumetric flask or in an oven-dried 8 mL screw cap septum vials in the proper solvent following the aforesaid procedure. After degassing by sparging nitrogen for 10-15 min, the vials were sealed with parafilm and introduced into a nitrogen filled glove box.

To a glass 96-well plate (internal well-diameter 7.5 mm) in a glove box, was dispensed the reagent under study, a base screening for instance, into the bottom of the well. Then, the previously fresh prepared stock solutions were added to reach a final volume of 60 μL (In the case of dilution studies the corresponding amount of solvent was added before the stock solution). The plate was then sealed with transparent sealing films PCR and immediately removed from the glove box and placed on the platform inside of the FLOSIM device described in section S2. The fan (medium speed) and Kessil lights were switched on and the reactions were carried out for the appropriate time. The plate was then removed from the light, cooled until room temperature, and the sealing

film was withdrawn. After the dilution of each well with 100 μL of acetonitrile, the reactions were transferred to a Nunc 96-well plate, diluted again with 950 μL of acetonitrile and analyzed by UPLC-MS. Yields were determined using 1,3,5-trimethoxybenzene as internal standard.

3.3. Reactions in continuous flow system.

3.3.1. Comparison with HTE.

Reactions using the UV-150 Vapourtec photoreactor were performed using a Vapourtec E-series unit equipped with a UV-150 module with blue LEDs of the specific wavelength (60W; 385 nm, 420 nm, 450 nm Gen-1). A reactor coil of 2 mL made of FEP tubing (inner diameter: 1.3 mm or 2.0 mm) was using for the comparative study between the flow and the HTE protocols.

Note: Total volume reaction vials of 3 – 6 mL were prepared as described for the reactions in batch section (S3.1) to get reproducible results with reaction scale and reactor-coil size.

Reactions using the PhotoSyn (Uniqsis) photoreactor were performed using a prototype unit equipped with LEDs (700W; 455 nm) in combination with a Rainin HPXL solvent delivery system pump and a water-cooling system. A 10 mL reactor coil (inner diameter: 1.0 mm) was used for both the comparison with HTE (50 μL/well) and the scale-up experiments.

Reaction setup followed the same procedure as batch reaction using the desired conditions in an 8 mL screw cap septum vial. The degassed vial, covered with aluminum foil, was connected to the inlet of the reactor coil under a positive pressure of nitrogen. After setting the reaction parameters (residence time, temperature, light intensity), the crude reaction mixture was collected in the steady state and analyzed by UPLC-MS. Yields were determined using 1,3,5-trimethoxybenzene as internal standard.

3.3.2. Scale up.

The Scale-up procedure was performed by using the PhotoSyn photoreactor or the UV-150 Vapourtec photoreactor equipped with a 10 mL reactor coil.

Reaction setup followed the same procedure as batch reaction using the desired homogeneous conditions in a flask under nitrogen. The degassed flask, covered with aluminum foil, was

connected to the inlet of the reactor coil under a positive pressure of nitrogen. After setting the reaction parameters (residence time, temperature, light intensity), the crude reaction mixture was collected in the steady state and analyzed by UPLC-MS and ^{1}H-NMR. Following the original conditions, the coupled products were isolated after an aqueous workup and a flash column chromatography obtaining the pure compound in a good yield.

4. Decarboxylative arylation

4.1. Light optimization in batch.

To an oven-dried 8 mL vial equipped with a Teflon septum and magnetic stir bar were added 1-bromo-4-(trifluoromethyl)-benzene (14.0 μL, 0.1 mmol, 1.0 equiv), *N*-Boc-Proline (Boc-Pro-OH) (32.3 mg, 0.15 mmol, 1.5 equiv), 1,3,5-trimethoxybenzene (16.86 mg, 0.1 mmol, 1.0 equiv), [Ir(dF(CF$_3$ppy)$_2$dtbbpy]PF$_6$ (**1**) (1.1 mg, 1 μmol, 1 mol%), NiCl$_2$·dme (1.1 mg, 5 μmol, 5 mol%), 4,4′-ditertbutyl-pyridine (1.4 mg, 5 μmol, 5 mol%) and Cs$_2$CO$_3$ (32.3 mg, 0.15 mmol, 1.5 equiv) in DMA (0.02 M). The solution was degassed by sparging with nitrogen for 15 minutes before sealing with parafilm. The reaction was stirred and irradiated using the 40 W PR160 Kessil LED (3 cm away without cooling fan to heat the reaction to approximately 35-45 °C) for 12 hours. The reaction mixture was cooled at room temperature and analyzed by UPLC or ^{1}H NMR vs. internal standard (Figure S8).

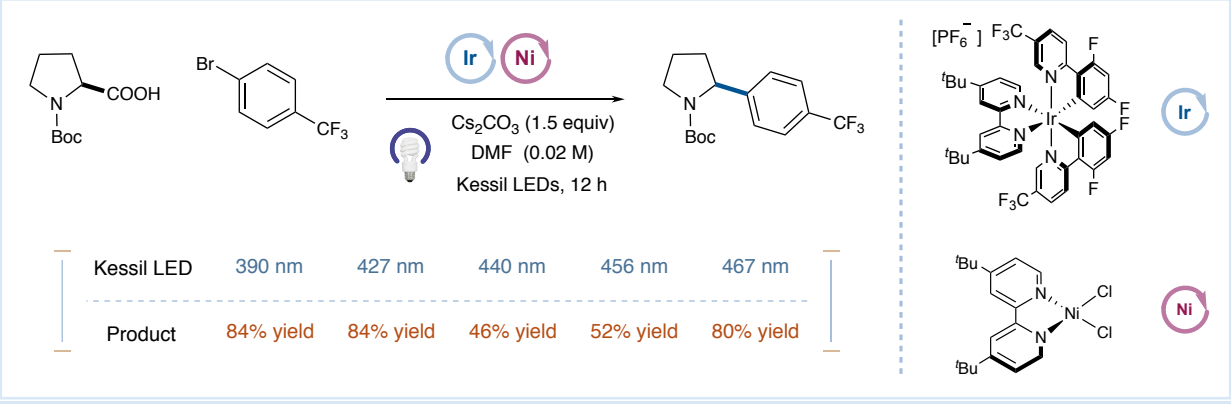

Fig. S8. Evaluation of the light source. Each data is an average of two reactions.

4.2. High-throughput experimentation screening.

For this optimization process we used the glass 96-well plate and the FLOSIM device described in the section 2. The final reaction volume for these screenings are related to the internal diameter which we need to compare it with (see section 2.2).

Recommendations for the preparation of stock solution. To avoid any damage on the glass 96-well plates during the setup of the reactions, the GeneVac is not using for these screenings. For

this reason, is necessary adjust the volume of the reaction stock solutions, reactants and solvents to reach a final volume of 60 µL for the regular cases (Vapourtec reactor coils with id= 1.3 mm) (see section 2.2, Figure S5). To facilitate this, it is recommended to prepare concentrated stock solutions with the major amount of the reactants, added variables we need to evaluated in the screening (if the reactant is liquid it should be added directly, and if it is a solid it is added as a stock solution). Lastly, if is needed the final volume is reached by addition of the corresponding dry solvent. Note: Insoluble reactants requires individual preparations, and they should be added as a suspension directly to the plate.

Base, solvent and concentration screening of the decarboxylative arylation of N-Boc-Proline.

Preparation of stock solution. To an oven-dried 8 mL vial equipped with a stir bar was added 1-bromo-4-(trifluoromethyl)-benzene (82.8 μL, 0.6 mmol, 1.0 equiv), *N*-Boc-Proline (Boc-Pro-OH) (193.7 mg, 0.9 mmol, 1.5 equiv), 1,3,5-trimethoxybenzene (100.9 mg, 0.6 mmol, 1.0 equiv), $[Ir(dF(CF_3ppy)_2dtbbpy]PF_6$ (6.7 mg, 6 μmol, 1 mol%), $NiCl_2$·dme (6.6 mg, 30 μmol, 5 mol%), 4,4´-ditertbutyl-pyridine (8.0 mg, 30 μmol, 5 mol%) in the evaluated solvent (3mL as final volume, 0.2 M). The solution was degassed by sparging with nitrogen for 15 minutes before sealing with parafilm. In this specific case in which the concentration is one of the evaluated parameters, a portion of this solution was taken to prepare two more diluted solutions (0.1 M and 0.05 M) which were also sparging with nitrogen for 15 minutes and sealed with parafilm. The internal standard is included in the reaction mixture instead in the workup of the reaction to obtain a better comparison with the flow system where we also need to include the internal standard with the rest of reactants.

Preparation of the 96-well plate. Experiments were set up inside a glovebox under a nitrogen atmosphere. To a vacuum-dried glass 96-well plate were added the corresponding bases (2.25 μmol – 9 μmol), solvent (until reach a final volume of 30 μL) and then 30 μL of the stock solution (completing the final volume of 60 μL), which correspond to 1-bromo-4-(trifluoromethyl)-benzene (1.5 – 6 μmol), *N*-Boc-Proline (Boc-Pro-OH) ((2.25 – 9 μmol, 1.5 equiv), 1,3,5-trimethoxybenzene (1.5 – 6 μmol), $[Ir(dF(CF_3ppy)_2dtbbpy]PF_6$ (15 – 60 nmol,), $NiCl_2$·dme (0.075 – 0.3 μmol), 4,4´-ditertbutyl-pyridine (0.075 – 0.3 μmol) in the corresponding solvent (0.025 – 0.1 M). The 96-well plate was sealed, placed in the HTE FLOSIM device and irradiated with 40W 427 nm Kessil LEDS for 30 minutes. Upon cooling the reaction at room temperature, the plate is opened to the air and

100 µL of acetonitrile was added. An aliquot of this diluted reaction mixtures (20 – 45 µL) was transferred into a separate Nunc 96-well plate followed by 950 µL of acetonitrile. Then the LC block was mounted on an automated UPLC instrument for analysis.

As we are looking for not only the best conditions in terms of reactivity but also in terms of cost, we have screened different soluble organic bases.

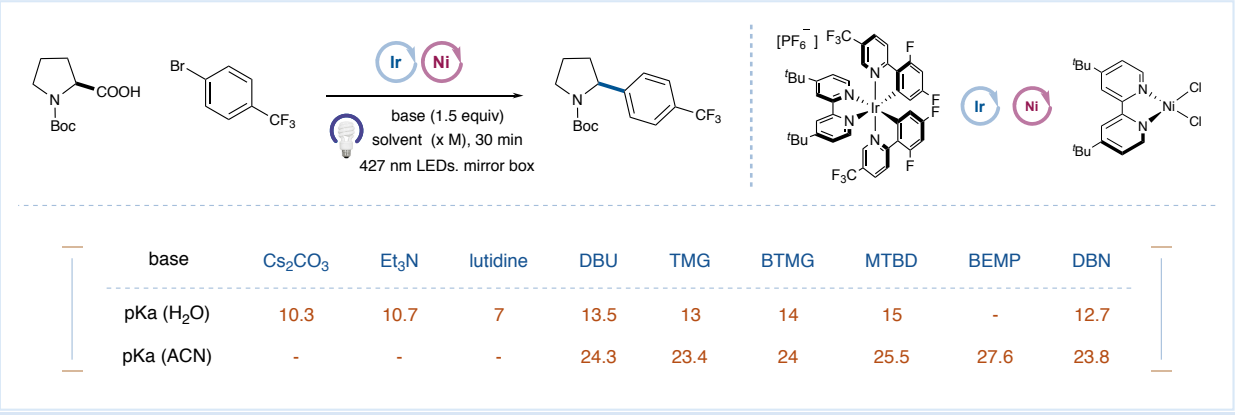

base	Cs_2CO_3	Et_3N	lutidine	DBU	TMG	BTMG	MTBD	BEMP	DBN
pKa (H_2O)	10.3	10.7	7	13.5	13	14	15	-	12.7
pKa (ACN)	-	-	-	24.3	23.4	24	25.5	27.6	23.8

Fig. S9. pKa of conjugated organic bases[4,5] to compare with standard inorganic base (Cs_2CO_3) for the decarboxylative arylation.

First, we have tested the reaction at higher concentrations to facilitate the reaction setup. At the same time, we have screened the influence of some organic bases and solvents. *Note: Due to the low melting point temperature of DMSO, we are using a mixture 1:1 DMSO:DMF to avoid any issue in the flow system during the reaction*.

We would expect good results using bases with similar or higher conjugate acid pKa values than the published carbonates (Figure S9). As shown Figure S10 the use of weak bases such as triethylamine or lutidine shows poor reactivity after 30 minutes of reaction. On the other hand, using strong bases (with pKa in acetonitrile higher than 23) the reaction takes place in good yields.

To probe the generality of our method, different conditions from the 96-well plate setup was submitted to the flow system and compare them. To accomplish this, we selected the following conditions: first, 4-(trifluoromethyl)-benzene (6 μmol, 1 equiv), *N*-Boc-Proline (1.5 equiv), 1,3,5-trimethoxybenzene (1 equiv), $[Ir(dF(CF_3ppy)_2dtbbpy]PF_6$ (1 mol%), $NiCl_2$·dme (5 mol%), 4,4´-ditertbutyl-pyridine (5 mol%), MTBD (1.5 equiv) in DMA (0.1 M) which present 50% yield in the

HTE screening (Figure S10, left table) after 30 minutes, and secondly using DBU as base in dioxane (0.1 M) the desired compound is observed in a 7% yield (Figure S10, right table).

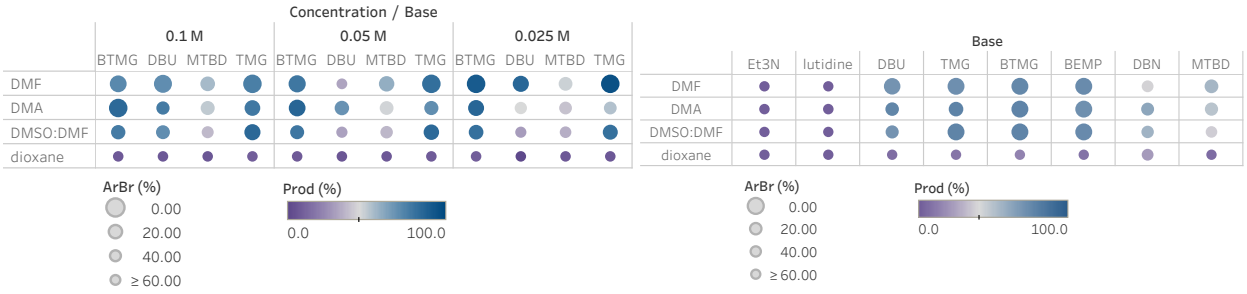

Fig. S10. Decarboxylative arylation high-throughtput screening. Bases vs solvents at different concentrations (*left*), base screening in different solvents at 0.1 M (*right*).

To increase the reproducibility with our results and to avoid human error resulted from the addition of small amounts of liquids, it was preferred the use of more concentrated solutions. In these cases, we observed the same range of yields (different between 1% and 10 %) for 0.1 M and 0.2 M solutions, so we continue our screening with the more concentrated reaction conditions. Although the use of bases such as BTMG or BEMP present good results we are focused on the less expensive organic bases such as TMG or DBU when it was possible. We also evaluated the use of different photocatalyst as well as different nickel sources or base loadings.

As shown Figure S11-top, the use of iridium photocatalyst (in particular the $[Ir(dF(Me)ppy)_2dtbbpy]PF_6$) as well as the organic dye 4CzIPN gave excellent results on the reaction. Also, we could observe good reactivities using any nickel source, so we based our election for the next steps on the price of the nickel salts. On the other hand, we also observed that the use of an excess amount of base do not improve the reactivity. Additionally, we observed high product yield with less than 10% of aryl bromide left using any base in the presence of $NiCl_2 \cdot 6H_2O$ as nickel source, $[Ir(dF(Me)ppy)_2dtbbpy]PF_6$ or 4CzIPN as photocatalyst, in DMA (0.2 M) (Figure S11, bottom).

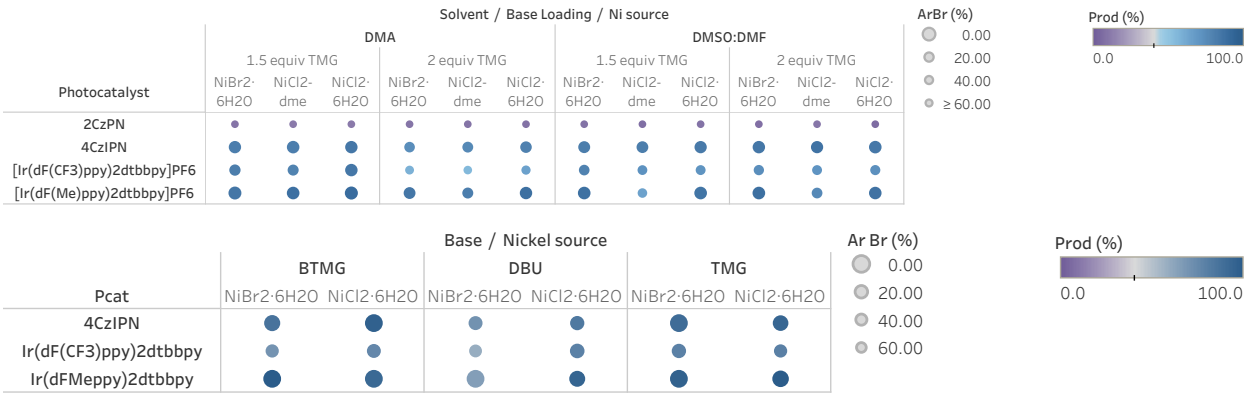

Fig. S11. Decarboxylative arylation high-throughtput screening. Photocatalyst (1 mol%) vs nickel source (5 mol%) and bases (1.5 equiv). Reactions were carried out at 12 μmol scale (0.2 M).

Next, we have examined some the two best bases and photocatalyst in combination with two different nickel sources and concentrations (Figure S12). We have observed good levels of reactivity in all cases, although when the concentration is increased the yield diminished by 5-10%, at the same time we could observed more aryl bromide left. At this point, we evaluated if it is more advantageous to use a higher concentration and increase the reaction time to consume the aryl bromides or, by contrast, maintain the previous reaction time in a lower concentration.

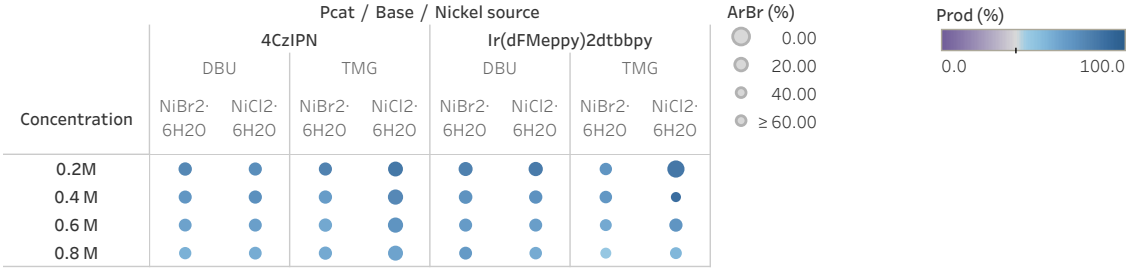

Fig. S12. Decarboxylative arylation high-throughtput screening. Concentration vs nickel source (5 mol%) and bases (1.5 equiv). Reactions were carried out at 12 – 48 μmol scale (0.2 – 0.8 M).

In our case, we decided to increase the concentration to 0.4 M in DMA. Unfortunately, after using TMG as base at 0.4 M (or higher), we detected salt formation during the course of the reaction, being possible the clogging of the continuous flow reactor coils, so we should avoid using these conditions. For this reason, we have continued the evaluation of the reaction parameters using both DBU and TMG in DMA at 0.4 M and 0.2 M respectively.

We have observed similar behaviors using both photocatalysts (Figures S13 and S14). However, the use of the iridium photocatalyst allows to reduce the catalyst loading maintaining the reactivity. Figure S13 shows that using a 5 mol% of nickel complex we can reduce the photocatalyst loading until 0.6 mol% obtaining the desired product in about 80% yield. The use of the organic photocatalyst led slightly lower yields. Although, the results using TMG as base are great (between 80 – 90% yield) we were not able to scale the reaction using these conditions due to the accumulation of salts into the reactor-coil.

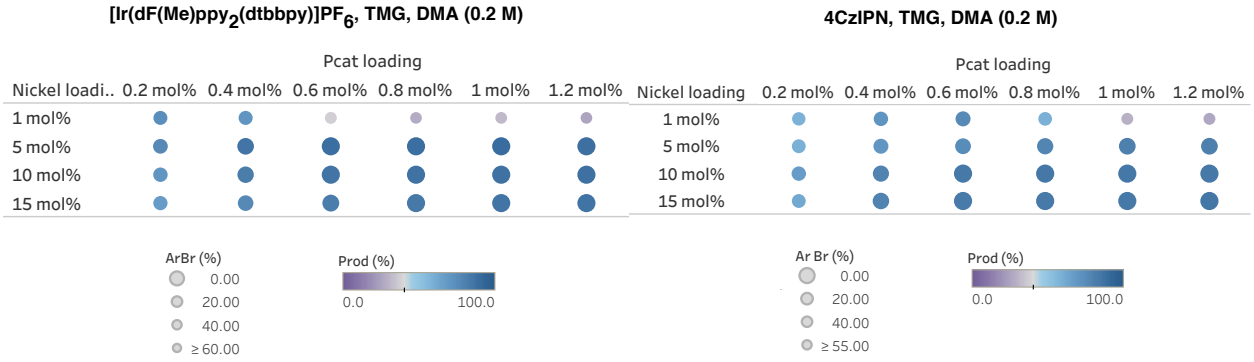

Fig. S13. Decarboxylative arylation high-throughtput screening. Photocatalyst loading vs Nickel loading using TMG as base. Reactions were carried out at 24 μmol scale (0.2 M).

We have obtained the similar results using DBU as base (Figure S14) in a more concentrated reaction solution (0.4 M). Here we observed that either using 1 mol% iridium photocatalyst or the organic photocatalyst, both conditions are comparable. Again, we were able to maintain the reactivity level only when the iridium photocatalyst loading is reduced (73% yield). However, when we reduce the photocatalyst loading of the 4CzIPN the yield decrease from 75% to 65% yield. Although we could use a 1 mol% of 4CzIPN photocatalyst we decided to continue our optimization using a lower amount of the iridium photocatalyst.

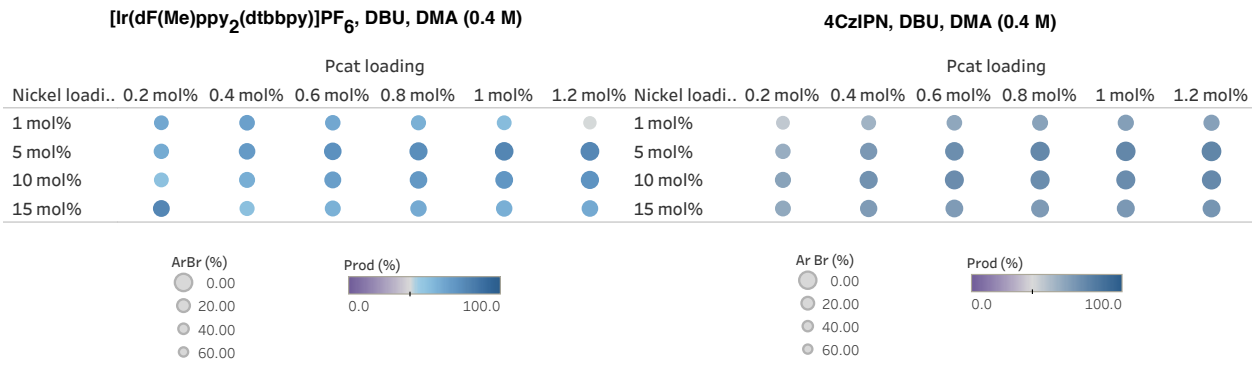

Fig. S14. Decarboxylative arylation high-throughtput screening. Photocatalyst loading vs nickel loading using DBU as base. Reactions were carried out at 48 μmol scale (0.4 M).

Finally, using the optimal conditions, we carried out the reaction at different reaction times, and we have also compared these results with the flow system reactions.

4.3. Reaction using continuous flow system and scale-up.

4.3.1. Continuous flow system results vs. HTE FLOSIM device results.

To an oven-dried 8 mL vial equipped with a Teflon septum and magnetic stir bar were added 1-bromo-4-(trifluoromethyl)-benzene (1.0 equiv), *N*-Boc-Proline (Boc-Pro-OH) (1.5 equiv), 1,3,5-trimethoxybenzene (1.0 equiv), photocatalyst (0 – 1 mol%), nickel source (5 – 10 mol%), 4,4′-ditertbutyl-pyridine (5 – 10 mol%) in the 3 mL of solvent. Then, the organic base was added (1.5 equiv) to the solution. The reaction mixture was stirred, degassed by sparging with nitrogen for 15 minutes before sealing with parafilm, and the vial was covered the vial with aluminum foil. Then, the reaction mixture was connected to the inlet of the reactor coil under a positive pressure of nitrogen. The flow system was purged with the degassed solvent and then, the reaction mixture was injected in the system using the corresponding reaction parameters such as flow rate or residence time (based on the conditions from the FLOSIM device), temperature (based on reaction temperature in plates, see Figure S7)), the crude reaction mixture was collected in the steady state and analyzed by UPLC-MS. Yields were determined using 1,3,5-trimethoxybenzene as internal standard.

The reaction was carried out using the best conditions described in the previous section. First, 1-bromo-4-(trifluoromethyl)-benzene (1.2 mmol, 1.0 equiv), *N*-Boc-Proline (Boc-Pro-OH) (1.5 equiv), 1,3,5-trimethoxybenzene (1.0 equiv), $[Ir(dF(Me)ppy)_2dtbbpy]PF_6$ or 4CzIPN (0.6 – 1 mol%), $NiCl_2 \cdot 6H_2O$ (5 mol%), 4,4´-ditertbutyl-pyridine (5 mol%) where combined with 6 mL of DMA (0.2 M). Then, the TMG was added (1.5 equiv) to the solution. Finally, the reaction solution was mixed and degassed with nitrogen. The reaction mixture was injected in a UV-150 Vapourtec E-Series, equipped with a 2 mL-reactor coil and the 420 nm LED light. The reaction was carried out at 36 degrees for 30 minutes of residence time (66 μL/min of flow rate) obtained the desired product in high yield. As shown the Figure S15 we observed very similar results between these yields and the ones obtained previously in the HTE FLOSIM device (entries 1 and 2). Unfortunately, using these conditions on a big scale which requires longer reaction times, has triggered the clogging of the reactor-coil due to salt accumulation.

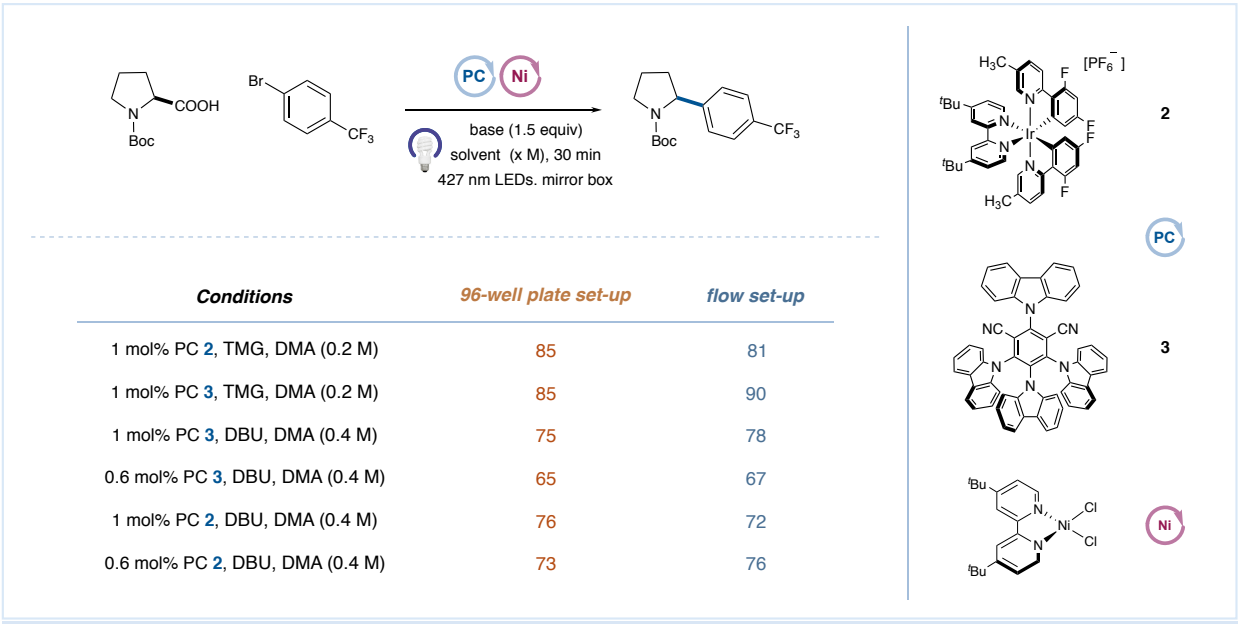

Conditions	96-well plate set-up	flow set-up
1 mol% PC **2**, TMG, DMA (0.2 M)	85	81
1 mol% PC **3**, TMG, DMA (0.2 M)	85	90
1 mol% PC **3**, DBU, DMA (0.4 M)	75	78
0.6 mol% PC **3**, DBU, DMA (0.4 M)	65	67
1 mol% PC **2**, DBU, DMA (0.4 M)	76	72
0.6 mol% PC **2**, DBU, DMA (0.4 M)	73	76

Fig. S15. Setup comparison using good conditions in the decarboxylattive arylation. Reaction takes place using 1 equiv of aryl bromide, 1.5 equiv of *N*-Boc-Proline, 5 mol% $NiCl_2 \cdot$dtbbpy for 30 minutes at 36 ºC. Reactions were carried out at 12 – 24 μmol scale (each data is an average of two – six points) for plates and 1.2 – 2.4 mmol scale for flow system (each data is an average of two reactions).

Similarly, 1-bromo-4-(trifluoromethyl)-benzene (2.4 mmol, 1.0 equiv), *N*-Boc-Proline (Boc-Pro-OH) (1.5 equiv), 1,3,5-trimethoxybenzene (1.0 equiv), $[Ir(dF(Me)ppy)_2dtbbpy]PF_6$ (0.6

mol%), $NiCl_2 \cdot 6H_2O$ (5 mol%), 4,4′-ditertbutyl-pyridine (5 mol%) were dissolved in 6 mL of DMA (0.4 M). Then, the DBU was added (1.5 equiv) to the solution. Finally, the reaction solution was mixed and degassed with nitrogen. The reaction mixture was injected in a UV-150 Vapourtec E-Series, equipped with a 2 mL-reactor coil and the 420 nm LED light. The reaction was carried out at 36 degrees with a 30 minutes of residence time (66 μL/min of flow rate). As shown Figure S15, the using DBU as base the reaction take place in good yields for both photocatalyst. However, only iridium photocatalyst allows a decrease in the photocatalyst loading without any variation in the yield (entries 3 – 6).

After this we evaluated the reaction time (Figure S16). To do this and have a fair comparison between the times and the setups and trying to avoid possible human error factors in the experiments, it was prepared a stock solution from which aliquots were taken for all the experiments (*the stock solution was covered with aluminum foil to avoid any background reaction*). Each time point was evaluated in 8 different wells, and the experiments using the flow system were run in duplicate considering the temperature data for each time point (Figure S7).

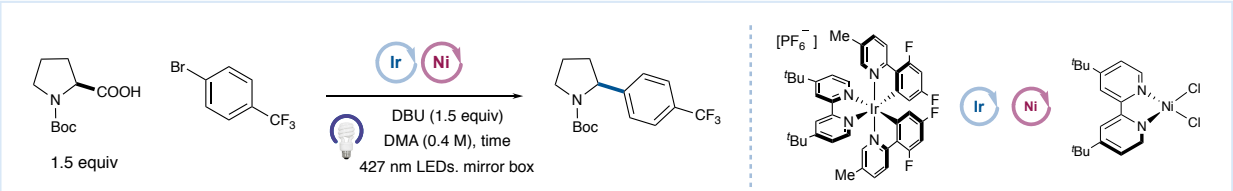

time	5 min	10 min	15 min	20 min	25 min	30 min	35 min	40 min	45 min
96-well plate set-up *(Pdt (%))*	**23**	**39**	**52**	**58**	**64**	**72**	**74**	**76**	**79**
ArBr (%)	77	58	44	35	27	21	11	8	3
flow set-up *(Pdt (%))*	**19**	**38**	**51**	**63**	**62**	**72**	**67**	**71**	**74**
ArBr (%)	83	63	46	38	27	19	13	10	0

Fig. S16. Reaction time comparison using the optimal conditions.. Reactions were carried out at 24 μmol scale (each data is an average of eight points) for plates and 1.6 mmol scale for flow system (each data is an average of two reactions).

Note: we have not observed any background reaction. To probe if we can keep the reaction in a flask and its only start to react when the light is turn on, we mixed all the reactants in a vial and we keep in darkness for a week (the vial was covered with aluminum foil and left at room

temperature). After one week, an aliquot of the reaction mixture was injected in the UPLC, achieving no product formation (0.5 % yield). Then, the reaction was injected in the Vapourtec system , observing similar amount of product formation as with freshly prepared reaction mixture.

Finally, as we mentioned in the section 4.2 (related to some data from Figure S10) we also compare different conditions to probe the generality of our method. To do this we selected two conditions showing moderate and poor yields of the cross-coupling product (Figure S17) and we were pleased to find a strong relation between setups for both.

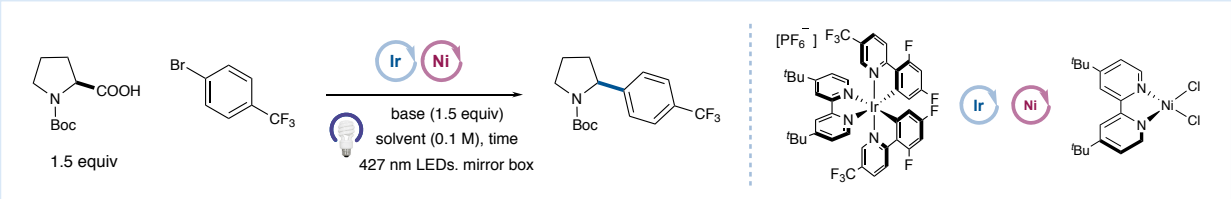

Conditions	96-well plate set-up	flow set-up
1 mol% Ir, 5 mol% $NiCl_2$·dtbbpy, 1.5 equiv MTBD, DMA (0.1 M)	50	56
1 mol% Ir, 5 mol% $NiCl_2$·dtbbpy, 1.5 equiv DBU, dioxane (0.1 M)	7	6

Fig. S17. Setup comparison using other conditions in the decarboxylattive arylation. Reactions takes place using 1 equiv of aryl bromide, 1.5 equiv of *N*-Boc-Proline for 30 minutes at 36 ºC. Reactions were carried out at 6 μmol scale (each data is an average of four points) for plates and 0.3 mmol scale for flow system (each data is an average of two reactions).

4.3.2. Scale up using the continuous flow system.

A oven-dried 250 mL round-bottom flask (RBF) or volumetric flask equipped with a Teflon septum and magnetic stir bar was charged with 1-bromo-4-(trifluoromethyl)-benzene (8.4 mL, 60 mmol, 1.0 equiv), *N*-Boc-Proline (Boc-Pro-OH) (19.4 g, 90 mmol, 1.5 equiv), 1,3,5-trimethoxybenzene (10.1 g, 60 mmol, 1.0 equiv), $[Ir(dF(Me)ppy)_2dtbbpy]PF_6$ (365 mg, 0.36 mmol, 0.6 mol%), $NiCl_2{\cdot}6H_2O$ (713 mg, 3 mmol, 5 mol%), 4,4´-ditertbutyl-pyridine (805 mg, 3 mmol, 5 mol%), DBU (13.57 mL, 90 mmol, 1.5 equiv) and DMA (0.4 M, 150 mL of total reaction volume). The reaction mixture was dissolved, degassed by sparging with nitrogen for 15 minutes before sealing with parafilm, and the flask was covered the vial with aluminum foil. The Vapourtec

system equipped with a 10 mL-reactor coil and 420 nm LED lights was purged, under nitrogen atmosphere, with the degassed DMA and then, the reaction mixture was injected into the system under nitrogen atmosphere. The reaction was run at 40 degrees in the heated mode with a 45 minutes of residence time (219 μL/min of flow rate) for 11.7 hours in total. The collection fraction was analyzed by ^{1}H-NMR and UPLC-MS (75 % yield). Then, the collection mixture was diluted with ethyl acetate (150 mL) and was washed with an aqueous solution of LiCl (2% w/v) (2 x 50 mL), water (2 x 100 mL). The aqueous layers were extracted with ethyl acetate (3 x 50 mL). The organic extracts were combined, washed with brine, dried over Na_2SO_4 and concentrated in vacuo. The residue was purified by flash column chromatography (hexane : ethyl acetate 9:1) to afford 13.2 g of the desired coupled product (pale yellow oil, 70% isolated yield). The spectroscopic properties of this compound are consistent with data reported in the literature.[6]

^{1}H NMR (500 MHz, $CDCl_3$) rotameric mixture: δ 7.56 (d, J = 8.1 Hz, 2H), 7.27 (d, J = 14.6 Hz, 2H), 4.98 (bs, 1H), 4.81 (bs, 1H), 3.71 – 3.47 (m, 2H), 2.46 – 2.24 (m, 1H), 1.97 – 1.73 (m, 2H), 1.46 (s, 3H), 1.18 (s, 6H).

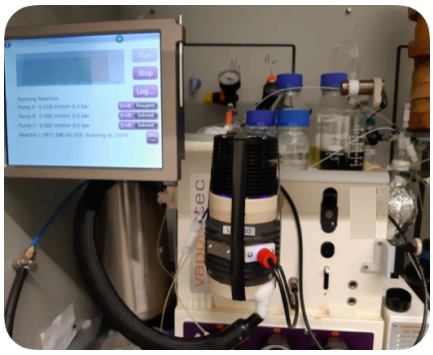

Fig. S18. Scale-up reaction setup.

Note: Before scale the reaction up, we have also tested the reaction under the optimized conditions using the 10 mL reactor-coil (with an injection of 13 mL of reaction mixture) reaching similar results.

5. Decarboxylative alkylation. C–N coupling.

5.1. Light optimization in batch.

To an oven-dried 8 mL vial equipped with a Teflon septum and magnetic stir bar were added $Ir(ppy)_3$ (1.3 mg, 2 µmol, 0.02 equiv.), $Cu(acac)_2$ (13.0 mg, 0.05 mmol, 0.50 equiv.), 3-chloro-1H-indazole (15.2 mg, 0.10 mmol, 1.0 equiv.), iodomesitylene O'[1],O[1]-3,3'-dimethyl bis(bicyclo[1.1.1]pentane-1,3-dicarboxylate) (116.8 mg, 0.2 mmol, 2.0 equiv.), 1,3,5-trimethoxybenzene (16.8 mg, 0.1 mmol, 1.0 equiv), and 1,4- dioxane (2.4 mL). The solution was sonicated for 3–5 minutes until it became homogeneous. The solution was degassed by sparging with nitrogen for 10 minutes before sealing with Parafilm. The reaction was stirred and irradiated using the 40 W PR160 Kessil LED (3 cm away without cooling fan, allowing the reaction to reach approximately 35-45 °C) for 1 hour. The reaction was cooled at room temperature and analyzed by UPLC or ^{1}H NMR vs. internal standard (Figure S19). As shown Figure S19 the reaction shows high yields in all cases, in particular, using 390 nm, 456 nm, or 467 nm LEDs present the best yields. Finally, we chose the 390 nm LEDs because lead to a cleaner reaction profile.

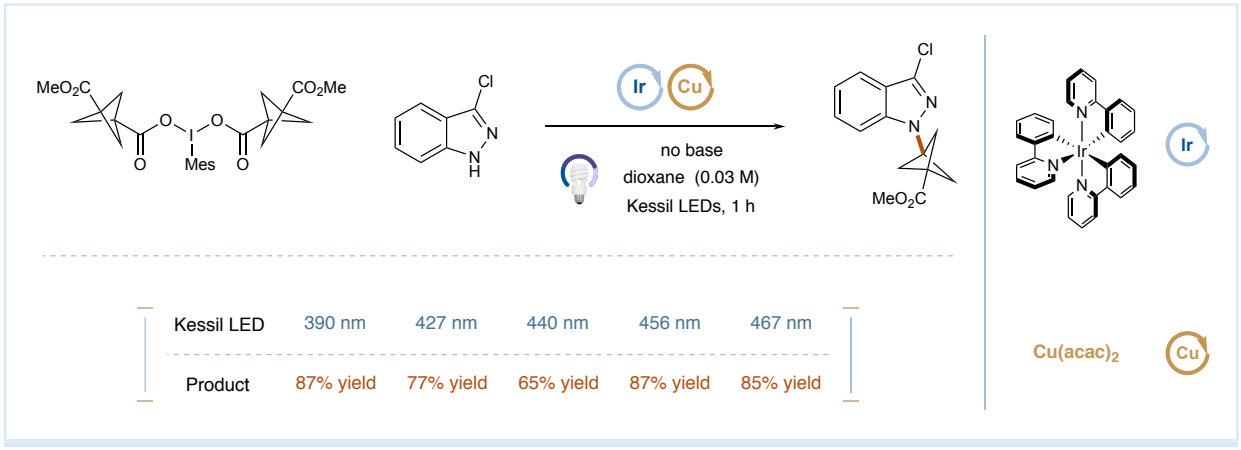

Fig. S19. Evaluation of the light source. Each data is an average of two reactions.

5.2. High-throughput experimentation screening.

To carry out these experiments we follow the same methodology described in detail in the previous sections: preparing concentrated stock solutions with all the reactants except the ones we are testing as a variable or by multiple stock solutions that must converge into the required final volume, usually 60 μL. All stock solutions were sonicated until became homogeneous solutions.

Catalyst screening. *Preparation of stock solution.* To an oven-dried 8 mL vial equipped with a stir bar was added 3-chloro-1H-indazole (45.8 mg, 54 μmol, 1.0 equiv.), iodomesitylene O'[1],O[1]-3,3'-dimethyl bis(bicyclo[1.1.1]pentane-1,3-dicarboxylate) (351.0 mg, 0.1 mmol, 2.0 equiv.), 1,3,5-trimethoxybenzene (50.5 mg, 54 μmol, 1.0 equiv), and the evaluated dry solvent (1.5 mL). On separate vials were also prepared two copper salt stock solution: $Cu(acac)_2$ (2.3 mg, 15 μmol; or 13.7 mg, 76 μmol) in 1.0 mL of solvent each (to reach 10 mol% or 50 mol% of catalyst in the final solution), and three photocatalyst stock solution: $Ir(ppy)_3$ (2.0 mg, 3 μmol); $[Ir(F(Me)ppy)_2dtbbpy]PF_6$ (2.5 mg, 3 μmol), and 4CzIPN (2.4 mg, 3 μmol) in 1 mL of the selected solvent. The solutions were sonicated for 5 minutes, degassed by sparging with nitrogen for 10 minutes before sealing with parafilm.

Preparation of the 96-well plate. Experiments were set up inside a glovebox under a nitrogen atmosphere. To a vacuum-dried glass 96-well plate was added the required amount of solvent to reach 60 μ*L total reaction volume* (0 or 10 μL), 10 μL of the photocatalyst stock solution (1 mol%), 10 or 20 μL of the $Cu(acac)_2$ stock solution (5 – 50 mol%) and then 30 μL of the stock solution [which correspond to 3-chloro-1H-indazole (3 μmol, 1.0 equiv.), iodomesitylene O'[1],O[1]-3,3'-dimethyl bis(bicyclo[1.1.1]pentane-1,3-dicarboxylate) (6 μmol, 2.0 equiv.), 1,3,5-trimethoxybenzene (3 μmol, 1.0 equiv), in the corresponding solvent (30 μL, 0.05 M final concentration). The 96-well plate was sealed, placed in the HTE FLOSIM device and irradiated with 40W 390 nm Kessil LEDS for 2, 5 or 10 minutes. Upon cooling the reaction at room temperature, the plate is opened to the air and 100 μL of acetonitrile was added. An aliquot of this diluted reaction mixtures (45 μL) was transferred into a separate Nunc 96-well plate followed by 950 μL of acetonitrile. Then the LC block was mounted on an automated UPLC instrument for analysis.

In the original publication this reaction takes place in only one hour, so we decided to explore this transformation using our protocol in shorter reaction times (less than 10 minutes). We started the evaluation of this reaction using the two best photocatalyst reported, as well as using of an inexpensive organic photocatalyst (4CzIPN) in combination with different copper catalyst loading in four organic solvents (Figure S20).

The reactions using both 2-Me-THF and dimethoxyethatne (DME) as solvents are not homogeneous and due to this the reactions shows low reactivities under the reaction conditions. As shown Figure S20 the reaction gave the best results for dioxane and DMA, and the copper can be diminished at longer reaction times. Then, we were able to detect good reactivities for any photocatalyst. Although the iridium photocatalysts are the ones used in the original paper we were pleased to find the organic photocatalyst gave even better yields (about 80% yield in dioxane).

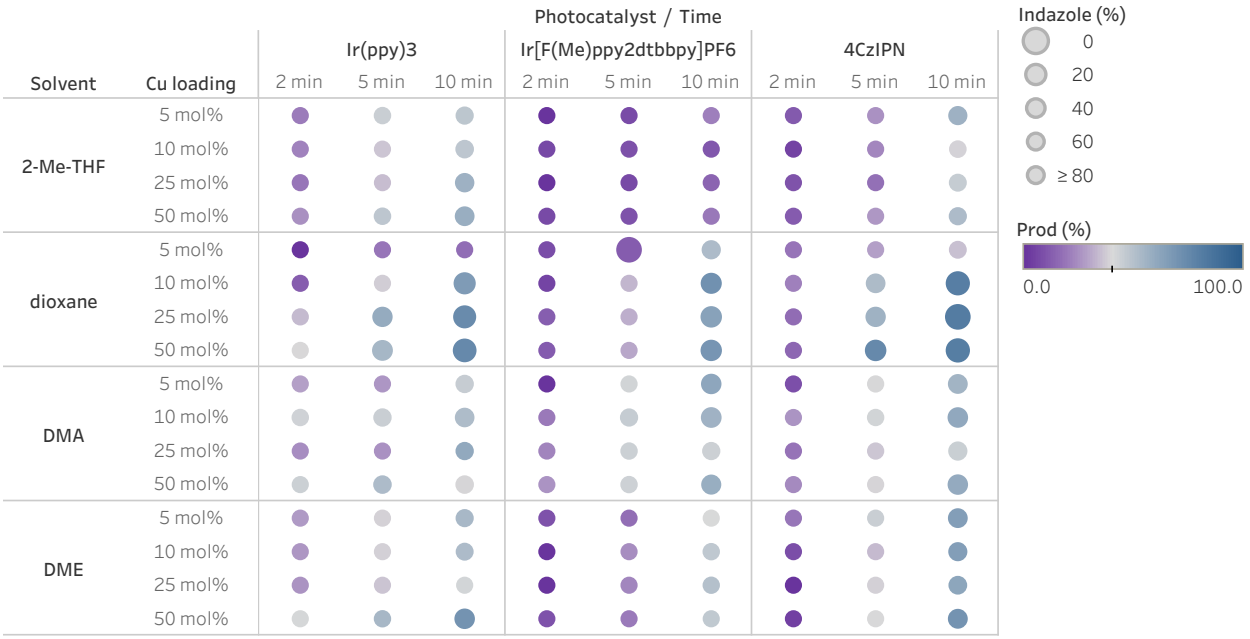

Fig. S20. C–N decarboxylative coupling high-throughtput screening. Photocatalyst vs copper loading and solvents. Reactions were carried out at 3 μmol scale at 3 different reaction times (0.05 M).

Then, we explored more carefully the copper catalyst loading in the reaction with one or two equivalents of iodomesitylene (generated from it corresponding carboxylic acid) in the presence of different photocatalysts (Figure S21 and S22). Broadly, we could observe greater reactivities achieving better yields and reaction conversions using an excess of carboxylic acid (Figure S21).

In particular, using 4CzIPN we were able to reduce both the copper loading (up to 30 mol%) and the carboxylic acid loading (up to 1.5 equiv) reaching higher reaction yields (Figure S22).

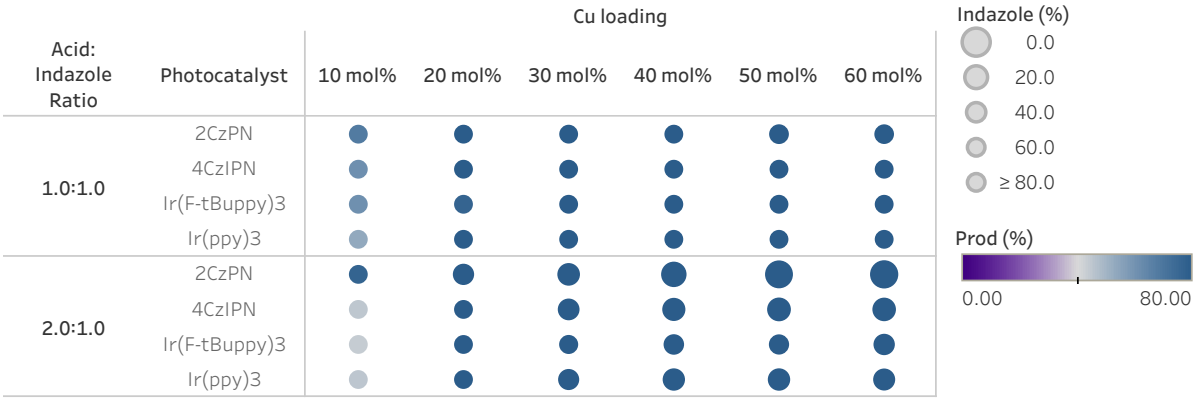

Fig. S21. C–N decarboxylative coupling high-throughtput screening. Photocatalyst vs copper loading and reagent stoichiometry. Reactions were carried out at 3 μmol scale for 10 minutes (0.05 M in dioxane).

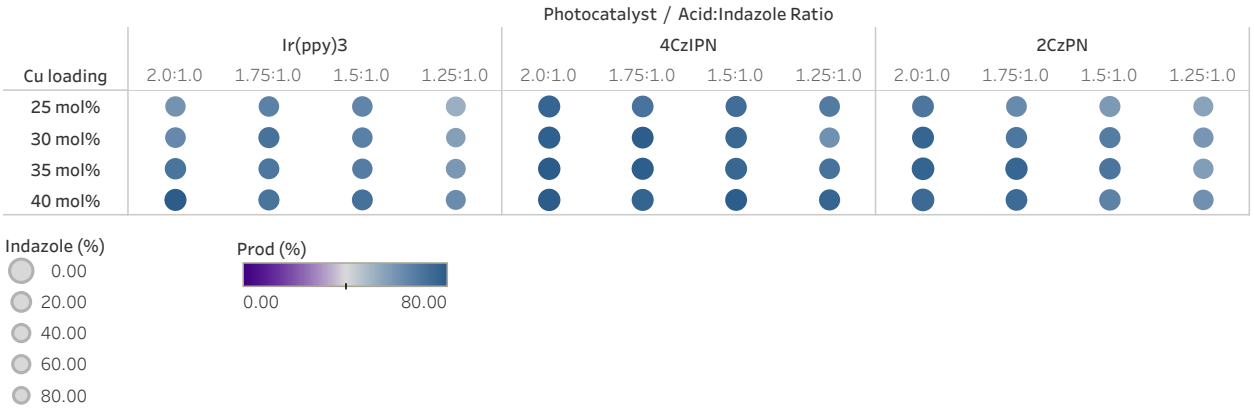

Fig. S22. C–N decarboxylative coupling high-throughtput screening. Photocatalyst vs copper loading and reagent stoichiometry. Reactions were carried out at 3 μmol scale for 10 minutes (0.05 M in dioxane).

Finally, we examined the effect on the reaction concentration in combination with the photocatalyst loading and two different copper loadings (Figure 23). As shown in Figure 23 we observed a decrease yield when the concentration is increased (up to 20% of difference). At the same time, we detected a trend between the photocatalyst loading and the concentration in which using lower reaction concentrations, lower amounts of the photocatalyst are required. Although the reaction took place successfully even for more concentrated reactions such as 0.075M or 0.1 M, during the course of the reaction salt formations were also detected, so we decided to continue

with 0.05 M as the optimal reaction concentration. As we could observe in the original manuscript some of the reactions did not need light. In these cases, the reactions were only copper-mediated, here we can see also this effect owing to if we increase the copper catalyst loading in absence of photocatalyst the reaction shows moderate reactivities and the yields became better for more diluted conditions.

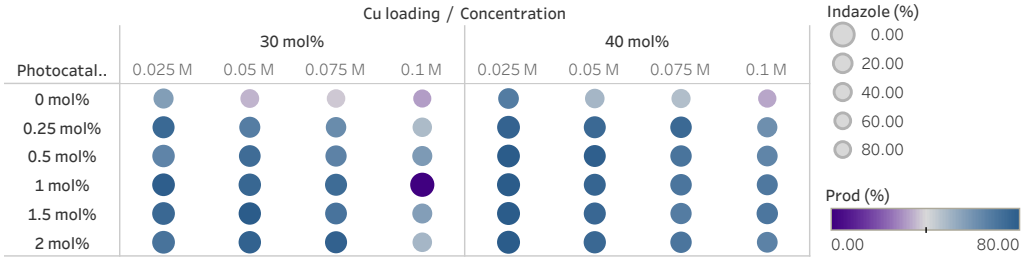

Fig. S23. C–N decarboxylative coupling high-throughtput screening. Photocatalyst loading vs copper loading and concentration. Reactions were carried out at 3 μmol scale for 10 minutes.

To sum up, we could conclude the best conditions in terms of product yield and reaction conversion involved the use of the *N*-nucleophile as the limiting reagent (indazole), 1.5 equiv. of activated carboxylic acid in combination with 30 mol% of copper loading and 1.5 mol% of 4CzIPN photocatalyst in dioxane.

5.3. Reaction using continuous flow system and scale-up.

5.3.1. Continuous flow system results vs. HTE FLOSIM device results.

We have first analyzed the reaction time under the optimal reaction conditions. Gratifyingly, we observed very similar results for both setups in every single evaluated time point and we could accomplish high yields from 6 minutes of reaction time. However, to observe a higher reaction conversion longer times are required (Figure S24).

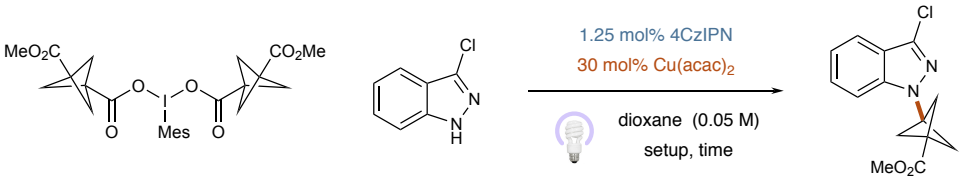

time	2 min	4 min	6 min	8 min	10 min	12 min
96-well plate set-up *(Pdt (%))*	**43**	**70**	**82**	**89**	**86**	**83**
Indazole (%)	56	29	18	10	8	11
flow set-up *(Pdt (%))*	**39**	**68**	**84**	**87**	**81**	**85**
Indazole (%)	59	34	16	11	8	12

Fig. S24. Reaction time comparison using the optimal conditions.. Reactions were carried out at 3 μmol scale (each data is an average of four points) for plates and 0.2 mmol scale for flow system (each data is an average of two reactions).

The reaction was carried out using the optimal conditions described in the Figure S24. First, using 3-chloro-1H-indazole (186.8 mg, 1.2 mmol, 1.0 equiv.), iodomesitylene O'^{1},O^1-3,3'-dimethyl bis(bicyclo[1.1.1]pentane-1,3-dicarboxylate) (1.1 g, 1.8 mmol, 1.5 equiv.), 1,3,5-trimethoxybenzene (201.8 mg, 1.2 mmol, 1.0 equiv), $Cu(acac)_2$ (65.4 mg, 0.36 mmol, 30 mol%), and 4CzIPN (14.2 mg, 18 μmol, 1.5 mol%) were combined in 24 mL of dioxane (0.05 M). The solution was sonicated for 5 minutes until it became homogeneous. Then, the mixture was degassed with nitrogen for 10 minutes and the reaction vessel was covered with aluminum foil. The reaction solution was injected in a UV-150 Vapourtec E-Series, equipped with a 2 mL-reactor coil and the 385 nm LED light on the heated mode (under the cooling mode the solvent is freezing with the subsequent reactor clogging). The reaction was carried out at 27 – 33 degrees from 2 – 12 minutes of residence time (from 1mL/min to 167 μL/min of flow rate).

Next, we also selected different conditions from the optimization process with moderate and poor yields of product formation, and we were pleased to find a strong relation between both setups demonstrating the robustness of our protocol (Figure S25).

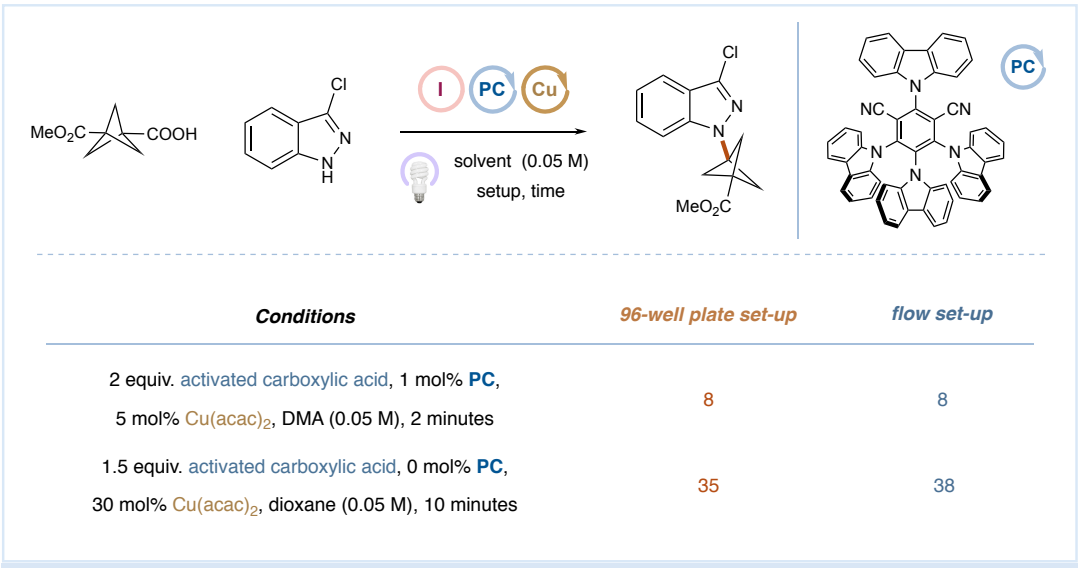

Conditions	*96-well plate set-up*	*flow set-up*
2 equiv. activated carboxylic acid, 1 mol% **PC**, 5 mol% $Cu(acac)_2$, DMA (0.05 M), 2 minutes	8	8
1.5 equiv. activated carboxylic acid, 0 mol% **PC**, 30 mol% $Cu(acac)_2$, dioxane (0.05 M), 10 minutes	35	38

Fig. S25. Setup comparison for moderate and poor results in the decarboxylattive C–N coupling. Reactions were carried out at 3 μmol scale (each data is an average of four points) for plates and 0.2 mmol scale for flow system (each data is an average of two reactions).

Normally, the size of the reactor-coil has not an impact on the reactivity of the reaction as long as the inner diameter will be constant. Based on that we are able to scale any reaction up with no variation in the yields between the 2 mL and 10 mL reactor-coil. However, in this case, when we tried to run the reaction using the 10 mL-reactor coils at 30°C or 31°C for 8 or 10 minutes of residence time respectively, we detected overpressure in the system. This was caused by the cooling mode on the Vapourtec system. It uses an air flowing system that is cooled by a dry ice-charged Dewar container. When the cooled air is coming to the reactor the temperature goes down fast and the dioxane freezes, clogging the reactor and stopping the reaction. For this reason, we were forced to use the heated mode. However, the minimum reliable homogeneous temperature to be control for this instrument in this mode is about 35 degrees, so before the scale-up we have to make sure there are substantial variations in the reaction yield (Figure S26).

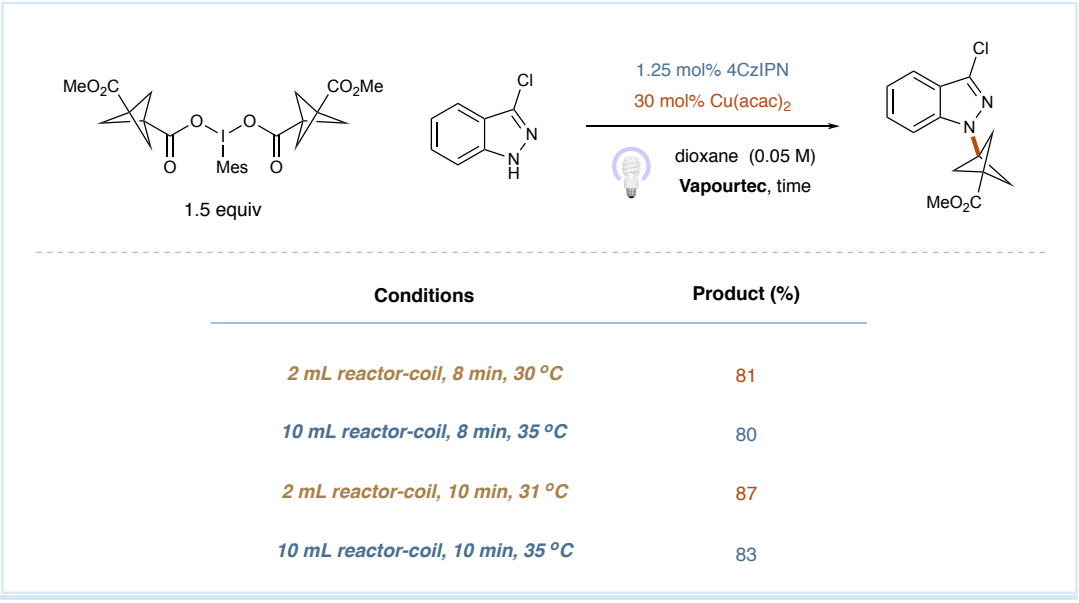

Conditions	Product (%)
2 mL reactor-coil, 8 min, 30 °C	81
10 mL reactor-coil, 8 min, 35 °C	80
2 mL reactor-coil, 10 min, 31 °C	87
10 mL reactor-coil, 10 min, 35 °C	83

Fig. S26. Decarboxylative C–N coupling flow reaction using cooled mode (brown) or heated mode (blue). Reactions were carried out at 0.2 or 0.6 mmol scale (each data is an average of two reactions)

Due to the iodomesitylene decomposition background reaction observed at higher temperatures and longer reaction times, we could potentially observe a decrease in reaction efficacy. Evaluation of small temperature changes showed minor variations in the product formation (Figure S26). However, when the temperature difference increase, we are able to observe these reaction yield variations. As shown in Figure S27, the reaction using the standard conditions for two minutes of residence time (also shown in Fig. S24) is 39% yield. This reaction take place at 27 degrees (according to the detected temperature on the FLOSIM device, see section 2.3), but if we increase the temperature until 40 degrees, we were able to accelerate the reaction achieving the N–coupled product in a 62% yield (Figure S27).

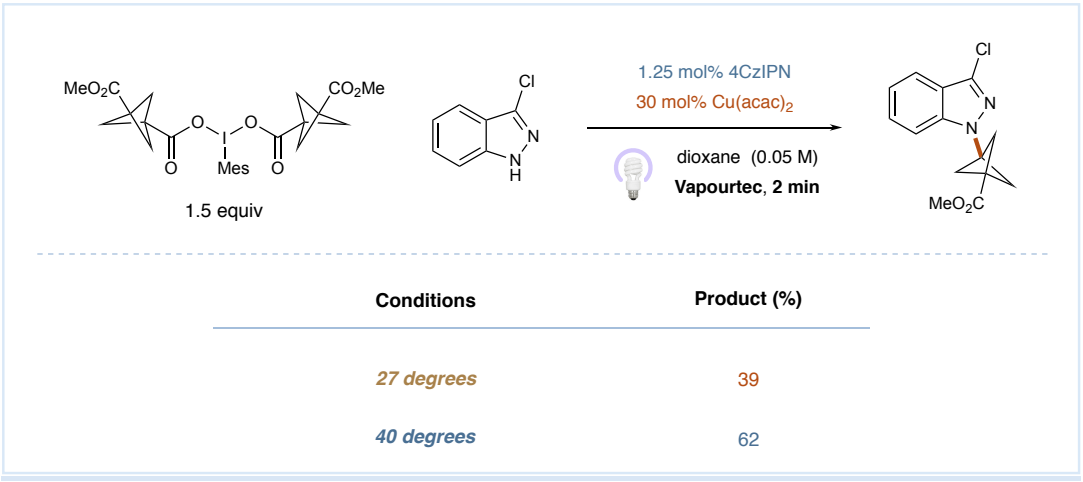

Conditions	Product (%)
27 degrees	39
40 degrees	62

Fig. S27. Decarboxylative C–N coupling flow reaction using heated mode. Reactions were carried out at 0.6 mmol scale

On a separate way, to undoubtably stablish our methodology, we wanted to demonstrate that other commercial flow systems are compatible with this approach. We examined a new photoreactor, the PhotoSyn instrument developed by Uniqsis Ltd and was made available in our lab for a brief testing period. The powerful LEDs (700W, 455 nm LEDs) equipped with a 10 mL reactor-coil (i.d. = 1.0 mm). Although this instrument has massive powerful LEDs, it is known that more than a third part of the power is lost in form of heat and if we want to compare this system with the HTE FLOSIM setup, we need to evaluate this parameter and find what is the right intensity that matches with the our light setup in the HTE FLOSIM device (with two lights) or with the Vapourtec system. This study was accomplished with the etherification reaction (see section 7.3.1). A 25% of light intensity was needed to reach the same level of reactivity than the observed in the HTE FLOSIM platform.

As we mentioned PhotoSyn photoreactor is equipped with a 455 nm LEDs and owing to the difference in wavelength in comparison with the Kessil lamps may lead to slightly different reactivity (it should be similar due to during the light optimization process we observed similar yields for 390 nm and 456 nm). Moreover, the reactor-coil tubing for this photoreactor is different, so we have to employ a different volume in plates to have a feasible comparison between both setups. Doing this, under the optimal reaction conditions [3-chloro-1H-indazole (1 equiv), iodomesitylene O'[1],O[1]-3,3'-dimethyl bis(bicyclo[1.1.1]pentane-1,3-dicarboxylate(1.5 equiv), of 1,3,5-trimethoxybenzene (1 equiv.), $Cu(acac)_2$ (30 mol%), and 4CzIPN (1.5 mol%) in dioxane

(0.05 M)] for a 50 μL as final volume in plates for 2 minutes a 28% of product yield was detected using the HTE FLOSIM device with two 456 nm LEDs. Next, we explored the same reaction conditions using the PhotoSyn system (25% light intensity) in which we were able to find a solid relation with the previous result (Figure S28, entries 1 and 2). We have demonstrated that increasing the reaction power we are able to accelerate the reaction rate (Figure S27). Thus, we envisioned that the use of a more powerful flow system such as PhotoSyn, could increase the reaction yield by increasing the light intensity maintaining the temperature, which may be beneficial for heat-sensitive reactions. Pleasantly, when the reaction was carried out under the same reaction conditions (2 minutes of residence time at 26 degrees) and 75 % light intensity the desired product was performed in a 64% yield (Figure S28, entry 3) verifying our previous hypothesis.

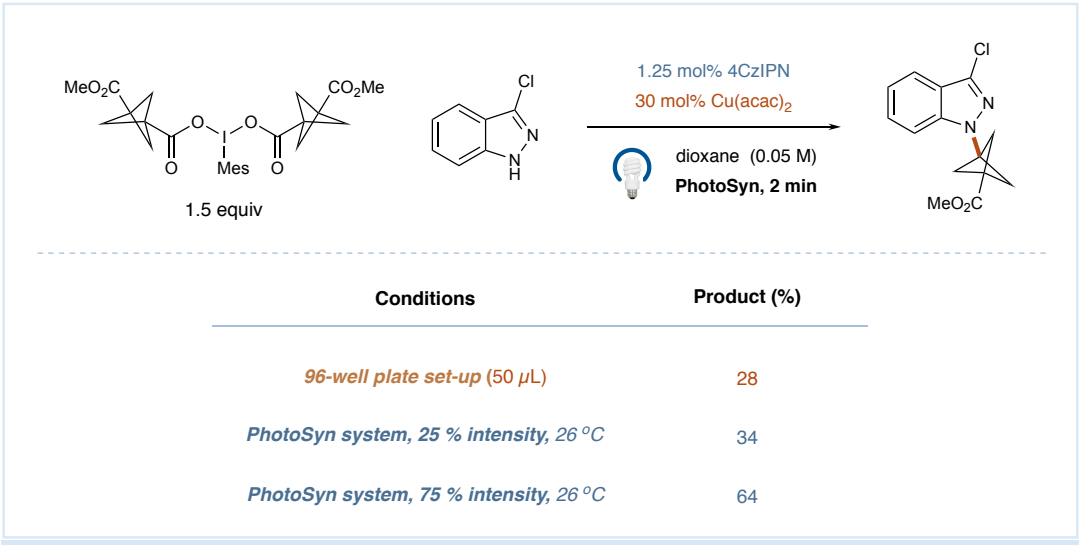

Conditions	Product (%)
96-well plate set-up (50 μL)	28
PhotoSyn system, 25 % intensity, 26 °C	34
PhotoSyn system, 75 % intensity, 26 °C	64

Fig. S28. Decarboxylative C–N coupling flow reaction using heated mode. Reactions were carried out at 3 μmol scale (each data is an average of four points) for plates and 0.6 mmol scale for flow system (each data is an average of two reactions).

5.3.2. Scale up using the continuous flow system.

An oven-dried 250 mL RBF or volumetric flask equipped with a Teflon septum and magnetic stir bar was charged with 4CzIPN (473.3 mg, 0.6 mmol, 0.015 equiv.), $Cu(acac)_2$ (2.18 g, 12 mmol, 0.30 equiv.), 3-chloro-1H-indazole (6.23 g, 40 mmol, 1.0 equiv.), iodomesitylene O'^{1},O^{1}-3,3'-

dimethyl bis(bicyclo[1.1.1]pentane-1,3-dicarboxylate) (35.1 g, 60 mmol, 1.5 equiv.), 1,3,5-trimethoxybenzene (6.73 g, 40 mmol, 1.0 equiv), and 1,4- dioxane (800 mL). The solution was sonicated for 5–10 minutes until it became homogeneous. The solution was degassed by sparging with nitrogen for 15 minutes before sealing with parafilm and covered the vessel with aluminum foil. The Vapourtec system equipped with a 10 mL-reactor coil and 385 nm LED lights was purged, under nitrogen atmosphere, with the degassed 1,4-dioxane and then, the reaction mixture was injected into the system under nitrogen atmosphere. The reaction was run at 35 degrees in the heated mode with an 8 minutes of residence time (1.25 mL/min of flow rate) for 10.7 hours in total. The collection fraction was analyzed by ^{1}H-NMR and UPLC-MS (70 % yield). Then, the collection mixture was diluted with ethyl acetate (150 mL) and was washed with an aqueous solution of ammonium hydroxide (3 x 50 mL), and water (2 x 100 mL). The aqueous layers were extracted with ethyl acetate (3 x 50 mL). The organic extracts were combined, washed with brine, dried over Na_2SO_4 and concentrated in vacuo. The residue was purified by flash column chromatography (hexane : ethyl acetate 4:1 to 0:1) to afford 7.6 g of the desired coupled product (white solid, 70% isolated yield). The spectroscopic properties of this compound are consistent with data reported in the literature.[7]

^{1}H NMR (500 MHz, $CDCl_3$): δ 7.68 (d, J = 8.1 Hz, 1H), 7.52 – 7.41 (m, 2H), 7.26 – 7.20 (m, 1H), 3.76 (s, 3H), 2.75 (s, 6H).

6. Cross-electrophile coupling.

6.1. Light optimization in batch.

To an oven-dried 8 mL vial equipped with a Teflon septum and magnetic stir bar were added methyl 4-bromo benzoate (22 mg, 0.1 mmol, 1.0 equiv), 4-bromotetrahydropyran (17 μL, 0.15 mmol, 1.5 equiv), 1,3,5-trimethoxybenzene (16.86 mg, 0.1 mmol, 1.0 equiv), tris(trimethylsilyl)silane (31 μL, 0.15 mmol, 1 equiv), 2,6-lutidine (23 μL, 1.0 mmol, 2 equiv), $[Ir(dF(CF_3ppy)_2dtbbpy]PF_6$ (1.12 mg, 1 μmol, 1 mol%), and dry DME was added (0.8 mL). To a separate vial was added $NiCl_2$·glyme (1.1 mg, 5 μmol, 5 mol%), 4,4′-ditertbutyl-pyridine (1.4 mg, 5 μmol, 5 mol%). The catalyst vial was sealed, purged with nitrogen then to it was added 2 mL of DME. The precatalyst solution was sonicated for 10 minutes, thereafter 0.2 mL (0.5 μmol, 0.005 equiv) was syringed into the reaction vessel. The solution was degassed by sparging with nitrogen for 15 minutes before sealing with Parafilm. The reaction was stirred and irradiated using the 40 W PR160 Kessil LED (3 cm away without cooling fan to heat the reaction to approximately 35-45 °C) for 16 hours. The reaction was cooled at room temperature and analyzed by UPLC or ^{1}H NMR vs. internal standard (1,3,5-trimethoxybenzene) (Figure S29).

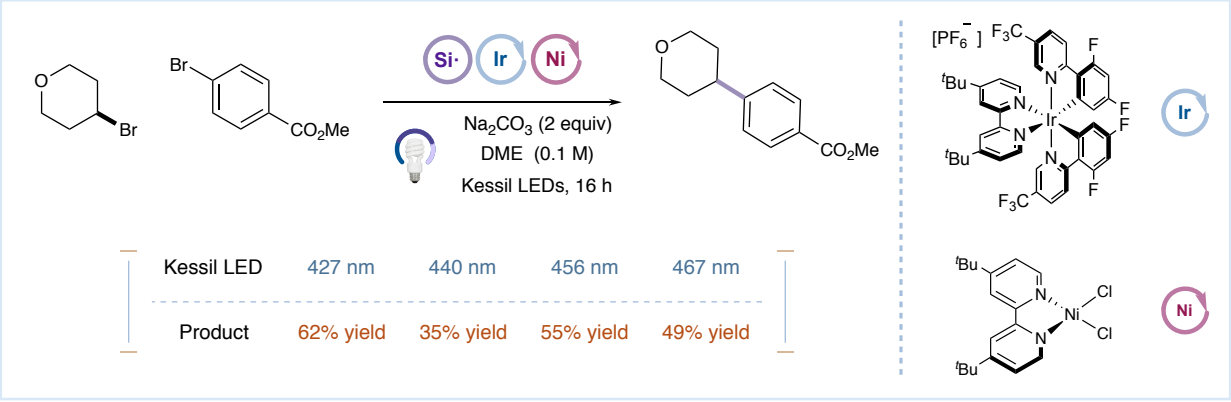

Fig. S29. Evaluation of the light source. Each data is an average of two reactions.

6.2. High-throughput experimentation screening.

To carry out these experiments we follow the same methodology described in detail in the previous sections preparing concentrated stock solutions with all the reactants except the ones we are testing as a variable.

Base and solvent screening. Preparation of stock solution. To an oven-dried 8 mL vial equipped with a stir bar was added methyl 4-bromo benzoate (64.5 mg, 0.3 mmol, 1.0 equiv), 4-bromotetrahydropyran (50.5 μL, 0.45 mmol, 1.5 equiv), 1,3,5-trimethoxybenzene (50.5 mg, 0.3 mmol, 1.0 equiv), tris(trimethylsilyl)silane (92.6 μL, 0.3 mmol, 1 equiv), $[Ir(dF(CF_3ppy)_2dtbbpy]PF_6$ (3.36 mg, $3\cdot10^{-3}$ μmol, 1 mol%), and the evaluated dry solvent was added (1.4 mL, 0.2 M). To a separate vial was added $NiCl_2\cdot$glyme (3.3 mg, 15 μmol, 5 mol%), 4,4′-ditertbutyl-pyridine (4.8 mg, 18 μmol, 6 mol%). The catalyst vial was sealed, purged with nitrogen then to it was added 1 mL of DME. The precatalyst solution was sonicated for 10 minutes, after which, 0.1 mL (1.5 μmol, 0.005 equiv) was added into the reaction vessel. The solution was degassed by sparging with nitrogen for 15 minutes before sealing with Parafilm. All bases and solvents are degassed by sparging with nitrogen for 15 minutes and sealed with Parafilm.

Preparation of the 96-well plate. Experiments were set up inside a glovebox under a nitrogen atmosphere. To a vacuum-dried glass 96-well plate were added the corresponding bases (12 μmol), solvent (until reach a final volume of 60 μL taking account the volume of base rest of the components in the reaction, in this case the different bases) and then 30 μL of the following stock solution [which correspond to methyl 4-bromo benzoate (6 μmol, 1.0 equiv), 4-bromotetrahydropyran (9 μmol, 1.5 equiv), 1,3,5-trimethoxybenzene (6 μmol, 1.0 equiv), tris(trimethylsilyl)silane (6 μmol, 1 equiv) $[Ir(dF(CF_3ppy)_2dtbbpy]PF_6$ (0.06 μmol, 1 mol%), and $NiCl_2\cdot$dtbbpy (0.03 μmol, 0.5 mol%), in the corresponding solvent (30 μL, 0.2 M). The 96-well plate was sealed, placed in the HTE FLOSIM device and irradiated with 40W 427 nm Kessil LEDS for 30 minutes. Upon cooling the reaction at room temperature, the plate was opened to the air and 100 μL of acetonitrile was added. An aliquot of this diluted reaction mixtures (45 μL) was transferred into a separate Nunc 96-well plate followed by 950 μL of acetonitrile. Then the LC block was mounted on an automated UPLC instrument for analysis.

We initiated the evaluation of this reaction using some soluble organic bases in combination with different organic solvents providing initially homogeneous reaction conditions. As we observed in previous studies of this reaction[8], 2,6-lutidine can act as an efficient base. As shown Figure S30, solvents such as acetone, ethyl acetate, DME or THF provides promising results and coordinating solvents like DMA or DMF provides lower reactivities. As we expect, the best bases for this transformation were 2,6-lutidine and 2,4,6-collidine. Using the non-efficient organic bases (TMG, NMM and DBU) or even without a base we could observe a more homogeneous reactivity using DMA as solvent.

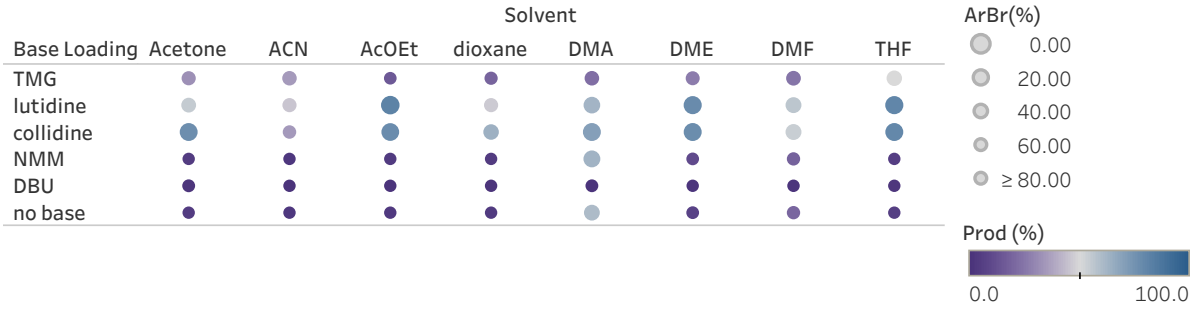

Fig. S30. sp^2-sp^3-Cross-electrophile coupling high-throughtput screening. Bases vs solvents. Reactions were carried out at 6 μmol scale (0.1 M)

Although we have observed good results using THF as solvent, we observed a competitive reaction that generates the THF-arylated compound as a major product under these conditions. For this reason, we have continued with the optimization using the other most promising solvents and bases testing different concentrations (Figure S31). We could observe similar levels of reactivity for more concentrated reactions being able to increase the concentration until 0.3 – 0.4 M without significant changes in terms of yield. The solvent study has not exhibited any difference from the previous screening, but despite acetone and ethyl acetate are promising candidates for this reaction. The use of the original solvent, DME, shows the best results at this point.

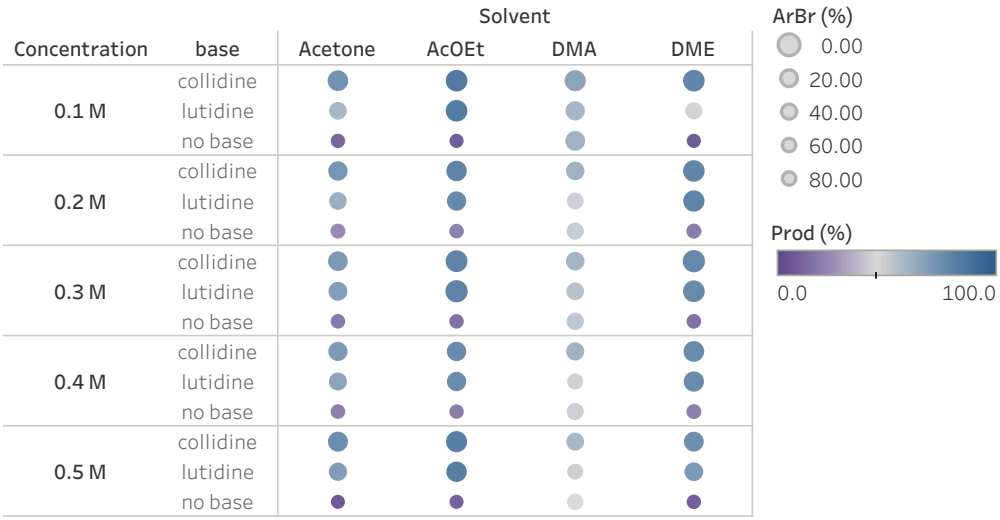

Fig. S31. sp^2-sp^3-Cross-electrophile coupling high-throughtput screening. Concentration vs bases and solvents. Reactions were carried out at 6 – 30 μmol scale (0.1 – 0.5 M)

A fundamental requirement to set up this reaction in batch-like conditions is the pre-complexation of the nickel source with the appropriate ligand. Despite this procedure is straightforward, we would like to test if this parameter is critical in the flow system as it could facilitate the reaction setup in big scales. Therefore, we have carried out the reaction testing three different nickel complex formation, by sonication as described the procedure in section 6.1 and 6.2, with no sonication where the nickel complex should be formed over the course of the reaction by simple stirring, or by isolation of the complex in a separate step. Based on the screening results shown in Figure S32, the use of any of these nickel catalyst generation sources should not interfere in the yield of this reaction in flow systems, being possible to adapt the setup conditions to our convenience. A comparison of the nickel catalyst loading was also tested (0.5 mol% and 1 mol%) obtaining similar results. Although normally we would continue the optimization process with the lower amount of material, we have chosen the 1 mol% to minimize the weighing errors in the preparation of the complex and to facilitate the reaction setup in plates. Notably we have obtained similar results with $NiCl_2$·dme and $NiCl_2$·$6H_2O$ as nickel sources, so we decided to continue the optimization with $NiCl_2$·$6H_2O$.

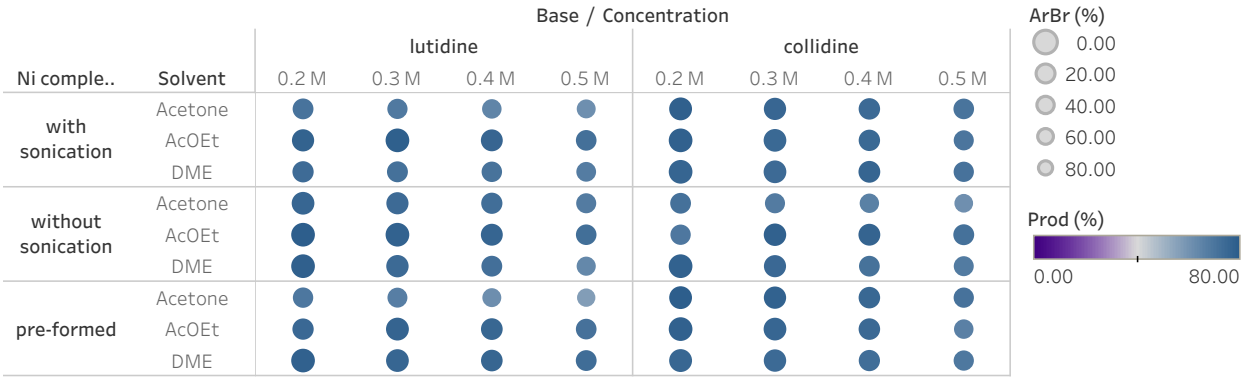

Fig. S32. sp^2-sp^3-Cross-electrophile coupling high-throughtput screening. Concentration vs solvents and nickel-complex formations. Reactions were carried out at 6 – 30 μmol scale (0.1 – 0.5 M)

One of the by-products observed in this reaction is the formation of a pyridinium bromide salts. The lutidinium bromide was identified the first time for this reaction in a previous report[6] using the integrated photoreactor designed by Merck. In this reaction a base is crucial to neutralize HBr formed via Si–H abstraction from the silane, which causes poor reaction efficiency if left unquenched. Accordingly, the lutidine forms an insoluble lutidinium bromide salt, which precipitates from the reaction mixture. Although this salt formation is beneficial due to help quenching the HBr, and do not affect the reactivity, the light penetration into a heterogeneous reaction mixture is hard. This issue is easily solved in small scale, using the integrated photoreactors, by a simple adjustment of the light intensity as well as the stirring rate. However, considering the narrow tubing of the flow system, the use of homogeneous conditions during the reaction process is one of the biggest requirements, so if the lutidinium bromide salt precipitates from the reaction mixture, could clog the flow reactor and prevent further reaction. In order to conduct this reaction on a larger scale, the solubilization of these salts is required to provide homogeneous or well-tolerated reaction conditions (Figures 33–38).

The solubility of this lutidinium bromide salt in DME is low (1 mg/mL) so we considered the identification of any parameter which enables a complete solubility. Inspired by the side product nature, rationally design lead us to introduce water into the reaction mixture. We evaluated the effect of different water loadings under different conditions (Figures S33 and S34). The reaction tolerates up to 10 equiv. of water without losses in the product yield. However, the reaction profile is independent of this screen showing only good reactivity for lutidine and collidine as base, and iridium photocatalyst. Similarly, salt formation was still detected on the wells under these

conditions. After this, different additives that potentially enable to dissolve this kind of salts were also tested such as ethylene glycol or methanol, without any positive result in terms of homogeneity (Figure S34).

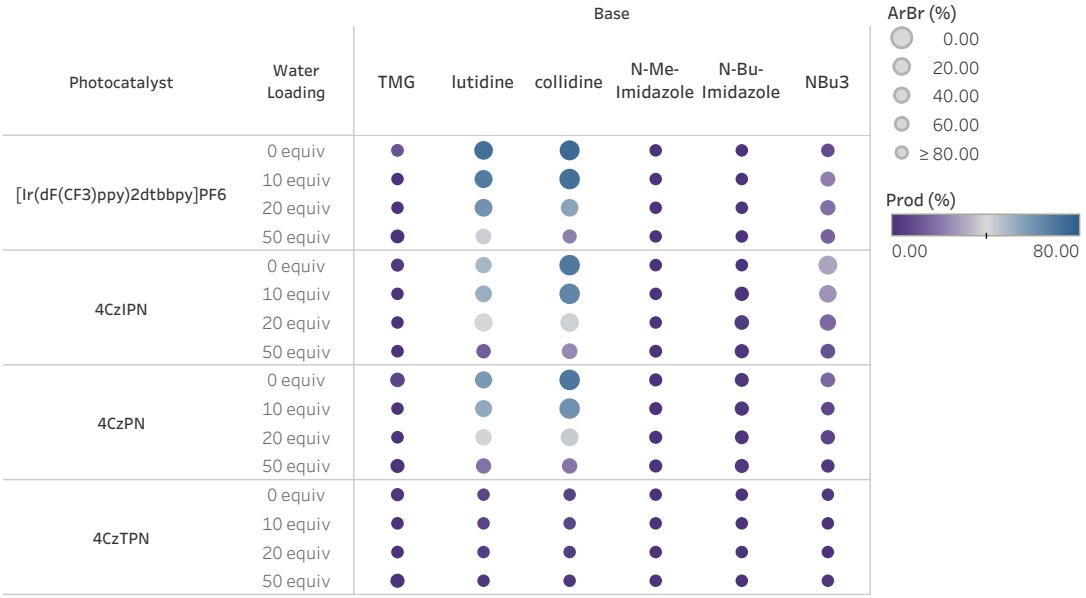

Fig. S33. sp^2-sp^3-Cross-electrophile coupling high-throughtput screening. Bases vs photocatalyst and water loading. Reactions were carried out at 18 μmol scale in DME as solvent (0.3 M)

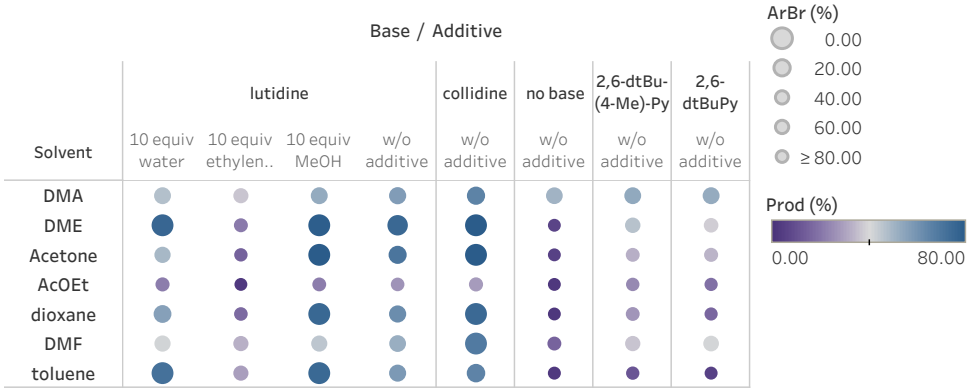

Fig. S34. sp^2-sp^3-Cross-electrophile coupling high-throughtput screening. Bases vs solvents and additives. Reactions were carried out at 18 μmol scale (0.3 M)

Although the use of solvents such as DMA or DMF have not provided good results in terms of reactivity (yields under 50%) we could observe a complete solubility, owing to this, we were moved our study using different solvent mixtures, solvents which provides great reactivity in conjunction with solvents which provides good solubilities. Furthermore, we also tested the

efficiency of the base loading in the reaction, due to reducing the base loadings involves a lower salt formation in the solution which could be easier to solubilize (Figure S35–S38).

At the same time, the ratio between the aryl bromide and alkyl bromide as well as the silane loading were also explored. Similar to the original conditions, the reaction shows better results when the aryl bromide is the limiting reactant, 1.5 equiv. of alkyl halide, and the same silane loading which allows a complete halogen-abstraction. Increasing the silane loading (2 or 3 equiv) leads to lower product yields (about 10% or 20% lower yields respectively). Moreover, an increment in the dehalogenated aryl side-product was also observed.

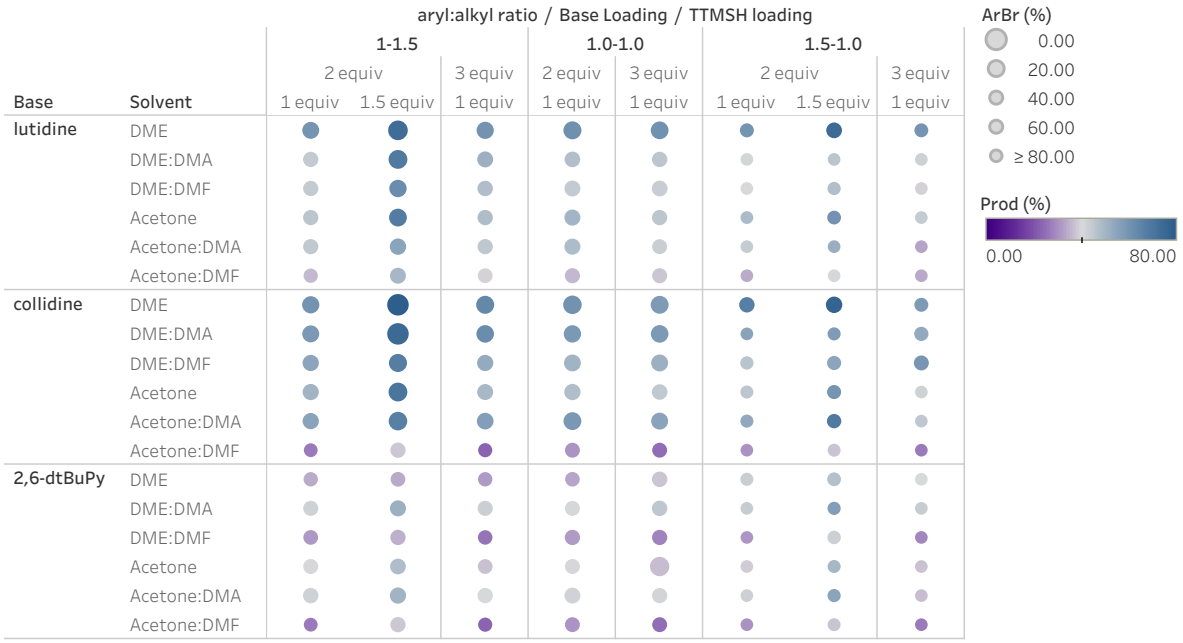

Fig. S35. sp^2-sp^3-Cross-electrophile coupling high-throughtput screening. Bases vs solvents and reagent loadings. Reactions were carried out at 18 μmol scale (0.3 M)

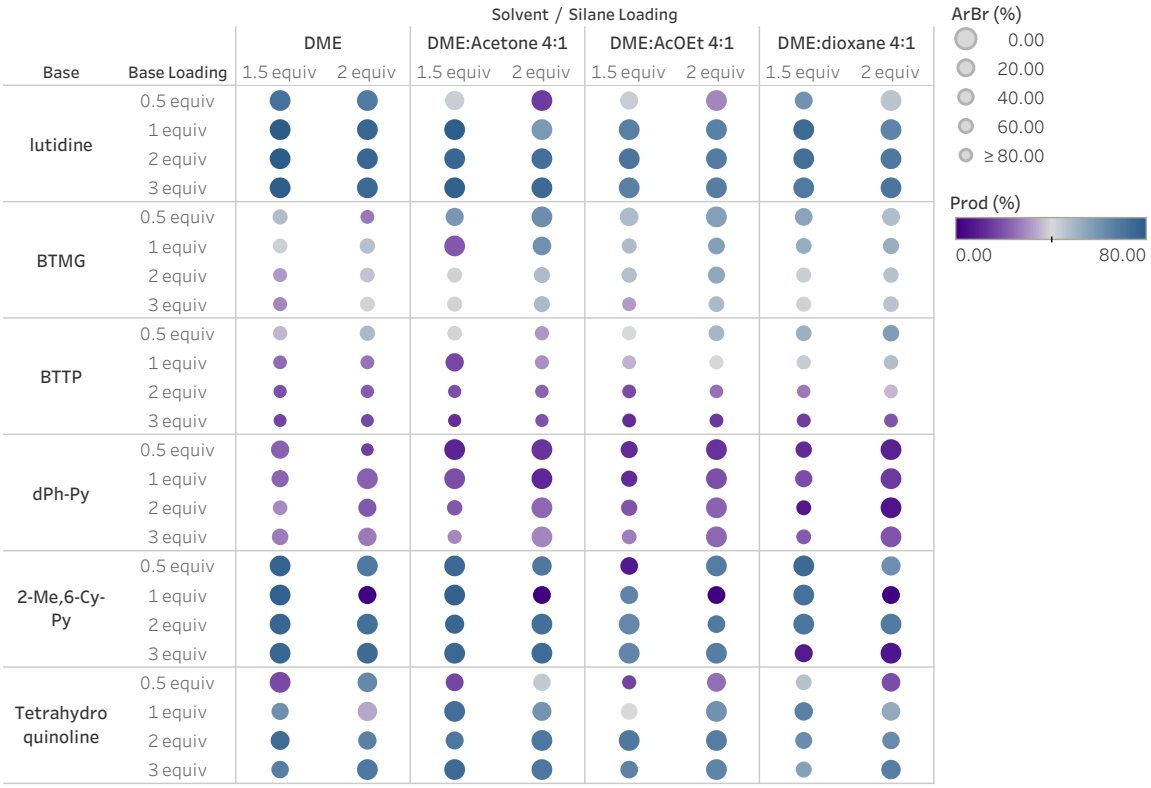

Fig. S36. sp^2-sp^3-Cross-electrophile coupling high-throughtput screening. Bases vs base loadings and solvents. Reactions were carried out at 18 μmol scale (0.3 M)

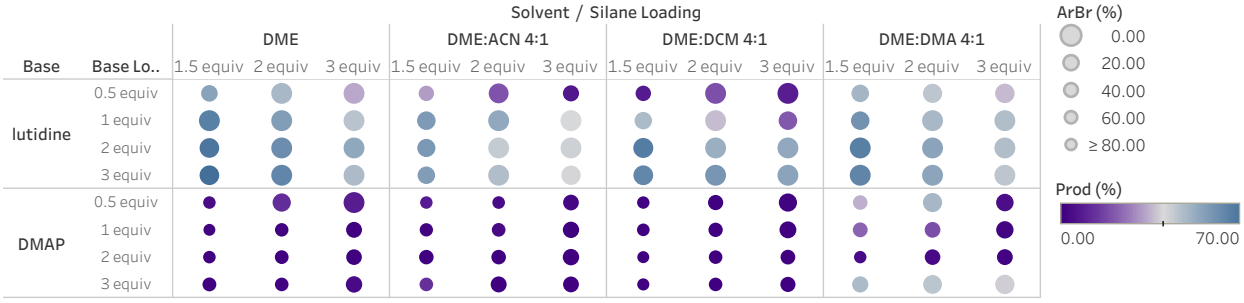

Fig. S37. sp^2-sp^3-Cross-electrophile coupling high-throughtput screening. Bases loadings vs solvent loadings. Reactions were carried out at 18 μmol scale (0.3 M)

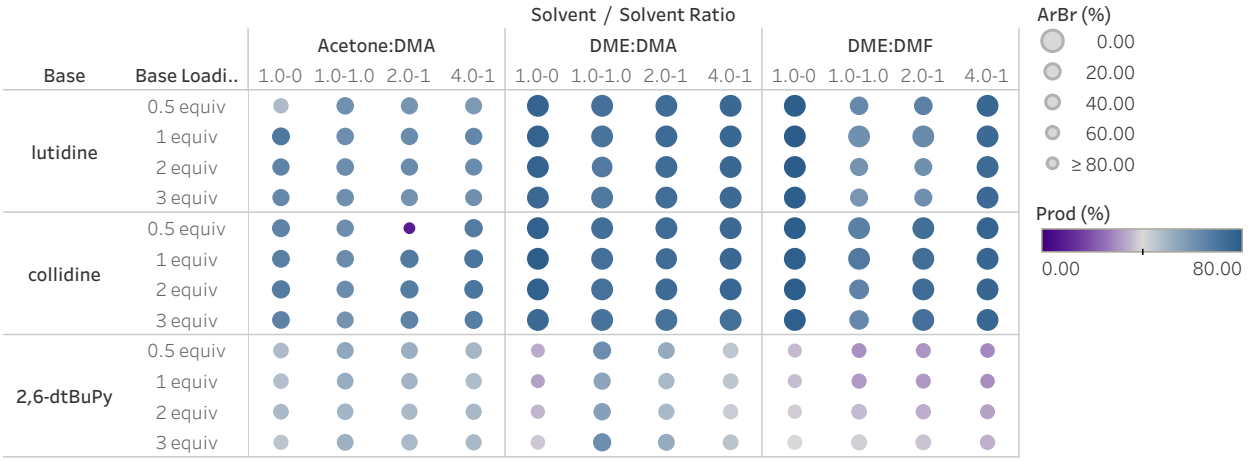

Fig. S38. sp^2-sp^3-Cross-electrophile coupling high-throughtput screening. Bases loadings vs solvent loadings. Reactions were carried out at 18 μmol scale (0.3 M)

Thereby, using DME as solvent or solvent mixtures with DME as the major solvent, we are able to reduce the base loading to 1 equiv. with no decrease in yield. The yield starts to decrease when the base loading is lower to 0.5 equiv. Unfortunately, even in those cases we could observed salt formation in the 96-well plates which can be translated to the clogging in a flow system.

On the other hand, as shown the Figures S31 and S32, the reaction took place in good yields for different concentration ranges, from 0.1 M to 0.3 M, though the usage of more concentrated solution is desirable in flow chemistry, the employment of these concentrated reactions makes more difficult the solubility of the salt. Therefore, the use of more diluted reaction mixtures turns to be another alternative to overcome the homogenization issues.

As an alternative, we have also imagined that using a thicker tubing, with higher inner diameter (i.d.), the flowing of the solutions allows a higher amount of salt and eventually solved the problem.

To do this, we were able to test some reactor prototypes with different characteristics. As we shown in the section 2.2 the use of a different reactor-coil with a different i.d. needs a new total volume for our reactions in plates. As shown Fig. S5 using a reactor coil with 2 mm of i.d. the calculated volume corresponds to 88.4 µL, but to facilitate the experimental procedure we would like to use 90 µL as final volume. To verify this approach, To verify this approach, a stock solution for the cross-electrophile coupling was prepared, showing similar results (Figure S39).

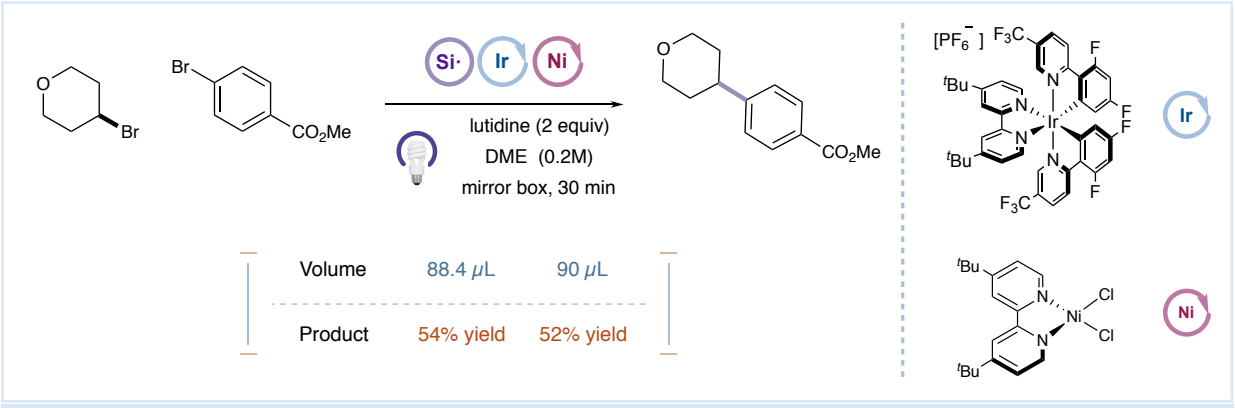

Fig. S39. Testing the calculated volume vs experimental volume. Each data is an average of 12 examples. Yields determined by UPLC using 1,3,5-trimethoxybenzene as internal standard. Reaction takes place using 1 equiv of aryl bromide, 1.5 equiv of alkyl bromide, 1.5 equiv of TTMS–H, 2 equiv of lutidine, 1 mol% PCat and 0.5 mol% of Ni-complex in DME (0.2 M) for 30 minutes in the HTE FLOSIM platform (427 nm LEDs). Reactions were carried out at 12 μmol scale.

According to the Beer-Lambert law, the penetration of visible light through a reaction medium decreases exponentially with increasing path length. This could suggest a possible loss of reaction efficiency using this new volume in plates (90 μL) which correspond directly a loss of efficiency in flow (reactor-coil tubing, i.d. 2mm). To test the efficiency of the reaction with the new volume, a screening was run under known conditions to study the effect of the base loading vs water loading or solvents (Figure S40 and S41).

As expected, the general behavior of the reaction is similar to the previous case, the use of a higher reaction volume implies a slightly diminished in the reactivity.

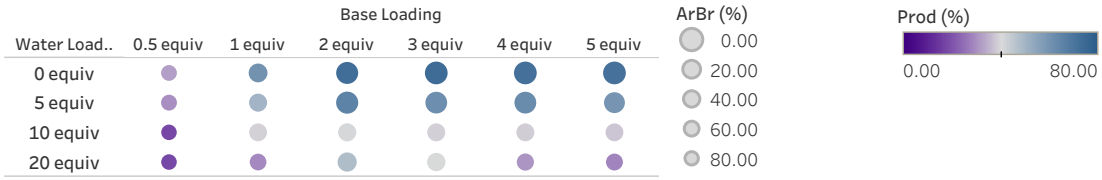

Fig. S40. sp^2–sp^3-Cross-electrophile coupling high-throughtput screening. 2,6-Lutidine loading vs water loading. Reaction takes place using 1 equiv of aryl bromide, 1.5 equiv of alkyl bromide, 1.5 equiv of TTMS–H, 1 mol% PCat and 1 mol% of Ni-complex in DME (0.2 M) for 30 minutes. Reactions were carried out at 12 μmol scale.

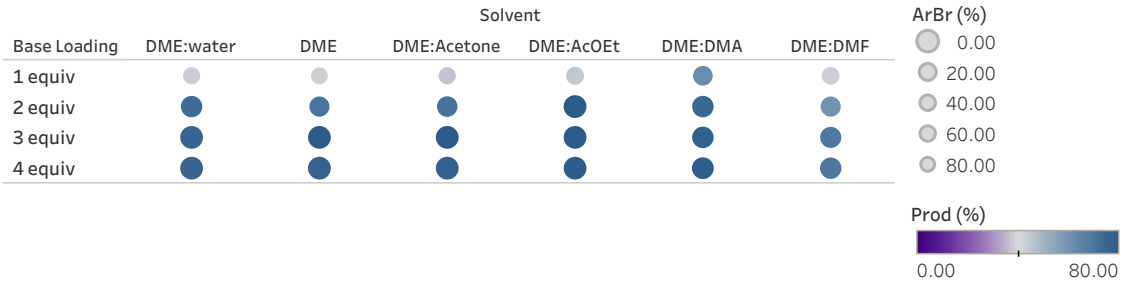

Fig. S41. sp^2–sp^3-Cross-electrophile coupling high-throughtput screening. 2,6-Lutidine loading vs solvents. Reaction takes place using 1 equiv of aryl bromide, 1.5 equiv of alkyl bromide, 1.5 equiv of TTMS–H, 1 mol% PCat and 1 mol% of Ni-complex for 30 minutes. Reactions were carried out at 12 μmol scale (0.2 M).

In this case, we have observed good reaction efficiency using up to 5 equiv. of water and two or more equivalents of base which means higher amount of lutidinium bromide formation (Fig. S40). The evaluation of the solvents provides similar information. The high reactivity is maintained when two or more equivalents of base are used independently of the used solvent mixture (Fig. S41), but this increase in the base loading may trigger higher accumulation of salts, and a subsequent reactor-coil clogging in the flow systems. We could identify a promising result in which using DMA as co-solvent and only 1 equiv. of lutidine the reaction works in a moderate yield in a less heterogeneous solution. Then, we have evaluated the effect of the water in different DME:DMA mixtures. As shown Figure S42, the reaction take place in good yields when DME is using at higher percentage (70 – 80%), the increase of DMA in the reaction either in the presence or absence of water leads to a drop-in reactivity and these factors are not helping with the solubility issues.

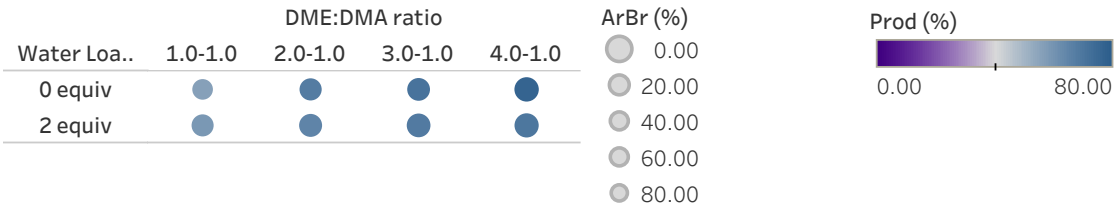

Fig. S42. sp^2–sp^3-Cross-electrophile coupling high-throughtput screening. Solvents ratio vs water loading. Reaction takes place using 1 equiv of aryl bromide, 1.5 equiv of alkyl bromide, 1.5 equiv of TTMS–H, 2 equiv of lutidine, 1 mol% PCat and 1 mol% of Ni-complex for 30 minutes. Reactions were carried out at 12 μmol scale (0.2 M)

After this, more variables were evaluating using DME:DMA mixtures (4:1 to 2:1) such as nickel source, and its loading, photocatalyst and its loadings with different amounts of bases and in the presence or absence of water (0 – 2 equiv). Although good reaction conditions were achieved in terms of reactivity, and the salt formation was diminished, when those conditions were transferred to a flow system, we obtained successful results for small scales. An increment of the scale results in a higher salt accumulation which may clog the reactor-coil (see next section).

We decided back our attention using once again the regular reactive volume (60 μL experimental volume in plates which correspond to 1.3 mm i.d. tubing), focusing on getting more homogeneous conditions even if we may have to sacrifice some reactivity.

To confirm the previous conditions, we could see the product formation is more dependent of the base loading than the photocatalyst or nickel loading in DME (Figure S43) but the reaction mixture after 30 minutes of reaction is completely heterogeneous.

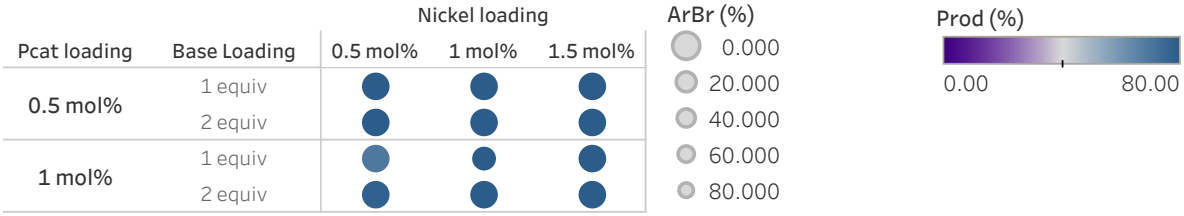

Fig. S43. sp^2–sp^3-Cross-electrophile coupling high-throughtput screening. Base vs PCat and Ni-complex loadings. Reactions were carried out at 12 μmol scale (0.2 M)

According to the Figure S30, the use of DMA as solvent provide a completely homogeneous solution but with moderate yield, so we have envisioned explore some variables in the reaction using the mentioned solvent to reach better yield. First, we evaluated the best bases for this reaction: collidine and lutidine as homogeneous organic bases, and a suspension of Na_2CO_3 in DMA (generated by sonication for almost two days). We have observed good reactivities when we used collidine or lutidine as bases which present better and more reproducible results with higher nickel-complex loadings (Figure S44). Although the use of collidine present higher yields, the corresponding pyridinium salt is more insoluble than the lutidinium salt even in DMA, so these conditions were not considered to further optimization.

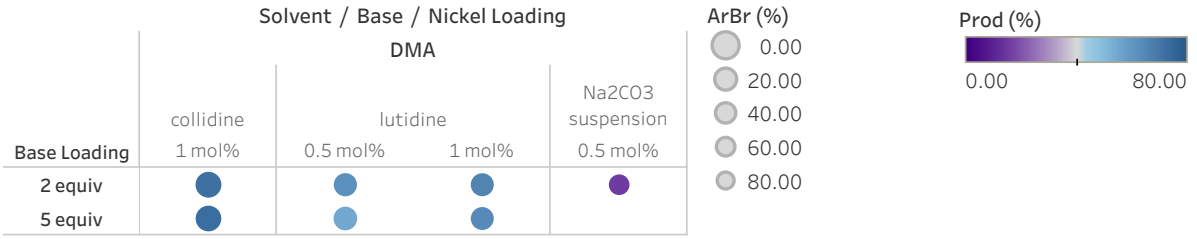

Fig. S44. sp^2–sp^3-Cross-electrophile coupling high-throughtput screening. Base and Ni-complex loadings vs bases. Reactions were carried out at 12 μmol scale (0.2 M)

Next, we evaluated different photocatalyst and nickel complexes in the reaction. The reaction took place in moderate yields when an iridium photocatalyst is used (Figure S45). When the reaction occurs in the presence of organic photocatalyst such as 4CzIPN the reactivity drops substantially. We also observed the reactivity is not dependent of the nickel source obtaining similar yields for $NiCl_2$ ($NiCl_2{\cdot}6H_2O$, $NiCl_2{\cdot}$dme) or $NiBr_2$ sources. The only parameter which affect the reactivity in the reaction apart from the base was the used ligand in the complexation of the nickel-complex but even in these screened cases the yield was not improved.

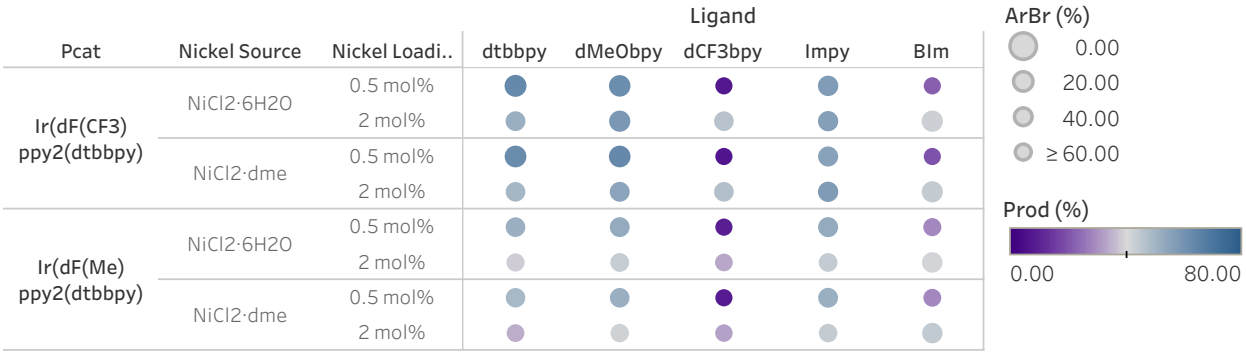

Fig. S45. sp^2–sp^3-Cross-electrophile coupling high-throughtput screening. Photocatalyst vs Nickel salt and ligand. Reactions were carried out at 12 μmol scale (0.2 M)

Finally, we have decided to explore the reaction time. Ideally, shorter times are preferred because decreasing the residence time allow us to synthesize higher amounts of material. Also, lower energy is required working with shorter reaction time *(the use of longer flow rates, up to one hour of residence time is also acceptable)*. Based on this we would explore the course of the reaction expecting an increase in yields when the time is also increased. We detected this trend in the Figure S46, observing higher yields by increasing the reaction time.

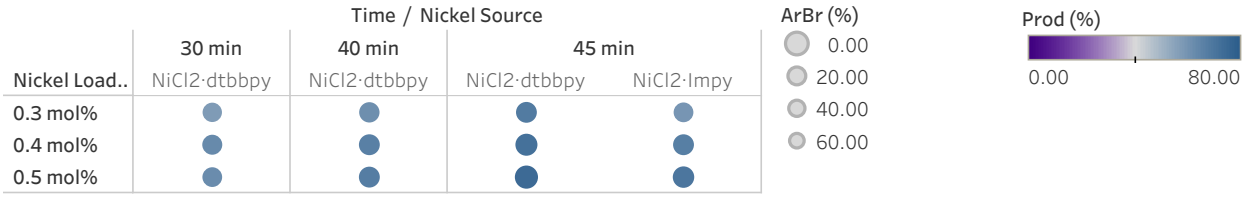

Fig. S46. sp^2–sp^3-Cross-electrophile coupling high-throughtput screening. Reaction time vs Ni-complex. Reactions were carried out at 12 μmol scale (0.2 M)

Although the reaction yield has been improved (up to 66% yield), we still observed some remaining aryl bromide (15-20%). This fact could be due to a slow oxidative addition of the aryl bromide to the nickel complex, so by increasing the amount of nickel we might accelerate this step and could achieve a full reaction and higher yields (Figure S47). Fortunately, we observed good results in all cases highlighted the best reproducibility when using 1 mol% Ni-complex.

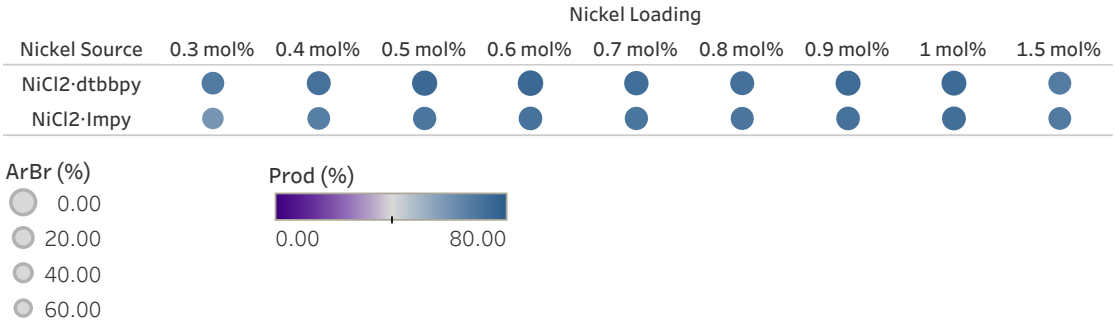

Fig. S47. sp^2–sp^3-Cross-electrophile coupling high-throughtput screening. Ni-complex vs Ni-complex loading. Reactions were carried out at 12 μmol scale (0.2 M)

Note: The use of dry DMA provides higher yields, so in these cases the control of the moisture and air in the system is crucial.

6.3. Reaction using continuous flow system and scale-up.

6.3.1. Continuous flow system results vs. HTE FLOSIM device results.

The reaction was carried out using the one of the best initial conditions described in Figure S43. First, using methyl 4-bromo benzoate (172.0 mg, 0.8 mmol, 1.0 equiv), 4-bromotetrahydropyran (134.7 μL, 1.2 mmol, 1.5 equiv), 1,3,5-trimethoxybenzene (134.5 mg, 0.8 mmol, 1.0 equiv), tris(trimethylsilyl)silane (370.2 μL, 1.2 mmol, 1.6 equiv), [Ir(dF(CF_3ppy)$_2$dtbbpy]PF_6 (8.97 mg, 8 μmol, 1 mol%), a pre-formed solution (by sonication as explain the previous section) in DME of $NiCl_2 \cdot 6H_2O$ (1.90 mg, 8 μmol, 1 mol%) with 4,4´-ditertbutyl-pyridine (2.58 mg, 9.6 μmol, 1.2 mol%) in DME (0.2 M). Finally, the solution was mixed and degassed with nitrogen for 10 minutes and the reaction vessel was covered with aluminum foil. The reaction mixture was injected in a UV-150 Vapourtec E-Series, equipped with a 2 mL-reactor coil and the 420 nm LED light. The reaction was carried out at 36 degrees for 30 minutes of residence time (66 μL/min of flow rate) obtained the desired product in high yields. As shown the Figure S48 we observed very similar results for both setups (entries 1 and 2). Unfortunately, using these conditions on a big scale which requires longer reaction times, we observed the clogging of the reactor-coil due to salt accumulation. As an example of this, we can appreciate the amount of salts generated over the course of the reaction (Figure S49, vials on the left represent the collected fraction in the steady state and vials on the right are collected during the cleaning up process). In general higher flow rates help with the movement inside of the flow system, so we tested the reaction in shorter reaction times, and even in these cases (0.133 mL/ min using the 2 mL-reactor coil or 0.666 mL/min for 10 mL-reactor coil), the formed salts reach to clog the system before the reaction could ends.

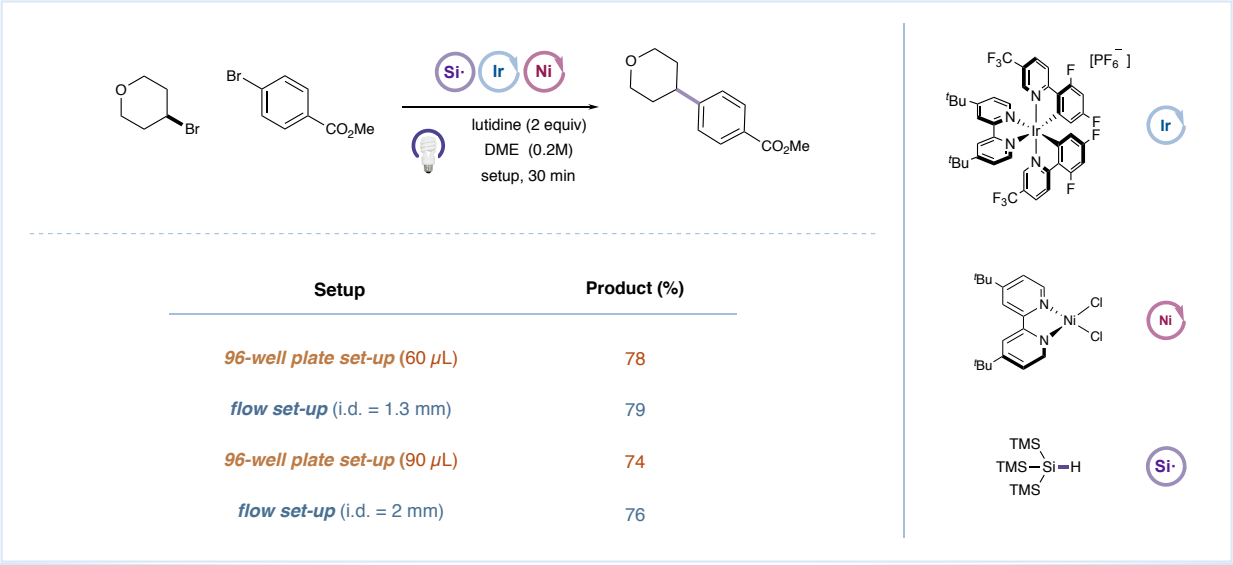

Setup	Product (%)
96-well plate set-up (60 μL)	78
flow set-up (i.d. = 1.3 mm)	79
96-well plate set-up (90 μL)	74
flow set-up (i.d. = 2 mm)	76

Fig. S48. Setup comparison using good conditions in the cross-electrophile coupling. Reaction takes place using 1 equiv of aryl bromide, 1.5 equiv of alkyl bromide, 1.5 equiv supersilane, 1 mol% photocatalyst, 1 mol% $NiCl_2$·dtbbpy for 30 minutes at 36 °C. Reactions were carried out at 12 or 18 μmol scale in plates (each data is an average of six points) for plates and 0.6 or 3 mmol scale for flow system (each data is an average of two reactions).

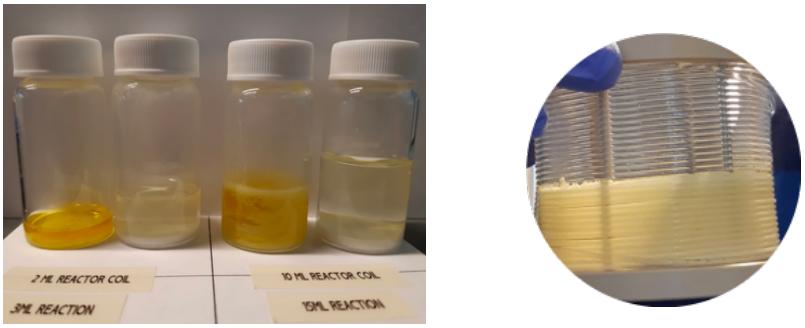

Fig. S49. Left: Collection fractions from the reactions and washed process for both sizes of reactor coils using concentrated solutions (0.3 M) and higher flow rate which correspond to a shorter residence time (15 minutes). Right: clogged 10-mL reactor-coil after reaction with a considerable acummulated salts.

As we have mentioned in the previous section, due to these salt formations and with the support of Vapourtec we have tested different reactor coils with different characteristics to solve the clogging issues. In this process, we were able to try different tubing bores changing both the internal and the external diameter of the tubing (from 1.6 mm to 3 mm), the position of the tubing in the reactor holder, helping the solution flowing through the system using the gravity as an

additional factor, or modifications in the software system. As expected, the use of these modifications helps, but the problem is not completely solved. Using a 13-mL reactor coil with a 2.0 mm of inner diameter with the output tubing on the bottom of the reactor and using an oscillation function, which makes the reaction mixture move distributing the salts more evenly and preventing clumping, we were able to obtain the desired product in a 76% of yield (31 mL injected volume, 6.2 mmol) with no clogging in the reactor, and we were happy to probe the result match with the value in plates using the corresponding reaction volume (Figure S48, entries 3 and 4). Despite this promising result, when the reaction was performed on a larger scale (12 mmol) the reactor clogged before all volume was injected stopping the reaction (Figure S50B). High amounts of salts were detected in the reactor (inside of the reactor clogging the system and the tubing ends, 1st and 3rd pictures on part B), in the collection fraction, and during the washed process (2nd and 4th pictures).

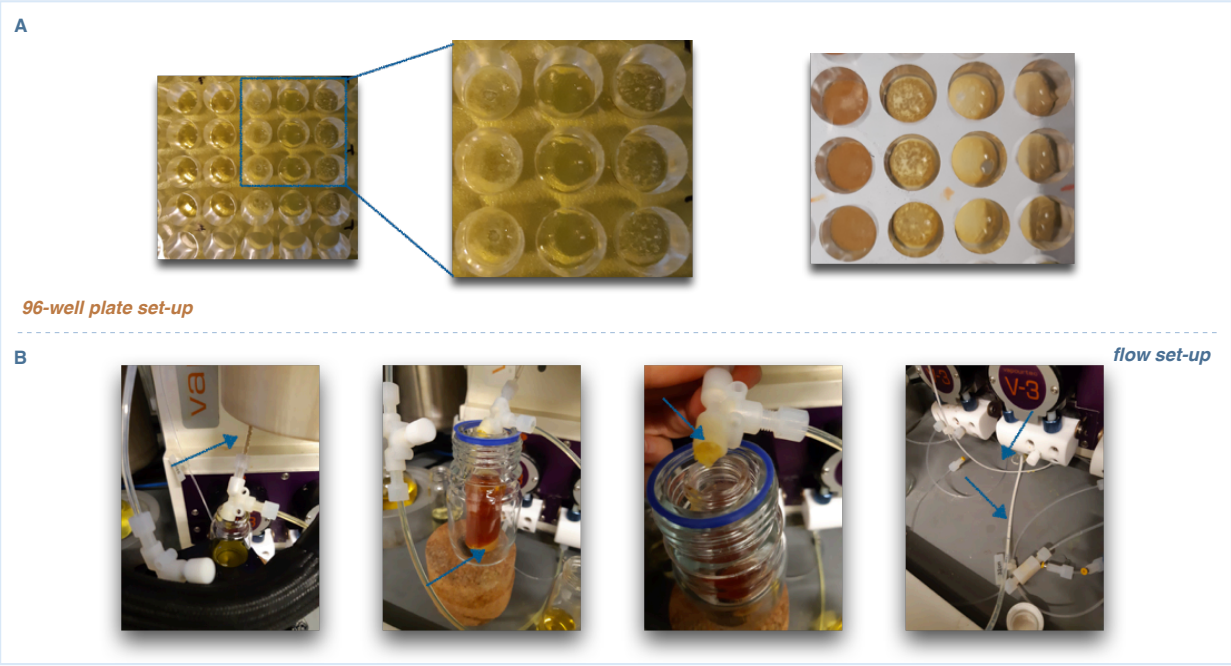

Fig. S50. A. 96-well plate after with different reaction mixture after the light exposure. B. Flow system during and after the reaction.

The use of the 96-well plate as a simulated platform for flow systems is not only valuable in terms of yield. As shown Figure S50A when the reaction is complete, we are able to see the morphology or status of the reaction mixture. In the Figure S50A (picture on the left and its

zooming, middle picture) we are able to differentiate diverse amounts of salts formation. We also saw this behavior on the right picture, where the first column presents a very high amount of salts, lower in the second one and almost no appreciable salt formation in the third and fourth one. This may offer an idea of how the reaction behavior will be in flow systems. The higher the amount of salts detected in plates, the easier the reactor coil will be clogged.

Next, we compared diverse-outcome conditions in the HTE platform and in the flow setup to probe the generality of our method. We selected reactions with moderate and poor yields of product formation and we were pleased to find a strong correlation between both setups in all cases ((Figure S51 and S52) and once again we could demonstrate the applicability of our method using different tubing bore sizes and their corresponding calculated volumes in plates.

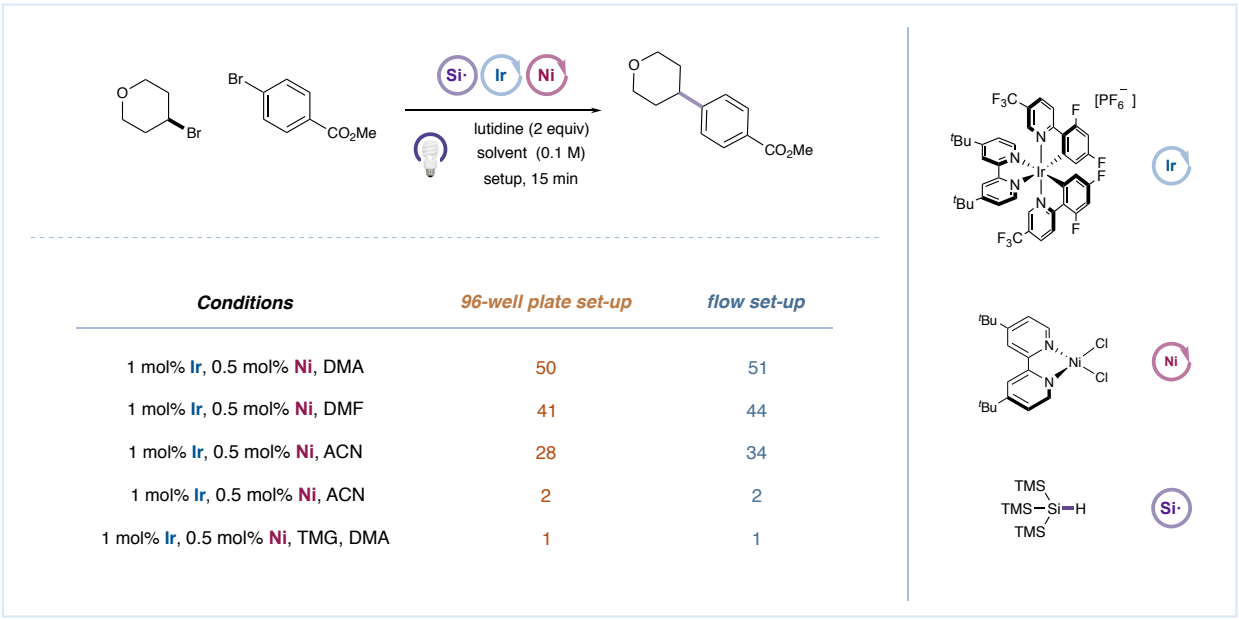

Conditions	96-well plate set-up	flow set-up
1 mol% Ir, 0.5 mol% Ni, DMA	50	51
1 mol% Ir, 0.5 mol% Ni, DMF	41	44
1 mol% Ir, 0.5 mol% Ni, ACN	28	34
1 mol% Ir, 0.5 mol% Ni, ACN	2	2
1 mol% Ir, 0.5 mol% Ni, TMG, DMA	1	1

Fig. S51. Setup comparison for moderates and poor results in the cross-electrophile coupling. Reaction takes place using 1 equiv of aryl bromide, 1.5 equiv of alkyl bromide, 1.0 equiv supersilane for 15 minutes at 33 °C. Reactions were carried out at 6 μmol scale in plates (each data is an average of six points, 60 μL total volume) for plates and 0.3 mmol scale for flow system (each data is an average of two reactions, 2 mL-reactor-coil, 1.3 mm of i.d.).

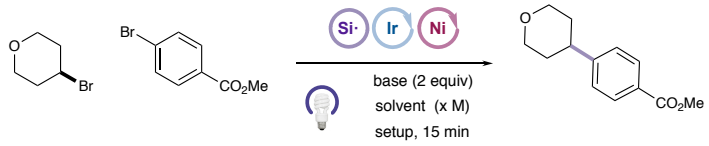

Conditions	96-well plate set-up	flow set-up
no base, DME (0.1 M)	4	2
NMM, DMF (0.1 M)	3	3
lutidine, DMA (0.1 M)	40	36
lutidine, DMF (0.1 M)	32	27
lutidine, DMA (0.2 M)	29	24
NMM, DMF (0.2 M)	12	10
TMG, DMA (0.2 M)	3	6

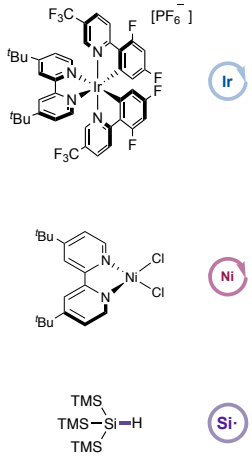

Fig. S52. Setup comparison for moderates and poor results in the cross-electrophile coupling. Reaction takes place using 1 equiv of aryl bromide, 1.5 equiv of alkyl bromide, 1.0 equiv supersilane for 15 minutes at 33 °C. Reactions were carried out at 9 or 18 μmol scale in plates (each data is an average of six points, 90 μL total volume) and 3 or 6 mmol scale for flow system (each data is an average of two reactions, 13 mL-reactor-coil, 2.0 mm of i.d.).

Finally, we found more homogeneous conditions that result in a high reactivity levels, which allowed a larger scaling up. Ahead of continuing with larger scales, we evaluated the reaction time (Figure S53). Similar to the previous cases it was prepared a stock solution of which were taken aliquots for all the experiments (*the stock solution was covered with aluminum foil to avoid any background reaction*). Each time was evaluated in 8 different wells, and the experiments using the flow system were run in duplicate taking account the achieved temperature for each time (Figure S53).

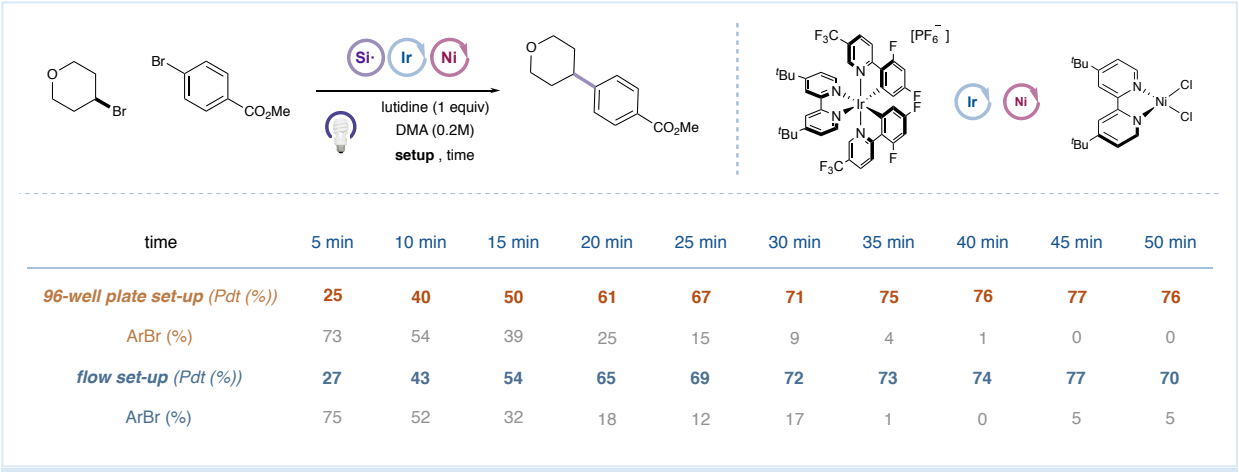

time	5 min	10 min	15 min	20 min	25 min	30 min	35 min	40 min	45 min	50 min
96-well plate set-up *(Pdt (%))*	**25**	**40**	**50**	**61**	**67**	**71**	**75**	**76**	**77**	**76**
ArBr (%)	73	54	39	25	15	9	4	1	0	0
flow set-up *(Pdt (%))*	**27**	**43**	**54**	**65**	**69**	**72**	**73**	**74**	**77**	**70**
ArBr (%)	75	52	32	18	12	17	1	0	5	5

Fig. S53. Reaction time comparison using the optimal conditions. Reactions were carried out at 12 μmol scale (each data is an average of eight points) for plates and 0.8 mmol scale for flow system (each data is an average of two reactions).

6.3.2. Continuous flow reactions.

As previously stated, the use of DMA as solvent, the reduction of the amount of base and the extension of the reaction time in the reaction mixture are important factors to maximize the homogeneity as well as to increase the reactivity.

Even when the lutidinium salt is more soluble in this coordinating solvent, the use of 2 equivalents of base increase the amount of salts, and if the reaction takes place in a large scale, they become more problematic. Reducing the base loading to 1 equivalent does not affect to the reactivity and the solution is completely clear. Figure S54 shows the difference in the collection fractions for two reactions, the first one (left) using two equivalents of base and the second one with only one equivalent.

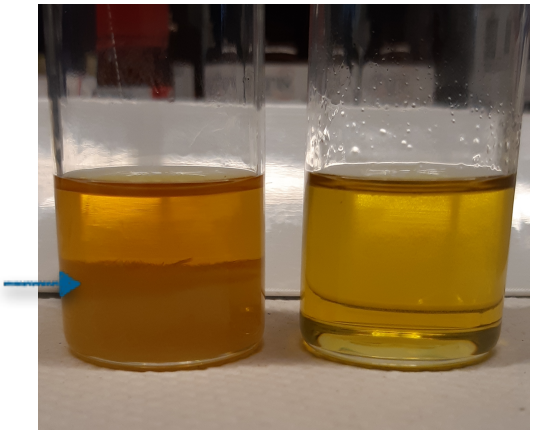

Fig. S54. Collection fractions from two reactions using the optimal conditions: 1 equiv of aryl bromide, 1.5 equiv of alkyl bromide, 1.5 equiv supersilane, 1 mol% photocatalyst, 1 mol% $NiCl_2$·dtbbpy for 45 minutes at 40 ºC. Reactions were carried out 2.4 mmol scale. Left vial: reaction took place using 2 equiv. of lutidine collecting a cloudy solution with some salts on the bottom. Right vial: reaction took place using 1 equiv. of lutidine and the collection fraction present a clear solution with no salts in it.

As we discussed in the section 5.3.1, we were interested in increasing our flow investigation, by applying our strategy to different flow reactors to demonstrate its robustness. We examined a new photoreactor, PhotoSyn, developed by Uniqsis Ltd and was made available in our lab for a brief testing period. The powerful LEDs (700W, 455 nm LEDs) equipped with a 10 mL reactor-coil (i.d. = 1.0 mm). Although more than a third part of the power is lost in form of heat, the real output power is much higher than the ones that Vapourtec provide in its E-Series instrument. This massive power could help with the light penetration pathway though thicker tubing or reducing the reaction times using a regular PFA tubing. We used the PhotoSyn instrument in combination with a water cooler to control the temperature in the reactor and a Rainin pump to inject our solution.

The optimization process for this reaction (section 6.2) was taken place using a 420 nm LEDs, so it was needed to run a control experiment. To do this, a reaction mixture was prepared under the optimal conditions developed in the previous section [1 equiv of aryl bromide, 1.5 equiv of alkyl bromide, 1.5 equiv of supersilane, 1 equiv of lutidine, 1 mol% photocatalyst, 1 mol% $NiCl_2$·dtbbpy in DMA (0.2 M)]. The reaction was carried out at 40 – 42 degrees, and 25% of light intensity for 45 minutes of residence time (222 μL/min of flow rate) obtained the desired product in a 49% yield. Then, to probe right our hypothesis, we decreased the reaction time at the same

time we increased the light intensity maintaining the rest of the conditions. If the relation between the reaction time and the light intensity is essentially lineal, we should obtain the same yield.

Pleasantly, when the reaction was carried out under the same reaction conditions using a faster flow rate (0.91 mL/min, 11 minutes of residence time) and 100% of light intensity the desired product was achieve in a 44% yield (Figure S55).

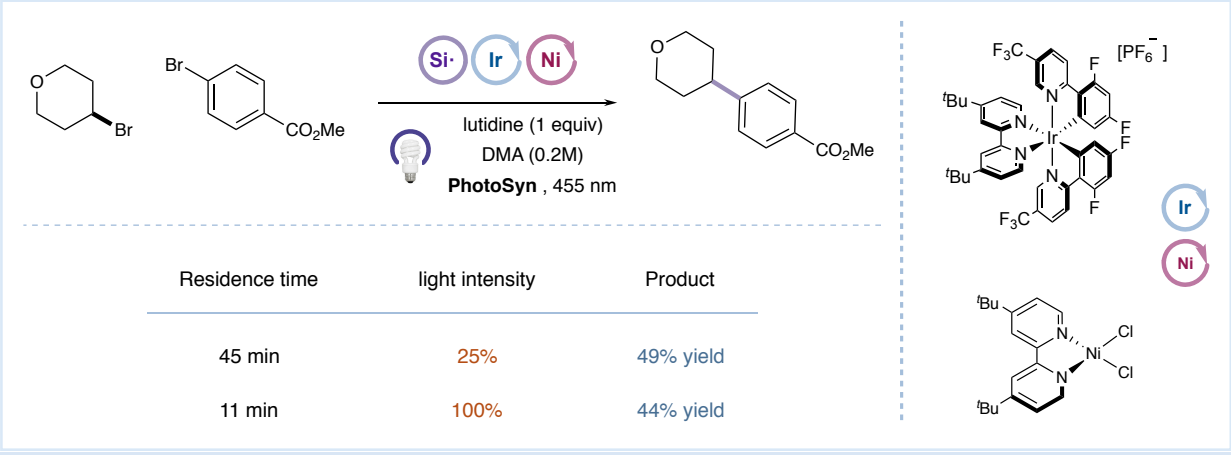

Fig. S55. Collection fractions from two reactions using the optimal conditions: 1 equiv of aryl bromide, 1.5 equiv of alkyl bromide, 1.5 equiv of supersilane, 1 equiv of lutidine, 1 mol% photocatalyst, 1 mol% $NiCl_2$·dtbbpy in DMA (0.2 M) at 40 °C. Reactions were carried out 3 mmol scale.

6.3.3. Scale up using the continuous flow system.

An oven-dried 250 mL RBF or volumetric flask equipped with a Teflon septum and magnetic stir bar was charged with methyl 4-bromo benzoate (13.2 g, 60 mmol, 1.0 equiv), 4-bromotetrahydropyran (10.4 mL, 90 mmol, 1.5 equiv), 1,3,5-trimethoxybenzene (10.1 g, 60 mmol, 1.0 equiv), tris(trimethylsilyl)silane (27.8 mL, 90 mmol, 1.5 equiv), 2,6-lutidine (6.99 mL, 60 mmol, 1 equiv), $[Ir(dF(CF_3ppy)_2dtbbpy]PF_6$ (673.2 mg, 0.6 mmol, 0.01 equiv) and DMA (250 mL, 0.2 M). To a separate vial was added $NiCl_2·6H_2O$ (171.1 mg, 0.72 mmol), 4,4´-ditertbutyl-pyridine (193.2 mg, 0.72 mmol). The catalyst vial was sealed, purged with nitrogen then to it was added 5.8 mL of DMA. The precatalyst solution was sonicated for 10 minutes, after which, 4.83 mL (0.6 mmol, 1 mol%) was syringed into the reaction vessel. The solution was degassed by sparging with nitrogen for 15 minutes before sealing with parafilm and covered the vessel with aluminum foil.

The Vapourtec system equipped with a 10 mL-reactor coil and 420 nm LED lights was purged, under nitrogen atmosphere, with the degassed DMA and then, the reaction mixture was injected into the system under nitrogen atmosphere. The reaction was run at 40 – 42 degrees in the heated mode with a 45 minutes of residence time (222 μL/min of flow rate) for 23 hours in total. The collection fraction was analyzed by ^{1}H-NMR and UPLC-MS (79 % yield). Then, the collection mixture was diluted with dichloromethane (150 mL) and was washed with an aqueous solution of $NaHCO_3$ (3 x 50 mL), an aqueous solution of LiCl (2% w/v) (2 x 50 mL), water (2 x 100 mL). The aqueous layers were extracted with dichloromethane (3 x 50 mL). The organic extracts were combined, washed with brine, dried over Na_2SO_4 and concentrated in vacuo. The residue was purified by flash column chromatography (hexane : ethyl acetate 4:1 to 0:1) to afford 10.25 g of the desired coupled product (colorless solid, 78% isolated yield). The spectroscopic properties of this compound are consistent with data reported in the literature.[9]

^{1}H NMR (500 MHz, $CDCl_3$): δ 7.99 (d, *J* = 8.3 Hz, 2H), 7.31 (d, *J* = 8.3 Hz, 2H), 4.19 – 4.02 (m, 2H), 3.91 (s, 3H), 3.54 (td, *J* = 11.3, 3.2 Hz, 2H), 2.82 (tt, *J* = 10.7, 5.6 Hz, 1H), 2.04 – 1.47 (m, 4H).

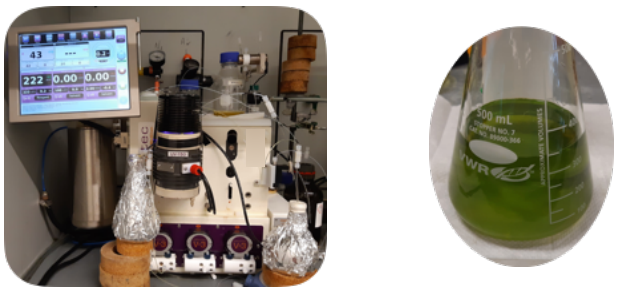

Fig. S56. Reaction setup and collected fraction for the scale up.

7. C–O coupling.

7.1. Light optimization in batch.

To an oven-dried 8 mL vial equipped with a Teflon septum and magnetic stir bar were added 4-bromoacetophenone (49.8 mg, 0.25 mmol, 1.0 equiv), 1,2:3,4-di-O-isopropylidene-D-galactopyranose (97.5 mg, 0.37 mmol, 1.5 equiv), quinuclidine (2.8 mg, 0.02 mmol, 0.1 equiv), 1,3,5-trimethoxybenzene (42.15 mg, 0.25 mmol, 1.0 equiv), potassium carbonate (34.5 mg, 0.25 mmol, 1 equiv), [Ir(dF(CF$_3$ppy)$_2$dtbbpy]PF$_6$ (2.8 mg, 2·10^{-3} mmol, 1 mol%), NiCl$_2$·dme (2.8 mg, 0.01 mmol, 5 mol%), 4,4′-ditertbutyl-pyridine (3.4 mg, 0.01 mmol, 5 mol%) and dry acetonitrile (1 mL). The solution was degassed by sparging with nitrogen for 15 minutes before sealing with Parafilm. The reaction was stirred and irradiated using the 40 W PR160 Kessil LED (3 cm away without cooling fan to heat the reaction to approximately 35–45 °C) for 24 hours. The reaction was cooled at room temperature and analyzed by UPLC or ^{1}H NMR vs. internal standard (Figure S57) identifying 456 nm LEDs as the best wavelength for this transformation.

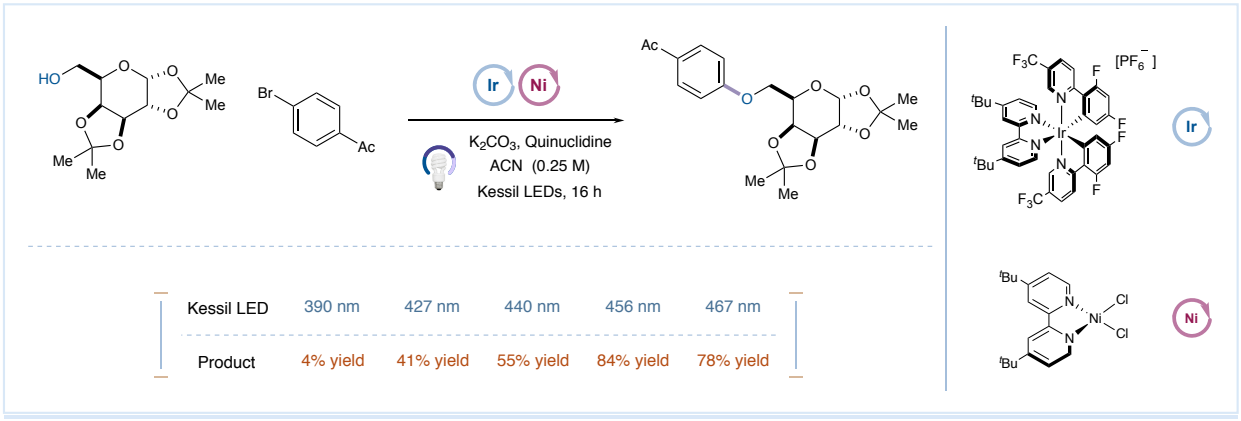

Fig. S57. Evaluation of the light source. Each data is an average of two reactions.

7.2. High-throughput experimentation screening.

To carry out these experiments we follow the same methodology explain in detail in the previous sections preparing concentrated stock solutions with all the reactants except the ones we are testing as a variable. Depending on the variables to screen, it was prepared a stock solution with

some reactants or multiple stock solutions with one reactant in the appropriate concentration to afford the desired screen conditions.

Our original publication uses blue LED strips or CFL bulb for this transformation. The reason behind this choice is that more energetic lights (e. g. Kessil LEDs) generate the formation of undesirable side-products such as alcohol-polymerization reaction compounds. Due to this cause, during the optimization process were also tested different light intensities (25%, 50%, 75% and 100%). Although in most of the cases a lower intensity is enough to achieve good results we decided to use and include only the full intensity results because the correlation with the flow system will be easier (*at the beginning of these screening we had a regular Vapourtec E-Series which is not able to control the light intensity. Only at the end and as a trial we could use a new power supply from Vapourtec as well as the PhotoSyn reactor which enables the control of the light intensity*). Furthermore, we thought the use of an active system in a short reaction time could help with the exclusive formation of the desired product and avoid these side products.

<u>*Base and solvent screening*</u>. *Preparation of stock solution.* To an oven-dried 8 mL vial equipped with a stir bar was added 4-bromoacetophenone (298.9 mg, 1.5 mmol, 1.0 equiv), 1,2:3,4-di-O-isopropylidene-D-galactopyranose (585.6 mg, 2.25 mmol, 1.5 equiv), 1,3,5-trimethoxybenzene (252.3 mg, 1.5 mmol, 1.0 equiv), quinuclidine (16.7 mg, 0.15 mmol, 10 mol%), $[Ir(dF(CF_3ppy)_2dtbbpy]PF_6$ (16.8 mg, 15 μmol, 1 mol%), $NiCl_2$·dme (16.5 mg, 0.08 mmol, 5 mol%), 4,4′-ditertbutyl-pyridine (20.1 mg, 0.08 mmol, 5 mol%) and the evaluated dry solvent (0.5 M). The solution was degassed by sparging with nitrogen for 15 minutes before sealing with parafilm. All bases and solvents are degassed by sparging with nitrogen for 15 minutes and sealed with parafilm.

Preparation of the 96-well plate. Experiments were set up inside a glovebox under a nitrogen atmosphere. To a vacuum-dried glass 96-well plate were added the corresponding bases (15 μmol), solvent (until reach a final volume of 60 μL taking account the volume of base rest of the components in the reaction, in this case the different bases) and then 30 μL of the stock solution [which correspond to added 4-bromoacetophenone (15 μmol, 1.0 equiv), 1,2:3,4-di-O-isopropylidene-D-galactopyranose (22.5 μmol, 1.5 equiv), 1,3,5-trimethoxybenzene (15 μmol, 1.0 equiv), quinuclidine (1.5 μmol, 10 mol%), $[Ir(dF(CF_3ppy)_2dtbbpy]PF_6$ (0.15 μmol, 1 mol%), $NiCl_2$·dme (0.75 mmol, 5 mol%), 4,4′-ditertbutyl-pyridine (0.75 mmol, 5 mol%) and the

corresponding dry solvent (30 μL, 0.5 M) to achieve a final concentration of 0.25 M]. The 96-well plate was sealed, placed in the HTE FLOSIM device and irradiated with 40W 456 nm Kessil LEDS for 30 minutes. Upon cooling the reaction at room temperature, the plate is opened to the air and 100 μL of acetonitrile was added. An aliquot of this diluted reaction mixtures (20 μL) was transferred into a separate Nunc 96-well plate followed by 950 μL of acetonitrile. Then the LC block was mounted on an automated UPLC instrument for analysis.

We started the evaluation of this reaction using some soluble organic bases in combination with different organic solvents providing initially homogeneous reaction conditions. In the original conditions acetonitrile was described as the best solvent followed by acetone or ethyl acetate.[4] However, for our system are preferred more coordinating solvents such as DMF or DMA. The use of acetonitrile also provides good reactivities in this case. As shown in Figure S58 the use of quinuclidine or TMG as base offer a more general reactivity pattern. The use of more expensive and strong bases such as BTMG or BEMP provides also the desired product in moderates yields. Although DMA gave moderates results (similar or lower yields than DMF) we chose to continue the screening only with acetonitrile and DMF as solvents due to these solvents present more reproducible results.

After some inconsistent results thought the optimization screening, we found there are some critical parameters to obtain reproducible and/or good results. The first one is the presence of water on the reaction mixture, although the water is tolerated the yields can be affected and for this reason is important the use of dry conditions. The pre-formation of the nickel complex by sonication for 5 – 10 minutes in a separate vial, is also beneficial. The sugar alcohol is a very dense oil, so to facilitate the addition of this reagent with high levels of reproducibility, a 2M stock solution of this alcohol was prepared and added to the reaction solution (with no variation on the final concentration). Finally, quinuclidine, a very moisture sensitive reagent which it has to be use it as a sacrificial reductant and under some conditions is used also as base, must to be dried and very pure. To do this, quinuclidine needs to be keep bottle on a glovebox and only take small amounts of quinuclidine just before used it. After this, the quinuclidine is recrystallized in diethyl ether, the white power solid is dried and used immediately. The remaining quinuclidine can be keep in a desiccator and use it in the next couple of days, after that it is necessary repeat the recrystallization process.

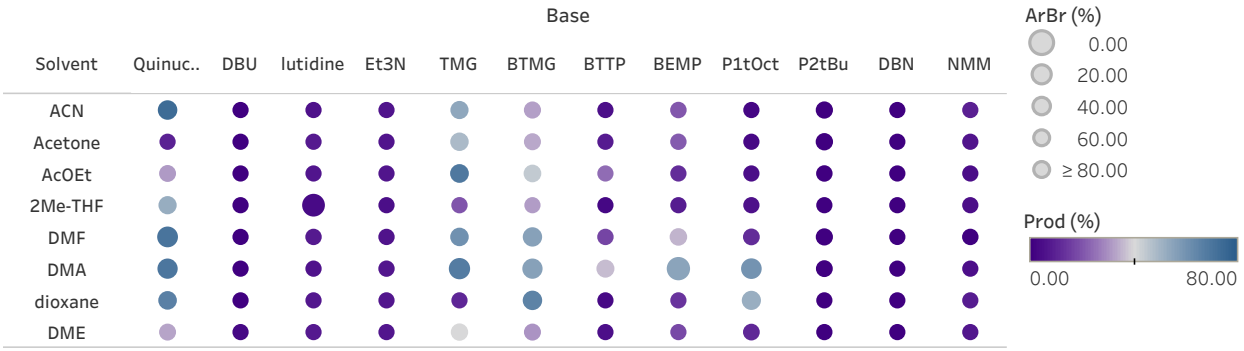

Fig. S58. C–O coupling high-throughtput screening. Bases vs solvents. Reactions were carried out at 15 μmol scale (0.25 M).

Next, we would like to assess the effect of the photocatalyst in this reaction (Figure S59 and S60) using both inorganic and organic photocatalyst. This reaction shows a more general reactivity using quinuclidine as base. Furthermore, in those cases we obtain good yields using either iridium photocatalyst, 4CzIPN or 4CzPN. However, the reaction yields drop when we used the TPN derivates due to low solubility in these solvents. The reaction was also tested with different photocatalyst loading (Figure S60). Here we can differentiate two different trends, using quinuclidine as base, a higher amount of photocatalyst is preferred (1 or 2 mol%) showing with the lower loadings a lower reactivity. Also, in the cases we used quinuclidine we detected salt formations which can affect in the reaction profile. On the other hand, we may reduce the photocatalyst loading when TMG is acting as base. The reaction takes place in good yields from for almost every case using iridium photocatalyst as well as 4CzIPN.

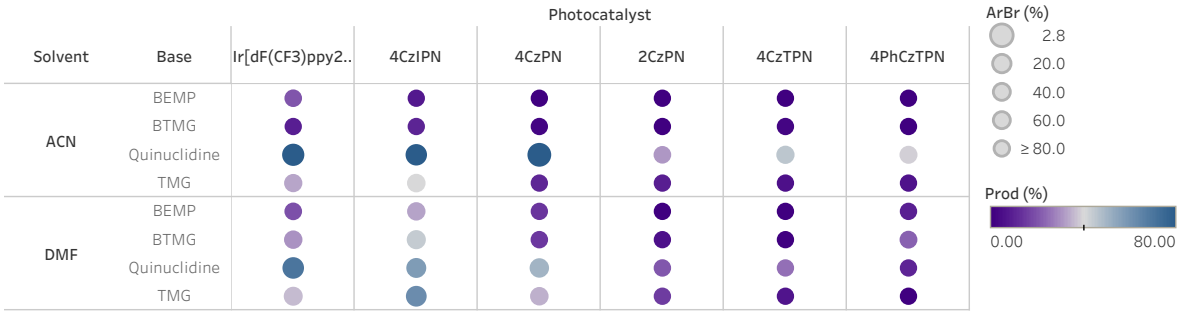

Fig. S59. C–O coupling high-throughtput screening. Bases vs solvents and photocatalyst. Reactions were carried out at 15 μmol scale (0.25 M).

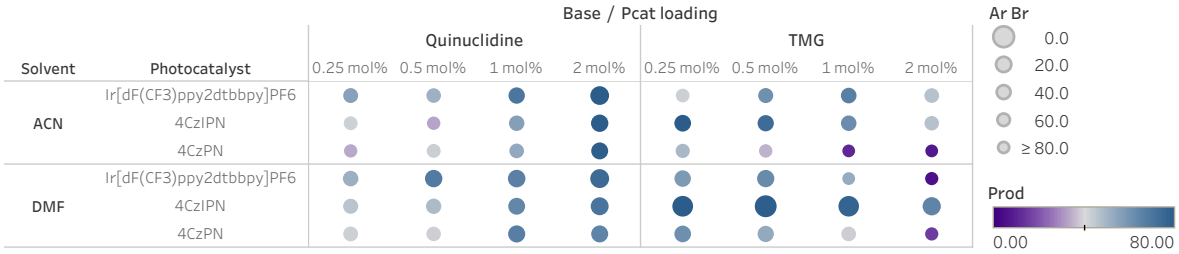

Fig. S60. C–O coupling high-throughtput screening. Solvents vs photocatalyst and photocatalyst loading. Reactions were carried out at 15 μmol scale (0.25 M).

To be sure that the reaction in acetonitrile requires higher amounts of photocatalyst or another parameter is influence on the reactivity we evaluate the effect of the base for two different photocatalyst loadings (Figure S61). This screening shows the base loading effect, in which an increasement on the amount of quinuclidine in the reaction helps, recovering again the high yields. This effect can explain based on the purity of the used quinuclidine, due to we are able to obtain similar results using 1 equiv. of freshly recrystallize quinuclidine or increasing the amount of quinuclidine in the reaction media, having in this case a large amount of salts in the reaction mixture which is not desirable. For this reason, an increasement in the TMG loading dos not affect the reactivity in the system.

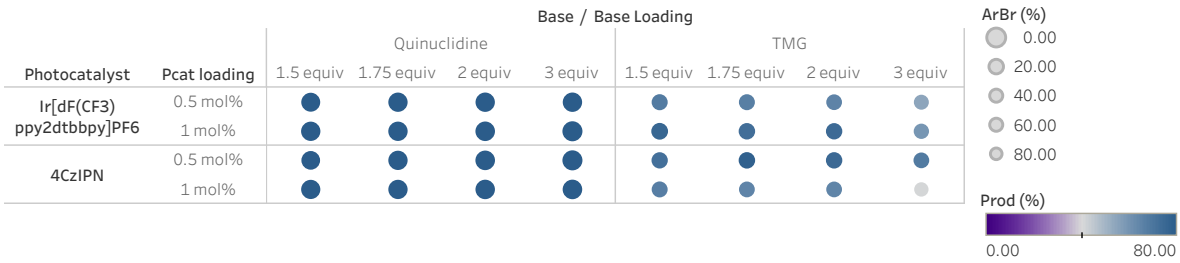

Fig. S61. C–O coupling high-throughtput screening. Base and base loading vs photocatalyst and photocatalyst loading. Reactions were carried out at 15 μmol scale (ACN, 0.25 M).

Once we established that an excess of base is not necessary, we evaluated the influence of the quinuclidine loading as a reductant in the reaction. Although an excess of base is not required, in general a sub-stoichiometric amount of base reduces the efficiency of the reaction. As shown in Figure S62 an increment on reductant loading (from 10 to 20 mol%) helps when the reaction works

in moderates yields to accomplishing better yields and also accelerates the reaction profile, achieving higher conversions.

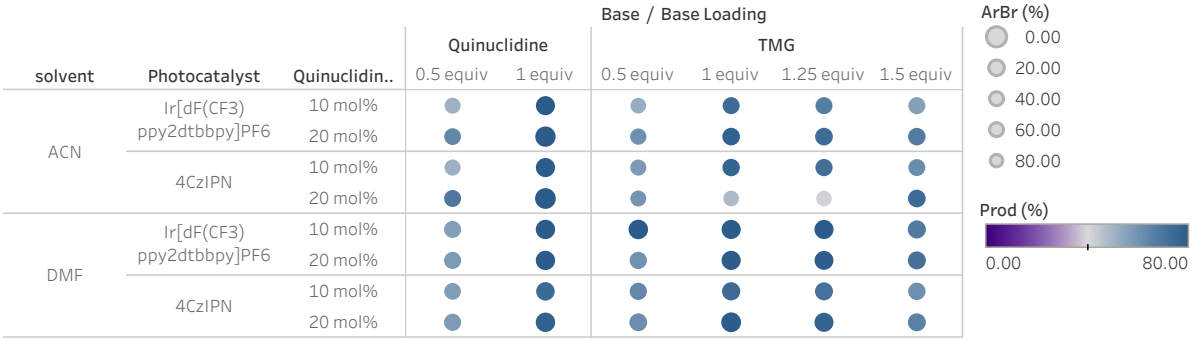

Fig. S62. C–O coupling high-throughtput screening. Base and base loading vs photocatalyst and photocatalyst loading. Reactions were carried out at 15 μmol scale (ACN and DMF, 0.25 M).

To have a general overview of the reaction profile, we tested the previous parameters all together in the same screening (Figure S63). Here, we observed similar reactivities when quinuclidine was used as base. Under these conditions and in combination with different amounts of reductant, photocatalyst and solvents afford better results. However, the reaction in acetonitrile presents a large amount of salts, thereby we decided to continue with DMF as solvent. On the other hand, TMG role as base also provided better reactivities in DMF and the use of 1 equivalent of base and a lower amount of photocatalyst loading afford higher yields.

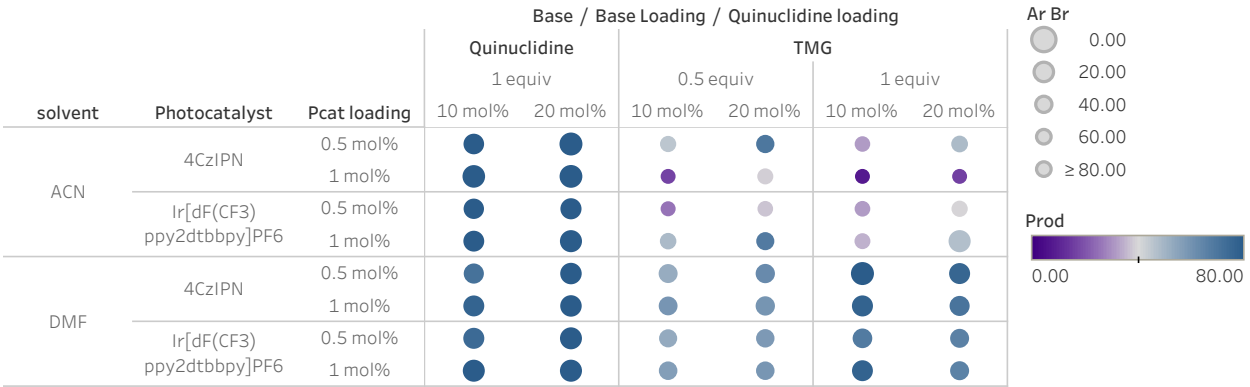

Fig. S63. C–O coupling high-throughtput screening. Reactions were carried out at 15 μmol scale (0.25 M).

Next, we turned our attention on the study of the employed nickel source and its loading for the three better conditions (0.5 mol% photocatalyst, 20 mol% quinuclidine as reductant and 1 equiv. of base). As shown Figure S64 the use of any halogenated nickel source shows great levels of reactivity and the catalyst loading can be reduced with almost no variation in the reaction yields. Due to quinuclidine is a more sensitive and expensive reactant, we decided to continue the optimization with a cheaper organic base such as TMG. Afterward, we examined a higher range of nickel catalyst loading obtaining great results for nickel bromide and chloride salts which being able to reduce the catalyst loading up to 2 mol% (detecting higher conversions between 2 and 5 mol%). The extension of the reaction time helps though its effect in the reactivity is not critical (Figure S65).

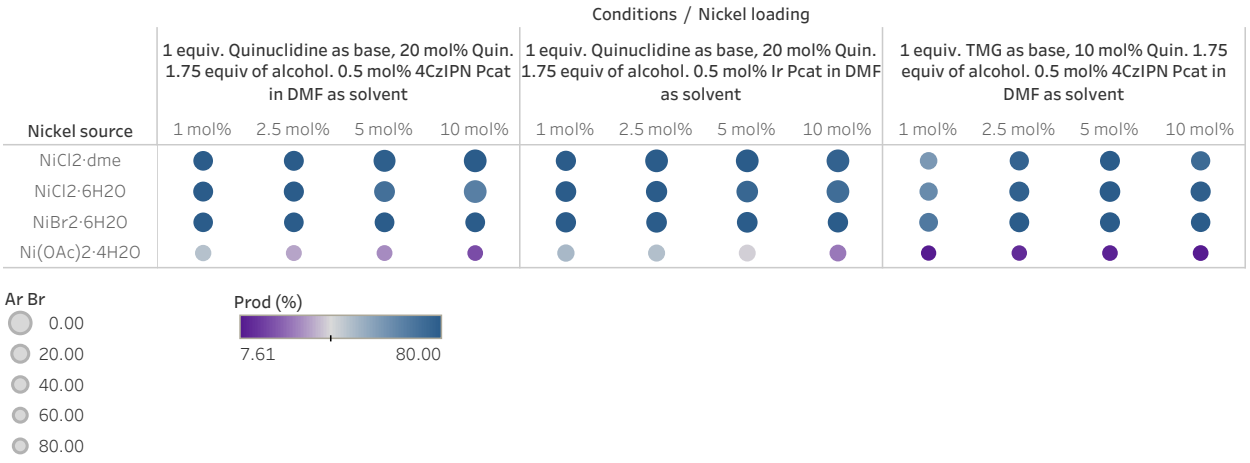

Fig. S64. C–O coupling high-throughtput screening. Nickel vs nickel catalyst loading. Reactions were carried out at 15 μmol scale (0.25 M).

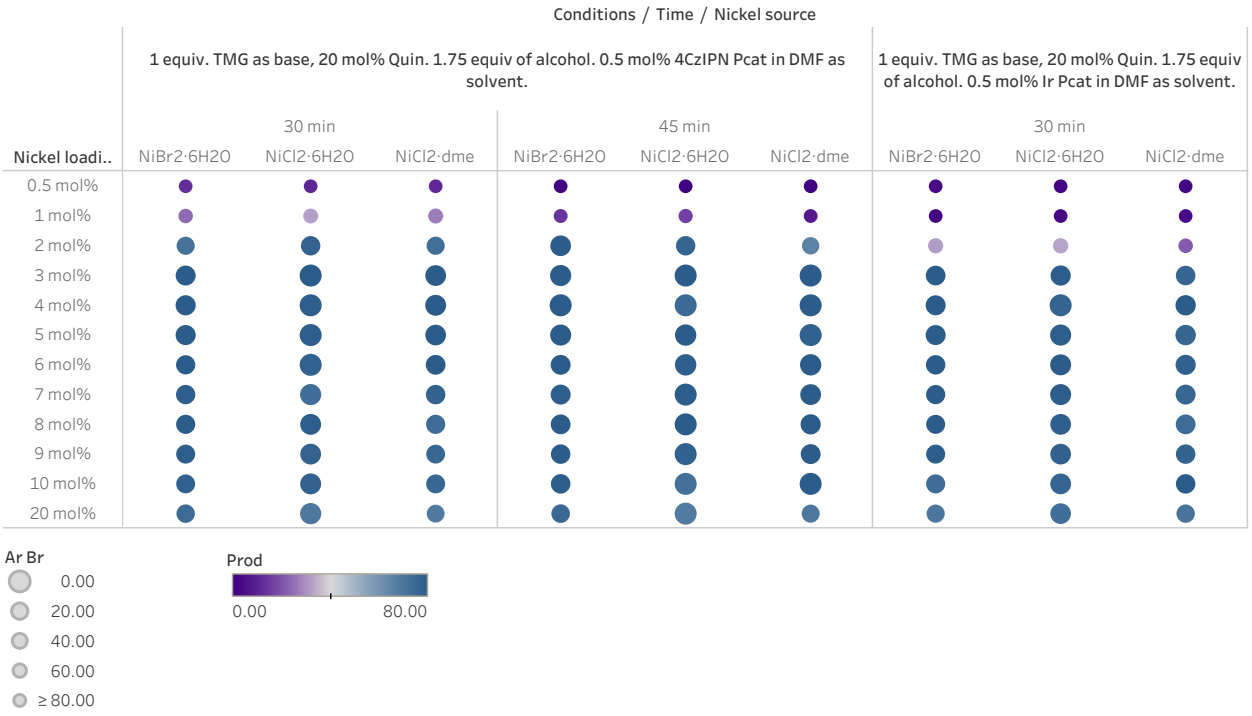

Fig. S65. C–O coupling high-throughtput screening. Nickel vs nickel catalyst loading and time. Reactions were carried out at 15 μmol scale (0.25 M).

A cheap nickel source, $NiCl_2 \cdot 6H_2O$, was selected to finish the optimization process according to its great reactivity. To accomplish this, we analyzed the best relationship between the photocatalyst, and the nickel loading ranges (Figure S66). Here we were able to identify that using 0.25 mol% of 4CzIPN in combination with 3 mol% of $NiCl_2 \cdot$dtbbpy provided the desired compound in an 80% yield with almost complete consumption of aryl bromide.

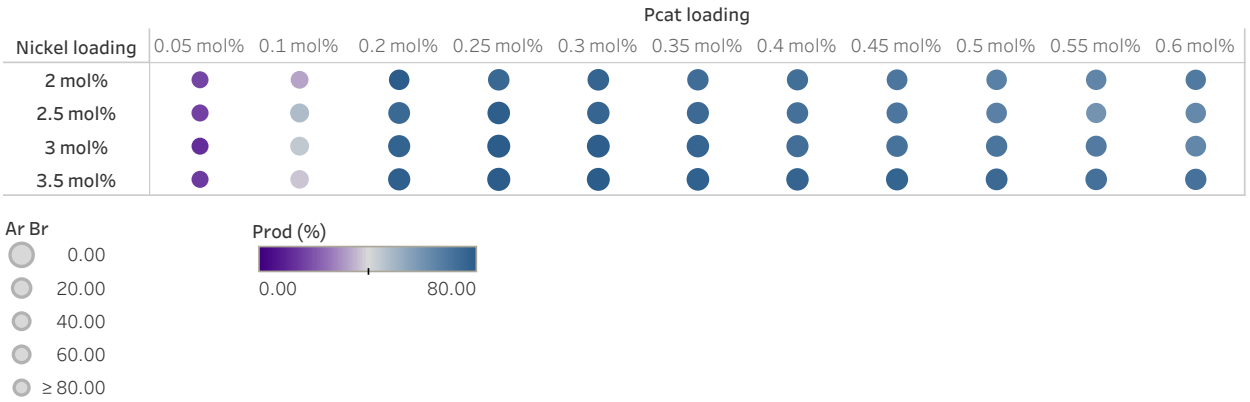

Fig. S66. C–O coupling high-throughtput screening. Photocatalyst loading vs nickel catalyst loading. Reactions were carried out at 15 μmol scale.

Finally, using the optimal reaction conditions we evaluated the ratio between the alcohol and the aryl bromide in the presence of different photocatalyst (Figure S67). Although we observed some amount of product with all of the photocatalysts, as we expected, 4CzIPN exhibited the best behavior using the alcohol reagent in superstoichiometric amounts (1.75 equiv.).

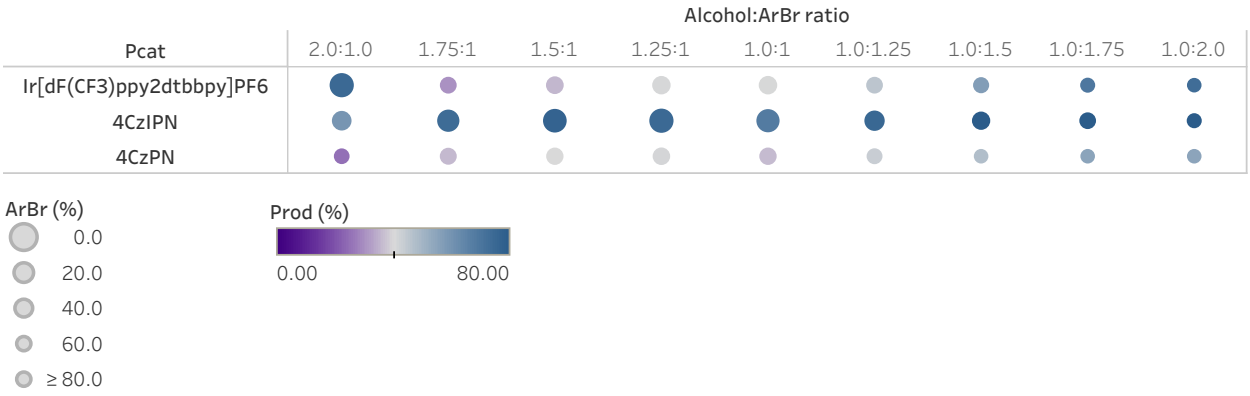

Fig. S67. C–O coupling high-throughtput screening. Photocatalyst vs reagents ratio. Reactions were carried out at 15 μmol scale.

As it was mentioned in Section 6, to expand the use of our methodology by increasing our flow investigation enables this optimization process not only with Vapourtec but also with other flow systems such as PhotoSyn. In this case, PhotoSyn is equipped with 455 nm LEDs which allows the comparison with the HTE FLOSIM device using this specific reaction due to as shown the Figure S46 the best wavelength for this transformation was using 456 nm Kessil LEDs. n section

2.1 we probed a high degree of homogeneity in the 96-wells using four lights instead of two in the FLOSIM device. So, we envisioned use this new light setup to try the linearity of the reaction according to the light intensity. We run the etherification reaction at 50% of light intensity (4 lights, ~ 24 W output power) for 15 minutes achieving an average of 23% yield. When we increased the light intensity up to 100% (4 lights, ~ 48 W output power) the desired product was obtained in a 56% yield (Figure S68). Although this relation is not perfectly linear, we believe it is possible device.

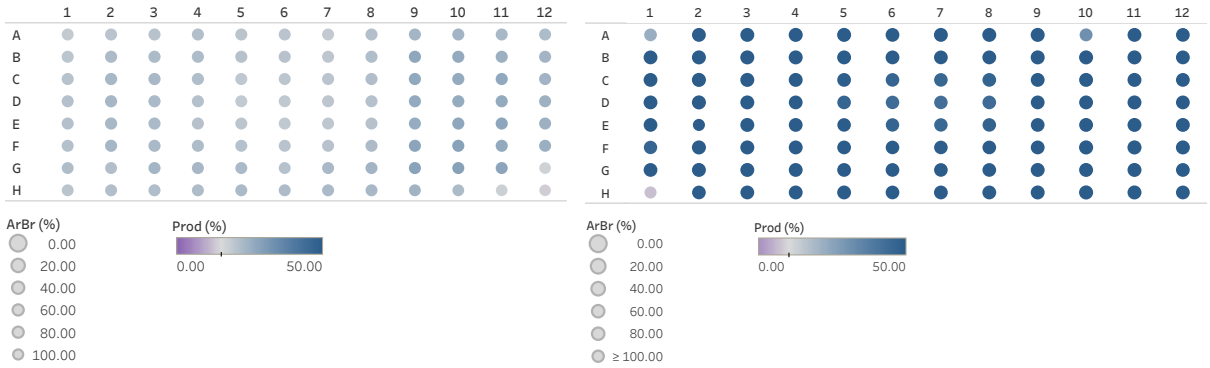

Fig. S68. Light intensity relation using the C–O coupling reaction. Left: reactions take place under optimal conditions using 4 lights with 50% of light intensity. Right: reactions take place under optimal conditions using 4 lights with 100% of light intensity. Reactions were carried out at 15 μmol scale.

According to this hypothesis, by increasing the light intensity we are able to obtain higher yields in the same reaction time. So, it would be possible to achieve the same pattern in the opposite way namely, increasing the light intensity we could reduce proportionally the reaction time maintaining similar levels of reactivity. This behavior was demonstrated using PhotoSyn photoreactor (Figure 5 on the manuscript, next section on this SI).

7.3. Reaction using continuous flow system and scale-up.

7.3.1. Continuous flow system results vs. HTE FLOSIM device results.

To compare the results between both setups, we follow the same procedure as in the previous sections using the conditions that were found during the screening process.

First, using 4-bromoacetophenone (199.3 mg, 1.0 mmol, 1.0 equiv), 1,2:3,4-di-O-isopropylidene-D-galactopyranose (2 M solution in DMF, 875 μL, 1.75 mmol, 1.75 equiv), 1,3,5-trimethoxybenzene (168.2 mg, 1.0 mmol, 1.0 equiv), quinuclidine (11.1 mg, 0.10 mmol, 10 mol%), base (1.0 mmol, 1.0 equiv), photocatalyst (0 – 10 μmol, 0 – 1 mol%), a pre-formed solution (by sonication as explain the previous section in the reaction solvent) of $NiCl_2$·dtbbpy (0.5 – 5 mol%), 4,4′-ditertbutyl-pyridine (20.1 mg, 0.08 mmol, 5 mol%) in the appropriate solvent (0.25 M). Finally, the reaction solution was mixed and degassed with nitrogen for 10 minutes and the reaction vessel was covered with aluminum foil. The reaction mixture was injected in a UV-150 Vapourtec E-Series, equipped with a 2 mL-reactor coil and the 450 nm LED light. The reaction was carried out at 36 degrees for 30 minutes of residence time (66.7 μL/min of flow rate) obtained the desired product in high yields.

As shown the Figure S69 we observed very similar results for both setups. The reaction using the optimal conditions for 30 minutes present high and similar reactivities. In the same way, comparing different conditions from the optimization process (section 7.2) with moderate and poor yields of product formation, we were pleased to find a strong relation between both setups for all cases (Figure S69, entries 2 – 5).

Finally, we carried out a reaction time study to achieve high reactivity levels ahead of continuing with larger scales (Figure S70). Similar to the previous cases it was prepared a stock solution from which were taken aliquots for all the experiments (*the stock solution was covered with aluminum foil to avoid any background reaction*). Each time was evaluated in 8 different wells, and the experiments using the flow system were run in duplicate taking account the achieved temperature for each time (Figure S70).

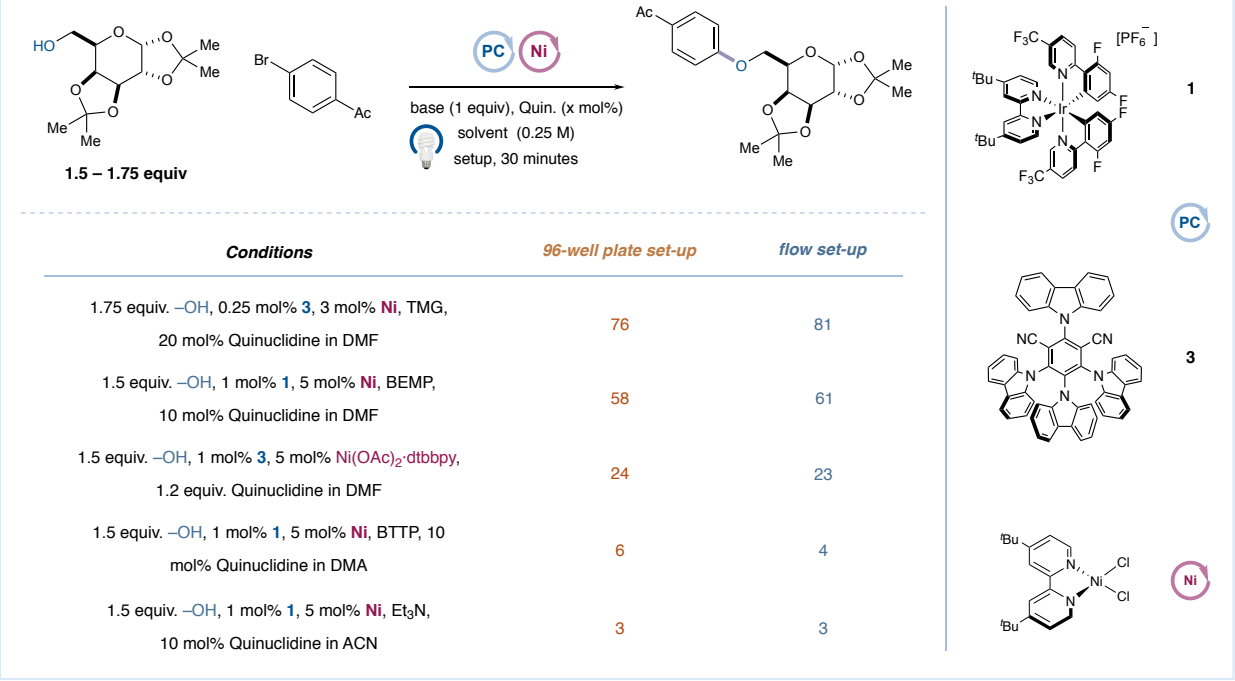

Conditions	96-well plate set-up	flow set-up
1.75 equiv. –OH, 0.25 mol% **3**, 3 mol% **Ni**, TMG, 20 mol% Quinuclidine in DMF	76	81
1.5 equiv. –OH, 1 mol% **1**, 5 mol% **Ni**, BEMP, 10 mol% Quinuclidine in DMF	58	61
1.5 equiv. –OH, 1 mol% **3**, 5 mol% Ni(OAc)$_2$·dtbbpy, 1.2 equiv. Quinuclidine in DMF	24	23
1.5 equiv. –OH, 1 mol% **1**, 5 mol% **Ni**, BTTP, 10 mol% Quinuclidine in DMA	6	4
1.5 equiv. –OH, 1 mol% **1**, 5 mol% **Ni**, Et$_3$N, 10 mol% Quinuclidine in ACN	3	3

Fig. S69. Setup comparison results in the etherification reaction. Reaction takes place at 36 °C for 30 minutes. Reactions were carried out at 15 μmol scale in plates (each data is an average of six points) and 1 mmol scale for flow system (each data is an average of two reactions, 2 mL-reactor-coil).

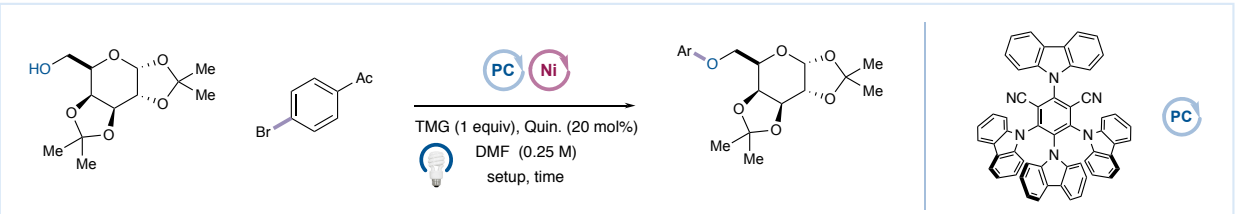

time	5 min	10 min	15 min	20 min	25 min	30 min	35 min	40 min
96-well plate set-up *(Pdt (%))*	**8**	**20**	**35**	**52**	**66**	**76**	**80**	**76**
ArBr (%)	91	77	57	39	23	11	6	3
flow set-up *(Pdt (%))*	**5**	**15**	**30**	**47**	**61**	**81**	**75**	**72**
ArBr (%)	95	83	63	41	25	7	7	3

Fig. S70. Reaction time comparison using the optimal conditions. Reaction takes place using 1 equiv of aryl bromide, 1.75 equiv. of alcohol (2M solution in DMF), 20 mol% of quinuclidine, 1 equiv. TMG, 0.25 mol% 4CzIPN and 3 mol% NiCl$_2$·dtbbpy for 35 minutes at 37 °C. Reactions were carried out at 15 μmol scale (each data is an average of eight points) for plates and 0.87 mmol scale for flow system (each data is an average of two reactions).

As we mentioned in the previous section, we also tested the PhotoSyn instrument by Uniqsis Ltd. and owing to its powerful LEDs we envisioned that we may decrease the reaction time with no variations in the reactivity by increasing the light intensity.

To perform this study, we used the PhotoSyn instrument (700W, 455 nm LEDs) equipped with a 10 mL reactor-coil (i.d. = 1.0 mm) in combination with a water cooler to control the temperature in the reactor and a Rainin pump to inject our solution (Figure S71).

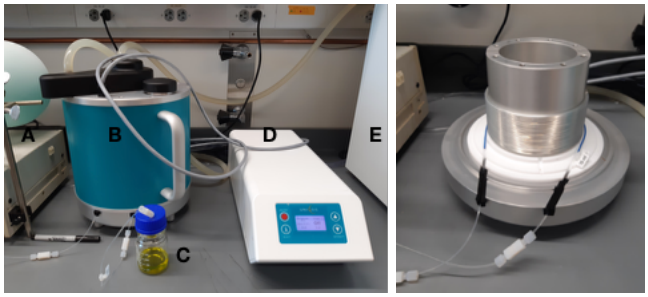

Fig. S71. PhotoSyn flow system. Left picture. A: Rainin pump; B: PhotoSyn reactor; C: collection fraction; D: photoreactor power supply; E: water cooler to control the temperature. Right picture: reactor-coil inside of the flow photoreactor.

Although PhotoSyn instrument has massive powerful LEDs, it is known that more than a third part of the power is lost in form of heat and besides, this testing instrument does not include any reflecting material on the case or covering the reactor holder, so the efficacy of the reflected light is lower than the other setups.

To establish the real output power and being able to compare with the HTE FLOSIM device, we carried out the reaction under the optimal conditions for different light intensities. First, we explore a range of low light intensities to identify which one correspond with the power used previously in the FLOSIM platform (with two LEDs) as well as the Vapourtec. For this testing instrument, we used a water cooler, so the control of the temperature was not as accurate as if we could use the polar bear cooler (by Uniqsis) or the previous Vapourtec cooling system and for this reason the temperature range in this section is a range of temperature (38 ºC – 42 ºC). As Figure S72 shown a 25% of intensity was needed to reach the same level of reactivity we obtained previously in the Vapourtec. To bear out this result, and since the reactor-coil tubing for this reactor has a smaller inner diameter we need to employ a different volume in plates to be able to compare the results between plates and this flow system. Doing this, under the optimal reaction conditions

for a 50 μL as final volume in plates a 79% of product yield was detected. This result match almost perfectly with the previous result using the PhotoSyn reactor (76% yield) so we can conclude PhotoSyn photoreactor at 25% light intensity is able to reproduce the results obtaining in the HTE FLOSIM platform using 2 Kessil LEDs as well as the results obtained from the Vapourtec (Figure S73).

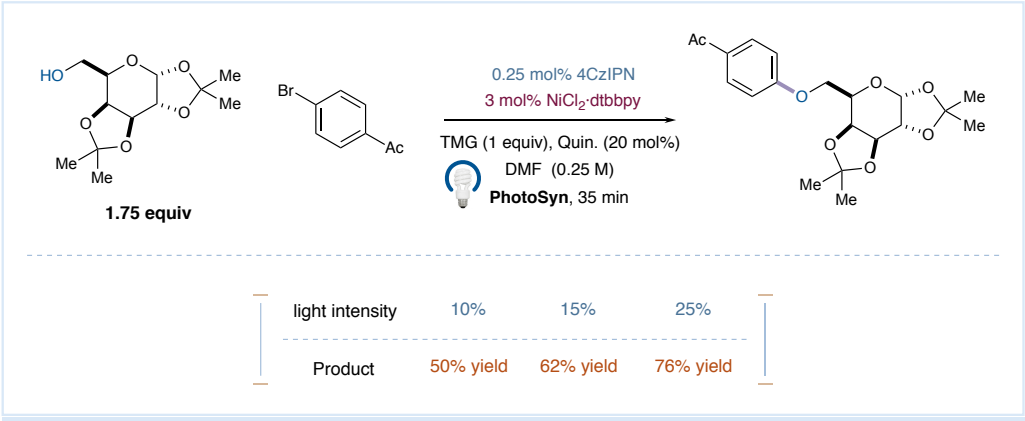

Fig. S72. Evaluation of the PhotoSyn light intensity under optimal conditions. Reactions were carried out at 3.75 mmol scale for flow system (each data is an average of two reactions).

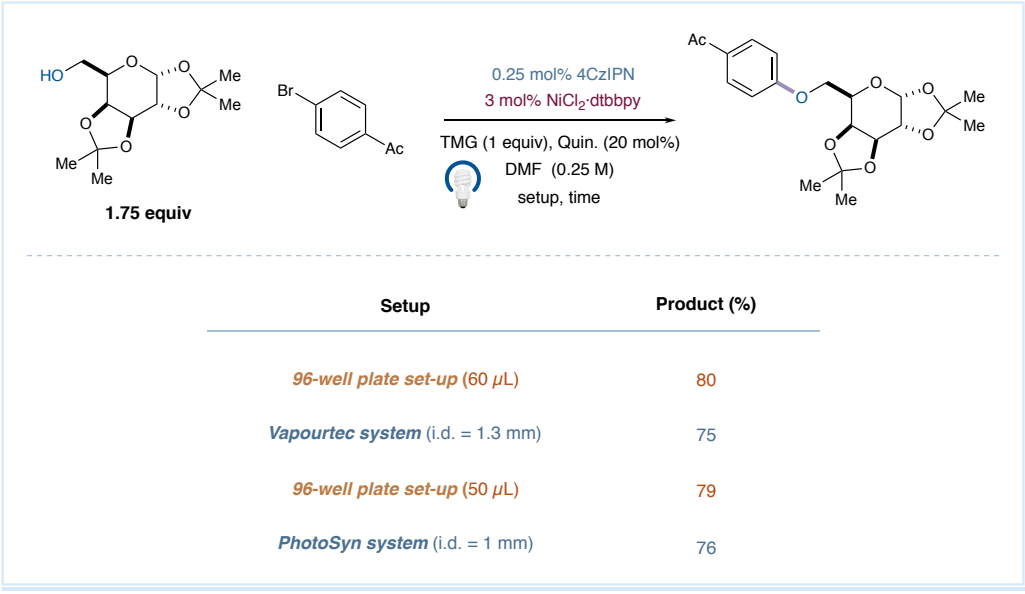

Setup	Product (%)
96-well plate set-up (60 μL)	80
Vapourtec system (i.d. = 1.3 mm)	75
96-well plate set-up (50 μL)	79
PhotoSyn system (i.d. = 1 mm)	76

Fig. S73. Setup comparison using the optimal conditions. Reactions were carried out at 15 μmol scale (each data is an average of eight points) for plates and 1 or 3.75 mmol scale for flow system (each data is an average of two reactions).

After we optimized the conditions, we needed to obtain the same level of reactivity than the other setups, we proceed to explore the relation between the light intensity and the reaction time using the PhotoSyn system. Therefore, a reaction mixture was prepared under the optimal conditions developed in the previous section [1 equiv of aryl bromide, 1.75 equiv of alkyl alcohol, 1 equiv of TMG, 20 mol% of quinuclidine, 0.25 mol% 4CzIPN, 3 mol% $NiCl_2$·dtbbpy in DMF (0.25 M)]. The reaction was carried out at 40 – 42 degrees and 25% of light intensity for 35 minutes of residence time (286.6 μL/min of flow rate) obtained the desired product in a 76% yield. Nicely, we were able to reduce the residence time until 17.5 min or 13.75 min (571.4 μL/min or 727.3 μL/min of flow rate, respectively) with no diminished yields in the collection fractions (Figure S74).

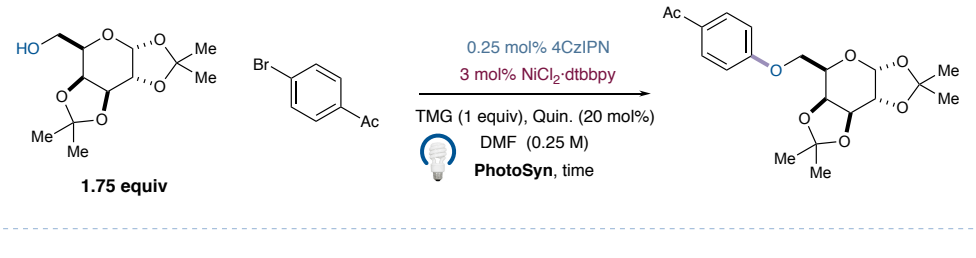

Residence time	light intensity	Product
35 min	25%	76% yield
17.5 min	50%	80% yield
13.75 min	75%	79% yield
8.75 min	100%	66% yield
12 min	100%	67% yield
4 min	100%	23% yield

Fig. S74. Evaluation of the PhotoSyn light intensity vs residence time. Reactions were carried out at 3.75 mmol scale for flow system (each data is an average of two reactions).

Unfortunately, when the residence time was reduced to 8.75 minutes (1.14 mL/min of flow rate) using a 100% light intensity the relation between these parameters became less linear, detecting a 66% product yield. Based on the detected light requirements in the original publication, in which the best results had found using less energetic light sources such as blue LED strips or CFL bulb,

it is not surprising that when a high light intensity is used the formation of alcohol side-products is favored. To support this, we were able to run different experiments using 100% of light intensity at different residence times (Figure S74, entries 5 and 6), reaching lower reactivities, with no complete consumption of the aryl bromide and not detection of dehalogenated aryl compound, which indicates the decomposition of the reaction mixture probably by polymerization of the alkyl alcohol. Moreover, this linear relation was successfully observed for the cross-electrophile coupling (section 6.3.2, Figure S55).

7.3.2. Scale up using the continuous flow systems.

First, using a Vapourtec system: an oven-dried 250 mL RBF or volumetric flask equipped with a Teflon septum and magnetic stir bar was charged with 4-bromoacetophenone (8.96 g, 45.0 mmol, 1.0 equiv), 1,2:3,4-di-O-isopropylidene-D-galactopyranose (2 M solution in DMF, 39.4 mL, 78.75 mmol, 1.75 equiv), 1,3,5-trimethoxybenzene (7.57 g, 45.0 mmol, 1.0 equiv), quinuclidine (1.0 g, 9.0 mmol, 20 mol%), TMG (5.65 mL, 45.0 mmol, 1.0 equiv), 4CzIPN (88.75 mg, 0.11 mmol, 0.25 mol%) in DMF (130 mL, 0.25 M). To a separate vial was added $NiCl_2 \cdot 6H_2O$ (385.1 mg, 1.62 mmol), 4,4′-ditertbutyl-pyridine (434.8 mg, 1.62 mmol). The catalyst vial was sealed, purged with nitrogen then to it was added 6 mL of DMF. The precatalyst solution was sonicated for 10 minutes, after which, 5.0 mL (1.35 mmol, 3 mol%) was syringed into the reaction vessel. The solution was degassed by sparging with nitrogen for 15 minutes before sealing with Parafilm and covered the vessel with aluminum foil. The Vapourtec system equipped with a 10 mL-reactor coil and 450 nm LED lights was purged, under nitrogen atmosphere, with the degassed DMF and then, the reaction mixture was injected into the system under nitrogen atmosphere. The reaction was run at 40 – 42 degrees in the heated mode with a 13.75 minutes of residence time (285.7 μL/min of flow rate) for 11 hours in total. The collection fraction was analyzed by ^{1}H-NMR and UPLC-MS (80 % yield). Then, the collection mixture was diluted with ethyl acetate (150 mL) and was washed with an aqueous solution of LiCl (2% w/v) (2 x 50 mL), water (2 x 100 mL). The aqueous layers were extracted with ethyl acetate (3 x 50 mL). The organic extracts were combined, washed with brine, dried over Na_2SO_4 and concentrated in vacuo. The residue was purified by flash column chromatography (hexane : ethyl acetate 9:1 to 4:1) to afford 12.23 g of the desired coupled product (colorless oil, 72% isolated yield).

Secondly, in the case of using a PhotoSyn instrument: to an oven-dried 250 mL RBF or volumetric flask equipped with a Teflon septum and magnetic stir bar was charged with 4-bromoacetophenone (1.92 g, 11.43 mmol, 1.0 equiv), 1,2:3,4-di-O-isopropylidene-D-galactopyranose (2 M solution in DMF, 10.0 mL, 20.0 mmol, 1.75 equiv), 1,3,5-trimethoxybenzene (1.92 g, 11.43 mmol, 1.0 equiv), quinuclidine (254.1 mg, 2.3 mmol, 20 mol%), TMG (1.43 mL, 11.43 mmol, 1.0 equiv), 4CzIPN (22.54 mg, 28.6 μmol, 0.25 mol%) in DMF (32.8 mL, 0.25 M). To a separate vial was added $NiCl_2 \cdot 6H_2O$ (97.8 mg, 0.41 mmol), 4,4′-ditertbutyl-pyridine (110.6 mg, 0.41 mmol). The catalyst vial was sealed, purged with nitrogen then to it was added 1.8 mL of DMF. The precatalyst solution was sonicated for 10 minutes, after which, 1.5 mL (0.34 mmol, 3 mol%) was syringed into the reaction vessel. The solution was degassed by sparging with nitrogen for 15 minutes before sealing with Parafilm and covered the vessel with aluminum foil. The PhotoSyn instrument equipped with a 10 mL-reactor coil and 455 nm LED lights was purged, under nitrogen atmosphere, with the degassed DMF and then, the reaction mixture was injected into the system under nitrogen atmosphere. The reaction was run at 40 – 42 degrees controlled with a water cooler, 13.75 minutes of residence time (727.3 μL/min of flow rate) for 77 minutes in total. The collection fraction was analyzed by ^{1}H-NMR and UPLC-MS (77 % yield). Then, the collection mixture was diluted with ethyl acetate (150 mL) and was washed with an aqueous solution of LiCl (2% w/v) (2 x 50 mL), water (2 x 100 mL). The aqueous layers were extracted with ethyl acetate (3 x 50 mL). The organic extracts were combined, washed with brine, dried over Na_2SO_4 and concentrated in vacuo. The residue was purified by flash column chromatography (hexane : ethyl acetate 9:1 to 4:1) to afford 3.1 g of the desired coupled product (colorless oil, 72% isolated yield).

The spectroscopic properties of this compound are consistent with data reported in the literature.[10]

^{1}H NMR (500 MHz, $CDCl_3$): δ 7.92 (d, J = 8.9 Hz, 1H), 6.98 (d, J = 8.9 Hz, 1H), 5.57 (d, J = 5.0 Hz, 1H), 4.66 (dd, J = 7.9, 2.5 Hz, 1H), 4.42 – 4.30 (m, 2H), 4.26 – 4.15 (m, 3H), 2.55 (s, 3H), 1.53 (s, 3H), 1.47 (s, 3H), 1.36 (s, 3H), 1.35 (s, 3H).

8. Extended data of Tableau optimization graphics.

8.1. Data from Section 2.

Data from Fig. S2. 2.5 cm between LEDs using lens F = –75.

Average (total plate) = 33, std (total plate) = 3.69; average (rows C – F) = 35, std (total plate) = 2.84.

ROW	COLUMN	Product (%)	ArBr (%)	Acid (%)
A	1	**30**	64	123
A	2	**29**	61	124
A	3	**28**	63	124
A	4	**29**	62	124
A	5	**25**	62	127
A	6	**26**	62	130
A	7	**25**	64	126
A	8	**30**	63	125
A	9	**30**	61	124
A	10	**29**	62	123
A	11	**28**	60	126
A	12	**30**	62	125
B	1	**28**	61	124
B	2	**32**	61	123
B	3	**31**	60	122
B	4	**33**	60	121
B	5	**33**	61	120
B	6	**31**	60	121
B	7	**34**	60	120
B	8	**32**	60	118
B	9	**33**	63	120
B	10	**31**	62	120
B	11	**33**	62	121
B	12	**29**	61	123
C	1	**32**	60	124
C	2	**32**	60	120
C	3	**34**	60	120
C	4	**33**	58	118
C	5	**38**	56	117

C	6	**37**	56	113
C	7	**37**	55	114
C	8	**37**	58	117
C	9	**35**	60	118
C	10	**33**	58	120
C	11	**34**	58	121
C	12	**31**	59	124
D	1	**33**	59	124
D	2	**34**	57	121
D	3	**33**	57	120
D	4	**35**	56	119
D	5	**37**	56	116
D	6	**42**	53	112
D	7	**40**	53	112
D	8	**38**	56	116
D	9	**34**	57	117
D	10	**36**	58	117
D	11	**35**	56	118
D	12	**32**	58	121
E	1	**31**	58	122
E	2	**33**	57	121
E	3	**35**	56	121
E	4	**36**	55	119
E	5	**39**	54	117
E	6	**41**	52	113
E	7	**41**	51	114
E	8	**36**	56	117
E	9	**36**	58	118
E	10	**34**	56	118
E	11	**33**	56	120
E	12	**34**	58	122
F	1	**33**	57	124
F	2	**35**	57	122
F	3	**33**	56	119
F	4	**33**	56	119
F	5	**37**	55	119
F	6	**39**	55	116
F	7	**37**	54	117
F	8	**37**	57	118
F	9	**33**	57	121

F	10	**32**	57	121
F	11	**32**	57	122
F	12	**30**	57	124
G	1	**31**	56	126
G	2	**32**	56	123
G	3	**34**	57	123
G	4	**33**	56	122
G	5	**34**	56	124
G	6	**32**	57	126
G	7	**30**	57	125
G	8	**30**	58	124
G	9	**29**	59	124
G	10	**30**	57	128
G	11	**31**	57	128
G	12	**29**	58	128
H	1	**32**	57	127
H	2	**32**	56	126
H	3	**32**	57	125
H	4	**31**	57	127
H	5	**28**	57	132
H	6	**25**	59	134
H	7	**25**	59	134
H	8	**27**	58	133
H	9	**27**	57	129
H	10	**29**	59	128
H	11	**29**	59	127
H	12	**27**	57	130

Data from Fig. S2. 2.5 cm between LEDs using lens F = –100.

Average (total plate) = 32, std (total plate) = 4.17; average (rows C – F) = 34, std (total plate) = 2.29.

ROW	COLUMN	Product (%)	ArBr (%)	Acid (%)
A	1	**31**	61	132
A	2	**31**	55	151
A	3	**29**	59	140
A	4	**27**	57	154
A	5	**23**	58	159
A	6	**22**	58	167
A	7	**20**	59	157

A	8	**23**	58	147
A	9	**28**	55	161
A	10	**33**	54	167
A	11	**28**	54	133
A	12	**31**	55	161
B	1	**34**	53	148
B	2	**38**	53	166
B	3	**36**	53	149
B	4	**32**	55	142
B	5	**29**	57	143
B	6	**26**	57	155
B	7	**27**	55	160
B	8	**33**	54	151
B	9	**34**	55	142
B	10	**36**	55	149
B	11	**34**	58	150
B	12	**32**	58	149
C	1	**31**	67	115
C	2	**35**	67	115
C	3	**36**	60	132
C	4	**37**	64	122
C	5	**32**	66	115
C	6	**33**	57	154
C	7	**31**	67	114
C	8	**34**	60	137
C	9	**36**	63	113
C	10	**35**	61	127
C	11	**33**	67	115
C	12	**30**	67	117
D	1	**34**	65	115
D	2	**36**	67	113
D	3	**38**	63	111
D	4	**37**	62	111
D	5	**37**	64	111
D	6	**34**	64	112
D	7	**37**	64	111
D	8	**34**	63	112
D	9	**36**	64	112
D	10	**36**	66	112
D	11	**32**	66	115

D	12	**33**	65	115
E	1	**35**	65	114
E	2	**34**	64	114
E	3	**37**	62	113
E	4	**38**	62	112
E	5	**37**	60	111
E	6	**36**	62	112
E	7	**36**	62	110
E	8	**36**	63	113
E	9	**33**	63	115
E	10	**35**	64	114
E	11	**31**	65	116
E	12	**30**	66	117
F	1	**35**	63	115
F	2	**34**	63	113
F	3	**37**	62	112
F	4	**36**	63	113
F	5	**35**	62	112
F	6	**35**	64	114
F	7	**34**	63	113
F	8	**35**	64	115
F	9	**34**	62	116
F	10	**34**	63	113
F	11	**32**	65	117
F	12	**28**	70	118
G	1	**36**	62	114
G	2	**34**	63	115
G	3	**33**	62	115
G	4	**34**	63	116
G	5	**31**	64	116
G	6	**29**	66	120
G	7	**27**	68	119
G	8	**31**	63	116
G	9	**29**	66	117
G	10	**32**	65	118
G	11	**29**	67	118
G	12	**28**	68	120
H	1	**31**	64	119
H	2	**31**	64	115
H	3	**32**	64	117

H	4	**32**	63	118
H	5	**25**	67	122
H	6	**21**	68	125
H	7	**23**	71	125
H	8	**24**	68	123
H	9	**28**	68	121
H	10	**29**	68	120
H	11	**26**	68	121
H	12	**28**	69	121

Data from Fig. S2. 2.5 cm between LEDs using lens F = –150.

Average (total plate) = 34, std (total plate) = 4.29; average (rows C – F) = 36, std (total plate) = 3.13.

ROW	COLUMN	Product (%)	ArBr (%)	Acid (%)
A	1	**33**	63	112
A	2	**30**	63	112
A	3	**31**	63	114
A	4	**27**	63	117
A	5	**27**	67	118
A	6	**23**	65	120
A	7	**25**	67	120
A	8	**26**	65	118
A	9	**30**	64	116
A	10	**31**	62	113
A	11	**30**	62	114
A	12	**29**	61	113
B	1	**33**	58	111
B	2	**33**	59	110
B	3	**36**	58	110
B	4	**32**	59	112
B	5	**31**	6	113
B	6	**29**	60	114
B	7	**30**	61	114
B	8	**34**	60	111
B	9	**33**	58	110
B	10	**35**	60	111
B	11	**33**	59	114
B	12	**33**	61	113

C	1	**32**	58	111
C	2	**33**	58	113
C	3	**37**	58	108
C	4	**36**	57	107
C	5	**38**	54	109
C	6	**35**	54	109
C	7	**38**	56	109
C	8	**38**	56	109
C	9	**36**	56	109
C	10	**36**	58	110
C	11	**35**	60	110
C	12	**30**	59	114
D	1	**34**	58	113
D	2	**33**	55	111
D	3	**36**	55	110
D	4	**38**	52	110
D	5	**42**	51	106
D	6	**41**	50	105
D	7	**41**	51	104
D	8	**41**	52	106
D	9	**40**	53	106
D	10	**34**	55	111
D	11	**34**	59	113
D	12	**33**	58	113
E	1	**35**	54	113
E	2	**34**	52	114
E	3	**36**	52	113
E	4	**39**	51	109
E	5	**39**	48	106
E	6	**43**	48	104
E	7	**41**	48	105
E	8	**40**	50	107
E	9	**35**	53	110
E	10	**36**	56	132
E	11	**33**	58	112
E	12	**30**	56	115
F	1	**35**	52	115
F	2	**34**	51	113
F	3	**37**	52	110
F	4	**39**	51	110

F	5	**40**	50	108
F	6	**38**	49	107
F	7	**40**	52	108
F	8	**39**	47	110
F	9	**34**	50	114
F	10	**34**	52	116
F	11	**31**	53	116
F	12	**32**	56	117
G	1	**33**	48	108
G	2	**35**	50	110
G	3	**37**	51	112
G	4	**36**	50	114
G	5	**36**	52	113
G	6	**31**	54	115
G	7	**32**	56	116
G	8	**31**	54	115
G	9	**31**	55	115
G	10	**33**	56	114
G	11	**31**	57	114
G	12	**29**	55	117
H	1	**33**	50	116
H	2	**35**	50	119
H	3	**34**	49	122
H	4	**32**	50	123
H	5	**29**	53	12
H	6	**24**	55	126
H	7	**24**	54	124
H	8	**25**	54	123
H	9	**29**	54	121
H	10	**29**	53	121
H	11	**29**	55	118
H	12	**28**	50	127

Data from Fig. S2. 2.2 cm between LEDs using lens F = –75.

Average (total plate) = 36, std (total plate) = 4.82; average (rows C – F) = 38, std (total plate) = 3.38.

ROW	COLUMN	Product (%)	ArBr (%)	Acid (%)
A	1	**37**	61	109

A	2	**35**	61	108
A	3	**36**	61	109
A	4	**31**	63	111
A	5	**27**	68	114
A	6	**23**	69	121
A	7	**23**	70	118
A	8	**27**	68	114
A	9	**35**	64	110
A	10	**35**	61	109
A	11	**39**	49	107
A	12	**36**	62	108
B	1	**34**	63	111
B	2	**33**	61	110
B	3	**35**	61	110
B	4	**36**	61	109
B	5	**33**	61	110
B	6	**28**	65	114
B	7	**32**	64	114
B	8	**32**	61	112
B	9	**32**	60	111
B	10	**33**	61	111
B	11	**32**	62	111
B	12	**34**	63	112
C	1	**34**	59	110
C	2	**35**	59	109
C	3	**38**	56	109
C	4	**38**	56	110
C	5	**38**	56	105
C	6	**40**	56	106
C	7	**38**	55	107
C	8	**39**	57	107
C	9	**34**	58	109
C	10	**34**	60	110
C	11	**34**	60	110
C	12	**35**	62	111
D	1	**37**	58	109
D	2	**37**	55	107
D	3	**39**	55	107
D	4	**37**	54	107
D	5	**40**	51	105

D	6	**47**	48	100
D	7	**44**	48	102
D	8	**41**	54	106
D	9	**37**	55	107
D	10	**39**	58	108
D	11	**36**	57	108
D	12	**34**	59	110
E	1	**38**	57	109
E	2	**37**	53	108
E	3	**37**	53	109
E	4	**38**	51	108
E	5	**43**	51	104
E	6	**46**	45	99
E	7	**47**	45	101
E	8	**41**	52	106
E	9	**38**	7	107
E	10	**38**	54	107
E	11	**37**	56	108
E	12	**35**	58	109
F	1	**38**	56	109
F	2	**36**	53	109
F	3	**38**	53	109
F	4	**36**	53	108
F	5	**42**	51	106
F	6	**44**	46	101
F	7	**44**	48	103
F	8	**37**	51	107
F	9	**36**	54	109
F	10	**38**	56	108
F	11	**38**	56	109
F	12	**33**	58	111
G	1	**41**	51	105
G	2	**40**	50	104
G	3	**40**	49	105
G	4	**39**	50	105
G	5	**44**	47	102
G	6	**43**	49	102
G	7	**40**	50	103
G	8	**41**	53	104
G	9	**39**	55	105

G	10	**37**	53	108
G	11	**39**	52	108
G	12	**35**	55	109
H	1	**32**	55	114
H	2	**30**	53	119
H	3	**32**	55	115
H	4	**32**	56	114
H	5	**30**	56	116
H	6	**28**	60	118
H	7	**32**	58	117
H	8	**29**	59	116
H	9	**28**	59	116
H	10	**29**	57	118
H	11	**28**	55	117
H	12	**29**	58	118

Data from Fig. S2. 2.2 cm between LEDs using lens F = –100.

Average (total plate) = 36, std (total plate) = 5.40; average (rows C – F) = 39, std (total plate) = 3.69.

ROW	COLUMN	Product (%)	ArBr (%)	Acid (%)
A	1	**29**	72	113
A	2	**34**	72	281
A	3	**33**	70	114
A	4	**27**	72	114
A	5	**24**	76	117
A	6	**24**	79	119
A	7	**21**	76	119
A	8	**24**	76	90
A	9	**31**	74	112
A	10	**33**	71	111
A	11	**34**	71	110
A	12	**29**	71	112
B	1	**38**	67	107
B	2	**36**	65	106
B	3	**39**	63	107
B	4	**35**	64	107
B	5	**32**	68	109
B	6	**29**	68	112
B	7	**31**	69	111

B	8	**35**	68	110
B	9	**37**	67	108
B	10	**36**	67	109
B	11	**34**	66	109
B	12	**32**	66	110
C	1	**36**	64	105
C	2	**40**	64	105
C	3	**43**	61	105
C	4	**39**	61	103
C	5	**43**	61	102
C	6	**41**	63	104
C	7	**37**	61	105
C	8	**37**	63	105
C	9	**40**	62	107
C	10	**39**	64	106
C	11	**34**	64	108
C	12	**33**	65	110
D	1	**36**	63	107
D	2	**40**	62	106
D	3	**43**	59	105
D	4	**40**	60	102
D	5	**42**	57	101
D	6	**44**	56	99
D	7	**44**	58	100
D	8	**42**	61	103
D	9	**38**	60	104
D	10	**36**	61	110
D	11	**36**	63	106
D	12	**34**	65	108
E	1	**37**	61	106
E	2	**39**	60	104
E	3	**42**	60	104
E	4	**44**	59	101
E	5	**43**	56	100
E	6	**47**	53	95
E	7	**47**	56	99
E	8	**40**	58	103
E	9	**38**	60	105
E	10	**36**	61	108
E	11	**35**	63	106

E	12	**34**	64	108
F	1	**36**	60	107
F	2	**39**	59	106
F	3	**39**	61	105
F	4	**40**	61	106
F	5	**39**	58	105
F	6	**42**	57	102
F	7	**43**	57	104
F	8	**37**	61	106
F	9	**38**	61	108
F	10	**34**	62	110
F	11	**34**	62	110
F	12	**32**	65	110
G	1	**37**	61	106
G	2	**39**	61	106
G	3	**36**	60	107
G	4	**36**	62	107
G	5	**38**	62	108
G	6	**37**	63	109
G	7	**32**	63	112
G	8	**35**	64	110
G	9	**31**	63	112
G	10	**31**	65	111
G	11	**31**	66	110
G	12	**32**	65	111
H	1	**34**	64	112
H	2	**33**	63	110
H	3	**33**	63	111
H	4	**31**	64	112
H	5	**31**	66	115
H	6	**24**	67	118
H	7	**24**	68	120
H	8	**26**	68	117
H	9	**28**	67	115
H	10	**30**	67	114
H	11	**29**	66	114
H	12	**30**	67	115

Data from Fig. S2. 2.2 cm between LEDs using lens F = –150.

Average (total plate) = 36, std (total plate) = 4.98; average (rows C – F) = 40, std (total plate) = 3.12.

ROW	COLUMN	Product (%)	ArBr (%)	Acid (%)
A	1	**34**	54	144
A	2	**35**	51	157
A	3	**36**	52	157
A	4	**32**	53	155
A	5	**25**	57	154
A	6	**24**	57	165
A	7	**24**	77	120
A	8	**26**	75	118
A	9	**26**	69	113
A	10	**29**	69	111
A	11	**31**	68	112
A	12	**30**	69	113
B	1	**37**	65	108
B	2	**37**	59	104
B	3	**37**	59	106
B	4	**38**	64	108
B	5	**34**	66	111
B	6	**30**	69	115
B	7	**30**	69	115
B	8	**34**	67	111
B	9	**34**	63	109
B	10	**34**	64	108
B	11	**33**	64	108
B	12	**33**	63	111
C	1	**35**	63	107
C	2	**37**	61	106
C	3	**42**	58	103
C	4	**43**	57	102
C	5	**40**	61	105
C	6	**39**	62	106
C	7	**39**	63	106
C	8	**41**	60	102
C	9	**42**	58	102
C	10	**36**	61	105
C	11	**36**	64	106
C	12	**33**	62	107

D	1	**37**	60	107
D	2	**38**	60	103
D	3	**42**	59	103
D	4	**42**	55	101
D	5	**42**	56	100
D	6	**42**	56	102
D	7	**42**	56	101
D	8	**41**	57	100
D	9	**40**	58	105
D	10	**36**	59	107
D	11	**38**	61	107
D	12	**37**	61	109
E	1	**39**	60	107
E	2	**39**	57	104
E	3	**40**	57	102
E	4	**42**	55	101
E	5	**46**	54	99
E	6	**43**	53	100
E	7	**45**	53	98
E	8	**45**	55	99
E	9	**42**	57	103
E	10	**40**	57	105
E	11	**36**	61	108
E	12	**35**	61	109
F	1	**35**	61	107
F	2	**38**	58	106
F	3	**43**	56	103
F	4	**44**	54	102
F	5	**41**	55	101
F	6	**41**	55	102
F	7	**39**	55	104
F	8	**41**	58	105
F	9	**37**	58	106
F	10	**38**	61	107
F	11	**34**	60	109
F	12	**36**	62	110
G	1	**36**	58	106
G	2	**41**	57	104
G	3	**38**	56	104
G	4	**38**	56	106

G	5	**39**	59	107
G	6	**38**	60	106
G	7	**34**	59	111
G	8	**38**	60	106
G	9	**35**	61	108
G	10	**37**	60	107
G	11	**33**	60	110
G	12	**33**	62	109
H	1	**37**	60	109
H	2	**37**	59	109
H	3	**34**	58	110
H	4	**33**	62	110
H	5	**31**	64	114
H	6	**26**	65	118
H	7	**28**	67	116
H	8	**29**	63	114
H	9	**30**	62	115
H	10	**29**	63	114
H	11	**32**	62	113
H	12	**32**	64	0

Data from Fig. S3. Reducing the heigh of the box (4”x8” FLOSIM device).

Average (total plate) = 34, std (total plate) = 4.29; average (rows C – F) = 36, std (total plate) = 3.34.

ROW	COLUMN	Product (%)	ArBr (%)	Acid (%)
A	1	**32**	66	100
A	2	**30**	64	101
A	3	**30**	64	102
A	4	**30**	67	104
A	5	**27**	69	107
A	6	**26**	69	108
A	7	**23**	71	112
A	8	**25**	70	111
A	9	**28**	67	106
A	10	**29**	66	105
A	11	**29**	66	105
A	12	**27**	67	106
B	1	**35**	77	127
B	2	**33**	72	118

B	3	**35**	71	117
B	4	**35**	70	117
B	5	**33**	73	118
B	6	**32**	74	119
B	7	**32**	71	118
B	8	**35**	69	115
B	9	**37**	68	114
B	10	**35**	69	114
B	11	**35**	71	118
B	12	**35**	70	119
C	1	**31**	75	117
C	2	**32**	71	121
C	3	**33**	71	119
C	4	**36**	68	118
C	5	**37**	66	118
C	6	**36**	69	118
C	7	**38**	66	115
C	8	**40**	63	115
C	9	**38**	66	116
C	10	**35**	68	116
C	11	**34**	72	121
C	12	**33**	71	118
D	1	**32**	72	122
D	2	**32**	71	20
D	3	**34**	70	121
D	4	**38**	59	152
D	5	**37**	58	147
D	6	**40**	56	112
D	7	**41**	54	110
D	8	**43**	48	111
D	9	**41**	52	110
D	10	**39**	57	116
D	11	**34**	58	118
D	12	**33**	58	117
E	1	**33**	69	135
E	2	**34**	69	124
E	3	**34**	66	119
E	4	**38**	65	119
E	5	**38**	63	118
E	6	**39**	65	117

E	7	**40**	61	115
E	8	**44**	58	110
E	9	**42**	59	112
E	10	**40**	64	113
E	11	**35**	67	119
E	12	**33**	66	117
F	1	**32**	68	120
F	2	**32**	68	118
F	3	**35**	67	118
F	4	**36**	65	116
F	5	**35**	65	115
F	6	**36**	66	117
F	7	**37**	64	115
F	8	**41**	60	110
F	9	**41**	61	111
F	10	**40**	58	116
F	11	**36**	65	117
F	12	**33**	67	118
G	1	**31**	68	119
G	2	**31**	67	118
G	3	**32**	66	118
G	4	**33**	66	117
G	5	**33**	66	119
G	6	**31**	67	120
G	7	**31**	67	118
G	8	**34**	64	114
G	9	**40**	63	113
G	10	**38**	62	111
G	11	**37**	62	112
G	12	**35**	62	114
H	1	**33**	59	105
H	2	**33**	59	104
H	3	**33**	59	106
H	4	**30**	61	110
H	5	**27**	61	113
H	6	**25**	65	115
H	7	**25**	65	114
H	8	**27**	62	110
H	9	**31**	62	107
H	10	**32**	60	109

H	11	**32**	59	110
H	12	**30**	59	111

Data from Fig. S4. Four lights setup. 50% light intensity.

Average (total plate) = 21, std (total plate) = 5.36; average (rows C – F) = 18, std (total plate) = 2.23.

ROW	COLUMN	Product (%)	ArBr (%)	Acid (%)
A	1	**43**	52	145
A	2	**46**	49	137
A	3	**31**	55	174
A	4	**29**	56	168
A	5	**28**	56	166
A	6	**24**	57	157
A	7	**24**	57	161
A	8	**25**	58	156
A	9	**25**	59	153
A	10	**24**	59	153
A	11	**24**	58	152
A	12	**25**	57	165
B	1	**38**	58	71
B	2	**35**	60	64
B	3	**33**	63	83
B	4	**22**	73	111
B	5	**20**	74	114
B	6	**18**	75	114
B	7	**18**	75	114
B	8	**20**	73	112
B	9	**21**	73	111
B	10	**21**	70	112
B	11	**22**	73	110
B	12	**21**	70	113
C	1	**21**	72	111
C	2	**22**	70	111
C	3	**21**	72	112
C	4	**18**	73	115
C	5	**17**	74	116
C	6	**15**	75	117
C	7	**16**	75	118
C	8	**17**	75	115

C	9	**19**	73	114
C	10	**20**	73	112
C	11	**20**	74	112
C	12	**20**	73	114
D	1	**20**	69	115
D	2	**21**	70	113
D	3	**19**	72	114
D	4	**17**	73	117
D	5	**15**	74	119
D	6	**14**	74	120
D	7	**14**	74	119
D	8	**16**	73	119
D	9	**17**	73	116
D	10	**19**	72	114
D	11	**20**	71	114
D	12	**19**	69	116
E	1	**21**	69	115
E	2	**21**	69	115
E	3	**19**	71	116
E	4	**17**	72	117
E	5	**15**	73	119
E	6	**15**	73	121
E	7	**14**	73	121
E	8	**16**	74	119
E	9	**17**	71	118
E	10	**18**	70	116
E	11	**19**	66	119
E	12	**19**	68	116
F	1	**22**	63	117
F	2	**22**	65	115
F	3	**20**	65	116
F	4	**19**	67	117
F	5	**17**	67	119
F	6	**15**	68	120
F	7	**16**	65	122
F	8	**17**	67	119
F	9	**19**	65	120
F	10	**20**	66	116
F	11	**20**	65	114
F	12	**20**	64	119

G	1	**21**	64	114
G	2	**23**	63	114
G	3	**22**	63	115
G	4	**21**	64	114
G	5	**20**	64	119
G	6	**18**	65	118
G	7	**19**	64	119
G	8	**20**	65	116
G	9	**21**	64	115
G	10	**21**	64	115
G	11	**21**	63	116
G	12	**21**	62	116
H	1	**22**	62	118
H	2	**21**	62	116
H	3	**22**	62	116
H	4	**22**	61	117
H	5	**21**	62	118
H	6	**20**	63	117
H	7	**20**	61	120
H	8	**21**	62	115
H	9	**21**	60	117
H	10	**21**	62	118
H	11	**21**	60	120
H	12	**20**	61	118

Data from Fig. S4. Four lights setup. 100% light intensity.

Average (total plate) =44, std (total plate) = 8.05; average (rows C – F) = 40, std (total plate) = 7.61.

ROW	COLUMN	Product (%)	ArBr (%)	Acid (%)
A	1	**54**	49	86
A	2	**53**	44	83
A	3	**55**	41	81
A	4	**55**	40	79
A	5	**53**	43	82
A	6	**45**	51	90
A	7	**44**	51	90
A	8	**46**	49	87
A	9	**47**	47	86
A	10	**45**	48	88

A	11	**46**	48	88
A	12	**63**	27	47
B	1	**51**	42	80
B	2	**55**	37	73
B	3	**54**	37	74
B	4	**54**	40	79
B	5	**48**	49	85
B	6	**40**	54	92
B	7	**40**	54	92
B	8	**45**	50	87
B	9	**48**	46	83
B	10	**48**	45	83
B	11	**64**	25	54
B	12	**65**	25	53
C	1	**49**	45	82
C	2	**52**	41	78
C	3	**49**	43	81
C	4	**44**	49	88
C	5	**36**	56	96
C	6	**32**	60	100
C	7	**33**	61	101
C	8	**37**	56	95
C	9	**43**	50	89
C	10	**46**	47	83
C	11	**47**	45	84
C	12	**61**	31	60
D	1	**45**	48	87
D	2	**48**	45	83
D	3	**44**	48	88
D	4	**35**	57	97
D	5	**30**	61	103
D	6	**26**	65	107
D	7	**27**	65	281
D	8	**30**	62	103
D	9	**34**	58	98
D	10	**41**	51	91
D	11	**44**	49	89
D	12	**40**	52	93
E	1	**45**	48	88
E	2	**46**	46	86

E	3	**42**	50	90
E	4	**34**	57	99
E	5	**30**	62	103
E	6	**27**	63	106
E	7	**27**	64	106
E	8	**31**	61	105
E	9	**35**	57	98
E	10	**41**	51	92
E	11	**42**	50	90
E	12	**40**	52	93
F	1	**47**	45	85
F	2	**49**	42	81
F	3	**46**	45	85
F	4	**41**	52	92
F	5	**36**	55	97
F	6	**33**	58	100
F	7	**33**	58	101
F	8	**37**	55	96
F	9	**41**	51	91
F	10	**44**	48	87
F	11	**45**	46	86
F	12	**43**	48	90
G	1	**55**	39	79
G	2	**52**	38	75
G	3	**50**	41	79
G	4	**47**	45	85
G	5	**43**	48	89
G	6	**40**	51	92
G	7	**40**	51	93
G	8	**43**	48	88
G	9	**46**	47	85
G	10	**46**	45	84
G	11	**46**	45	85
G	12	**44**	44	88
H	1	**47**	44	84
H	2	**48**	42	83
H	3	**49**	42	85
H	4	**48**	43	83
H	5	**46**	45	88
H	6	**44**	46	88

H	7	**44**	47	90
H	8	**45**	46	88
H	9	**46**	46	85
H	10	**44**	46	88
H	11	**43**	47	89
H	12	**42**	49	92

8.2. Data from Section 2.4. Use of Analytical Sales HTE platform.

Use of 420 nm lens mat and active cooling base (100% intensity inside of the glove box).

Average (total plate) =42, std (total plate) = 2.97; average (rows C – F) = 42, std (total plate) = 3.44.

ROW	COLUMN	Product (%)	ArBr (%)	Acid (%)
A	1	**37**	24	46
A	2	**41**	19	42
A	3	**41**	17	40
A	4	**44**	14	37
A	5	**44**	15	38
A	6	**40**	19	43
A	7	**43**	16	38
A	8	**44**	15	39
A	9	**44**	15	38
A	10	**44**	15	38
A	11	**41**	18	41
A	12	**41**	19	41
B	1	**39**	20	42
B	2	**44**	15	37
B	3	**44**	14	37
B	4	**46**	12	35
B	5	**44**	14	37
B	6	**43**	15	38
B	7	**44**	8	173
B	8	**45**	13	36
B	9	**43**	15	38
B	10	**43**	16	38
B	11	**42**	17	39
B	12	**41**	18	40
C	1	**41**	18	41
C	2	**43**	15	37
C	3	**43**	16	39

C	4	**45**	13	36
C	5	**46**	12	34
C	6	**44**	14	37
C	7	**45**	13	35
C	8	**44**	13	36
C	9	**43**	15	38
C	10	**45**	13	35
C	11	**43**	16	39
C	12	**40**	19	41
D	1	**40**	19	43
D	2	**43**	15	38
D	3	**44**	13	35
D	4	**44**	14	37
D	5	**42**	16	38
D	6	**40**	18	42
D	7	**44**	14	37
D	8	**43**	15	38
D	9	**44**	14	37
D	10	**44**	14	37
D	11	**44**	15	38
D	12	**39**	22	44
E	1	**27**	29	44
E	2	**41**	19	41
E	3	**43**	15	37
E	4	**43**	16	39
E	5	**40**	19	43
E	6	**41**	18	41
E	7	**41**	18	41
E	8	**43**	15	39
E	9	**44**	14	37
E	10	**38**	22	45
E	11	**35**	26	49
E	12	**35**	26	49
F	1	**40**	19	41
F	2	**43**	15	37
F	3	**46**	13	35
F	4	**42**	16	39
F	5	**45**	14	36
F	6	**42**	16	38
F	7	**44**	14	37

F	8	**42**	16	39
F	9	**47**	11	34
F	10	**46**	11	35
F	11	**42**	18	39
F	12	**39**	22	47
G	1	**37**	23	46
G	2	**41**	18	43
G	3	**44**	14	37
G	4	**44**	16	38
G	5	**40**	19	42
G	6	**43**	17	40
G	7	**44**	17	40
G	8	**43**	16	39
G	9	**42**	16	40
G	10	**45**	14	37
G	11	**41**	18	41
G	12	**36**	24	47
H	1	**38**	23	44
H	2	**44**	15	37
H	3	**43**	15	37
H	4	**41**	19	41
H	5	**43**	17	39
H	6	**38**	23	44
H	7	**41**	19	41
H	8	**43**	17	39
H	9	**45**	13	36
H	10	**46**	14	36
H	11	**44**	15	37
H	12	**35**	26	48

Use of 420 nm lens mat and active cooling base (100% intensity outside of the glove box). Average (total plate) =39, std (total plate) = 7.84; average (rows C – F) = 38, std (total plate) = 7.76.

ROW	COLUMN	Product (%)	ArBr (%)	Acid (%)
A	1	**43**	22	40
A	2	**42**	19	40
A	3	**43**	17	38
A	4	**45**	16	35
A	5	**45**	17	37

A	6	**42**	20	40
A	7	**40**	19	40
A	8	**39**	20	40
A	9	**25**	31	28
A	10	**40**	20	39
A	11	**41**	17	37
A	12	**40**	20	40
B	1	**41**	18	36
B	2	**42**	16	35
B	3	**42**	16	36
B	4	**42**	17	35
B	5	**42**	17	35
B	6	**43**	15	35
B	7	**42**	17	35
B	8	**40**	19	37
B	9	**42**	15	24
B	10	**19**	37	23
B	11	**42**	17	36
B	12	**36**	19	23
C	1	**43**	16	36
C	2	**41**	17	36
C	3	**44**	14	32
C	4	**27**	28	21
C	5	**45**	12	30
C	6	**24**	32	22
C	7	**45**	13	32
C	8	**44**	14	33
C	9	**38**	18	22
C	10	**28**	26	21
C	11	**44**	12	23
C	12	**31**	24	21
D	1	**40**	19	38
D	2	**40**	20	39
D	3	**42**	17	35
D	4	**43**	16	34
D	5	**42**	16	36
D	6	**42**	17	38
D	7	**46**	11	29
D	8	**41**	17	37
D	9	**36**	19	23

D	10	**25**	31	22
D	11	**43**	14	31
D	12	**41**	18	35
E	1	**43**	16	34
E	2	**44**	14	33
E	3	**32**	22	18
E	4	**46**	11	29
E	5	**37**	17	20
E	6	**45**	12	32
E	7	**44**	12	33
E	8	**44**	13	33
E	9	**21**	34	21
E	10	**29**	27	23
E	11	**45**	12	29
E	12	**45**	12	29
F	1	**46**	12	32
F	2	**32**	23	20
F	3	**42**	13	18
F	4	**23**	32	20
F	5	**31**	23	20
F	6	**47**	9	20
F	7	**46**	10	29
F	8	**46**	10	30
F	9	**46**	11	31
F	10	**29**	26	21
F	11	**24**	31	18
F	12	**29**	26	15
G	1	**46**	12	33
G	2	**22**	33	20
G	3	**25**	30	18
G	4	**23**	32	19
G	5	**46**	11	31
G	6	**32**	22	13
G	7	**48**	8	25
G	8	**34**	19	17
G	9	**25**	29	19
G	10	**46**	11	30
G	11	**45**	14	34
G	12	**32**	22	15
H	1	**44**	13	34

H	2	**45**	14	34
H	3	**47**	3	29
H	4	**48**	10	28
H	5	**49**	7	20
H	6	**47**	11	184
H	7	**46**	12	30
H	8	**49**	7	22
H	9	**49**	7	23
H	10	**23**	32	19
H	11	**37**	17	18
H	12	**42**	16	34

8.3. Data from Decarboxylative arylation high-throughput screening.

Data from Fig. S10. Bases vs solvents at different concentrations.

Solvent	Base	Concentration	Product (%)	ArBr (%)	Acid (%)
DMF	DBU	0.025 M	**85**	5	38
DMF	TMG	0.025 M	**96**	0	20
DMF	BTMG	0.025 M	**91**	0	26
DMF	MTBD	0.025 M	**48**	21	43
DMF	DBU	0.05 M	**31**	57	91
DMF	TMG	0.05 M	**82**	0	34
DMF	BTMG	0.05 M	**79**	2	38
DMF	MTBD	0.05 M	**59**	9	54
DMF	DBU	0.1 M	**70**	0	56
DMF	TMG	0.1 M	**76**	0	43
DMF	BTMG	0.1 M	**72**	3	43
DMF	MTBD	0.1 M	**55**	14	70
DMA	DBU	0.025 M	**45**	36	71
DMA	TMG	0.025 M	**52**	31	35
DMA	BTMG	0.025 M	**86**	6	22
DMA	MTBD	0.025 M	**39**	31	58
DMA	DBU	0.05 M	**68**	15	77
DMA	TMG	0.05 M	**70**	18	39
DMA	BTMG	0.05 M	**86**	3	34
DMA	MTBD	0.05 M	**47**	21	70
DMA	DBU	0.1 M	**77**	26	76
DMA	TMG	0.1 M	**78**	8	42
DMA	BTMG	0.1 M	**84**	0	33

DMA	MTBD	0.1 M	**50**	19	70
DMSO:DMF	DBU	0.025 M	**29**	51	81
DMSO:DMF	TMG	0.025 M	**81**	12	21
DMSO:DMF	BTMG	0.025 M	**82**	14	35
DMSO:DMF	MTBD	0.025 M	**34**	45	66
DMSO:DMF	DBU	0.05 M	**30**	50	114
DMSO:DMF	TMG	0.05 M	**84**	9	37
DMSO:DMF	BTMG	0.05 M	**79**	19	43
DMSO:DMF	MTBD	0.05 M	**36**	34	66
DMSO:DMF	DBU	0.1 M	**70**	20	75
DMSO:DMF	TMG	0.1 M	**85**	5	40
DMSO:DMF	BTMG	0.1 M	**77**	16	40
DMSO:DMF	MTBD	0.1 M	**37**	40	72
dioxane	DBU	0.025 M	**0**	98	130
dioxane	TMG	0.025 M	**6**	96	126
dioxane	BTMG	0.025 M	**9**	96	126
dioxane	MTBD	0.025 M	**6**	96	128
dioxane	DBU	0.05 M	**5**	94	139
dioxane	TMG	0.05 M	**7**	91	133
dioxane	BTMG	0.05 M	**7**	91	138
dioxane	MTBD	0.05 M	**6**	92	134
dioxane	DBU	0.1 M	**6**	86	144
dioxane	TMG	0.1 M	**9**	84	138
dioxane	BTMG	0.1 M	**7**	87	144
dioxane	MTBD	0.1 M	**6**	87	141

Data from Fig. S10. Base screening in different solvents at 0.1 M.

Solvent	Base	Product (%)	ArBr (%)	Acid (%)
DMF	Et_3N	**0**	60	140
DMF	lutidine	**0**	61	136
DMF	DBU	**70**	0	56
DMF	TMG	**72**	0	38
DMF	BTMG	**76**	0	34
DMF	BEMP	**74**	0	36
DMF	DBN	**38**	36	67
DMF	MTBD	**55**	14	70
DMA	Et_3N	**0**	58	149
DMA	lutidine	**0**	57	147

DMA	DBU	**77**	16	76
DMA	TMG	**78**	8	42
DMA	BTMG	**78**	0	40
DMA	BEMP	**72**	0	52
DMA	DBN	**62**	22	68
DMA	MTBD	**49**	19	70
DMSO:DMF	Et_3N	**0**	69	144
DMSO:DMF	lutidine	**0**	72	140
DMSO:DMF	DBU	**70**	20	75
DMSO:DMF	TMG	**78**	0	31
DMSO:DMF	BTMG	**78**	0	30
DMSO:DMF	BEMP	**75**	0	39
DMSO:DMF	DBN	**56**	28	64
DMSO:DMF	MTBD	**37**	40	72
dioxane	Et_3N	**0**	67	142
dioxane	lutidine	**0**	62	140
dioxane	DBU	**6**	86	144
dioxane	TMG	**9**	84	138
dioxane	BTMG	**14**	69	121
dioxane	BEMP	**8**	71	132
dioxane	DBN	**22**	37	78
dioxane	MTBD	**6**	87	141

Data from Fig. S11. Photocatalyst (1 mol%) vs nickel source (5 mol%) and bases (1.5 equiv).

Solvent	Ni source	Base loading	Photocatalyst	Product (%)	ArBr (%)	Acid (%)
DMSO:DMF	$NiCl_2{\cdot}6H_2O$	1.5 equiv TMG	$[Ir(dF(CF_3)ppy)_2dtbbpy]PF_6$	**72**	23	63
DMSO:DMF	$NiCl_2$-dme	1.5 equiv TMG	$[Ir(dF(CF_3)ppy)_2dtbbpy]PF_6$	**72**	24	69
DMSO:DMF	$NiBr_2{\cdot}6H_2O$	1.5 equiv TMG	$[Ir(dF(CF_3)ppy)_2dtbbpy]PF_6$	**80**	14	59
DMSO:DMF	$NiCl_2{\cdot}6H_2O$	2 equiv TMG	$[Ir(dF(CF_3)ppy)_2dtbbpy]PF_6$	**73**	20	59
DMSO:DMF	$NiCl_2$-dme	2 equiv TMG	$[Ir(dF(CF_3)ppy)_2dtbbpy]PF_6$	**71**	23	67
DMSO:DMF	$NiBr_2{\cdot}6H_2O$	2 equiv TMG	$[Ir(dF(CF_3)ppy)_2dtbbpy]PF_6$	**74**	18	60
DMA	$NiCl_2{\cdot}6H_2O$	1.5 equiv TMG	$[Ir(dF(CF_3)ppy)_2dtbbpy]PF_6$	**85**	2	43
DMA	$NiCl_2$-dme	1.5 equiv TMG	$[Ir(dF(CF_3)ppy)_2dtbbpy]PF_6$	**79**	11	52
DMA	$NiBr_2{\cdot}6H_2O$	1.5 equiv TMG	$[Ir(dF(CF_3)ppy)_2dtbbpy]PF_6$	**82**	9	51
DMA	$NiCl_2{\cdot}6H_2O$	2 equiv TMG	$[Ir(dF(CF_3)ppy)_2dtbbpy]PF_6$	**65**	32	71
DMA	$NiCl_2$-dme	2 equiv TMG	$[Ir(dF(CF_3)ppy)_2dtbbpy]PF_6$	**55**	42	81
DMA	$NiBr_2{\cdot}6H_2O$	2 equiv TMG	$[Ir(dF(CF_3)ppy)_2dtbbpy]PF_6$	**58**	38	77
DMSO:DMF	$NiCl_2{\cdot}6H_2O$	1.5 equiv TMG	$[Ir(dF(Me)ppy)_2dtbbpy]PF_6$	**86**	1	42

DMSO:DMF	$NiCl_2$-dme	1.5 equiv TMG	$[Ir(dF(Me)ppy)_2dtbbpy]PF_6$	**64**	27	68
DMSO:DMF	$NiBr_2{\cdot}6H_2O$	1.5 equiv TMG	$[Ir(dF(Me)ppy)_2dtbbpy]PF_6$	**88**	1	43
DMSO:DMF	$NiCl_2{\cdot}6H_2O$	2 equiv TMG	$[Ir(dF(Me)ppy)_2dtbbpy]PF_6$	**87**	2	38
DMSO:DMF	$NiCl_2$-dme	2 equiv TMG	$[Ir(dF(Me)ppy)_2dtbbpy]PF_6$	**76**	13	53
DMSO:DMF	$NiBr_2{\cdot}6H_2O$	2 equiv TMG	$[Ir(dF(Me)ppy)_2dtbbpy]PF_6$	**89**	1	39
DMA	$NiCl_2{\cdot}6H_2O$	1.5 equiv TMG	$[Ir(dF(Me)ppy)_2dtbbpy]PF_6$	**90**	0	35
DMA	$NiCl_2$-dme	1.5 equiv TMG	$[Ir(dF(Me)ppy)_2dtbbpy]PF_6$	**88**	1	38
DMA	$NiBr_2{\cdot}6H_2O$	1.5 equiv TMG	$[Ir(dF(Me)ppy)_2dtbbpy]PF_6$	**86**	1	39
DMA	$NiCl_2{\cdot}6H_2O$	2 equiv TMG	$[Ir(dF(Me)ppy)_2dtbbpy]PF_6$	**89**	2	41
DMA	$NiCl_2$-dme	2 equiv TMG	$[Ir(dF(Me)ppy)_2dtbbpy]PF_6$	**82**	11	50
DMA	$NiBr_2{\cdot}6H_2O$	2 equiv TMG	$[Ir(dF(Me)ppy)_2dtbbpy]PF_6$	**85**	5	44
DMSO:DMF	$NiCl_2{\cdot}6H_2O$	1.5 equiv TMG	4CzIPN	**84**	3	48
DMSO:DMF	$NiCl_2$-dme	1.5 equiv TMG	4CzIPN	**82**	5	51
DMSO:DMF	$NiBr_2{\cdot}6H_2O$	1.5 equiv TMG	4CzIPN	**82**	4	51
DMSO:DMF	$NiCl_2{\cdot}6H_2O$	2 equiv TMG	4CzIPN	**85**	2	49
DMSO:DMF	$NiCl_2$-dme	2 equiv TMG	4CzIPN	**87**	3	48
DMSO:DMF	$NiBr_2{\cdot}6H_2O$	2 equiv TMG	4CzIPN	**85**	2	50
DMA	$NiCl_2{\cdot}6H_2O$	1.5 equiv TMG	4CzIPN	**85**	2	44
DMA	$NiCl_2$-dme	1.5 equiv TMG	4CzIPN	**82**	2	47
DMA	$NiBr_2{\cdot}6H_2O$	1.5 equiv TMG	4CzIPN	**82**	2	48
DMA	$NiCl_2{\cdot}6H_2O$	2 equiv TMG	4CzIPN	**81**	7	56
DMA	$NiCl_2$-dme	2 equiv TMG	4CzIPN	**77**	12	59
DMA	$NiBr_2{\cdot}6H_2O$	2 equiv TMG	4CzIPN	**75**	15	61
DMSO:DMF	$NiCl_2{\cdot}6H_2O$	1.5 equiv TMG	2CzPN	**8**	78	133
DMSO:DMF	$NiCl_2$-dme	1.5 equiv TMG	2CzPN	**7**	79	134
DMSO:DMF	$NiBr_2{\cdot}6H_2O$	1.5 equiv TMG	2CzPN	**8**	79	133
DMSO:DMF	$NiCl_2{\cdot}6H_2O$	2 equiv TMG	2CzPN	**5**	83	134
DMSO:DMF	$NiCl_2$-dme	2 equiv TMG	2CzPN	**9**	80	133
DMSO:DMF	$NiBr_2{\cdot}6H_2O$	2 equiv TMG	2CzPN	**7**	83	134
DMA	$NiCl_2{\cdot}6H_2O$	1.5 equiv TMG	2CzPN	**11**	77	126
DMA	$NiCl_2$-dme	1.5 equiv TMG	2CzPN	**11**	76	127
DMA	$NiBr_2{\cdot}6H_2O$	1.5 equiv TMG	2CzPN	**9**	77	126
DMA	$NiCl_2{\cdot}6H_2O$	2 equiv TMG	2CzPN	**8**	83	128
DMA	$NiCl_2$-dme	2 equiv TMG	2CzPN	**8**	83	129
DMA	$NiBr_2{\cdot}6H_2O$	2 equiv TMG	2CzPN	**9**	83	129

Data from Fig. S11. Photocatalyst (1 mol%) vs nickel source (5 mol%) and bases (1.5 equiv).

Photocatalyst	Base	Nickel Source	Product (%)	ArBr (%)	Acid (%)
$[Ir(dF(CF_3)ppy)_2dtbbpy]PF_6$	TMG	$NiCl_2{\cdot}6H_2O$	**80**	31	78

$[Ir(dF(CF_3)ppy)_2dtbbpy]PF_6$	DBU	$NiCl_2{\cdot}6H_2O$	**79**	15	65
$[Ir(dF(CF_3)ppy)_2dtbbpy]PF_6$	BTMG	$NiCl_2{\cdot}6H_2O$	**76**	22	63
$[Ir(dF(CF_3)ppy)_2dtbbpy]PF_6$	TMG	$NiBr_2{\cdot}6H_2O$	**79**	18	62
$[Ir(dF(CF_3)ppy)_2dtbbpy]PF_6$	DBU	$NiBr_2{\cdot}6H_2O$	**59**	36	88
$[Ir(dF(CF_3)ppy)_2dtbbpy]PF_6$	BTMG	$NiBr_2{\cdot}6H_2O$	**70**	31	73
$[Ir(dF(Me)ppy)_2dtbbpy]PF_6$	TMG	$NiCl_2{\cdot}6H_2O$	**102**	2	65
$[Ir(dF(Me)ppy)_2dtbbpy]PF_6$	DBU	$NiCl_2{\cdot}6H_2O$	**95**	5	78
$[Ir(dF(Me)ppy)_2dtbbpy]PF_6$	BTMG	$NiCl_2{\cdot}6H_2O$	**93**	0	69
$[Ir(dF(Me)ppy)_2dtbbpy]PF_6$	TMG	$NiBr_2{\cdot}6H_2O$	**97**	0	nd
$[Ir(dF(Me)ppy)_2dtbbpy]PF_6$	DBU	$NiBr_2{\cdot}6H_2O$	**65**	0	nd
$[Ir(dF(Me)ppy)_2dtbbpy]PF_6$	BTMG	$NiBr_2{\cdot}6H_2O$	**105**	0	nd
4CzIPN	TMG	$NiCl_2{\cdot}6H_2O$	**95**	7	67
4CzIPN	DBU	$NiCl_2{\cdot}6H_2O$	**84**	18	84
4CzIPN	BTMG	$NiCl_2{\cdot}6H_2O$	**97**	0	0
4CzIPN	TMG	$NiBr_2{\cdot}6H_2O$	**91**	0	75
4CzIPN	DBU	$NiBr_2{\cdot}6H_2O$	**71**	22	96
4CzIPN	BTMG	$NiBr_2{\cdot}6H_2O$	**87**	4	91

Data from Fig. S12. Concentration vs nickel source (5 mol%) and bases (1.5 equiv).

Pcat	Base	Nickel source	Concentration	c	ArBr (%)	Acid (%)
$[Ir(dF(Me)ppy)_2dtbbpy]PF_6$	TMG	$NiCl_2{\cdot}6H_2O$	0.2M	**85**	0	47
$[Ir(dF(Me)ppy)_2dtbbpy]PF_6$	DBU	$NiCl_2{\cdot}6H_2O$	0.2M	**83**	10	59
$[Ir(dF(Me)ppy)_2dtbbpy]PF_6$	TMG	$NiBr_2{\cdot}6H_2O$	0.2M	**71**	27	67
$[Ir(dF(Me)ppy)_2dtbbpy]PF_6$	DBU	$NiBr_2{\cdot}6H_2O$	0.2M	**80**	12	62
4CzIPN	TMG	$NiCl_2{\cdot}6H_2O$	0.2M	**85**	6	53
4CzIPN	DBU	$NiCl_2{\cdot}6H_2O$	0.2M	**74**	19	71
4CzIPN	TMG	$NiBr_2{\cdot}6H_2O$	0.2M	**80**	19	76
4CzIPN	DBU	$NiBr_2{\cdot}6H_2O$	0.2M	**77**	17	66
$[Ir(dF(Me)ppy)_2dtbbpy]PF_6$	TMG	$NiCl_2{\cdot}6H_2O$	0.4 M	**90**	71	55
$[Ir(dF(Me)ppy)_2dtbbpy]PF_6$	DBU	$NiCl_2{\cdot}6H_2O$	0.4 M	**73**	18	66
$[Ir(dF(Me)ppy)_2dtbbpy]PF_6$	TMG	$NiBr_2{\cdot}6H_2O$	0.4 M	**70**	26	69
$[Ir(dF(Me)ppy)_2dtbbpy]PF_6$	DBU	$NiBr_2{\cdot}6H_2O$	0.4 M	**72**	16	65
4CzIPN	TMG	$NiCl_2{\cdot}6H_2O$	0.4 M	**77**	5	55
4CzIPN	DBU	$NiCl_2{\cdot}6H_2O$	0.4 M	**74**	19	70
4CzIPN	TMG	$NiBr_2{\cdot}6H_2O$	0.4 M	**67**	18	76
4CzIPN	DBU	$NiBr_2{\cdot}6H_2O$	0.4 M	**70**	20	68
$[Ir(dF(Me)ppy)_2dtbbpy]PF_6$	TMG	$NiCl_2{\cdot}6H_2O$	0.6 M	**71**	18	63
$[Ir(dF(Me)ppy)_2dtbbpy]PF_6$	DBU	$NiCl_2{\cdot}6H_2O$	0.6 M	**66**	21	70

$[Ir(dF(Me)ppy)_2dtbbpy]PF_6$	TMG	$NiBr_2{\cdot}6H_2O$	0.6 M	**62**	33	78
$[Ir(dF(Me)ppy)_2dtbbpy]PF_6$	DBU	$NiBr_2{\cdot}6H_2O$	0.6 M	**68**	20	69
4CzIPN	TMG	$NiCl_2{\cdot}6H_2O$	0.6 M	**71**	5	58
4CzIPN	DBU	$NiCl_2{\cdot}6H_2O$	0.6 M	**66**	21	73
4CzIPN	TMG	$NiBr_2{\cdot}6H_2O$	0.6 M	**62**	18	79
4CzIPN	DBU	$NiBr_2{\cdot}6H_2O$	0.6 M	**64**	23	72
$[Ir(dF(Me)ppy)_2dtbbpy]PF_6$	TMG	$NiCl_2{\cdot}6H_2O$	0.8 M	**56**	34	78
$[Ir(dF(Me)ppy)_2dtbbpy]PF_6$	DBU	$NiCl_2{\cdot}6H_2O$	0.8 M	**61**	26	75
$[Ir(dF(Me)ppy)_2dtbbpy]PF_6$	TMG	$NiBr_2{\cdot}6H_2O$	0.8 M	**48**	46	92
$[Ir(dF(Me)ppy)_2dtbbpy]PF_6$	DBU	$NiBr_2{\cdot}6H_2O$	0.8 M	**68**	22	72
4CzIPN	TMG	$NiCl_2{\cdot}6H_2O$	0.8 M	**64**	6	63
4CzIPN	DBU	$NiCl_2{\cdot}6H_2O$	0.8 M	**61**	23	77
4CzIPN	TMG	$NiBr_2{\cdot}6H_2O$	0.8 M	**62**	19	82
4CzIPN	DBU	$NiBr_2{\cdot}6H_2O$	0.8 M	**59**	28	79

Data from Fig. S13. Photocatalyst loading vs Nickel loading using $[Ir(dF(Me)ppy)_2dtbbpy]PF_6$ as photocatalyst and TMG as base in DMA (0.2M).

Nickel Source loading	Photocatalyst loading	Product (%)	ArBr (%)	Acid (%)
1 mol%	0.2 mol%	**74**	25	75
1 mol%	0.4 mol%	**71**	24	64
1 mol%	0.6 mol%	**38**	54	85
1 mol%	0.8 mol%	**27**	61	91
1 mol%	1 mol%	**31**	59	86
1 mol%	1.2 mol%	**25**	64	92
5 mol%	0.2 mol%	**77**	16	62
5 mol%	0.4 mol%	**86**	3	50
5 mol%	0.6 mol%	**89**	0	44
5 mol%	0.8 mol%	**89**	0	42
5 mol%	1 mol%	**90**	0	40
5 mol%	1.2 mol%	**88**	0	41
10 mol%	0.2 mol%	**71**	19	66
10 mol%	0.4 mol%	**83**	4	53
10 mol%	0.6 mol%	**86**	0	47
10 mol%	0.8 mol%	**87**	0	44
10 mol%	1 mol%	**88**	0	43
10 mol%	1.2 mol%	**88**	0	41
15 mol%	0.2 mol%	**67**	22	68
15 mol%	0.4 mol%	**77**	9	57
15 mol%	0.6 mol%	**82**	2	51

15 mol%	0.8 mol%	**84**	0	48
15 mol%	1 mol%	**86**	0	45
15 mol%	1.2 mol%	**87**	0	44

Data from Fig. S13. Photocatalyst loading vs Nickel loading using 4CzIPN as photocatalyst and TMG as base in DMA (0.2M).

Nickel Source loading	Photocatalyst loading	Product (%)	ArBr (%)	Acid (%)
1 mol%	0.2 mol%	**58**	32	78
1 mol%	0.4 mol%	**71**	20	65
1 mol%	0.6 mol%	**76**	14	58
1 mol%	0.8 mol%	**59**	28	64
1 mol%	1 mol%	**29**	57	87
1 mol%	1.2 mol%	**26**	59	89
5 mol%	0.2 mol%	**59**	26	74
5 mol%	0.4 mol%	**70**	14	62
5 mol%	0.6 mol%	**75**	8	56
5 mol%	0.8 mol%	**78**	5	53
5 mol%	1 mol%	**81**	3	50
5 mol%	1.2 mol%	**81**	3	49
10 mol%	0.2 mol%	**67**	20	67
10 mol%	0.4 mol%	**80**	6	53
10 mol%	0.6 mol%	**84**	0	47
10 mol%	0.8 mol%	**85**	0	45
10 mol%	1 mol%	**85**	0	43
10 mol%	1.2 mol%	**85**	0	43
15 mol%	0.2 mol%	**62**	26	73
15 mol%	0.4 mol%	**79**	4	52
15 mol%	0.6 mol%	**83**	0	46
15 mol%	0.8 mol%	**84**	0	43
15 mol%	1 mol%	**85**	0	42
15 mol%	1.2 mol%	**86**	0	41

Data from Fig. S14. Photocatalyst loading vs Nickel loading using $[Ir(dF(Me)ppy)_2dtbbpy]PF_6$ as photocatalyst and DBU as base in DMA (0.4M).

Nickel Source loading	Photocatalyst loading	Product (%)	ArBr (%)	Acid (%)
1 mol%	0.2 mol%	**62**	37	85
1 mol%	0.4 mol%	**65**	29	79

1 mol%	0.6 mol%	**62**	30	78
1 mol%	0.8 mol%	**59**	34	79
1 mol%	1 mol%	**54**	36	81
1 mol%	1.2 mol%	**40**	51	91
5 mol%	0.2 mol%	**61**	31	81
5 mol%	0.4 mol%	**68**	22	73
5 mol%	0.6 mol%	**73**	15	68
5 mol%	0.8 mol%	**74**	12	64
5 mol%	1 mol%	**78**	9	61
5 mol%	1.2 mol%	**77**	9	61
10 mol%	0.2 mol%	**52**	36	85
10 mol%	0.4 mol%	**60**	26	77
10 mol%	0.6 mol%	**66**	19	71
10 mol%	0.8 mol%	**69**	15	68
10 mol%	1 mol%	**70**	14	65
10 mol%	1.2 mol%	**72**	11	63
15 mol%	0.2 mol%	**78**	20	116
15 mol%	0.4 mol%	**52**	34	84
15 mol%	0.6 mol%	**58**	26	79
15 mol%	0.8 mol%	**61**	23	75
15 mol%	1 mol%	**59**	23	76
15 mol%	1.2 mol%	**61**	21	74

Data from Fig. S14. Photocatalyst loading vs Nickel loading using 4CzIPN as photocatalyst and DBU as base in DMA (0.4M).

Nickel Source loading	Photocatalyst loading	Product (%)	ArBr (%)	Acid (%)
1 mol%	0.2 mol%	**47**	43	93
1 mol%	0.4 mol%	**56**	33	84
1 mol%	0.6 mol%	**61**	26	77
1 mol%	0.8 mol%	**63**	23	73
1 mol%	1 mol%	**65**	21	70
1 mol%	1.2 mol%	**64**	22	70
5 mol%	0.2 mol%	**58**	28	81
5 mol%	0.4 mol%	**68**	14	68
5 mol%	0.6 mol%	**73**	7	61
5 mol%	0.8 mol%	**76**	5	58
5 mol%	1 mol%	**76**	4	57
5 mol%	1.2 mol%	**77**	3	57
10 mol%	0.2 mol%	**63**	22	75

10 mol%	0.4 mol%	**71**	9	64
10 mol%	0.6 mol%	**74**	6	61
10 mol%	0.8 mol%	**73**	5	60
10 mol%	1 mol%	**74**	5	60
10 mol%	1.2 mol%	**75**	5	59
15 mol%	0.2 mol%	**60**	24	78
15 mol%	0.4 mol%	**67**	14	69
15 mol%	0.6 mol%	**66**	11	67
15 mol%	0.8 mol%	**67**	10	66
15 mol%	1 mol%	**68**	10	65
15 mol%	1.2 mol%	**69**	11	65

8.4. Data from Decarboxylative alkylation. C–N coupling.

Data from Fig. S20. Photocatalyst vs copper loading and solvents.

Time	Cu loading	Photocatalyst	Solvent	Product (%)	Indazole (%)	Iodo-mesytilene (%)
2 min	5 mol%	$Ir(ppy)_3$	dioxane	**0**	115	119
2 min	10 mol%	$Ir(ppy)_3$	dioxane	**12**	87	104
2 min	25 mol%	$Ir(ppy)_3$	dioxane	**34**	79	111
2 min	50 mol%	$Ir(ppy)_3$	dioxane	**40**	78	40
2 min	5 mol%	$Ir[F(Me)ppy_2dtbbpy]PF_6$	dioxane	**7**	83	0
2 min	10 mol%	$Ir[F(Me)ppy_2dtbbpy]PF_6$	dioxane	**5**	142	0
2 min	25 mol%	$Ir[F(Me)ppy_2dtbbpy]PF_6$	dioxane	**12**	132	0
2 min	50 mol%	$Ir[F(Me)ppy_2dtbbpy]PF_6$	dioxane	**11**	131	0
2 min	5 mol%	4CzIPN	dioxane	**18**	127	0
2 min	10 mol%	4CzIPN	dioxane	**21**	102	103
2 min	25 mol%	4CzIPN	dioxane	**16**	108	0
2 min	50 mol%	4CzIPN	dioxane	**15**	117	0
2 min	5 mol%	$Ir(ppy)_3$	DME	**27**	109	125
2 min	10 mol%	$Ir(ppy)_3$	DME	**26**	111	0
2 min	25 mol%	$Ir(ppy)_3$	DME	**25**	215	0
2 min	50 mol%	$Ir(ppy)_3$	DME	**41**	106	0
2 min	5 mol%	$Ir[F(Me)ppy_2dtbbpy]PF_6$	DME	**9**	145	0
2 min	10 mol%	$Ir[F(Me)ppy_2dtbbpy]PF_6$	DME	**0**	153	0
2 min	25 mol%	$Ir[F(Me)ppy_2dtbbpy]PF_6$	DME	**0**	202	0
2 min	50 mol%	$Ir[F(Me)ppy_2dtbbpy]PF_6$	DME	**9**	152	0
2 min	5 mol%	4CzIPN	DME	**18**	134	0
2 min	10 mol%	4CzIPN	DME	**8**	128	0

2 min	25 mol%	4CzIPN	DME	**0**	193	0
2 min	50 mol%	4CzIPN	DME	**4**	136	0
2 min	5 mol%	$Ir(ppy)_3$	2-Me-THF	**20**	156	0
2 min	10 mol%	$Ir(ppy)_3$	2-Me-THF	**22**	111	0
2 min	25 mol%	$Ir(ppy)_3$	2-Me-THF	**18**	107	0
2 min	50 mol%	$Ir(ppy)_3$	2-Me-THF	**25**	104	0
2 min	5 mol%	$Ir[F(Me)ppy_2dtbbpy]PF_6$	2-Me-THF	**0**	177	0
2 min	10 mol%	$Ir[F(Me)ppy_2dtbbpy]PF_6$	2-Me-THF	**6**	145	0
2 min	25 mol%	$Ir[F(Me)ppy_2dtbbpy]PF_6$	2-Me-THF	**0**	148	0
2 min	50 mol%	$Ir[F(Me)ppy_2dtbbpy]PF_6$	2-Me-THF	**7**	145	0
2 min	5 mol%	4CzIPN	2-Me-THF	**11**	136	0
2 min	10 mol%	4CzIPN	2-Me-THF	**5**	135	0
2 min	25 mol%	4CzIPN	2-Me-THF	**9**	137	0
2 min	50 mol%	4CzIPN	2-Me-THF	**11**	136	0
2 min	5 mol%	$Ir(ppy)_3$	DMA	**28**	98	183
2 min	10 mol%	$Ir(ppy)_3$	DMA	**43**	74	173
2 min	25 mol%	$Ir(ppy)_3$	DMA	**24**	96	132
2 min	50 mol%	$Ir(ppy)_3$	DMA	**44**	334	39
2 min	5 mol%	$Ir[F(Me)ppy_2dtbbpy]PF_6$	DMA	**0**	134	134
2 min	10 mol%	$Ir[F(Me)ppy_2dtbbpy]PF_6$	DMA	**19**	111	182
2 min	25 mol%	$Ir[F(Me)ppy_2dtbbpy]PF_6$	DMA	**22**	109	142
2 min	50 mol%	$Ir[F(Me)ppy_2dtbbpy]PF_6$	DMA	**25**	112	182
2 min	5 mol%	4CzIPN	DMA	**8**	84	0
2 min	10 mol%	4CzIPN	DMA	**25**	109	0
2 min	25 mol%	4CzIPN	DMA	**18**	112	0
2 min	50 mol%	4CzIPN	DMA	**23**	110	0
5 min	5 mol%	$Ir(ppy)_3$	dioxane	**18**	90	129
5 min	10 mol%	$Ir(ppy)_3$	dioxane	**38**	121	198
5 min	25 mol%	$Ir(ppy)_3$	dioxane	**59**	31	150
5 min	50 mol%	$Ir(ppy)_3$	dioxane	**54**	26	0
5 min	5 mol%	$Ir[F(Me)ppy_2dtbbpy]PF_6$	dioxane	**12**	0	62
5 min	10 mol%	$Ir[F(Me)ppy_2dtbbpy]PF_6$	dioxane	**33**	85	0
5 min	25 mol%	$Ir[F(Me)ppy_2dtbbpy]PF_6$	dioxane	**31**	86	0
5 min	50 mol%	$Ir[F(Me)ppy_2dtbbpy]PF_6$	dioxane	**30**	85	0
5 min	5 mol%	4CzIPN	dioxane	**28**	129	0
5 min	10 mol%	4CzIPN	dioxane	**52**	39	0
5 min	25 mol%	4CzIPN	dioxane	**56**	31	0
5 min	50 mol%	4CzIPN	dioxane	**75**	19	0
5 min	5 mol%	$Ir(ppy)_3$	DME	**38**	80	0
5 min	10 mol%	$Ir(ppy)_3$	DME	**38**	82	0

5 min	25 mol%	$Ir(ppy)_3$	DME	**36**	83	0
5 min	50 mol%	$Ir(ppy)_3$	DME	**54**	76	0
5 min	5 mol%	$Ir[F(Me)ppy_2dtbbpy]PF_6$	DME	**16**	121	0
5 min	10 mol%	$Ir[F(Me)ppy_2dtbbpy]PF_6$	DME	**24**	115	0
5 min	25 mol%	$Ir[F(Me)ppy_2dtbbpy]PF_6$	DME	**22**	121	0
5 min	50 mol%	$Ir[F(Me)ppy_2dtbbpy]PF_6$	DME	**20**	122	0
5 min	5 mol%	4CzIPN	DME	**44**	94	0
5 min	10 mol%	4CzIPN	DME	**34**	87	0
5 min	25 mol%	4CzIPN	DME	**38**	90	0
5 min	50 mol%	4CzIPN	DME	**40**	83	0
5 min	5 mol%	$Ir(ppy)_3$	2-Me-THF	**45**	74	0
5 min	10 mol%	$Ir(ppy)_3$	2-Me-THF	**36**	83	0
5 min	25 mol%	$Ir(ppy)_3$	2-Me-THF	**34**	83	0
5 min	50 mol%	$Ir(ppy)_3$	2-Me-THF	**48**	73	0
5 min	5 mol%	$Ir[F(Me)ppy_2dtbbpy]PF_6$	2-Me-THF	**7**	143	0
5 min	10 mol%	$Ir[F(Me)ppy_2dtbbpy]PF_6$	2-Me-THF	**9**	140	0
5 min	25 mol%	$Ir[F(Me)ppy_2dtbbpy]PF_6$	2-Me-THF	**6**	143	0
5 min	50 mol%	$Ir[F(Me)ppy_2dtbbpy]PF_6$	2-Me-THF	**9**	137	0
5 min	5 mol%	4CzIPN	2-Me-THF	**25**	107	0
5 min	10 mol%	4CzIPN	2-Me-THF	**22**	113	0
5 min	25 mol%	4CzIPN	2-Me-THF	**17**	119	0
5 min	50 mol%	4CzIPN	2-Me-THF	**26**	106	0
5 min	5 mol%	$Ir(ppy)_3$	DMA	**26**	103	0
5 min	10 mol%	$Ir(ppy)_3$	DMA	**44**	59	0
5 min	25 mol%	$Ir(ppy)_3$	DMA	**25**	109	0
5 min	50 mol%	$Ir(ppy)_3$	DMA	**52**	56	0
5 min	5 mol%	$Ir[F(Me)ppy_2dtbbpy]PF_6$	DMA	**42**	84	0
5 min	10 mol%	$Ir[F(Me)ppy_2dtbbpy]PF_6$	DMA	**45**	61	0
5 min	25 mol%	$Ir[F(Me)ppy_2dtbbpy]PF_6$	DMA	**44**	75	0
5 min	50 mol%	$Ir[F(Me)ppy_2dtbbpy]PF_6$	DMA	**43**	75	0
5 min	5 mol%	4CzIPN	DMA	**40**	78	0
5 min	10 mol%	4CzIPN	DMA	**42**	76	0
5 min	25 mol%	4CzIPN	DMA	**36**	78	0
5 min	50 mol%	4CzIPN	DMA	**39**	79	0
10 min	5 mol%	$Ir(ppy)_3$	dioxane	**16**	91	0
10 min	10 mol%	$Ir(ppy)_3$	dioxane	**66**	14	0
10 min	25 mol%	$Ir(ppy)_3$	dioxane	**74**	7	0
10 min	50 mol%	$Ir(ppy)_3$	dioxane	**75**	4	0
10 min	5 mol%	$Ir[F(Me)ppy_2dtbbpy]PF_6$	dioxane	**52**	46	0
10 min	10 mol%	$Ir[F(Me)ppy_2dtbbpy]PF_6$	dioxane	**71**	23	0

10 min	25 mol%	Ir[F(Me)ppy$_2$dtbbpy]PF$_6$	dioxane	**63**	19	0
10 min	50 mol%	Ir[F(Me)ppy$_2$dtbbpy]PF$_6$	dioxane	**69**	20	0
10 min	5 mol%	4CzIPN	dioxane	**35**	67	0
10 min	10 mol%	4CzIPN	dioxane	**81**	2	0
10 min	25 mol%	4CzIPN	dioxane	**82**	0	0
10 min	50 mol%	4CzIPN	dioxane	**81**	2	0
10 min	5 mol%	Ir(ppy)$_3$	DME	**54**	62	0
10 min	10 mol%	Ir(ppy)$_3$	DME	**52**	66	0
10 min	25 mol%	Ir(ppy)$_3$	DME	**42**	87	0
10 min	50 mol%	Ir(ppy)$_3$	DME	**70**	29	0
10 min	5 mol%	Ir[F(Me)ppy$_2$dtbbpy]PF$_6$	DME	**40**	94	0
10 min	10 mol%	Ir[F(Me)ppy$_2$dtbbpy]PF$_6$	DME	**47**	75	0
10 min	25 mol%	Ir[F(Me)ppy$_2$dtbbpy]PF$_6$	DME	**50**	76	0
10 min	50 mol%	Ir[F(Me)ppy$_2$dtbbpy]PF$_6$	DME	**47**	82	0
10 min	5 mol%	4CzIPN	DME	**65**	38	0
10 min	10 mol%	4CzIPN	DME	**65**	47	0
10 min	25 mol%	4CzIPN	DME	**62**	53	0
10 min	50 mol%	4CzIPN	DME	**70**	37	0
10 min	5 mol%	Ir(ppy)$_3$	2-Me-THF	**48**	61	0
10 min	10 mol%	Ir(ppy)$_3$	2-Me-THF	**48**	55	0
10 min	25 mol%	Ir(ppy)$_3$	2-Me-THF	**57**	43	0
10 min	50 mol%	Ir(ppy)$_3$	2-Me-THF	**58**	39	0
10 min	5 mol%	Ir[F(Me)ppy$_2$dtbbpy]PF$_6$	2-Me-THF	**21**	127	0
10 min	10 mol%	Ir[F(Me)ppy$_2$dtbbpy]PF$_6$	2-Me-THF	**10**	134	0
10 min	25 mol%	Ir[F(Me)ppy$_2$dtbbpy]PF$_6$	2-Me-THF	**14**	129	0
10 min	50 mol%	Ir[F(Me)ppy$_2$dtbbpy]PF$_6$	2-Me-THF	**19**	121	0
10 min	5 mol%	4CzIPN	2-Me-THF	**57**	47	0
10 min	10 mol%	4CzIPN	2-Me-THF	**39**	72	0
10 min	25 mol%	4CzIPN	2-Me-THF	**45**	65	0
10 min	50 mol%	4CzIPN	2-Me-THF	**52**	62	0
10 min	5 mol%	Ir(ppy)$_3$	DMA	**45**	59	0
10 min	10 mol%	Ir(ppy)$_3$	DMA	**52**	40	0
10 min	25 mol%	Ir(ppy)$_3$	DMA	**60**	59	0
10 min	50 mol%	Ir(ppy)$_3$	DMA	**39**	56	0
10 min	5 mol%	Ir[F(Me)ppy$_2$dtbbpy]PF$_6$	DMA	**61**	30	0
10 min	10 mol%	Ir[F(Me)ppy$_2$dtbbpy]PF$_6$	DMA	**56**	27	0
10 min	25 mol%	Ir[F(Me)ppy$_2$dtbbpy]PF$_6$	DMA	**44**	61	0
10 min	50 mol%	Ir[F(Me)ppy$_2$dtbbpy]PF$_6$	DMA	**58**	34	0
10 min	5 mol%	4CzIPN	DMA	**56**	38	0
10 min	10 mol%	4CzIPN	DMA	**61**	29	0

10 min	25 mol%	4CzIPN	DMA	**44**	46	0
10 min	50 mol%	4CzIPN	DMA	**60**	30	0

Data from Fig. S21. Photocatalyst vs copper loading and reagent stoichiometry in dioxane (0.05 M).

Time	Cu loading	Photocatalyst	Acid : indazole ratio	Product (%)	Indazole (%)	Iodo-mesytilene (%)
5 min	10 mol%	$Ir(ppy)_3$	2:1	**17**	95	0
5 min	20 mol%	$Ir(ppy)_3$	2:1	**48**	55	0
5 min	30 mol%	$Ir(ppy)_3$	2:1	**61**	37	0
5 min	40 mol%	$Ir(ppy)_3$	2:1	**66**	29	0
5 min	50 mol%	$Ir(ppy)_3$	2:1	**63**	29	0
5 min	60 mol%	$Ir(ppy)_3$	2:1	**65**	34	0
5 min	10 mol%	$Ir(ppy)_3$	1:1	**28**	88	0
5 min	20 mol%	$Ir(ppy)_3$	1:1	**40**	67	0
5 min	30 mol%	$Ir(ppy)_3$	1:1	**41**	133	0
5 min	40 mol%	$Ir(ppy)_3$	1:1	**45**	65	0
5 min	50 mol%	$Ir(ppy)_3$	1:1	**45**	64	0
5 min	60 mol%	$Ir(ppy)_3$	1:1	**49**	63	0
5 min	10 mol%	$Ir(F\text{-}^tBuppy)_3$	2:1	**16**	100	0
5 min	20 mol%	$Ir(F\text{-}^tBuppy)_3$	2:1	**43**	63	0
5 min	30 mol%	$Ir(F\text{-}^tBuppy)_3$	2:1	**47**	54	0
5 min	40 mol%	$Ir(F\text{-}^tBuppy)_3$	2:1	**53**	48	0
5 min	50 mol%	$Ir(F\text{-}^tBuppy)_3$	2:1	**52**	47	0
5 min	60 mol%	$Ir(F\text{-}^tBuppy)_3$	2:1	**57**	40	0
5 min	10 mol%	$Ir(F\text{-}^tBuppy)_3$	1:1	**25**	88	0
5 min	20 mol%	$Ir(F\text{-}^tBuppy)_3$	1:1	**32**	79	0
5 min	30 mol%	$Ir(F\text{-}^tBuppy)_3$	1:1	**34**	73	0
5 min	40 mol%	$Ir(F\text{-}^tBuppy)_3$	1:1	**39**	69	0
5 min	50 mol%	$Ir(F\text{-}^tBuppy)_3$	1:1	**37**	73	0
5 min	60 mol%	$Ir(F\text{-}^tBuppy)_3$	1:1	**40**	71	0
5 min	10 mol%	4CzIPN	2:1	**21**	110	0
5 min	20 mol%	4CzIPN	2:1	**51**	49	0
5 min	30 mol%	4CzIPN	2:1	**64**	37	0
5 min	40 mol%	4CzIPN	2:1	**69**	25	0
5 min	50 mol%	4CzIPN	2:1	**67**	22	0
5 min	60 mol%	4CzIPN	2:1	**70**	25	0
5 min	10 mol%	4CzIPN	1:1	**31**	84	0
5 min	20 mol%	4CzIPN	1:1	**40**	68	0

5 min	30 mol%	4CzIPN	1:1	**41**	66	0
5 min	40 mol%	4CzIPN	1:1	**40**	74	0
5 min	50 mol%	4CzIPN	1:1	**38**	79	0
5 min	60 mol%	4CzIPN	1:1	**34**	87	0
5 min	10 mol%	2CzPN	2:1	**24**	97	0
5 min	20 mol%	2CzPN	2:1	**64**	24	0
5 min	30 mol%	2CzPN	2:1	**61**	29	0
5 min	40 mol%	2CzPN	2:1	**73**	12	0
5 min	50 mol%	2CzPN	2:1	**82**	2	0
5 min	60 mol%	2CzPN	2:1	**81**	1	0
5 min	10 mol%	2CzPN	1:1	**33**	74	0
5 min	20 mol%	2CzPN	1:1	**42**	60	0
5 min	30 mol%	2CzPN	1:1	**50**	43	0
5 min	40 mol%	2CzPN	1:1	**48**	50	0
5 min	50 mol%	2CzPN	1:1	**49**	40	0
5 min	60 mol%	2CzPN	1:1	**61**	30	0
10 min	10 mol%	$Ir(ppy)_3$	2:1	**29**	76	0
10 min	20 mol%	$Ir(ppy)_3$	2:1	**44**	55	0
10 min	30 mol%	$Ir(ppy)_3$	2:1	**73**	12	0
10 min	40 mol%	$Ir(ppy)_3$	2:1	**78**	7	0
10 min	50 mol%	$Ir(ppy)_3$	2:1	**77**	7	0
10 min	60 mol%	$Ir(ppy)_3$	2:1	**73**	6	0
10 min	10 mol%	$Ir(ppy)_3$	1:1	**25**	91	0
10 min	20 mol%	$Ir(ppy)_3$	1:1	**46**	59	0
10 min	30 mol%	$Ir(ppy)_3$	1:1	**48**	53	0
10 min	40 mol%	$Ir(ppy)_3$	1:1	**54**	49	0
10 min	50 mol%	$Ir(ppy)_3$	1:1	**53**	48	0
10 min	60 mol%	$Ir(ppy)_3$	1:1	**59**	41	0
10 min	10 mol%	$Ir(F\text{-}^tBuppy)_3$	2:1	**27**	80	0
10 min	20 mol%	$Ir(F\text{-}^tBuppy)_3$	2:1	**45**	53	0
10 min	30 mol%	$Ir(F\text{-}^tBuppy)_3$	2:1	**63**	22	0
10 min	40 mol%	$Ir(F\text{-}^tBuppy)_3$	2:1	**73**	9	0
10 min	50 mol%	$Ir(F\text{-}^tBuppy)_3$	2:1	**73**	14	0
10 min	60 mol%	$Ir(F\text{-}^tBuppy)_3$	2:1	**72**	7	0
10 min	10 mol%	$Ir(F\text{-}^tBuppy)_3$	1:1	**36**	69	0
10 min	20 mol%	$Ir(F\text{-}^tBuppy)_3$	1:1	**45**	59	0
10 min	30 mol%	$Ir(F\text{-}^tBuppy)_3$	1:1	**47**	55	0
10 min	40 mol%	$Ir(F\text{-}^tBuppy)_3$	1:1	**51**	52	0
10 min	50 mol%	$Ir(F\text{-}^tBuppy)_3$	1:1	**51**	52	0
10 min	60 mol%	$Ir(F\text{-}^tBuppy)_3$	1:1	**53**	50	0

10 min	10 mol%	4CzIPN	2:1	**24**	89	0
10 min	20 mol%	4CzIPN	2:1	**48**	53	0
10 min	30 mol%	4CzIPN	2:1	**81**	5	0
10 min	40 mol%	4CzIPN	2:1	**82**	3	0
10 min	50 mol%	4CzIPN	2:1	**81**	1	0
10 min	60 mol%	4CzIPN	2:1	**83**	0	0
10 min	10 mol%	4CzIPN	1:1	**30**	84	0
10 min	20 mol%	4CzIPN	1:1	**58**	44	0
10 min	30 mol%	4CzIPN	1:1	**61**	38	0
10 min	40 mol%	4CzIPN	1:1	**58**	39	0
10 min	50 mol%	4CzIPN	1:1	**55**	49	0
10 min	60 mol%	4CzIPN	1:1	**61**	37	0
10 min	10 mol%	2CzPN	2:1	**53**	34	0
10 min	20 mol%	2CzPN	2:1	**67**	23	0
10 min	30 mol%	2CzPN	2:1	**79**	4	0
10 min	40 mol%	2CzPN	2:1	**81**	0	0
10 min	50 mol%	2CzPN	2:1	**76**	0	0
10 min	60 mol%	2CzPN	2:1	**81**	0	0
10 min	10 mol%	2CzPN	1:1	**35**	68	0
10 min	20 mol%	2CzPN	1:1	**49**	47	0
10 min	30 mol%	2CzPN	1:1	**53**	39	0
10 min	40 mol%	2CzPN	1:1	**59**	31	0
10 min	50 mol%	2CzPN	1:1	**63**	27	0
10 min	60 mol%	2CzPN	1:1	**55**	38	0

Data from Fig. S22. Photocatalyst vs copper loading and reagent stoichiometry in dioxane (0.05 M).

Time	**Cu loading**	**Photocatalyst**	**Acid : Indazole ratio**	**Product (%)**	**Indazole (%)**
5 min	25 mol%	$Ir(ppy)_3$	2.0:1.0	**60**	19
5 min	25 mol%	$Ir(ppy)_3$	1.75:1.0	**66**	17
5 min	25 mol%	$Ir(ppy)_3$	1.5:1.0	**65**	17
5 min	25 mol%	$Ir(ppy)_3$	1.25:1.0	**52**	24
5 min	25 mol%	4CzIPN	2.0:1.0	**77**	5
5 min	25 mol%	4CzIPN	1.75:1.0	**71**	7
5 min	25 mol%	4CzIPN	1.5:1.0	**73**	11
5 min	25 mol%	4CzIPN	1.25:1.0	**68**	15
5 min	25 mol%	2CzPN	2.0:1.0	**70**	7
5 min	25 mol%	2CzPN	1.75:1.0	**63**	15

5 min	25 mol%	2CzPN	1.5:1.0	**58**	12
5 min	25 mol%	2CzPN	1.25:1.0	**55**	23
5 min	30 mol%	$Ir(ppy)_3$	2.0:1.0	**64**	16
5 min	30 mol%	$Ir(ppy)_3$	1.75:1.0	**71**	12
5 min	30 mol%	$Ir(ppy)_3$	1.5:1.0	**67**	18
5 min	30 mol%	$Ir(ppy)_3$	1.25:1.0	**57**	29
5 min	30 mol%	4CzIPN	2.0:1.0	**79**	5
5 min	30 mol%	4CzIPN	1.75:1.0	**80**	6
5 min	30 mol%	4CzIPN	1.5:1.0	**76**	8
5 min	30 mol%	4CzIPN	1.25:1.0	**61**	20
5 min	30 mol%	2CzPN	2.0:1.0	**77**	6
5 min	30 mol%	2CzPN	1.75:1.0	**70**	10
5 min	30 mol%	2CzPN	1.5:1.0	**68**	11
5 min	30 mol%	2CzPN	1.25:1.0	**59**	19
5 min	35 mol%	$Ir(ppy)_3$	2.0:1.0	**71**	9
5 min	35 mol%	$Ir(ppy)_3$	1.75:1.0	**70**	13
5 min	35 mol%	$Ir(ppy)_3$	1.5:1.0	**68**	19
5 min	35 mol%	$Ir(ppy)_3$	1.25:1.0	**59**	24
5 min	35 mol%	4CzIPN	2.0:1.0	**83**	3
5 min	35 mol%	4CzIPN	1.75:1.0	**79**	4
5 min	35 mol%	4CzIPN	1.5:1.0	**76**	5
5 min	35 mol%	4CzIPN	1.25:1.0	**72**	15
5 min	35 mol%	2CzPN	2.0:1.0	**77**	2
5 min	35 mol%	2CzPN	1.75:1.0	**76**	4
5 min	35 mol%	2CzPN	1.5:1.0	**71**	9
5 min	35 mol%	2CzPN	1.25:1.0	**57**	19
5 min	40 mol%	$Ir(ppy)_3$	2.0:1.0	**80**	5
5 min	40 mol%	$Ir(ppy)_3$	1.75:1.0	**71**	12
5 min	40 mol%	$Ir(ppy)_3$	1.5:1.0	**72**	13
5 min	40 mol%	$Ir(ppy)_3$	1.25:1.0	**62**	23
5 min	40 mol%	4CzIPN	2.0:1.0	**83**	3
5 min	40 mol%	4CzIPN	1.75:1.0	**77**	5
5 min	40 mol%	4CzIPN	1.5:1.0	**80**	6
5 min	40 mol%	4CzIPN	1.25:1.0	**77**	12
5 min	40 mol%	2CzPN	2.0:1.0	**75**	2
5 min	40 mol%	2CzPN	1.75:1.0	**74**	7
5 min	40 mol%	2CzPN	1.5:1.0	**66**	9
5 min	40 mol%	2CzPN	1.25:1.0	**61**	18

Data from Fig. S23. Photocatalyst loading (4CzIPN) vs copper loading ($Cu(acac)_2$) and concentration (dioxane).

Concentration	Cu loading	Photocatalyst loading	Product (%)	Indazole (%)
0.025 M	30 mol%	0 mol%	**57**	25
0.025 M	30 mol%	0.25 mol%	**75**	7
0.025 M	30 mol%	0.5 mol%	**65**	4
0.025 M	30 mol%	1 mol%	**79**	3
0.025 M	30 mol%	1.5 mol%	**75**	3
0.025 M	30 mol%	2 mol%	**71**	3
0.025 M	40 mol%	0 mol%	**68**	18
0.025 M	40 mol%	0.25 mol%	**77**	3
0.025 M	40 mol%	0.5 mol%	**82**	3
0.025 M	40 mol%	1 mol%	**83**	2
0.025 M	40 mol%	1.5 mol%	**83**	2
0.025 M	40 mol%	2 mol%	**83**	2
0.05 M	30 mol%	0 mol%	**35**	44
0.05 M	30 mol%	0.25 mol%	**68**	15
0.05 M	30 mol%	0.5 mol%	**74**	9
0.05 M	30 mol%	1 mol%	**76**	5
0.05 M	30 mol%	1.5 mol%	**80**	5
0.05 M	30 mol%	2 mol%	**78**	5
0.05 M	40 mol%	0 mol%	**50**	32
0.05 M	40 mol%	0.25 mol%	**75**	7
0.05 M	40 mol%	0.5 mol%	**79**	8
0.05 M	40 mol%	1 mol%	**77**	7
0.05 M	40 mol%	1.5 mol%	**76**	7
0.05 M	40 mol%	2 mol%	**75**	5
0.075 M	30 mol%	0 mol%	**38**	48
0.075 M	30 mol%	0.25 mol%	**63**	21
0.075 M	30 mol%	0.5 mol%	**66**	13
0.075 M	30 mol%	1 mol%	**74**	7
0.075 M	30 mol%	1.5 mol%	**71**	9
0.075 M	30 mol%	2 mol%	**78**	7
0.075 M	40 mol%	0 mol%	**47**	38
0.075 M	40 mol%	0.25 mol%	**75**	11
0.075 M	40 mol%	0.5 mol%	**71**	12
0.075 M	40 mol%	1 mol%	**70**	11
0.075 M	40 mol%	1.5 mol%	**68**	13
0.075 M	40 mol%	2 mol%	**71**	12

0.1 M	30 mol%	0 mol%	**32**	56
0.1 M	30 mol%	0.25 mol%	**48**	34
0.1 M	30 mol%	0.5 mol%	**58**	26
0.1 M	30 mol%	1 mol%	nd	nd
0.1 M	30 mol%	1.5 mol%	**57**	27
0.1 M	30 mol%	2 mol%	**50**	32
0.1 M	40 mol%	0 mol%	**33**	52
0.1 M	40 mol%	0.25 mol%	**62**	24
0.1 M	40 mol%	0.5 mol%	**65**	18
0.1 M	40 mol%	1 mol%	**69**	15
0.1 M	40 mol%	1.5 mol%	**70**	11
0.1 M	40 mol%	2 mol%	**66**	18

8.5. Data from cross-electrophile coupling.

Data from Fig. S30. Bases vs solvents using $NiCl_2$·dme as nickel source and $[Ir(dF(CF_3)ppy)_2dtbbpy]PF_6$ as photocatalyst.

Solvent	Base	Product (%)	ArBr (%)	ArH (%)
DMA	TMG	**22**	33	21
DME	TMG	**26**	44	11
DMF	TMG	**24**	31	20
dioxane	TMG	**19**	60	7
ACN	TMG	**35**	34	18
THF	TMG	**50**	20	16
Acetone	TMG	**32**	40	16
AcOEt	TMG	**15**	73	6
DMA	lutidine	**63**	7	12
DME	lutidine	**78**	0	4
DMF	lutidine	**57**	15	12
dioxane	lutidine	**47**	41	4
ACN	lutidine	**46**	41	10
THF	lutidine	**81**	0	5
Acetone	lutidine	**55**	29	9
AcOEt	lutidine	**82**	0	5
DMA	collidine	**70**	1	11
DME	collidine	**78**	1	4
DMF	collidine	**54**	14	12
dioxane	collidine	**64**	19	5
ACN	collidine	**34**	54	9
THF	collidine	**80**	1	5

Acetone	collidine	**77**	1	9
AcOEt	collidine	**78**	1	6
DMA	NMM	**63**	6	12
DME	NMM	**10**	72	12
DMF	NMM	**18**	58	10
dioxane	NMM	**3**	87	5
ACN	NMM	**2**	94	5
THF	NMM	**5**	80	9
Acetone	NMM	**4**	85	7
AcOEt	NMM	**3**	88	6
DMA	DBU	**0**	69	15
DME	DBU	**1**	89	3
DMF	DBU	**1**	78	10
dioxane	DBU	**0**	92	2
ACN	DBU	**0**	89	8
THF	DBU	**2**	85	5
Acetone	DBU	**1**	68	17
AcOEt	DBU	**0**	93	3
DMA	no base	**60**	16	10
DME	no base	**6**	71	15
DMF	no base	**20**	57	10
dioxane	no base	**3**	87	5
ACN	no base	**2**	94	5
THF	no base	**5**	80	9
Acetone	no base	**4**	87	6
AcOEt	no base	**2**	88	6

Data from Fig. S31. Concentration vs bases and solvents.

Solvent	**Base**	**Concentration**	**Product (%)**	**ArBr (%)**	**ArH (%)**
DMA	lutidine	0.1 M	**58**	10	10
DME	lutidine	0.1 M	**47**	31	11
Acetone	lutidine	0.1 M	**58**	24	6
AcOEt	lutidine	0.1 M	**84**	1	3
DMA	collidine	0.1 M	**66**	2	10
DME	collidine	0.1 M	**79**	0	3
Acetone	collidine	0.1 M	**73**	3	4
AcOEt	collidine	0.1 M	**84**	0	3
DMA	no base	0.1 M	**60**	7	11

DME	no base	0.1 M	**7**	74	10
Acetone	no base	0.1 M	**12**	69	8
AcOEt	no base	0.1 M	**8**	74	9
DMA	lutidine	0.2 M	**48**	32	6
DME	lutidine	0.2 M	**80**	1	3
Acetone	lutidine	0.2 M	**61**	24	3
AcOEt	lutidine	0.2 M	**77**	10	3
DMA	collidine	0.2 M	**61**	16	7
DME	collidine	0.2 M	**79**	1	3
Acetone	collidine	0.2 M	**72**	9	3
AcOEt	collidine	0.2 M	**80**	4	2
DMA	no base	0.2 M	**49**	28	8
DME	no base	0.2 M	**19**	59	11
Acetone	no base	0.2 M	**23**	61	7
AcOEt	no base	0.2 M	**20**	67	7
DMA	lutidine	0.3 M	**54**	23	8
DME	lutidine	0.3 M	**77**	0	3
Acetone	lutidine	0.3 M	**68**	13	4
AcOEt	lutidine	0.3 M	**80**	0	3
DMA	collidine	0.3 M	**59**	16	8
DME	collidine	0.3 M	**77**	0	3
Acetone	collidine	0.3 M	**70**	7	4
AcOEt	collidine	0.3 M	**80**	0	3
DMA	no base	0.3 M	**52**	27	8
DME	no base	0.3 M	**15**	65	12
Acetone	no base	0.3 M	**18**	67	7
AcOEt	no base	0.3 M	**15**	68	10
DMA	lutidine	0.4 M	**43**	43	6
DME	lutidine	0.4 M	**76**	4	3
Acetone	lutidine	0.4 M	**65**	20	4
AcOEt	lutidine	0.4 M	**76**	10	3
DMA	collidine	0.4 M	**60**	19	6
DME	collidine	0.4 M	**76**	3	3
Acetone	collidine	0.4 M	**70**	11	4
AcOEt	collidine	0.4 M	**76**	9	2
DMA	no base	0.4 M	**49**	31	8
DME	no base	0.4 M	**20**	61	10
Acetone	no base	0.4 M	**20**	66	7
AcOEt	no base	0.4 M	**19**	69	7
DMA	lutidine	0.5 M	**43**	43	5

DME	lutidine	0.5 M	**70**	14	3
Acetone	lutidine	0.5 M	**68**	19	5
AcOEt	lutidine	0.5 M	**82**	4	3
DMA	collidine	0.5 M	**58**	22	6
DME	collidine	0.5 M	**74**	6	3
Acetone	collidine	0.5 M	**75**	6	5
AcOEt	collidine	0.5 M	**82**	2	3
DMA	no base	0.5 M	**45**	40	7
DME	no base	0.5 M	**9**	69	12
Acetone	no base	0.5 M	**7**	76	9
AcOEt	no base	0.5 M	**10**	76	8

Data from Fig. S32. Concentration vs solvents and nickel-complex formations.

Solvent	**Nickel Complex Formation**	**Concentration**	**Base**	**Product (%)**	**ArBr (%)**	**ArH (%)**
Acetone	with sonication	0.2 M	lutidine	**71**	8	4
Acetone	with sonication	0.3 M	lutidine	**69**	12	5
Acetone	with sonication	0.4 M	lutidine	**65**	18	4
Acetone	with sonication	0.5 M	lutidine	**62**	23	4
Acetone	without sonication	0.2 M	lutidine	**76**	1	5
Acetone	without sonication	0.3 M	lutidine	**75**	2	5
Acetone	without sonication	0.4 M	lutidine	**73**	6	4
Acetone	without sonication	0.5 M	lutidine	**68**	14	4
Acetone	pre-formed	0.2 M	lutidine	**70**	11	5
Acetone	pre-formed	0.3 M	lutidine	**67**	14	5
Acetone	pre-formed	0.4 M	lutidine	**62**	23	4
Acetone	pre-formed	0.5 M	lutidine	**57**	29	4
Acetone	with sonication	0.2 M	collidine	**79**	1	5
Acetone	with sonication	0.3 M	collidine	**76**	2	5
Acetone	with sonication	0.4 M	collidine	**75**	5	4
Acetone	with sonication	0.5 M	collidine	**71**	10	4
Acetone	without sonication	0.2 M	collidine	**72**	9	5
Acetone	without sonication	0.3 M	collidine	**68**	13	5
Acetone	without sonication	0.4 M	collidine	**66**	19	5
Acetone	without sonication	0.5 M	collidine	**61**	26	5
Acetone	pre-formed	0.2 M	collidine	**79**	1	5

Acetone	pre-formed	0.3 M	collidine	**78**	2	5
Acetone	pre-formed	0.4 M	collidine	**76**	5	5
Acetone	pre-formed	0.5 M	collidine	**72**	12	5
DME	with sonication	0.2 M	lutidine	**74**	6	4
DME	with sonication	0.3 M	lutidine	**72**	8	3
DME	with sonication	0.4 M	lutidine	**71**	11	3
DME	with sonication	0.5 M	lutidine	**68**	16	3
DME	without sonication	0.2 M	lutidine	**79**	0	3
DME	without sonication	0.3 M	lutidine	**75**	2	3
DME	without sonication	0.4 M	lutidine	**73**	8	3
DME	without sonication	0.5 M	lutidine	**64**	21	3
DME	pre-formed	0.2 M	lutidine	**78**	0	3
DME	pre-formed	0.3 M	lutidine	**76**	1	3
DME	pre-formed	0.4 M	lutidine	**76**	4	3
DME	pre-formed	0.5 M	lutidine	**73**	9	3
DME	with sonication	0.2 M	collidine	**77**	0	3
DME	with sonication	0.3 M	collidine	**75**	1	3
DME	with sonication	0.4 M	collidine	**77**	4	3
DME	with sonication	0.5 M	collidine	**72**	12	3
DME	without sonication	0.2 M	collidine	**78**	0	3
DME	without sonication	0.3 M	collidine	**75**	2	3
DME	without sonication	0.4 M	collidine	**72**	9	3
DME	without sonication	0.5 M	collidine	**69**	14	3
DME	pre-formed	0.2 M	collidine	**76**	1	3
DME	pre-formed	0.3 M	collidine	**75**	2	3
DME	pre-formed	0.4 M	collidine	**73**	6	3
DME	pre-formed	0.5 M	collidine	**70**	12	3
AcOEt	with sonication	0.2 M	lutidine	**78**	2	4
AcOEt	with sonication	0.3 M	lutidine	**79**	0	3
AcOEt	with sonication	0.4 M	lutidine	**76**	3	3
AcOEt	with sonication	0.5 M	lutidine	**72**	10	3
AcOEt	without sonication	0.2 M	lutidine	**79**	0	3
AcOEt	without sonication	0.3 M	lutidine	**78**	0	3
AcOEt	without sonication	0.4 M	lutidine	**77**	3	3
AcOEt	without sonication	0.5 M	lutidine	**73**	10	3

AcOEt	pre-formed	0.2 M	lutidine	**75**	6	4
AcOEt	pre-formed	0.3 M	lutidine	**77**	1	3
AcOEt	pre-formed	0.4 M	lutidine	**76**	4	3
AcOEt	pre-formed	0.5 M	lutidine	**72**	9	3
AcOEt	with sonication	0.2 M	collidine	**78**	0	3
AcOEt	with sonication	0.3 M	collidine	**75**	1	3
AcOEt	with sonication	0.4 M	collidine	**75**	5	3
AcOEt	with sonication	0.5 M	collidine	**71**	13	3
AcOEt	without sonication	0.2 M	collidine	**70**	12	5
AcOEt	without sonication	0.3 M	collidine	**78**	2	3
AcOEt	without sonication	0.4 M	collidine	**77**	3	3
AcOEt	without sonication	0.5 M	collidine	**72**	8	3
AcOEt	pre-formed	0.2 M	collidine	**78**	0	3
AcOEt	pre-formed	0.3 M	collidine	**76**	1	3
AcOEt	pre-formed	0.4 M	collidine	**75**	5	3
AcOEt	pre-formed	0.5 M	collidine	**66**	18	3

Data from Fig. S33. Bases vs photocatalyst and water loading in DME as solvent (0.3 M).

Water loading	Base	Photocatalyst	Product (%)	ArBr (%)	ArH (%)
0 equiv	TMG	$[Ir(dF(CF_3)ppy)_2dtbbpy]PF_6$	**11**	73	8
10 equiv	TMG	$[Ir(dF(CF_3)ppy)_2dtbbpy]PF_6$	**0**	88	5
20 equiv	TMG	$[Ir(dF(CF_3)ppy)_2dtbbpy]PF_6$	**0**	82	6
50 equiv	TMG	$[Ir(dF(CF_3)ppy)_2dtbbpy]PF_6$	**0**	55	5
0 equiv	TMG	4CzIPN	**3**	69	7
10 equiv	TMG	4CzIPN	**0**	86	7
20 equiv	TMG	4CzIPN	**0**	86	5
50 equiv	TMG	4CzIPN	**0**	77	4
0 equiv	lutidine	$[Ir(dF(CF_3)ppy)_2dtbbpy]PF_6$	**73**	4	9
10 equiv	lutidine	$[Ir(dF(CF_3)ppy)_2dtbbpy]PF_6$	**68**	7	10
20 equiv	lutidine	$[Ir(dF(CF_3)ppy)_2dtbbpy]PF_6$	**60**	9	13
50 equiv	lutidine	$[Ir(dF(CF_3)ppy)_2dtbbpy]PF_6$	**38**	27	14
0 equiv	lutidine	4CzIPN	**49**	21	14
10 equiv	lutidine	4CzIPN	**52**	17	16
20 equiv	lutidine	4CzIPN	**41**	6	29
50 equiv	lutidine	4CzIPN	**13**	46	21
0 equiv	collidine	$[Ir(dF(CF_3)ppy)_2dtbbpy]PF_6$	**75**	0	8
10 equiv	collidine	$[Ir(dF(CF_3)ppy)_2dtbbpy]PF_6$	**72**	0	10

20 equiv	collidine	$[Ir(dF(CF_3)ppy)_2dtbbpy]PF_6$	**55**	10	14
50 equiv	collidine	$[Ir(dF(CF_3)ppy)_2dtbbpy]PF_6$	**22**	49	10
0 equiv	collidine	4CzIPN	**69**	0	12
10 equiv	collidine	4CzIPN	**65**	0	15
20 equiv	collidine	4CzIPN	**42**	4	22
50 equiv	collidine	4CzIPN	**24**	28	19
0 equiv	*N*-Methyl-imidazole	$[Ir(dF(CF_3)ppy)_2dtbbpy]PF_6$	**0**	86	6
10 equiv	*N*-Methyl-imidazole	$[Ir(dF(CF_3)ppy)_2dtbbpy]PF_6$	**0**	84	6
20 equiv	*N*-Methyl-imidazole	$[Ir(dF(CF_3)ppy)_2dtbbpy]PF_6$	**0**	87	5
50 equiv	*N*-Methyl-imidazole	$[Ir(dF(CF_3)ppy)_2dtbbpy]PF_6$	**0**	85	6
0 equiv	*N*-Methyl-imidazole	4CzIPN	**0**	79	11
10 equiv	*N*-Methyl-imidazole	4CzIPN	**0**	80	10
20 equiv	*N*-Methyl-imidazole	4CzIPN	**0**	80	10
50 equiv	*N*-Methyl-imidazole	4CzIPN	**0**	73	10
0 equiv	*N*-Butyl-imidazole	$[Ir(dF(CF_3)ppy)_2dtbbpy]PF_6$	**0**	89	5
10 equiv	*N*-Butyl-imidazole	$[Ir(dF(CF_3)ppy)_2dtbbpy]PF_6$	**0**	83	8
20 equiv	*N*-Butyl-imidazole	$[Ir(dF(CF_3)ppy)_2dtbbpy]PF_6$	**0**	82	9
50 equiv	*N*-Butyl-imidazole	$[Ir(dF(CF_3)ppy)_2dtbbpy]PF_6$	**0**	87	7
0 equiv	*N*-Butyl-imidazole	4CzIPN	**0**	78	11
10 equiv	*N*-Butyl-imidazole	4CzIPN	**0**	48	25
20 equiv	*N*-Butyl-imidazole	4CzIPN	**3**	43	25
50 equiv	*N*-Butyl-imidazole	4CzIPN	**1**	49	25
0 equiv	NBu_3	$[Ir(dF(CF_3)ppy)_2dtbbpy]PF_6$	**8**	60	13
10 equiv	NBu_3	$[Ir(dF(CF_3)ppy)_2dtbbpy]PF_6$	**22**	37	17
20 equiv	NBu_3	$[Ir(dF(CF_3)ppy)_2dtbbpy]PF_6$	**18**	33	16
50 equiv	NBu_3	$[Ir(dF(CF_3)ppy)_2dtbbpy]PF_6$	**14**	44	7
0 equiv	NBu_3	4CzIPN	**30**	3	31
10 equiv	NBu_3	4CzIPN	**26**	10	37
20 equiv	NBu_3	4CzIPN	**16**	21	26
50 equiv	NBu_3	4CzIPN	**10**	41	23
0 equiv	TMG	4CzPN	**7**	44	11
10 equiv	TMG	4CzPN	**0**	79	10
20 equiv	TMG	4CzPN	**0**	77	10

50 equiv	TMG	4CzPN	**0**	51	6
0 equiv	TMG	4CzTPN	**1**	66	13
10 equiv	TMG	4CzTPN	**0**	77	14
20 equiv	TMG	4CzTPN	**0**	76	11
50 equiv	TMG	4CzTPN	**0**	50	6
0 equiv	lutidine	4CzPN	**59**	13	13
10 equiv	lutidine	4CzPN	**53**	14	17
20 equiv	lutidine	4CzPN	**39**	20	21
50 equiv	lutidine	4CzPN	**19**	33	21
0 equiv	lutidine	4CzTPN	**6**	87	3
10 equiv	lutidine	4CzTPN	**6**	87	3
20 equiv	lutidine	4CzTPN	**3**	90	3
50 equiv	lutidine	4CzTPN	**1**	92	3
0 equiv	collidine	4CzPN	**70**	0	14
10 equiv	collidine	4CzPN	**61**	0	17
20 equiv	collidine	4CzPN	**44**	9	21
50 equiv	collidine	4CzPN	**20**	32	21
0 equiv	collidine	4CzTPN	**5**	89	3
10 equiv	collidine	4CzTPN	**6**	87	3
20 equiv	collidine	4CzTPN	**3**	89	3
50 equiv	collidine	4CzTPN	**1**	90	3
0 equiv	*N*-Methyl-imidazole	4CzPN	**0**	68	18
10 equiv	*N*-Methyl-imidazole	4CzPN	**0**	69	18
20 equiv	*N*-Methyl-imidazole	4CzPN	**0**	68	18
50 equiv	*N*-Methyl-imidazole	4CzPN	**0**	67	15
0 equiv	*N*-Methyl-imidazole	4CzTPN	**0**	83	9
10 equiv	*N*-Methyl-imidazole	4CzTPN	**0**	83	10
20 equiv	*N*-Methyl-imidazole	4CzTPN	**0**	88	6
50 equiv	*N*-Methyl-imidazole	4CzTPN	**0**	84	5
0 equiv	*N*-Butyl-imidazole	4CzPN	**1**	54	21
10 equiv	*N*-Butyl-imidazole	4CzPN	**1**	49	22
20 equiv	*N*-Butyl-imidazole	4CzPN	**1**	56	21
50 equiv	*N*-Butyl-imidazole	4CzPN	**2**	52	20
0 equiv	*N*-Butyl-imidazole	4CzTPN	**0**	80	11

10 equiv	*N*-Butyl-imidazole	4CzTPN	**0**	81	10
20 equiv	*N*-Butyl-imidazole	4CzTPN	**0**	87	6
50 equiv	*N*-Butyl-imidazole	4CzTPN	**0**	84	4
0 equiv	NBu_3	4CzPN	**16**	42	21
10 equiv	NBu_3	4CzPN	**7**	60	18
20 equiv	NBu_3	4CzPN	**6**	47	26
50 equiv	NBu_3	4CzPN	**2**	63	21
0 equiv	NBu_3	4CzTPN	**2**	87	4
10 equiv	NBu_3	4CzTPN	**0**	92	2
20 equiv	NBu_3	4CzTPN	**1**	94	1
50 equiv	NBu_3	4CzTPN	**1**	93	1

Data from Fig. S34. Bases vs solvents and additives (0.3 M).

Solvent	**Base**	**Additive**	**Product (%)**	**ArBr (%)**	**ArH (%)**
DMA	2,6-d^{t}Bu-pyridine	w/o additive	**53**	24	11
DMA	2,6-d^{t}Bu-(4-Me)-pyridine	w/o additive	**54**	25	10
DMA	lutidine	w/o additive	**57**	22	8
DMA	collidine	w/o additive	**66**	13	7
DMA	no base	w/o additive	**51**	26	10
DMA	lutidine	10 equiv water	**47**	24	13
DMA	lutidine	10 equiv ethylene glycol	**36**	45	9
DMA	lutidine	10 equiv MeOH	**53**	24	9
DME	2,6-d^{t}Bu-pyridine	w/o additive	**38**	52	7
DME	2,6-d^{t}Bu-(4-Me)-pyridine	w/o additive	**46**	41	6
DME	lutidine	w/o additive	**75**	2	4
DME	collidine	w/o additive	**81**	0	4
DME	no base	w/o additive	**6**	81	10
DME	lutidine	10 equiv water	**76**	0	10
DME	lutidine	10 equiv ethylene glycol	**21**	62	10
DME	lutidine	10 equiv MeOH	**79**	0	8
Acetone	2,6-d^{t}Bu-pyridine	w/o additive	**33**	60	3
Acetone	2,6-d^{t}Bu-(4-Me)-pyridine	w/o additive	**32**	63	3
Acetone	lutidine	w/o additive	**70**	14	4
Acetone	collidine	w/o additive	**81**	0	4
Acetone	no base	w/o additive	**5**	80	10
Acetone	lutidine	10 equiv water	**49**	31	12

Acetone	lutidine	10 equiv ethylene glycol	**14**	71	7
Acetone	lutidine	10 equiv MeOH	**80**	0	9
AcOEt	2,6-d^{t}Bu-pyridine	w/o additive	**18**	74	4
AcOEt	2,6-d^{t}Bu-(4-Me)-pyridine	w/o additive	**24**	70	4
AcOEt	lutidine	w/o additive	**26**	68	4
AcOEt	collidine	w/o additive	**28**	59	6
AcOEt	no base	w/o additive	**2**	86	7
AcOEt	lutidine	10 equiv water	**21**	60	11
AcOEt	lutidine	10 equiv ethylene glycol	**2**	87	5
AcOEt	lutidine	10 equiv MeOH	**21**	64	8
DMF	2,6-d^{t}Bu-pyridine	w/o additive	**41**	38	11
DMF	2,6-d^{t}Bu-(4-Me)-pyridine	w/o additive	**36**	43	9
DMF	lutidine	w/o additive	**52**	26	9
DMF	collidine	w/o additive	**69**	0	11
DMF	no base	w/o additive	**15**	63	13
DMF	lutidine	10 equiv water	**42**	32	12
DMF	lutidine	10 equiv ethylene glycol	**32**	44	11
DMF	lutidine	10 equiv MeOH	**45**	33	9
dioxane	2,6-d^{t}Bu-pyridine	w/o additive	**15**	75	6
dioxane	2,6-d^{t}Bu-(4-Me)-pyridine	w/o additive	**27**	64	5
dioxane	lutidine	w/o additive	**62**	22	5
dioxane	collidine	w/o additive	**75**	0	5
dioxane	no base	w/o additive	**1**	85	7
dioxane	lutidine	10 equiv water	**56**	16	12
dioxane	lutidine	10 equiv ethylene glycol	**17**	67	8
dioxane	lutidine	10 equiv MeOH	**76**	0	7
toluene	2,6-d^{t}Bu-pyridine	w/o additive	**5**	78	3
toluene	2,6-d^{t}Bu-(4-Me)-pyridine	w/o additive	**11**	72	3
toluene	lutidine	w/o additive	**58**	23	3
toluene	collidine	w/o additive	**65**	11	4
toluene	no base	w/o additive	**2**	78	4
toluene	lutidine	10 equiv water	**72**	0	7
toluene	lutidine	10 equiv ethylene glycol	**29**	45	7
toluene	lutidine	10 equiv MeOH	**75**	0	5

Data from Fig. S35. Bases vs solvents and reagent loadings (0.3 M).

Solvent	Base	Base loading	Aryl : Alkyl ratio	TTMSH loading	Product (%)	ArBr (%)	ArH (%)
DME	lutidine	2 equiv	1:1.5	1 equiv	**60**	21	3
DME	lutidine	3 equiv	1:1.5	1 equiv	**60**	19	3
DME	lutidine	2 equiv	1:1.5	1.5 equiv	**74**	4	3
DME	lutidine	2 equiv	1:1	1 equiv	**61**	12	4
DME	lutidine	3 equiv	1:1	1 equiv	**61**	14	4
DME	lutidine	2 equiv	1.5:1	1 equiv	**60**	58	7
DME	lutidine	3 equiv	1.5:1	1 equiv	**60**	59	7
DME	lutidine	2 equiv	1.5:1	1.5 equiv	**74**	34	9
DME	collidine	2 equiv	1:1.5	1 equiv	**60**	19	3
DME	collidine	3 equiv	1:1.5	1 equiv	**64**	12	3
DME	collidine	2 equiv	1:1.5	1.5 equiv	**79**	0	3
DME	collidine	2 equiv	1:1	1 equiv	**61**	9	4
DME	collidine	3 equiv	1:1	1 equiv	**58**	13	4
DME	collidine	2 equiv	1.5:1	1 equiv	**67**	38	8
DME	collidine	3 equiv	1.5:1	1 equiv	**58**	58	6
DME	collidine	2 equiv	1.5:1	1.5 equiv	**77**	26	9
DME	2,6-^{t}Bupyridine	2 equiv	1:1.5	1 equiv	**34**	53	6
DME	2,6-^{t}Bupyridine	3 equiv	1:1.5	1 equiv	**31**	52	7
DME	2,6-^{t}Bupyridine	2 equiv	1:1.5	1.5 equiv	**34**	47	8
DME	2,6-^{t}Bupyridine	2 equiv	1:1	1 equiv	**33**	48	10
DME	2,6-^{t}Bupyridine	3 equiv	1:1	1 equiv	**37**	37	10
DME	2,6-^{t}Bupyridine	2 equiv	1.5:1	1 equiv	**43**	73	14
DME	2,6-^{t}Bupyridine	3 equiv	1.5:1	1 equiv	**40**	80	12
DME	2,6-^{t}Bupyridine	2 equiv	1.5:1	1.5 equiv	**47**	61	17
Acetone	lutidine	2 equiv	1:1.5	1 equiv	**45**	41	3
Acetone	lutidine	3 equiv	1:1.5	1 equiv	**48**	39	3
Acetone	lutidine	2 equiv	1:1.5	1.5 equiv	**68**	14	4
Acetone	lutidine	2 equiv	1:1	1 equiv	**50**	30	5
Acetone	lutidine	3 equiv	1:1	1 equiv	**45**	40	4
Acetone	lutidine	2 equiv	1.5:1	1 equiv	**48**	78	6
Acetone	lutidine	3 equiv	1.5:1	1 equiv	**44**	84	5
Acetone	lutidine	2 equiv	1.5:1	1.5 equiv	**60**	61	9
Acetone	collidine	2 equiv	1:1.5	1 equiv	**50**	29	3

Acetone	collidine	3 equiv	1:1.5	1 equiv	**49**	31	3
Acetone	collidine	2 equiv	1:1.5	1.5 equiv	**71**	8	5
Acetone	collidine	2 equiv	1:1	1 equiv	**47**	28	5
Acetone	collidine	3 equiv	1:1	1 equiv	**45**	36	5
Acetone	collidine	2 equiv	1.5:1	1 equiv	**45**	73	6
Acetone	collidine	3 equiv	1.5:1	1 equiv	**42**	84	5
Acetone	collidine	2 equiv	1.5:1	1.5 equiv	**60**	57	9
Acetone	2,6-d^{t}Bupyridine	2 equiv	1:1.5	1 equiv	**40**	44	4
Acetone	2,6-d^{t}Bupyridine	3 equiv	1:1.5	1 equiv	**37**	47	5
Acetone	2,6-d^{t}Bupyridine	2 equiv	1:1.5	1.5 equiv	**48**	34	7
Acetone	2,6-d^{t}Bupyridine	2 equiv	1:1	1 equiv	**40**	43	7
Acetone	2,6-d^{t}Bupyridine	3 equiv	1:1	1 equiv	**36**	5	6
Acetone	2,6-d^{t}Bupyridine	2 equiv	1.5:1	1 equiv	**38**	90	7
Acetone	2,6-d^{t}Bupyridine	3 equiv	1.5:1	1 equiv	**37**	92	7
Acetone	2,6-d^{t}Bupyridine	2 equiv	1.5:1	1.5 equiv	**49**	74	10
DME:DMF	lutidine	2 equiv	1:1.5	1 equiv	**44**	40	5
DME:DMF	lutidine	3 equiv	1:1.5	1 equiv	**47**	38	6
DME:DMF	lutidine	2 equiv	1:1.5	1.5 equiv	**63**	18	6
DME:DMF	lutidine	2 equiv	1:1	1 equiv	**44**	32	8
DME:DMF	lutidine	3 equiv	1:1	1 equiv	**43**	33	8
DME:DMF	lutidine	2 equiv	1.5:1	1 equiv	**40**	81	9
DME:DMF	lutidine	3 equiv	1.5:1	1 equiv	**39**	81	9
DME:DMF	lutidine	2 equiv	1.5:1	1.5 equiv	**47**	70	10
DME:DMF	collidine	2 equiv	1:1.5	1 equiv	**55**	28	5
DME:DMF	collidine	3 equiv	1:1.5	1 equiv	**53**	29	5
DME:DMF	collidine	2 equiv	1:1.5	1.5 equiv	**67**	12	5
DME:DMF	collidine	2 equiv	1:1	1 equiv	**51**	22	8
DME:DMF	collidine	3 equiv	1:1	1 equiv	**51**	21	7
DME:DMF	collidine	2 equiv	1.5:1	1 equiv	**46**	69	10
DME:DMF	collidine	3 equiv	1.5:1	1 equiv	**59**	44	14
DME:DMF	collidine	2 equiv	1.5:1	1.5 equiv	**55**	56	12
DME:DMF	2,6-d^{t}Bupyridine	2 equiv	1:1.5	1 equiv	**31**	47	12
DME:DMF	2,6-d^{t}Bupyridine	3 equiv	1:1.5	1 equiv	**25**	51	12
DME:DMF	2,6-d^{t}Bupyridine	2 equiv	1:1.5	1.5 equiv	**34**	39	13
DME:DMF	2,6-d^{t}Bupyridine	2 equiv	1:1	1 equiv	**31**	39	14

DME:DMF	2,6-d^{t}Bupyridine	3 equiv	1:1	1 equiv	**28**	41	16
DME:DMF	2,6-d^{t}Bupyridine	2 equiv	1.5:1	1 equiv	**31**	80	16
DME:DMF	2,6-d^{t}Bupyridine	3 equiv	1.5:1	1 equiv	**28**	83	16
DME:DMF	2,6-d^{t}Bupyridine	2 equiv	1.5:1	1.5 equiv	**43**	66	19
Acetone:DMF	lutidine	2 equiv	1:1.5	1 equiv	**36**	53	5
Acetone:DMF	lutidine	3 equiv	1:1.5	1 equiv	**39**	46	5
Acetone:DMF	lutidine	2 equiv	1:1.5	1.5 equiv	**49**	32	6
Acetone:DMF	lutidine	2 equiv	1:1	1 equiv	**36**	41	7
Acetone:DMF	lutidine	3 equiv	1:1	1 equiv	**37**	42	7
Acetone:DMF	lutidine	2 equiv	1.5:1	1 equiv	**34**	89	9
Acetone:DMF	lutidine	3 equiv	1.5:1	1 equiv	**34**	87	8
Acetone:DMF	lutidine	2 equiv	1.5:1	1.5 equiv	**41**	82	10
Acetone:DMF	collidine	2 equiv	1:1.5	1 equiv	**26**	61	10
Acetone:DMF	collidine	3 equiv	1:1.5	1 equiv	**22**	55	10
Acetone:DMF	collidine	2 equiv	1:1.5	1.5 equiv	**38**	40	12
Acetone:DMF	collidine	2 equiv	1:1	1 equiv	**30**	45	12
Acetone:DMF	collidine	3 equiv	1:1	1 equiv	**24**	44	12
Acetone:DMF	collidine	2 equiv	1.5:1	1 equiv	**30**	85	14
Acetone:DMF	collidine	3 equiv	1.5:1	1 equiv	**26**	88	14
Acetone:DMF	collidine	2 equiv	1.5:1	1.5 equiv	**37**	75	19
Acetone:DMF	2,6-d^{t}Bupyridine	2 equiv	1:1.5	1 equiv	**26**	61	10
Acetone:DMF	2,6-d^{t}Bupyridine	3 equiv	1:1.5	1 equiv	**22**	55	10
Acetone:DMF	2,6-d^{t}Bupyridine	2 equiv	1:1.5	1.5 equiv	**38**	40	12
Acetone:DMF	2,6-d^{t}Bupyridine	2 equiv	1:1	1 equiv	**30**	45	12
Acetone:DMF	2,6-d^{t}Bupyridine	3 equiv	1:1	1 equiv	**24**	44	12
Acetone:DMF	2,6-d^{t}Bupyridine	2 equiv	1.5:1	1 equiv	**30**	85	14
Acetone:DMF	2,6-d^{t}Bupyridine	3 equiv	1.5:1	1 equiv	**26**	88	14
Acetone:DMF	2,6-d^{t}Bupyridine	2 equiv	1.5:1	1.5 equiv	**37**	75	19
DME:DMA	lutidine	2 equiv	1:1.5	1 equiv	**44**	40	5
DME:DMA	lutidine	3 equiv	1:1.5	1 equiv	**52**	31	6
DME:DMA	lutidine	2 equiv	1:1.5	1.5 equiv	**69**	7	6
DME:DMA	lutidine	2 equiv	1:1	1 equiv	**47**	36	7
DME:DMA	lutidine	3 equiv	1:1	1 equiv	**45**	38	7
DME:DMA	lutidine	2 equiv	1.5:1	1 equiv	**41**	84	9
DME:DMA	lutidine	3 equiv	1.5:1	1 equiv	**42**	84	9

DME:DMA	lutidine	2 equiv	1.5:1	1.5 equiv	**46**	82	9
DME:DMA	collidine	2 equiv	1:1.5	1 equiv	**59**	21	5
DME:DMA	collidine	3 equiv	1:1.5	1 equiv	**62**	16	5
DME:DMA	collidine	2 equiv	1:1.5	1.5 equiv	**75**	0	5
DME:DMA	collidine	2 equiv	1:1	1 equiv	**59**	18	7
DME:DMA	collidine	3 equiv	1:1	1 equiv	**58**	16	7
DME:DMA	collidine	2 equiv	1.5:1	1 equiv	**55**	83	14
DME:DMA	collidine	3 equiv	1.5:1	1 equiv	**53**	54	12
DME:DMA	collidine	2 equiv	1.5:1	1.5 equiv	**58**	72	13
DME:DMA	2,6-d^{t}Bupyridine	2 equiv	1:1.5	1 equiv	**42**	42	11
DME:DMA	2,6-d^{t}Bupyridine	3 equiv	1:1.5	1 equiv	**43**	41	12
DME:DMA	2,6-d^{t}Bupyridine	2 equiv	1:1.5	1.5 equiv	**51**	30	11
DME:DMA	2,6-d^{t}Bupyridine	2 equiv	1:1	1 equiv	**41**	43	14
DME:DMA	2,6-d^{t}Bupyridine	3 equiv	1:1	1 equiv	**45**	38	13
DME:DMA	2,6-d^{t}Bupyridine	2 equiv	1.5:1	1 equiv	**44**	86	15
DME:DMA	2,6-d^{t}Bupyridine	3 equiv	1.5:1	1 equiv	**44**	84	15
DME:DMA	2,6-d^{t}Bupyridine	2 equiv	1.5:1	1.5 equiv	**57**	71	16
Acetone:DMA	lutidine	2 equiv	1:1.5	1 equiv	**45**	41	5
Acetone:DMA	lutidine	3 equiv	1:1.5	1 equiv	**45**	40	6
Acetone:DMA	lutidine	2 equiv	1:1.5	1.5 equiv	**55**	27	7
Acetone:DMA	lutidine	2 equiv	1:1	1 equiv	**48**	30	8
Acetone:DMA	lutidine	3 equiv	1:1	1 equiv	**43**	44	9
Acetone:DMA	lutidine	2 equiv	1.5:1	1 equiv	**44**	88	11
Acetone:DMA	lutidine	3 equiv	1.5:1	1 equiv	**33**	100	9
Acetone:DMA	lutidine	2 equiv	1.5:1	1.5 equiv	**52**	79	12
Acetone:DMA	collidine	2 equiv	1:1.5	1 equiv	**55**	28	5
Acetone:DMA	collidine	3 equiv	1:1.5	1 equiv	**57**	24	6
Acetone:DMA	collidine	2 equiv	1:1.5	1.5 equiv	**67**	9	6
Acetone:DMA	collidine	2 equiv	1:1	1 equiv	**59**	14	8
Acetone:DMA	collidine	3 equiv	1:1	1 equiv	**55**	21	9
Acetone:DMA	collidine	2 equiv	1.5:1	1 equiv	**54**	73	12
Acetone:DMA	collidine	3 equiv	1.5:1	1 equiv	**45**	86	10
Acetone:DMA	collidine	2 equiv	1.5:1	1.5 equiv	**69**	52	13
Acetone:DMA	2,6-d^{t}Bupyridine	2 equiv	1:1.5	1 equiv	**42**	38	11
Acetone:DMA	2,6-d^{t}Bupyridine	3 equiv	1:1.5	1 equiv	**40**	39	11

Acetone:DMA	2,6-d^{t}Bupyridine	2 equiv	1:1.5	1.5 equiv	**50**	29	11
Acetone:DMA	2,6-d^{t}Bupyridine	2 equiv	1:1	1 equiv	**42**	32	13
Acetone:DMA	2,6-d^{t}Bupyridine	3 equiv	1:1	1 equiv	**41**	40	16
Acetone:DMA	2,6-d^{t}Bupyridine	2 equiv	1.5:1	1 equiv	**43**	85	18
Acetone:DMA	2,6-d^{t}Bupyridine	3 equiv	1.5:1	1 equiv	**36**	90	16
Acetone:DMA	2,6-d^{t}Bupyridine	2 equiv	1.5:1	1.5 equiv	**55**	70	18

Data from Fig. S36. Bases vs base loadings and solvents (0.3 M).

Solvent	Base	Base loading	TTMSH loading	Product (%)	ArBr (%)	ArH (%)
DME	lutidine	0.5 equiv	1.5 equiv	**72**	0	9
DME	BTMG	0.5 equiv	1.5 equiv	**48**	39	4
DME	BTTP	0.5 equiv	1.5 equiv	**35**	51	4
DME	dPh-pyridine	0.5 equiv	1.5 equiv	**22**	8	30
DME	2-Me,6-Cy-pyridine	0.5 equiv	1.5 equiv	**77**	0	4
DME	Tetrahydroquinoline	0.5 equiv	1.5 equiv	**18**	0	37
DME	lutidine	0.5 equiv	2 equiv	**69**	0	9
DME	BTMG	0.5 equiv	2 equiv	**26**	57	6
DME	BTTP	0.5 equiv	2 equiv	**49**	36	4
DME	dPh-pyridine	0.5 equiv	2 equiv	**16**	88	nd
DME	2-Me,6-Cy-pyridine	0.5 equiv	2 equiv	**69**	0	8
DME	Tetrahydroquinoline	0.5 equiv	2 equiv	**63**	2	9
DME	lutidine	1 equiv	1.5 equiv	**81**	0	3
DME	BTMG	1 equiv	1.5 equiv	**42**	44	3
DME	BTTP	1 equiv	1.5 equiv	**24**	60	4
DME	dPh-pyridine	1 equiv	1.5 equiv	**22**	15	26
DME	2-Me,6-Cy-pyridine	1 equiv	1.5 equiv	**78**	0	4
DME	Tetrahydroquinoline	1 equiv	1.5 equiv	**61**	15	9
DME	lutidine	1 equiv	2 equiv	**76**	0	4
DME	BTMG	1 equiv	2 equiv	**47**	35	5
DME	BTTP	1 equiv	2 equiv	**25**	58	4
DME	dPh-pyridine	1 equiv	2 equiv	**22**	0	nd
DME	2-Me,6-Cy-pyridine	1 equiv	2 equiv	**0**	9	nd
DME	Tetrahydroquinoline	1 equiv	2 equiv	**33**	2	25
DME	lutidine	2 equiv	1.5 equiv	**80**	0	3
DME	BTMG	2 equiv	1.5 equiv	**31**	55	3
DME	BTTP	2 equiv	1.5 equiv	**19**	70	5

DME	dPh-pyridine	2 equiv	1.5 equiv	**29**	46	11
DME	2-Me,6-Cy-pyridine	2 equiv	1.5 equiv	**76**	0	4
DME	Tetrahydroquinoline	2 equiv	1.5 equiv	**74**	4	5
DME	lutidine	2 equiv	2 equiv	**76**	0	4
DME	BTMG	2 equiv	2 equiv	**37**	45	4
DME	BTTP	2 equiv	2 equiv	**21**	66	6
DME	dPh-pyridine	2 equiv	2 equiv	**20**	8	32
DME	2-Me,6-Cy-pyridine	2 equiv	2 equiv	**73**	0	5
DME	Tetrahydroquinoline	2 equiv	2 equiv	**66**	7	6
DME	lutidine	3 equiv	1.5 equiv	**79**	0	3
DME	BTMG	3 equiv	1.5 equiv	**28**	55	3
DME	BTTP	3 equiv	1.5 equiv	**17**	75	6
DME	dPh-pyridine	3 equiv	1.5 equiv	**27**	22	22
DME	2-Me,6-Cy-pyridine	3 equiv	1.5 equiv	**76**	0	4
DME	Tetrahydroquinoline	3 equiv	1.5 equiv	**67**	13	4
DME	lutidine	3 equiv	2 equiv	**75**	0	4
DME	BTMG	3 equiv	2 equiv	**39**	42	4
DME	BTTP	3 equiv	2 equiv	**17**	75	7
DME	dPh-pyridine	3 equiv	2 equiv	**26**	6	31
DME	2-Me,6-Cy-pyridine	3 equiv	2 equiv	**74**	0	4
DME	Tetrahydroquinoline	3 equiv	2 equiv	**70**	0	6
DME:Acetone 4:1	lutidine	0.5 equiv	1.5 equiv	**43**	3	21
DME:Acetone 4:1	BTMG	0.5 equiv	1.5 equiv	**59**	8	10
DME:Acetone 4:1	BTTP	0.5 equiv	1.5 equiv	**39**	44	5
DME:Acetone 4:1	dPh-pyridine	0.5 equiv	1.5 equiv	**10**	0	48
DME:Acetone 4:1	2-Me,6-Cy-pyridine	0.5 equiv	1.5 equiv	**75**	0	6
DME:Acetone 4:1	Tetrahydroquinoline	0.5 equiv	1.5 equiv	**17**	10	33
DME:Acetone 4:1	lutidine	0.5 equiv	2 equiv	**15**	0	43
DME:Acetone 4:1	BTMG	0.5 equiv	2 equiv	**62**	0	12
DME:Acetone 4:1	BTTP	0.5 equiv	2 equiv	**31**	51	5
DME:Acetone 4:1	dPh-pyridine	0.5 equiv	2 equiv	**13**	0	44
DME:Acetone 4:1	2-Me,6-Cy-pyridine	0.5 equiv	2 equiv	**69**	2	8
DME:Acetone 4:1	Tetrahydroquinoline	0.5 equiv	2 equiv	**44**	14	2
DME:Acetone 4:1	lutidine	1 equiv	1.5 equiv	**79**	0	5
DME:Acetone 4:1	BTMG	1 equiv	1.5 equiv	**20**	nd	5
DME:Acetone 4:1	BTTP	1 equiv	1.5 equiv	**17**	7	7
DME:Acetone 4:1	dPh-pyridine	1 equiv	1.5 equiv	**19**	0	40
DME:Acetone 4:1	2-Me,6-Cy-pyridine	1 equiv	1.5 equiv	**78**	0	4
DME:Acetone 4:1	Tetrahydroquinoline	1 equiv	1.5 equiv	**73**	0	7
DME:Acetone 4:1	lutidine	1 equiv	2 equiv	**58**	0	13

DME:Acetone 4:1	BTMG	1 equiv	2 equiv	**61**	5	7
DME:Acetone 4:1	BTTP	1 equiv	2 equiv	**30**	54	7
DME:Acetone 4:1	dPh-pyridine	1 equiv	2 equiv	**10**	0	45
DME:Acetone 4:1	2-Me,6-Cy-pyridine	1 equiv	2 equiv	**0**	10	nd
DME:Acetone 4:1	Tetrahydroquinoline	1 equiv	2 equiv	**60**	4	14
DME:Acetone 4:1	lutidine	2 equiv	1.5 equiv	**76**	0	4
DME:Acetone 4:1	BTMG	2 equiv	1.5 equiv	**42**	40	4
DME:Acetone 4:1	BTTP	2 equiv	1.5 equiv	**19**	69	7
DME:Acetone 4:1	dPh-pyridine	2 equiv	1.5 equiv	**20**	35	20
DME:Acetone 4:1	2-Me,6-Cy-pyridine	2 equiv	1.5 equiv	**76**	3	5
DME:Acetone 4:1	Tetrahydroquinoline	2 equiv	1.5 equiv	**70**	9	5
DME:Acetone 4:1	lutidine	2 equiv	2 equiv	**73**	0	4
DME:Acetone 4:1	BTMG	2 equiv	2 equiv	**48**	27	8
DME:Acetone 4:1	BTTP	2 equiv	2 equiv	**22**	65	7
DME:Acetone 4:1	dPh-pyridine	2 equiv	2 equiv	**23**	0	38
DME:Acetone 4:1	2-Me,6-Cy-pyridine	2 equiv	2 equiv	**73**	0	5
DME:Acetone 4:1	Tetrahydroquinoline	2 equiv	2 equiv	**70**	0	6
DME:Acetone 4:1	lutidine	3 equiv	1.5 equiv	**78**	0	4
DME:Acetone 4:1	BTMG	3 equiv	1.5 equiv	**39**	39	4
DME:Acetone 4:1	BTTP	3 equiv	1.5 equiv	**12**	71	8
DME:Acetone 4:1	dPh-pyridine	3 equiv	1.5 equiv	**28**	53	8
DME:Acetone 4:1	2-Me,6-Cy-pyridine	3 equiv	1.5 equiv	**75**	0	5
DME:Acetone 4:1	Tetrahydroquinoline	3 equiv	1.5 equiv	**74**	0	5
DME:Acetone 4:1	lutidine	3 equiv	2 equiv	**75**	0	4
DME:Acetone 4:1	BTMG	3 equiv	2 equiv	**48**	27	6
DME:Acetone 4:1	BTTP	3 equiv	2 equiv	**20**	70	8
DME:Acetone 4:1	dPh-pyridine	3 equiv	2 equiv	**28**	0	33
DME:Acetone 4:1	2-Me,6-Cy-pyridine	3 equiv	2 equiv	**74**	0	6
DME:Acetone 4:1	Tetrahydroquinoline	3 equiv	2 equiv	**70**	0	8
DME:dioxane 4:1	lutidine	0.5 equiv	1.5 equiv	**60**	11	12
DME:dioxane 4:1	BTMG	0.5 equiv	1.5 equiv	**55**	12	14
DME:dioxane 4:1	BTTP	0.5 equiv	1.5 equiv	**52**	31	4
DME:dioxane 4:1	dPh-pyridine	0.5 equiv	1.5 equiv	**11**	23	31
DME:dioxane 4:1	2-Me,6-Cy-pyridine	0.5 equiv	1.5 equiv	**75**	0	6
DME:dioxane 4:1	Tetrahydroquinoline	0.5 equiv	1.5 equiv	**46**	29	12
DME:dioxane 4:1	lutidine	0.5 equiv	2 equiv	**46**	0	21
DME:dioxane 4:1	BTMG	0.5 equiv	2 equiv	**48**	10	20
DME:dioxane 4:1	BTTP	0.5 equiv	2 equiv	**57**	22	5
DME:dioxane 4:1	dPh-pyridine	0.5 equiv	2 equiv	**9**	0	5
DME:dioxane 4:1	2-Me,6-Cy-pyridine	0.5 equiv	2 equiv	**62**	3	12

DME:dioxane 4:1	Tetrahydroquinoline	0.5 equiv	2 equiv	**18**	5	34
DME:dioxane 4:1	lutidine	1 equiv	1.5 equiv	**74**	0	4
DME:dioxane 4:1	BTMG	1 equiv	1.5 equiv	**53**	30	4
DME:dioxane 4:1	BTTP	1 equiv	1.5 equiv	**43**	51	5
DME:dioxane 4:1	dPh-pyridine	1 equiv	1.5 equiv	**18**	15	33
DME:dioxane 4:1	2-Me,6-Cy-pyridine	1 equiv	1.5 equiv	**72**	0	5
DME:dioxane 4:1	Tetrahydroquinoline	1 equiv	1.5 equiv	**67**	6	8
DME:dioxane 4:1	lutidine	1 equiv	2 equiv	**65**	0	11
DME:dioxane 4:1	BTMG	1 equiv	2 equiv	**52**	24	7
DME:dioxane 4:1	BTTP	1 equiv	2 equiv	**47**	48	5
DME:dioxane 4:1	dPh-pyridine	1 equiv	2 equiv	**14**	0	42
DME:dioxane 4:1	2-Me,6-Cy-pyridine	1 equiv	2 equiv	**0**	10	nd
DME:dioxane 4:1	Tetrahydroquinoline	1 equiv	2 equiv	**53**	5	16
DME:dioxane 4:1	lutidine	2 equiv	1.5 equiv	**73**	0	4
DME:dioxane 4:1	BTMG	2 equiv	1.5 equiv	**43**	39	4
DME:dioxane 4:1	BTTP	2 equiv	1.5 equiv	**26**	66	7
DME:dioxane 4:1	dPh-pyridine	2 equiv	1.5 equiv	**7**	41	23
DME:dioxane 4:1	2-Me,6-Cy-pyridine	2 equiv	1.5 equiv	**70**	0	5
DME:dioxane 4:1	Tetrahydroquinoline	2 equiv	1.5 equiv	**62**	17	5
DME:dioxane 4:1	lutidine	2 equiv	2 equiv	**70**	0	4
DME:dioxane 4:1	BTMG	2 equiv	2 equiv	**46**	34	5
DME:dioxane 4:1	BTTP	2 equiv	2 equiv	**36**	61	8
DME:dioxane 4:1	dPh-pyridine	2 equiv	2 equiv	**6**	0	43
DME:dioxane 4:1	2-Me,6-Cy-pyridine	2 equiv	2 equiv	**68**	0	6
DME:dioxane 4:1	Tetrahydroquinoline	2 equiv	2 equiv	**63**	13	6
DME:dioxane 4:1	lutidine	3 equiv	1.5 equiv	**69**	0	4
DME:dioxane 4:1	BTMG	3 equiv	1.5 equiv	**42**	39	4
DME:dioxane 4:1	BTTP	3 equiv	1.5 equiv	**15**	57	7
DME:dioxane 4:1	dPh-pyridine	3 equiv	1.5 equiv	**21**	43	18
DME:dioxane 4:1	2-Me,6-Cy-pyridine	3 equiv	1.5 equiv	**7**	9	39
DME:dioxane 4:1	Tetrahydroquinoline	3 equiv	1.5 equiv	**56**	28	5
DME:dioxane 4:1	lutidine	3 equiv	2 equiv	**71**	0	4
DME:dioxane 4:1	BTMG	3 equiv	2 equiv	**46**	32	5
DME:dioxane 4:1	BTTP	3 equiv	2 equiv	**20**	59	8
DME:dioxane 4:1	dPh-pyridine	3 equiv	2 equiv	**20**	0	38
DME:dioxane 4:1	2-Me,6-Cy-pyridine	3 equiv	2 equiv	**6**	0	43
DME:dioxane 4:1	Tetrahydroquinoline	3 equiv	2 equiv	**67**	2	7
DME:AcOEt 4:1	lutidine	0.5 equiv	1.5 equiv	**43**	9	22
DME:AcOEt 4:1	BTMG	0.5 equiv	1.5 equiv	**48**	5	21
DME:AcOEt 4:1	BTTP	0.5 equiv	1.5 equiv	**40**	51	5

DME:AcOEt 4:1	dPh-pyridine	0.5 equiv	1.5 equiv	**11**	17	35
DME:AcOEt 4:1	2-Me,6-Cy-pyridine	0.5 equiv	1.5 equiv	**7**	12	nd
DME:AcOEt 4:1	Tetrahydroquinoline	0.5 equiv	1.5 equiv	**16**	53	15
DME:AcOEt 4:1	lutidine	0.5 equiv	2 equiv	**28**	0	31
DME:AcOEt 4:1	BTMG	0.5 equiv	2 equiv	**56**	0	16
DME:AcOEt 4:1	BTTP	0.5 equiv	2 equiv	**50**	30	7
DME:AcOEt 4:1	dPh-pyridine	0.5 equiv	2 equiv	**13**	0	43
DME:AcOEt 4:1	2-Me,6-Cy-pyridine	0.5 equiv	2 equiv	**68**	0	9
DME:AcOEt 4:1	Tetrahydroquinoline	0.5 equiv	2 equiv	**24**	4	30
DME:AcOEt 4:1	lutidine	1 equiv	1.5 equiv	**67**	0	9
DME:AcOEt 4:1	BTMG	1 equiv	1.5 equiv	**48**	39	4
DME:AcOEt 4:1	BTTP	1 equiv	1.5 equiv	**35**	58	8
DME:AcOEt 4:1	dPh-pyridine	1 equiv	1.5 equiv	**11**	25	29
DME:AcOEt 4:1	2-Me,6-Cy-pyridine	1 equiv	1.5 equiv	**65**	9	nd
DME:AcOEt 4:1	Tetrahydroquinoline	1 equiv	1.5 equiv	**40**	20	21
DME:AcOEt 4:1	lutidine	1 equiv	2 equiv	**66**	0	5
DME:AcOEt 4:1	BTMG	1 equiv	2 equiv	**56**	19	6
DME:AcOEt 4:1	BTTP	1 equiv	2 equiv	**40**	53	8
DME:AcOEt 4:1	dPh-pyridine	1 equiv	2 equiv	**19**	0	38
DME:AcOEt 4:1	2-Me,6-Cy-pyridine	1 equiv	2 equiv	**0**	11	nd
DME:AcOEt 4:1	Tetrahydroquinoline	1 equiv	2 equiv	**61**	0	12
DME:AcOEt 4:1	lutidine	2 equiv	1.5 equiv	**71**	0	4
DME:AcOEt 4:1	BTMG	2 equiv	1.5 equiv	**47**	35	5
DME:AcOEt 4:1	BTTP	2 equiv	1.5 equiv	**18**	60	8
DME:AcOEt 4:1	dPh-pyridine	2 equiv	1.5 equiv	**20**	24	28
DME:AcOEt 4:1	2-Me,6-Cy-pyridine	2 equiv	1.5 equiv	**64**	0	5
DME:AcOEt 4:1	Tetrahydroquinoline	2 equiv	1.5 equiv	**69**	0	1
DME:AcOEt 4:1	lutidine	2 equiv	2 equiv	**68**	0	4
DME:AcOEt 4:1	BTMG	2 equiv	2 equiv	**54**	16	6
DME:AcOEt 4:1	BTTP	2 equiv	2 equiv	**25**	64	9
DME:AcOEt 4:1	dPh-pyridine	2 equiv	2 equiv	**22**	0	36
DME:AcOEt 4:1	2-Me,6-Cy-pyridine	2 equiv	2 equiv	**69**	11	nd
DME:AcOEt 4:1	Tetrahydroquinoline	2 equiv	2 equiv	**68**	0	6
DME:AcOEt 4:1	lutidine	3 equiv	1.5 equiv	**67**	0	4
DME:AcOEt 4:1	BTMG	3 equiv	1.5 equiv	**32**	57	5
DME:AcOEt 4:1	BTTP	3 equiv	1.5 equiv	**11**	59	8
DME:AcOEt 4:1	dPh-pyridine	3 equiv	1.5 equiv	**27**	45	18
DME:AcOEt 4:1	2-Me,6-Cy-pyridine	3 equiv	1.5 equiv	**65**	0	6
DME:AcOEt 4:1	Tetrahydroquinoline	3 equiv	1.5 equiv	**66**	12	nd
DME:AcOEt 4:1	lutidine	3 equiv	2 equiv	**67**	0	4

DME:AcOEt 4:1	BTMG	3 equiv	2 equiv	**49**	31	5
DME:AcOEt 4:1	BTTP	3 equiv	2 equiv	**14**	59	8
DME:AcOEt 4:1	dPh-pyridine	3 equiv	2 equiv	**23**	0	36
DME:AcOEt 4:1	2-Me,6-Cy-pyridine	3 equiv	2 equiv	**67**	0	5
DME:AcOEt 4:1	Tetrahydroquinoline	3 equiv	2 equiv	**65**	0	7

Data from Fig. S37. Bases loadings vs solvent loadings (0.3 M).

Solvent	Base	Base loading	TTMSH loading	Product (%)	ArBr (%)	ArH (%)
DME	lutidine	0.5 equiv	1.5 equiv	**55**	18	12
DME	DMAP	0.5 equiv	1.5 equiv	**3**	69	9
DME	lutidine	0.5 equiv	2 equiv	**49**	0	21
DME	DMAP	0.5 equiv	2 equiv	**12**	7	42
DME	lutidine	0.5 equiv	3 equiv	**33**	0	32
DME	DMAP	0.5 equiv	3 equiv	**8**	0	46
DME	lutidine	1 equiv	1.5 equiv	**67**	0	9
DME	DMAP	1 equiv	1.5 equiv	**1**	84	5
DME	lutidine	1 equiv	2 equiv	**57**	0	9
DME	DMAP	1 equiv	2 equiv	**0**	54	27
DME	lutidine	1 equiv	3 equiv	**46**	0	11
DME	DMAP	1 equiv	3 equiv	**1**	25	44
DME	lutidine	2 equiv	1.5 equiv	**70**	2	6
DME	DMAP	2 equiv	1.5 equiv	**0**	69	13
DME	lutidine	2 equiv	2 equiv	**62**	0	8
DME	DMAP	2 equiv	2 equiv	**0**	50	28
DME	lutidine	2 equiv	3 equiv	**54**	0	9
DME	DMAP	2 equiv	3 equiv	**0**	27	44
DME	lutidine	3 equiv	1.5 equiv	**73**	2	6
DME	DMAP	3 equiv	1.5 equiv	**0**	49	21
DME	lutidine	3 equiv	2 equiv	**64**	0	8
DME	DMAP	3 equiv	2 equiv	**1**	53	23
DME	lutidine	3 equiv	3 equiv	**48**	0	11
DME	DMAP	3 equiv	3 equiv	**3**	20	38
DME:DMA 4:1	lutidine	0.5 equiv	1.5 equiv	**50**	11	23
DME:DMA 4:1	DMAP	0.5 equiv	1.5 equiv	**35**	39	12
DME:DMA 4:1	lutidine	0.5 equiv	2 equiv	**45**	3	31
DME:DMA 4:1	DMAP	0.5 equiv	2 equiv	**49**	3	27
DME:DMA 4:1	lutidine	0.5 equiv	3 equiv	**36**	2	2
DME:DMA 4:1	DMAP	0.5 equiv	3 equiv	**4**	11	36

DME:DMA 4:1	lutidine	1 equiv	1.5 equiv	**61**	6	15
DME:DMA 4:1	DMAP	1 equiv	1.5 equiv	**23**	37	18
DME:DMA 4:1	lutidine	1 equiv	2 equiv	**49**	0	28
DME:DMA 4:1	DMAP	1 equiv	2 equiv	**18**	26	23
DME:DMA 4:1	lutidine	1 equiv	3 equiv	**48**	0	17
DME:DMA 4:1	DMAP	1 equiv	3 equiv	**2**	12	40
DME:DMA 4:1	lutidine	2 equiv	1.5 equiv	**67**	0	10
DME:DMA 4:1	DMAP	2 equiv	1.5 equiv	**3**	71	9
DME:DMA 4:1	lutidine	2 equiv	2 equiv	**55**	0	14
DME:DMA 4:1	DMAP	2 equiv	2 equiv	**3**	28	35
DME:DMA 4:1	lutidine	2 equiv	3 equiv	**47**	0	16
DME:DMA 4:1	DMAP	2 equiv	3 equiv	**1**	25	38
DME:DMA 4:1	lutidine	3 equiv	1.5 equiv	**65**	0	10
DME:DMA 4:1	DMAP	3 equiv	1.5 equiv	**48**	21	18
DME:DMA 4:1	lutidine	3 equiv	2 equiv	**55**	0	15
DME:DMA 4:1	DMAP	3 equiv	2 equiv	**46**	4	29
DME:DMA 4:1	lutidine	3 equiv	3 equiv	**45**	0	19
DME:DMA 4:1	DMAP	3 equiv	3 equiv	**38**	2	32
DME:DCM 4:1	lutidine	0.5 equiv	1.5 equiv	**7**	29	32
DME:DCM 4:1	DMAP	0.5 equiv	1.5 equiv	**1**	71	12
DME:DCM 4:1	lutidine	0.5 equiv	2 equiv	**19**	0	31
DME:DCM 4:1	DMAP	0.5 equiv	2 equiv	**1**	32	38
DME:DCM 4:1	lutidine	0.5 equiv	3 equiv	**8**	0	39
DME:DCM 4:1	DMAP	0.5 equiv	3 equiv	**1**	7	53
DME:DCM 4:1	lutidine	1 equiv	1.5 equiv	**48**	12	17
DME:DCM 4:1	DMAP	1 equiv	1.5 equiv	**0**	68	18
DME:DCM 4:1	lutidine	1 equiv	2 equiv	**36**	0	28
DME:DCM 4:1	DMAP	1 equiv	2 equiv	**0**	43	34
DME:DCM 4:1	lutidine	1 equiv	3 equiv	**20**	5	36
DME:DCM 4:1	DMAP	1 equiv	3 equiv	**0**	16	46
DME:DCM 4:1	lutidine	2 equiv	1.5 equiv	**68**	1	6
DME:DCM 4:1	DMAP	2 equiv	1.5 equiv	**0**	79	9
DME:DCM 4:1	lutidine	2 equiv	2 equiv	**52**	0	10
DME:DCM 4:1	DMAP	2 equiv	2 equiv	**0**	53	29
DME:DCM 4:1	lutidine	2 equiv	3 equiv	**54**	0	8
DME:DCM 4:1	DMAP	2 equiv	3 equiv	**0**	38	37
DME:DCM 4:1	lutidine	3 equiv	1.5 equiv	**64**	1	7
DME:DCM 4:1	DMAP	3 equiv	1.5 equiv	**0**	76	11
DME:DCM 4:1	lutidine	3 equiv	2 equiv	**59**	0	8
DME:DCM 4:1	DMAP	3 equiv	2 equiv	**0**	53	28

DME:DCM 4:1	lutidine	3 equiv	3 equiv	**55**	0	8
DME:DCM 4:1	DMAP	3 equiv	3 equiv	**0**	33	38
DME:ACN 4:1	lutidine	0.5 equiv	1.5 equiv	**32**	30	23
DME:ACN 4:1	DMAP	0.5 equiv	1.5 equiv	**8**	71	6
DME:ACN 4:1	lutidine	0.5 equiv	2 equiv	**20**	1	37
DME:ACN 4:1	DMAP	0.5 equiv	2 equiv	**3**	67	14
DME:ACN 4:1	lutidine	0.5 equiv	3 equiv	**7**	22	37
DME:ACN 4:1	DMAP	0.5 equiv	3 equiv	**2**	26	35
DME:ACN 4:1	lutidine	1 equiv	1.5 equiv	**58**	5	12
DME:ACN 4:1	DMAP	1 equiv	1.5 equiv	**1**	57	23
DME:ACN 4:1	lutidine	1 equiv	2 equiv	**54**	0	14
DME:ACN 4:1	DMAP	1 equiv	2 equiv	**3**	52	23
DME:ACN 4:1	lutidine	1 equiv	3 equiv	**40**	0	21
DME:ACN 4:1	DMAP	1 equiv	3 equiv	**0**	20	39
DME:ACN 4:1	lutidine	2 equiv	1.5 equiv	**59**	7	10
DME:ACN 4:1	DMAP	2 equiv	1.5 equiv	**0**	40	34
DME:ACN 4:1	lutidine	2 equiv	2 equiv	**44**	0	16
DME:ACN 4:1	DMAP	2 equiv	2 equiv	**0**	40	34
DME:ACN 4:1	lutidine	2 equiv	3 equiv	**42**	0	16
DME:ACN 4:1	DMAP	2 equiv	3 equiv	**0**	20	39
DME:ACN 4:1	lutidine	3 equiv	1.5 equiv	**57**	11	9
DME:ACN 4:1	DMAP	3 equiv	1.5 equiv	**12**	52	16
DME:ACN 4:1	lutidine	3 equiv	2 equiv	**47**	0	15
DME:ACN 4:1	DMAP	3 equiv	2 equiv	**0**	24	39
DME:ACN 4:1	lutidine	3 equiv	3 equiv	**39**	2	19
DME:ACN 4:1	DMAP	3 equiv	3 equiv	**0**	25	38

Data from Fig. S38. Bases loadings vs. solvent loadings (0.3 M).

Base	Base loading	Solvent	Solvent ratio	Product (%)	ArBr (%)	ArH (%)
lutidine	0.5 equiv	DME:DMF	1:0	**79**	0	5
lutidine	0.5 equiv	DME:DMF	4:1	**76**	0	8
lutidine	0.5 equiv	DME:DMF	2:1	**66**	8	10
lutidine	0.5 equiv	DME:DMF	1:1	**63**	8	11
collidine	0.5 equiv	DME:DMF	1:0	**79**	0	4
collidine	0.5 equiv	DME:DMF	4:1	**77**	0	6
collidine	0.5 equiv	DME:DMF	2:1	**73**	0	9
collidine	0.5 equiv	DME:DMF	1:1	**67**	0	12
2,6-d^{t}Bupyridine	0.5 equiv	DME:DMF	1:0	**36**	47	10
2,6-d^{t}Bupyridine	0.5 equiv	DME:DMF	4:1	**29**	41	19

2,6-d^{t}Bupyridine	0.5 equiv	DME:DMF	2:1	**30**	37	20
2,6-d^{t}Bupyridine	0.5 equiv	DME:DMF	1:1	**30**	38	19
lutidine	1 equiv	DME:DMF	1:0	**80**	0	4
lutidine	1 equiv	DME:DMF	4:1	**75**	0	8
lutidine	1 equiv	DME:DMF	2:1	**63**	0	5
lutidine	1 equiv	DME:DMF	1:1	**61**	0	5
collidine	1 equiv	DME:DMF	1:0	**79**	0	4
collidine	1 equiv	DME:DMF	4:1	**76**	0	6
collidine	1 equiv	DME:DMF	2:1	**73**	0	8
collidine	1 equiv	DME:DMF	1:1	**69**	0	11
2,6-d^{t}Bupyridine	1 equiv	DME:DMF	1:0	**36**	47	10
2,6-d^{t}Bupyridine	1 equiv	DME:DMF	4:1	**30**	42	19
2,6-d^{t}Bupyridine	1 equiv	DME:DMF	2:1	**31**	36	20
2,6-d^{t}Bupyridine	1 equiv	DME:DMF	1:1	**31**	34	21
lutidine	2 equiv	DME:DMF	1:0	**81**	0	4
lutidine	2 equiv	DME:DMF	4:1	**74**	0	8
lutidine	2 equiv	DME:DMF	2:1	**61**	12	11
lutidine	2 equiv	DME:DMF	1:1	**60**	10	12
collidine	2 equiv	DME:DMF	1:0	**80**	0	4
collidine	2 equiv	DME:DMF	4:1	**76**	0	6
collidine	2 equiv	DME:DMF	2:1	**74**	0	8
collidine	2 equiv	DME:DMF	1:1	**65**	3	11
2,6-d^{t}Bupyridine	2 equiv	DME:DMF	1:0	**38**	44	10
2,6-d^{t}Bupyridine	2 equiv	DME:DMF	4:1	**32**	36	19
2,6-d^{t}Bupyridine	2 equiv	DME:DMF	2:1	**34**	32	20
2,6-d^{t}Bupyridine	2 equiv	DME:DMF	1:1	**36**	29	21
lutidine	3 equiv	DME:DMF	1:0	**79**	0	4
lutidine	3 equiv	DME:DMF	4:1	**75**	0	8
lutidine	3 equiv	DME:DMF	2:1	**61**	11	8
lutidine	3 equiv	DME:DMF	1:1	**59**	11	12
collidine	3 equiv	DME:DMF	1:0	**79**	0	4
collidine	3 equiv	DME:DMF	4:1	**75**	0	7
collidine	3 equiv	DME:DMF	2:1	**72**	0	8
collidine	3 equiv	DME:DMF	1:1	**63**	4	11
2,6-d^{t}Bupyridine	3 equiv	DME:DMF	1:0	**40**	37	13
2,6-d^{t}Bupyridine	3 equiv	DME:DMF	4:1	**35**	33	20
2,6-d^{t}Bupyridine	3 equiv	DME:DMF	2:1	**37**	28	21
2,6-d^{t}Bupyridine	3 equiv	DME:DMF	1:1	**39**	25	21
lutidine	0.5 equiv	DME:DMA	1:0	**77**	0	6
lutidine	0.5 equiv	DME:DMA	4:1	**75**	0	7

lutidine	0.5 equiv	DME:DMA	2:1	**73**	0	9
lutidine	0.5 equiv	DME:DMA	1:1	**72**	0	10
collidine	0.5 equiv	DME:DMA	1:0	**78**	0	4
collidine	0.5 equiv	DME:DMA	4:1	**75**	0	6
collidine	0.5 equiv	DME:DMA	2:1	**74**	0	6
collidine	0.5 equiv	DME:DMA	1:1	**73**	0	8
2,6-d^{t}Bupyridine	0.5 equiv	DME:DMA	1:0	**34**	49	10
2,6-d^{t}Bupyridine	0.5 equiv	DME:DMA	4:1	**45**	28	15
2,6-d^{t}Bupyridine	0.5 equiv	DME:DMA	2:1	**53**	20	14
2,6-d^{t}Bupyridine	0.5 equiv	DME:DMA	1:1	**62**	11	11
lutidine	1 equiv	DME:DMA	1:0	**77**	0	5
lutidine	1 equiv	DME:DMA	4:1	**76**	0	7
lutidine	1 equiv	DME:DMA	2:1	**74**	0	8
lutidine	1 equiv	DME:DMA	1:1	**71**	0	10
collidine	1 equiv	DME:DMA	1:0	**79**	0	4
collidine	1 equiv	DME:DMA	4:1	**75**	0	6
collidine	1 equiv	DME:DMA	2:1	**74**	0	7
collidine	1 equiv	DME:DMA	1:1	**73**	0	8
2,6-d^{t}Bupyridine	1 equiv	DME:DMA	1:0	**32**	48	11
2,6-d^{t}Bupyridine	1 equiv	DME:DMA	4:1	**45**	29	14
2,6-d^{t}Bupyridine	1 equiv	DME:DMA	2:1	**49**	24	14
2,6-d^{t}Bupyridine	1 equiv	DME:DMA	1:1	**55**	16	13
lutidine	2 equiv	DME:DMA	1:0	**77**	0	5
lutidine	2 equiv	DME:DMA	4:1	**76**	0	7
lutidine	2 equiv	DME:DMA	2:1	**73**	0	8
lutidine	2 equiv	DME:DMA	1:1	**69**	1	11
collidine	2 equiv	DME:DMA	1:0	**78**	0	4
collidine	2 equiv	DME:DMA	4:1	**76**	0	6
collidine	2 equiv	DME:DMA	2:1	**74**	0	7
collidine	2 equiv	DME:DMA	1:1	**72**	0	8
2,6-d^{t}Bupyridine	2 equiv	DME:DMA	1:0	**35**	45	11
2,6-d^{t}Bupyridine	2 equiv	DME:DMA	4:1	**43**	32	13
2,6-d^{t}Bupyridine	2 equiv	DME:DMA	2:1	**49**	24	14
2,6-d^{t}Bupyridine	2 equiv	DME:DMA	1:1	**56**	15	13
lutidine	3 equiv	DME:DMA	1:0	**75**	0	6
lutidine	3 equiv	DME:DMA	4:1	**75**	0	8
lutidine	3 equiv	DME:DMA	2:1	**73**	0	9
lutidine	3 equiv	DME:DMA	1:1	**69**	0	12
collidine	3 equiv	DME:DMA	1:0	**75**	0	5
collidine	3 equiv	DME:DMA	4:1	**72**	0	7

collidine	3 equiv	DME:DMA	2:1	**72**	0	8
collidine	3 equiv	DME:DMA	1:1	**72**	0	9
2,6-d^{t}Bupyridine	3 equiv	DME:DMA	1:0	**38**	40	12
2,6-d^{t}Bupyridine	3 equiv	DME:DMA	4:1	**46**	29	15
2,6-d^{t}Bupyridine	3 equiv	DME:DMA	2:1	**53**	19	15
2,6-d^{t}Bupyridine	3 equiv	DME:DMA	1:1	**62**	10	12
lutidine	0.5 equiv	Acetone:DMA	1:0	**48**	32	11
lutidine	0.5 equiv	Acetone:DMA	4:1	**58**	18	10
lutidine	0.5 equiv	Acetone:DMA	2:1	**60**	17	9
lutidine	0.5 equiv	Acetone:DMA	1:1	**61**	15	9
collidine	0.5 equiv	Acetone:DMA	1:0	**65**	12	7
collidine	0.5 equiv	Acetone:DMA	4:1	**68**	10	7
collidine	0.5 equiv	Acetone:DMA	2:1	**8**	86	8
collidine	0.5 equiv	Acetone:DMA	1:1	**62**	16	8
2,6-d^{t}Bupyridine	0.5 equiv	Acetone:DMA	1:0	**48**	30	10
2,6-d^{t}Bupyridine	0.5 equiv	Acetone:DMA	4:1	**50**	21	15
2,6-d^{t}Bupyridine	0.5 equiv	Acetone:DMA	2:1	**52**	19	14
2,6-d^{t}Bupyridine	0.5 equiv	Acetone:DMA	1:1	**54**	18	13
lutidine	1 equiv	Acetone:DMA	1:0	**69**	12	7
lutidine	1 equiv	Acetone:DMA	4:1	**64**	16	7
lutidine	1 equiv	Acetone:DMA	2:1	**62**	16	8
lutidine	1 equiv	Acetone:DMA	1:1	**62**	15	8
collidine	1 equiv	Acetone:DMA	1:0	**67**	13	6
collidine	1 equiv	Acetone:DMA	4:1	**70**	7	7
collidine	1 equiv	Acetone:DMA	2:1	**68**	10	7
collidine	1 equiv	Acetone:DMA	1:1	**63**	15	7
2,6-d^{t}Bupyridine	1 equiv	Acetone:DMA	1:0	**47**	31	10
2,6-d^{t}Bupyridine	1 equiv	Acetone:DMA	4:1	**48**	24	15
2,6-d^{t}Bupyridine	1 equiv	Acetone:DMA	2:1	**50**	23	14
2,6-d^{t}Bupyridine	1 equiv	Acetone:DMA	1:1	**52**	20	13
lutidine	2 equiv	Acetone:DMA	1:0	**65**	16	6
lutidine	2 equiv	Acetone:DMA	4:1	**63**	17	7
lutidine	2 equiv	Acetone:DMA	2:1	**63**	16	7
lutidine	2 equiv	Acetone:DMA	1:1	**62**	14	8
collidine	2 equiv	Acetone:DMA	1:0	**68**	10	6
collidine	2 equiv	Acetone:DMA	4:1	**70**	7	7
collidine	2 equiv	Acetone:DMA	2:1	**68**	10	7
collidine	2 equiv	Acetone:DMA	1:1	**62**	15	8
2,6-d^{t}Bupyridine	2 equiv	Acetone:DMA	1:0	**49**	29	10
2,6-d^{t}Bupyridine	2 equiv	Acetone:DMA	4:1	**49**	24	14

2,6-d^{t}Bupyridine	2 equiv	Acetone:DMA	2:1	**49**	24	14
2,6-d^{t}Bupyridine	2 equiv	Acetone:DMA	1:1	**50**	21	14
lutidine	3 equiv	Acetone:DMA	1:0	**64**	17	7
lutidine	3 equiv	Acetone:DMA	4:1	**61**	18	7
lutidine	3 equiv	Acetone:DMA	2:1	**60**	18	7
lutidine	3 equiv	Acetone:DMA	1:1	**61**	15	9
collidine	3 equiv	Acetone:DMA	1:0	**66**	13	6
collidine	3 equiv	Acetone:DMA	4:1	**67**	11	7
collidine	3 equiv	Acetone:DMA	2:1	**65**	13	7
collidine	3 equiv	Acetone:DMA	1:1	**60**	18	8
2,6-d^{t}Bupyridine	3 equiv	Acetone:DMA	1:0	**45**	35	10
2,6-d^{t}Bupyridine	3 equiv	Acetone:DMA	4:1	**49**	25	15
2,6-d^{t}Bupyridine	3 equiv	Acetone:DMA	2:1	**49**	23	15
2,6-d^{t}Bupyridine	3 equiv	Acetone:DMA	1:1	**51**	20	14

Data from Fig. S40. 2,6-Lutidine loading vs water loading (0.2 M).

Water loading	Base loading	Product (%)	ArBr (%)	ArH (%)
0 equiv	0.5 equiv	**35**	56	7
0 equiv	1 equiv	**54**	30	8
0 equiv	2 equiv	**51**	33	7
0 equiv	3 equiv	**48**	36	7
0 equiv	4 equiv	**46**	38	7
0 equiv	5 equiv	**44**	41	6
5 equiv	0.5 equiv	**28**	55	9
5 equiv	1 equiv	**34**	44	9
5 equiv	2 equiv	**35**	42	10
5 equiv	3 equiv	**35**	41	10
5 equiv	4 equiv	**35**	40	11
5 equiv	5 equiv	**35**	41	11
10 equiv	0.5 equiv	**17**	60	12
10 equiv	1 equiv	**28**	48	10
10 equiv	2 equiv	**26**	50	10
10 equiv	3 equiv	**25**	52	10
10 equiv	4 equiv	**25**	51	10
10 equiv	5 equiv	**24**	52	10
20 equiv	0.5 equiv	**7**	71	11
20 equiv	1 equiv	**21**	52	13
20 equiv	2 equiv	**19**	59	10
20 equiv	3 equiv	**19**	58	11

20 equiv	4 equiv	**17**	61	11
20 equiv	5 equiv	**16**	64	10

Data from Fig. S41. 2,6-Lutidine loading vs. solvents (0.2 M).

Base loading	Solvent	Product (%)	ArBr (%)	ArH (%)
1 equiv	DME:water	**43**	51	18
1 equiv	DME	**38**	56	10
1 equiv	DME:Acetone	**37**	51	13
1 equiv	DME:AcOEt	**45**	38	14
1 equiv	DME:DMA	**62**	16	14
1 equiv	DME:DMF	**38**	39	18
2 equiv	DME:water	**74**	3	12
2 equiv	DME	**71**	11	9
2 equiv	DME:Acetone	**72**	8	10
2 equiv	DME:AcOEt	**81**	0	6
2 equiv	DME:DMA	**76**	3	10
2 equiv	DME:DMF	**60**	11	17
3 equiv	DME:water	**76**	0	12
3 equiv	DME	**81**	0	7
3 equiv	DME:Acetone	**81**	0	7
3 equiv	DME:AcOEt	**83**	0	6
3 equiv	DME:DMA	**78**	3	8
3 equiv	DME:DMF	**69**	5	14
4 equiv	DME:water	**76**	0	9
4 equiv	DME	**77**	0	8
4 equiv	DME:Acetone	**78**	0	7
4 equiv	DME:AcOEt	**81**	0	6
4 equiv	DME:DMA	**79**	2	9
4 equiv	DME:DMF	**70**	3	14

Data from Fig. S42. Solvents ratio vs water loading in DME:DMA (0.2 M).

DME:DMA ratio	Water loading	Product (%)	ArBr (%)	ArH (%)
4.0-1.0	0 equiv	**77**	2	7
3.0-1.0	0 equiv	**71**	10	7
2.0-1.0	0 equiv	**68**	15	7
1.0-1.0	0 equiv	**56**	31	8
4.0-1.0	2 equiv	**70**	3	13

3.0-1.0	2 equiv	**69**	5	13
2.0-1.0	2 equiv	**65**	9	13
1.0-1.0	2 equiv	**59**	16	14

Data from Fig. S43. Base vs photocatalyst and Ni-complex loadings.

Photocatalyst loading	Nickel loading	Base loading	Product (%)	ArBr (%)	ArH (%)
0.5 mol%	0.5 mol%	1 equiv	**81**	0	14
0.5 mol%	1 mol%	1 equiv	**86**	0	7
0.5 mol%	1.5 mol%	1 equiv	**85**	0	7
0.5 mol%	0.5 mol%	2 equiv	**81**	0	9
0.5 mol%	1 mol%	2 equiv	**84**	0	6
0.5 mol%	1.5 mol%	2 equiv	**85**	0	6
1 mol%	0.5 mol%	1 equiv	**69**	0	16
1 mol%	1 mol%	1 equiv	**84**	8	7
1 mol%	1.5 mol%	1 equiv	**84**	0	7
1 mol%	0.5 mol%	2 equiv	**78**	0	10
1 mol%	1 mol%	2 equiv	**82**	0	7
1 mol%	1.5 mol%	2 equiv	**82**	0	6
0.5 mol%	0.5 mol%	1 equiv	**23**	74	4
0.5 mol%	1 mol%	1 equiv	**14**	85	3
0.5 mol%	1.5 mol%	1 equiv	**12**	88	3
0.5 mol%	0.5 mol%	2 equiv	**26**	68	5
0.5 mol%	1 mol%	2 equiv	**19**	77	4
0.5 mol%	1.5 mol%	2 equiv	**16**	81	4
1 mol%	0.5 mol%	1 equiv	**26**	71	5
1 mol%	1 mol%	1 equiv	**17**	82	3
1 mol%	1.5 mol%	1 equiv	**15**	84	3
1 mol%	0.5 mol%	2 equiv	**33**	60	6
1 mol%	1 mol%	2 equiv	**23**	74	5
1 mol%	1.5 mol%	2 equiv	**19**	77	4

Data from Fig. S44. Base and Ni-complex loadings vs bases.

Base	Base loading	Nickel loading	Product (%)	ArBr (%)	ArH (%)
Na_2CO_3 suspension	2 equiv	0.5 mol%	**15**	44	19
lutidine	5 equiv	0.5 mol%	**55**	14	15

lutidine	2 equiv	0.5 mol%	**68**	6	10
lutidine	2 equiv	1 mol%	**67**	10	nd
lutidine	5 equiv	1 mol%	**64**	19	nd
collidine	2 equiv	1 mol%	**72**	3	nd
collidine	5 equiv	1 mol%	**73**	3	nd

Data from Fig. S45. Photocatalyst vs Nickel salt and ligand.

Photocatalyst	Nickel source	Ligand	Nickel complex loading	Product (%)	ArBr (%)	ArH (%)
$[Ir(dF(CF_3)ppy)_2dtbbpy]PF_6$	$NiCl_2{\cdot}6H_2O$	dtbbpy	0.5 mol%	**64**	16	10
$[Ir(dF(CF_3)ppy)_2dtbbpy]PF_6$	$NiCl_2{\cdot}6H_2O$	dMeObpy	0.5 mol%	**62**	19	10
$[Ir(dF(CF_3)ppy)_2dtbbpy]PF_6$	$NiCl_2{\cdot}6H_2O$	dCF_3bpy	0.5 mol%	**7**	72	14
$[Ir(dF(CF_3)ppy)_2dtbbpy]PF_6$	$NiCl_2{\cdot}6H_2O$	Impy	0.5 mol%	**57**	27	8
$[Ir(dF(CF_3)ppy)_2dtbbpy]PF_6$	$NiCl_2{\cdot}6H_2O$	BIm	0.5 mol%	**22**	60	13
$[Ir(dF(CF_3)ppy)_2dtbbpy]PF_6$	$NiCl_2{\cdot}dme$	dtbbpy	0.5 mol%	**63**	17	10
$[Ir(dF(CF_3)ppy)_2dtbbpy]PF_6$	$NiCl_2{\cdot}dme$	dMeObpy	0.5 mol%	**63**	18	10
$[Ir(dF(CF_3)ppy)_2dtbbpy]PF_6$	$NiCl_2{\cdot}dme$	dCF_3bpy	0.5 mol%	**6**	75	13
$[Ir(dF(CF_3)ppy)_2dtbbpy]PF_6$	$NiCl_2{\cdot}dme$	Impy	0.5 mol%	**56**	30	8
$[Ir(dF(CF_3)ppy)_2dtbbpy]PF_6$	$NiCl_2{\cdot}dme$	BIm	0.5 mol%	**19**	66	10
$[Ir(dF(CF_3)ppy)_2dtbbpy]PF_6$	$NiCl_2{\cdot}6H_2O$	dtbbpy	2 mol%	**52**	32	8
$[Ir(dF(CF_3)ppy)_2dtbbpy]PF_6$	$NiCl_2{\cdot}6H_2O$	dMeObpy	2 mol%	**59**	21	10
$[Ir(dF(CF_3)ppy)_2dtbbpy]PF_6$	$NiCl_2{\cdot}6H_2O$	dCF_3bpy	2 mol%	**46**	34	15
$[Ir(dF(CF_3)ppy)_2dtbbpy]PF_6$	$NiCl_2{\cdot}6H_2O$	Impy	2 mol%	**56**	28	8
$[Ir(dF(CF_3)ppy)_2dtbbpy]PF_6$	$NiCl_2{\cdot}6H_2O$	BIm	2 mol%	**42**	20	24
$[Ir(dF(CF_3)ppy)_2dtbbpy]PF_6$	$NiCl_2{\cdot}dme$	dtbbpy	2 mol%	**50**	34	9
$[Ir(dF(CF_3)ppy)_2dtbbpy]PF_6$	$NiCl_2{\cdot}dme$	dMeObpy	2 mol%	**55**	32	7
$[Ir(dF(CF_3)ppy)_2dtbbpy]PF_6$	$NiCl_2{\cdot}dme$	dCF_3bpy	2 mol%	**47**	34	14
$[Ir(dF(CF_3)ppy)_2dtbbpy]PF_6$	$NiCl_2{\cdot}dme$	Impy	2 mol%	**58**	28	7
$[Ir(dF(CF_3)ppy)_2dtbbpy]PF_6$	$NiCl_2{\cdot}dme$	BIm	2 mol%	**44**	21	23
$[Ir(dF(Me)ppy)_2dtbbpy]PF_6$	$NiCl_2{\cdot}6H_2O$	dtbbpy	0.5 mol%	**52**	34	10
$[Ir(dF(Me)ppy)_2dtbbpy]PF_6$	$NiCl_2{\cdot}6H_2O$	dMeObpy	0.5 mol%	**53**	32	10
$[Ir(dF(Me)ppy)_2dtbbpy]PF_6$	$NiCl_2{\cdot}6H_2O$	dCF_3bpy	0.5 mol%	**8**	64	17
$[Ir(dF(Me)ppy)_2dtbbpy]PF_6$	$NiCl_2{\cdot}6H_2O$	Impy	0.5 mol%	**53**	30	9
$[Ir(dF(Me)ppy)_2dtbbpy]PF_6$	$NiCl_2{\cdot}6H_2O$	BIm	0.5 mol%	**28**	49	13
$[Ir(dF(Me)ppy)_2dtbbpy]PF_6$	$NiCl_2{\cdot}dme$	dtbbpy	0.5 mol%	**49**	35	9
$[Ir(dF(Me)ppy)_2dtbbpy]PF_6$	$NiCl_2{\cdot}dme$	dMeObpy	0.5 mol%	**52**	34	9
$[Ir(dF(Me)ppy)_2dtbbpy]PF_6$	$NiCl_2{\cdot}dme$	dCF_3bpy	0.5 mol%	**8**	67	15

$[Ir(dF(Me)ppy)_2dtbbpy]PF_6$	$NiCl_2$·dme	Impy	0.5 mol%	**52**	32	9
$[Ir(dF(Me)ppy)_2dtbbpy]PF_6$	$NiCl_2$·dme	BIm	0.5 mol%	**28**	52	12
$[Ir(dF(Me)ppy)_2dtbbpy]PF_6$	$NiCl_2·6H_2O$	dtbbpy	2 mol%	**38**	48	7
$[Ir(dF(Me)ppy)_2dtbbpy]PF_6$	$NiCl_2·6H_2O$	dMeObpy	2 mol%	**43**	42	8
$[Ir(dF(Me)ppy)_2dtbbpy]PF_6$	$NiCl_2·6H_2O$	dCF_3bpy	2 mol%	**33**	53	10
$[Ir(dF(Me)ppy)_2dtbbpy]PF_6$	$NiCl_2·6H_2O$	Impy	2 mol%	**44**	43	8
$[Ir(dF(Me)ppy)_2dtbbpy]PF_6$	$NiCl_2·6H_2O$	BIm	2 mol%	**41**	26	20
$[Ir(dF(Me)ppy)_2dtbbpy]PF_6$	$NiCl_2$·dme	dtbbpy	2 mol%	**34**	53	7
$[Ir(dF(Me)ppy)_2dtbbpy]PF_6$	$NiCl_2$·dme	dMeObpy	2 mol%	**42**	46	7
$[Ir(dF(Me)ppy)_2dtbbpy]PF_6$	$NiCl_2$·dme	dCF_3bpy	2 mol%	**32**	56	9
$[Ir(dF(Me)ppy)_2dtbbpy]PF_6$	$NiCl_2$·dme	Impy	2 mol%	**44**	45	7
$[Ir(dF(Me)ppy)_2dtbbpy]PF_6$	$NiCl_2$·dme	BIm	2 mol%	**44**	27	19

Data from Fig. S46. Reaction time vs nickel-complex.

Nickel source	Nickel loading	Time	Product (%)	ArBr (%)	ArH (%)
$NiCl_2$·dtbbpy	0.3 mol%	30 min	**58**	23	11
$NiCl_2$·dtbbpy	0.4 mol%	30 min	**63**	17	11
$NiCl_2$·dtbbpy	0.5 mol%	30 min	**62**	20	10
$NiCl_2$·dtbbpy	0.3 mol%	40 min	**62**	14	12
$NiCl_2$·dtbbpy	0.4 mol%	40 min	**66**	10	11
$NiCl_2$·dtbbpy	0.5 mol%	40 min	**68**	10	11
$NiCl_2$·dtbbpy	0.3 mol%	45 min	**68**	11	15
$NiCl_2$·dtbbpy	0.4 mol%	45 min	**72**	4	13
$NiCl_2$·dtbbpy	0.5 mol%	45 min	**75**	1	12
$NiCl_2$·Impy	0.3 mol%	45 min	**59**	19	11
$NiCl_2$·Impy	0.4 mol%	45 min	**67**	11	11
$NiCl_2$·Impy	0.5 mol%	45 min	**70**	7	11

Data from Fig. S47. Ni-complex vs Ni-complex loading.

Nickel source	Nickel loading	Product (%)	ArBr (%)	ArH (%)
$NiCl_2$·dtbbpy	0.3 mol%	**68**	11	15
$NiCl_2$·dtbbpy	0.4 mol%	**72**	4	13
$NiCl_2$·dtbbpy	0.5 mol%	**75**	1	12
$NiCl_2$·dtbbpy	0.6 mol%	**75**	0	11
$NiCl_2$·dtbbpy	0.7 mol%	**73**	3	11
$NiCl_2$·dtbbpy	0.8 mol%	**72**	4	11
$NiCl_2$·dtbbpy	0.9 mol%	**74**	1	11
$NiCl_2$·dtbbpy	1 mol%	**75**	1	10
$NiCl_2$·dtbbpy	1.5 mol%	**68**	9	10

$NiCl_2$·dtbbpy	2 mol%	**59**	19	9
$NiCl_2$·Impy	0.3 mol%	**59**	19	11
$NiCl_2$·Impy	0.4 mol%	**67**	11	11
$NiCl_2$·Impy	0.5 mol%	**70**	7	11
$NiCl_2$·Impy	0.6 mol%	**72**	6	10
$NiCl_2$·Impy	0.7 mol%	**71**	7	10
$NiCl_2$·Impy	0.8 mol%	**70**	8	10
$NiCl_2$·Impy	0.9 mol%	**72**	6	10
$NiCl_2$·Impy	1 mol%	**73**	5	9
$NiCl_2$·Impy	1.5 mol%	**69**	10	9
$NiCl_2$·Impy	2 mol%	**63**	17	9

8.6. Data from C–O cross-coupling.

Data from Fig. S58. Bases vs solvents.

Solvent	Base	Product (%)	ArBr (%)	ArH (%)
ACN	Quinuclidine	**74**	28	4
ACN	DBU	**0**	92	6
ACN	lutidine	**5**	86	1
ACN	Et_3N	**6**	82	0
ACN	TMG	**54**	46	0
ACN	BTMG	**32**	63	3
ACN	BTTP	**4**	87	9
ACN	BEMP	**20**	75	5
ACN	$P_1{}^t$Oct	**2**	95	1
ACN	$P_2{}^t$Bu	**nd**	61	5
ACN	DBN	**0**	92	4
ACN	NMM	**9**	88	1
Acetone	Quinuclidine	**9**	89	3
Acetone	DBU	**0**	95	0
Acetone	lutidine	**7**	82	0
Acetone	Et_3N	**6**	81	0
Acetone	TMG	**49**	42	1
Acetone	BTMG	**33**	65	2
Acetone	BTTP	**8**	84	8
Acetone	BEMP	**21**	77	3
Acetone	$P_1{}^t$Oct	**2**	94	1
Acetone	$P_2{}^t$Bu	**nd**	59	0
Acetone	DBN	**0**	93	0
Acetone	NMM	**6**	89	1

AcOEt	Quinuclidine	**31**	67	2
AcOEt	DBU	**0**	99	0
AcOEt	lutidine	**6**	84	1
AcOEt	Et_3N	**6**	85	1
AcOEt	TMG	**69**	38	1
AcOEt	BTMG	**44**	54	1
AcOEt	BTTP	**24**	93	47
AcOEt	BEMP	**12**	85	3
AcOEt	$P_1{}^t$Oct	**4**	84	1
AcOEt	$P_2{}^t$Bu	**nd**	75	7
AcOEt	DBN	**0**	96	1
AcOEt	NMM	**4**	90	1
2-Me-THF	Quinuclidine	**52**	45	3
2-Me-THF	DBU	**0**	99	0
2-Me-THF	lutidine	**3**	3	2
2-Me-THF	Et_3N	**4**	85	3
2-Me-THF	TMG	**20**	78	1
2-Me-THF	BTMG	**32**	80	2
2-Me-THF	BTTP	**2**	97	2
2-Me-THF	BEMP	**8**	90	3
2-Me-THF	$P_1{}^t$Oct	**5**	79	1
2-Me-THF	$P_2{}^t$Bu	**nd**	81	6
2-Me-THF	DBN	**0**	97	1
2-Me-THF	NMM	**4**	86	3
DMF	Quinuclidine	**71**	15	2
DMF	DBU	**0**	91	6
DMF	lutidine	**7**	76	1
DMF	Et_3N	**6**	78	1
DMF	TMG	**61**	41	1
DMF	BTMG	**56**	30	2
DMF	BTTP	**17**	76	4
DMF	BEMP	**35**	56	3
DMF	$P_1{}^t$Oct	**12**	70	2
DMF	$P_2{}^t$Bu	**nd**	62	12
DMF	DBN	**0**	92	3
DMF	NMM	**0**	75	6
DMA	Quinuclidine	**70**	20	1
DMA	DBU	**0**	95	4
DMA	lutidine	**5**	79	0
DMA	Et_3N	**6**	77	1

DMA	TMG	**68**	11	0
DMA	BTMG	**56**	20	0
DMA	BTTP	**36**	48	4
DMA	BEMP	**55**	1	2
DMA	$P_1{}^t$Oct	**60**	16	1
DMA	$P_2{}^t$Bu	**0**	68	9
DMA	DBN	**0**	94	0
DMA	NMM	**4**	81	1
dioxane	Quinuclidine	**66**	40	0
dioxane	DBU	**0**	98	0
dioxane	lutidine	**7**	84	0
dioxane	Et_3N	**7**	84	1
dioxane	TMG	**10**	83	2
dioxane	BTMG	**66**	29	1
dioxane	BTTP	**3**	87	4
dioxane	BEMP	**13**	81	3
dioxane	$P_1{}^t$Oct	**52**	32	1
dioxane	$P_2{}^t$Bu	**nd**	87	3
dioxane	DBN	**0**	99	0
dioxane	NMM	**8**	84	0
DME	Quinuclidine	**33**	66	2
DME	DBU	**2**	96	1
DME	lutidine	**7**	81	2
DME	Et_3N	**7**	81	3
DME	TMG	**40**	59	1
DME	BTMG	**30**	65	1
DME	BTTP	**4**	93	2
DME	BEMP	**18**	81	2
DME	$P_1{}^t$Oct	**11**	70	1
DME	$P_2{}^t$Bu	**nd**	79	6
DME	DBN	**0**	98	0
DME	NMM	**6**	85	2

Data from Fig. S59. Bases vs. solvents and photocatalyst.

Solvent	Base	Photocatalyst	Photocatalyst loading	Product (%)	ArBr (%)	ArH (%)
ACN	Quinuclidine	$[Ir(dF(CF_3)ppy)_2dtbbpy]PF_6$	0.5 mol%	**8**	94	0
ACN	Quinuclidine	$[Ir(dF(CF_3)ppy)_2dtbbpy]PF_6$	1 mol%	**99**	7	2
ACN	Quinuclidine	4CzIPN	0.5 mol%	**105**	0	0
ACN	Quinuclidine	4CzIPN	1 mol%	**91**	13	0

ACN	Quinuclidine	4CzPN	0.5 mol%	**101**	4	0
ACN	Quinuclidine	4CzPN	1 mol%	**103**	3	0
ACN	Quinuclidine	2CzPN	0.5 mol%	**30**	73	0
ACN	Quinuclidine	2CzPN	1 mol%	**31**	73	0
ACN	Quinuclidine	4CzTPN	0.5 mol%	**48**	57	0
ACN	Quinuclidine	4CzTPN	1 mol%	**45**	59	0
ACN	Quinuclidine	4PhCzTPN	0.5 mol%	**31**	72	0
ACN	Quinuclidine	4PhCzTPN	1 mol%	**39**	65	0
ACN	TMG	$[Ir(dF(CF_3)ppy)_2dtbbpy]PF_6$	0.5 mol%	**26**	67	2
ACN	TMG	$[Ir(dF(CF_3)ppy)_2dtbbpy]PF_6$	1 mol%	**33**	59	2
ACN	TMG	4CzIPN	0.5 mol%	**45**	53	1
ACN	TMG	4CzIPN	1 mol%	**40**	53	1
ACN	TMG	4CzPN	0.5 mol%	**22**	77	0
ACN	TMG	4CzPN	1 mol%	**10**	84	1
ACN	TMG	2CzPN	0.5 mol%	**10**	88	0
ACN	TMG	2CzPN	1 mol%	**8**	89	0
ACN	TMG	4CzTPN	0.5 mol%	**6**	93	0
ACN	TMG	4CzTPN	1 mol%	**5**	93	0
ACN	TMG	4PhCzTPN	0.5 mol%	**5**	94	0
ACN	TMG	4PhCzTPN	1 mol%	**6**	93	0
ACN	BTMG	$[Ir(dF(CF_3)ppy)_2dtbbpy]PF_6$	0.5 mol%	**9**	85	3
ACN	BTMG	$[Ir(dF(CF_3)ppy)_2dtbbpy]PF_6$	1 mol%	**8**	82	3
ACN	BTMG	4CzIPN	0.5 mol%	**12**	87	1
ACN	BTMG	4CzIPN	1 mol%	**10**	87	1
ACN	BTMG	4CzPN	0.5 mol%	**1**	95	1
ACN	BTMG	4CzPN	1 mol%	**2**	95	1
ACN	BTMG	2CzPN	0.5 mol%	**0**	97	0
ACN	BTMG	2CzPN	1 mol%	**0**	97	0
ACN	BTMG	4CzTPN	0.5 mol%	**0**	95	1
ACN	BTMG	4CzTPN	1 mol%	**2**	96	1
ACN	BTMG	4PhCzTPN	0.5 mol%	**0**	97	1
ACN	BTMG	4PhCzTPN	1 mol%	**0**	97	0
ACN	BEMP	$[Ir(dF(CF_3)ppy)_2dtbbpy]PF_6$	0.5 mol%	**19**	74	4
ACN	BEMP	$[Ir(dF(CF_3)ppy)_2dtbbpy]PF_6$	1 mol%	**20**	74	5
ACN	BEMP	4CzIPN	0.5 mol%	**7**	88	3
ACN	BEMP	4CzIPN	1 mol%	**7**	89	3
ACN	BEMP	4CzPN	0.5 mol%	**2**	95	1
ACN	BEMP	4CzPN	1 mol%	**0**	95	1
ACN	BEMP	2CzPN	0.5 mol%	**0**	97	0
ACN	BEMP	2CzPN	1 mol%	**0**	97	0

ACN	BEMP	4CzTPN	0.5 mol%	**0**	95	2
ACN	BEMP	4CzTPN	1 mol%	**0**	96	2
ACN	BEMP	4PhCzTPN	0.5 mol%	**0**	95	2
ACN	BEMP	4PhCzTPN	1 mol%	**0**	96	1
DMF	Quinuclidine	$[Ir(dF(CF_3)ppy)_2dtbbpy]PF_6$	0.5 mol%	**73**	13	2
DMF	Quinuclidine	$[Ir(dF(CF_3)ppy)_2dtbbpy]PF_6$	1 mol%	**70**	12	2
DMF	Quinuclidine	4CzIPN	0.5 mol%	**48**	44	1
DMF	Quinuclidine	4CzIPN	1 mol%	**58**	30	1
DMF	Quinuclidine	4CzPN	0.5 mol%	**64**	26	0
DMF	Quinuclidine	4CzPN	1 mol%	**50**	38	1
DMF	Quinuclidine	2CzPN	0.5 mol%	**13**	83	0
DMF	Quinuclidine	2CzPN	1 mol%	**20**	77	0
DMF	Quinuclidine	4CzTPN	0.5 mol%	**31**	65	0
DMF	Quinuclidine	4CzTPN	1 mol%	**24**	712	0
DMF	Quinuclidine	4PhCzTPN	0.5 mol%	**18**	78	0
DMF	Quinuclidine	4PhCzTPN	1 mol%	**10**	86	0
DMF	TMG	$[Ir(dF(CF_3)ppy)_2dtbbpy]PF_6$	0.5 mol%	**35**	46	1
DMF	TMG	$[Ir(dF(CF_3)ppy)_2dtbbpy]PF_6$	1 mol%	**36**	46	1
DMF	TMG	4CzIPN	0.5 mol%	**60**	24	0
DMF	TMG	4CzIPN	1 mol%	**62**	20	1
DMF	TMG	4CzPN	0.5 mol%	**42**	45	0
DMF	TMG	4CzPN	1 mol%	**34**	54	0
DMF	TMG	2CzPN	0.5 mol%	**14**	82	0
DMF	TMG	2CzPN	1 mol%	**15**	79	1
DMF	TMG	4CzTPN	0.5 mol%	**9**	89	0
DMF	TMG	4CzTPN	1 mol%	**6**	90	0
DMF	TMG	4PhCzTPN	0.5 mol%	**0**	95	1
DMF	TMG	4PhCzTPN	1 mol%	**0**	96	1
DMF	BTMG	$[Ir(dF(CF_3)ppy)_2dtbbpy]PF_6$	0.5 mol%	**26**	59	2
DMF	BTMG	$[Ir(dF(CF_3)ppy)_2dtbbpy]PF_6$	1 mol%	**30**	56	2
DMF	BTMG	4CzIPN	0.5 mol%	**35**	51	2
DMF	BTMG	4CzIPN	1 mol%	**44**	43	2
DMF	BTMG	4CzPN	0.5 mol%	**16**	75	1
DMF	BTMG	4CzPN	1 mol%	**14**	76	1
DMF	BTMG	2CzPN	0.5 mol%	**5**	91	0
DMF	BTMG	2CzPN	1 mol%	**5**	91	0
DMF	BTMG	4CzTPN	0.5 mol%	**0**	94	0
DMF	BTMG	4CzTPN	1 mol%	**0**	95	0
DMF	BTMG	4PhCzTPN	0.5 mol%	**22**	66	4
DMF	BTMG	4PhCzTPN	1 mol%	**22**	68	6

DMF	BEMP	[Ir(dF(CF$_3$)ppy)$_2$dtbbpy]PF$_6$	0.5 mol%	**25**	68	3
DMF	BEMP	[Ir(dF(CF$_3$)ppy)$_2$dtbbpy]PF$_6$	1 mol%	**19**	73	4
DMF	BEMP	4CzIPN	0.5 mol%	**29**	63	3
DMF	BEMP	4CzIPN	1 mol%	**33**	56	3
DMF	BEMP	4CzPN	0.5 mol%	**9**	84	2
DMF	BEMP	4CzPN	1 mol%	**14**	82	2
DMF	BEMP	2CzPN	0.5 mol%	**3**	94	0
DMF	BEMP	2CzPN	1 mol%	**0**	96	0
DMF	BEMP	4CzTPN	0.5 mol%	**2**	95	1
DMF	BEMP	4CzTPN	1 mol%	**0**	95	2
DMF	BEMP	4PhCzTPN	0.5 mol%	**16**	77	5
DMF	BEMP	4PhCzTPN	1 mol%	**9**	79	7

Data from Fig. S60. Solvents vs. photocatalyst and photocatalyst loading.

Solvent	**Base**	**Photocatalyst**	**Photocatalyst loading**	**Product (%)**	**ArBr (%)**	**ArH (%)**
DMF	Quinuclidine	[Ir(dF(CF$_3$)ppy)$_2$dtbbpy]PF$_6$	0.25 mol%	**51**	39	2
DMF	Quinuclidine	[Ir(dF(CF$_3$)ppy)$_2$dtbbpy]PF$_6$	0.5 mol%	**68**	19	2
DMF	Quinuclidine	[Ir(dF(CF$_3$)ppy)$_2$dtbbpy]PF$_6$	1 mol%	**66**	18	2
DMF	Quinuclidine	[Ir(dF(CF$_3$)ppy)$_2$dtbbpy]PF$_6$	2 mol%	**74**	9	3
DMF	Quinuclidine	4CzIPN	0.25 mol%	**46**	45	1
DMF	Quinuclidine	4CzIPN	0.5 mol%	**48**	41	1
DMF	Quinuclidine	4CzIPN	1 mol%	**64**	24	1
DMF	Quinuclidine	4CzIPN	2 mol%	**71**	15	2
DMF	Quinuclidine	4CzPN	0.25 mol%	**42**	47	1
DMF	Quinuclidine	4CzPN	0.5 mol%	**38**	52	1
DMF	Quinuclidine	4CzPN	1 mol%	**67**	22	1
DMF	Quinuclidine	4CzPN	2 mol%	**65**	23	1
DMF	TMG	[Ir(dF(CF$_3$)ppy)$_2$dtbbpy]PF$_6$	0.25 mol%	**58**	28	1
DMF	TMG	[Ir(dF(CF$_3$)ppy)$_2$dtbbpy]PF$_6$	0.5 mol%	**63**	20	1
DMF	TMG	[Ir(dF(CF$_3$)ppy)$_2$dtbbpy]PF$_6$	1 mol%	**53**	106	1
DMF	TMG	[Ir(dF(CF$_3$)ppy)$_2$dtbbpy]PF$_6$	2 mol%	**5**	72	2
DMF	TMG	4CzIPN	0.25 mol%	**83**	1	1
DMF	TMG	4CzIPN	0.5 mol%	**79**	0	1
DMF	TMG	4CzIPN	1 mol%	**77**	2	1
DMF	TMG	4CzIPN	2 mol%	**65**	13	1
DMF	TMG	4CzPN	0.25 mol%	**61**	26	0
DMF	TMG	4CzPN	0.5 mol%	**53**	30	0
DMF	TMG	4CzPN	1 mol%	**38**	50	1
DMF	TMG	4CzPN	2 mol%	**15**	72	1

ACN	Quinuclidine	[Ir(dF(CF$_3$)ppy)$_2$dtbbpy]PF$_6$	0.25 mol%	**56**	47	2
ACN	Quinuclidine	[Ir(dF(CF$_3$)ppy)$_2$dtbbpy]PF$_6$	0.5 mol%	**51**	51	3
ACN	Quinuclidine	[Ir(dF(CF$_3$)ppy)$_2$dtbbpy]PF$_6$	1 mol%	**70**	29	2
ACN	Quinuclidine	[Ir(dF(CF$_3$)ppy)$_2$dtbbpy]PF$_6$	2 mol%	**93**	10	3
ACN	Quinuclidine	4CzIPN	0.25 mol%	**42**	62	1
ACN	Quinuclidine	4CzIPN	0.5 mol%	**33**	69	2
ACN	Quinuclidine	4CzIPN	1 mol%	**56**	40	2
ACN	Quinuclidine	4CzIPN	2 mol%	**80**	20	2
ACN	Quinuclidine	4CzPN	0.25 mol%	**33**	71	1
ACN	Quinuclidine	4CzPN	0.5 mol%	**43**	61	1
ACN	Quinuclidine	4CzPN	1 mol%	**54**	50	2
ACN	Quinuclidine	4CzPN	2 mol%	**79**	23	0
ACN	TMG	[Ir(dF(CF$_3$)ppy)$_2$dtbbpy]PF$_6$	0.25 mol%	**42**	64	1
ACN	TMG	[Ir(dF(CF$_3$)ppy)$_2$dtbbpy]PF$_6$	0.5 mol%	**61**	45	1
ACN	TMG	[Ir(dF(CF$_3$)ppy)$_2$dtbbpy]PF$_6$	1 mol%	**67**	37	2
ACN	TMG	[Ir(dF(CF$_3$)ppy)$_2$dtbbpy]PF$_6$	2 mol%	**47**	49	3
ACN	TMG	4CzIPN	0.25 mol%	**84**	26	1
ACN	TMG	4CzIPN	0.5 mol%	**74**	30	1
ACN	TMG	4CzIPN	1 mol%	**62**	39	1
ACN	TMG	4CzIPN	2 mol%	**46**	52	1
ACN	TMG	4CzPN	0.25 mol%	**49**	57	0
ACN	TMG	4CzPN	0.5 mol%	**35**	68	0
ACN	TMG	4CzPN	1 mol%	**10**	87	1
ACN	TMG	4CzPN	2 mol%	**7**	92	1

Data from Fig. S61. Base and base loading vs. photocatalyst and photocatalyst loading.

Photocatalyst	Photocatalyst loading	Base	Base loading	Product (%)	ArBr (%)	ArH (%)
[Ir(dF(CF$_3$)ppy)$_2$dtbbpy]PF$_6$	0.5 mol%	Quinuclidine	1.5 equiv	**96**	2	1
[Ir(dF(CF$_3$)ppy)$_2$dtbbpy]PF$_6$	0.5 mol%	Quinuclidine	1.75 equiv	**97**	1	1
[Ir(dF(CF$_3$)ppy)$_2$dtbbpy]PF$_6$	0.5 mol%	Quinuclidine	2 equiv	**98**	1	1
[Ir(dF(CF$_3$)ppy)$_2$dtbbpy]PF$_6$	0.5 mol%	Quinuclidine	3 equiv	**97**	1	1
[Ir(dF(CF$_3$)ppy)$_2$dtbbpy]PF$_6$	0.5 mol%	TMG	1.5 equiv	**68**	29	1
[Ir(dF(CF$_3$)ppy)$_2$dtbbpy]PF$_6$	0.5 mol%	TMG	1.75 equiv	**67**	30	1
[Ir(dF(CF$_3$)ppy)$_2$dtbbpy]PF$_6$	0.5 mol%	TMG	2 equiv	**65**	34	1
[Ir(dF(CF$_3$)ppy)$_2$dtbbpy]PF$_6$	0.5 mol%	TMG	3 equiv	**55**	46	1
[Ir(dF(CF$_3$)ppy)$_2$dtbbpy]PF$_6$	1 mol%	Quinuclidine	1.5 equiv	**98**	1	1
[Ir(dF(CF$_3$)ppy)$_2$dtbbpy]PF$_6$	1 mol%	Quinuclidine	1.75 equiv	**95**	1	1
[Ir(dF(CF$_3$)ppy)$_2$dtbbpy]PF$_6$	1 mol%	Quinuclidine	2 equiv	**99**	0	1

$[Ir(dF(CF_3)ppy)_2dtbbpy]PF_6$	1 mol%	Quinuclidine	3 equiv	**98**	0	2
$[Ir(dF(CF_3)ppy)_2dtbbpy]PF_6$	1 mol%	TMG	1.5 equiv	**76**	20	1
$[Ir(dF(CF_3)ppy)_2dtbbpy]PF_6$	1 mol%	TMG	1.75 equiv	**73**	23	1
$[Ir(dF(CF_3)ppy)_2dtbbpy]PF_6$	1 mol%	TMG	2 equiv	**75**	24	1
$[Ir(dF(CF_3)ppy)_2dtbbpy]PF_6$	1 mol%	TMG	3 equiv	**59**	41	1
4CzIPN	0.5 mol%	Quinuclidine	1.5 equiv	**95**	3	1
4CzIPN	0.5 mol%	Quinuclidine	1.75 equiv	**98**	1	1
4CzIPN	0.5 mol%	Quinuclidine	2 equiv	**99**	0	1
4CzIPN	0.5 mol%	Quinuclidine	3 equiv	**100**	0	1
4CzIPN	0.5 mol%	TMG	1.5 equiv	**72**	25	0
4CzIPN	0.5 mol%	TMG	1.75 equiv	**78**	23	0
4CzIPN	0.5 mol%	TMG	2 equiv	**75**	24	0
4CzIPN	0.5 mol%	TMG	3 equiv	**68**	34	1
4CzIPN	1 mol%	Quinuclidine	1.5 equiv	**97**	1	1
4CzIPN	1 mol%	Quinuclidine	1.75 equiv	**97**	1	1
4CzIPN	1 mol%	Quinuclidine	2 equiv	**96**	1	1
4CzIPN	1 mol%	Quinuclidine	3 equiv	**98**	0	1
4CzIPN	1 mol%	TMG	1.5 equiv	**67**	30	1
4CzIPN	1 mol%	TMG	1.75 equiv	**65**	33	1
4CzIPN	1 mol%	TMG	2 equiv	**65**	33	1
4CzIPN	1 mol%	TMG	3 equiv	**41**	59	1

Data from Fig. S62. Base and base loading vs photocatalyst and photocatalyst loading.

Solvent	Photocatalyst	Quinuclidine loading	Base	Base loading	Product (%)	ArBr (%)	ArH (%)
ACN	$[Ir(dF(CF_3)ppy)_2dtbbpy]PF_6$	10 mol%	Quinuclidine	0.5 equiv	**51**	46	1
ACN	$[Ir(dF(CF_3)ppy)_2dtbbpy]PF_6$	10 mol%	Quinuclidine	1 equiv	**94**	8	1
ACN	$[Ir(dF(CF_3)ppy)_2dtbbpy]PF_6$	10 mol%	TMG	0.5 equiv	**52**	52	0
ACN	$[Ir(dF(CF_3)ppy)_2dtbbpy]PF_6$	10 mol%	TMG	1 equiv	**74**	30	1
ACN	$[Ir(dF(CF_3)ppy)_2dtbbpy]PF_6$	10 mol%	TMG	1.25 equiv	**67**	30	2
ACN	$[Ir(dF(CF_3)ppy)_2dtbbpy]PF_6$	10 mol%	TMG	1.5 equiv	**56**	29	2
DMF	$[Ir(dF(CF_3)ppy)_2dtbbpy]PF_6$	10 mol%	Quinuclidine	0.5 equiv	**57**	30	1
DMF	$[Ir(dF(CF_3)ppy)_2dtbbpy]PF_6$	10 mol%	Quinuclidine	1 equiv	**80**	6	2
DMF	$[Ir(dF(CF_3)ppy)_2dtbbpy]PF_6$	10 mol%	TMG	0.5 equiv	**85**	5	0
DMF	$[Ir(dF(CF_3)ppy)_2dtbbpy]PF_6$	10 mol%	TMG	1 equiv	**83**	8	0
DMF	$[Ir(dF(CF_3)ppy)_2dtbbpy]PF_6$	10 mol%	TMG	1.25 equiv	**83**	8	0
DMF	$[Ir(dF(CF_3)ppy)_2dtbbpy]PF_6$	10 mol%	TMG	1.5 equiv	**69**	17	1
ACN	$[Ir(dF(CF_3)ppy)_2dtbbpy]PF_6$	20 mol%	Quinuclidine	0.5 equiv	**64**	33	1
ACN	$[Ir(dF(CF_3)ppy)_2dtbbpy]PF_6$	20 mol%	Quinuclidine	1 equiv	**100**	2	0
ACN	$[Ir(dF(CF_3)ppy)_2dtbbpy]PF_6$	20 mol%	TMG	0.5 equiv	**61**	41	1

ACN	$[Ir(dF(CF_3)ppy)_2dtbbpy]PF_6$	20 mol%	TMG	1 equiv	**78**	22	2
ACN	$[Ir(dF(CF_3)ppy)_2dtbbpy]PF_6$	20 mol%	TMG	1.25 equiv	**74**	21	2
ACN	$[Ir(dF(CF_3)ppy)_2dtbbpy]PF_6$	20 mol%	TMG	1.5 equiv	**68**	23	4
DMF	$[Ir(dF(CF_3)ppy)_2dtbbpy]PF_6$	20 mol%	Quinuclidine	0.5 equiv	**58**	29	2
DMF	$[Ir(dF(CF_3)ppy)_2dtbbpy]PF_6$	20 mol%	Quinuclidine	1 equiv	**83**	6	2
DMF	$[Ir(dF(CF_3)ppy)_2dtbbpy]PF_6$	20 mol%	TMG	0.5 equiv	**61**	26	0
DMF	$[Ir(dF(CF_3)ppy)_2dtbbpy]PF_6$	20 mol%	TMG	1 equiv	**86**	8	0
DMF	$[Ir(dF(CF_3)ppy)_2dtbbpy]PF_6$	20 mol%	TMG	1.25 equiv	**79**	10	0
DMF	$[Ir(dF(CF_3)ppy)_2dtbbpy]PF_6$	20 mol%	TMG	1.5 equiv	**72**	18	1
ACN	4CzIPN	10 mol%	Quinuclidine	0.5 equiv	**51**	43	0
ACN	4CzIPN	10 mol%	Quinuclidine	1 equiv	**97**	7	0
ACN	4CzIPN	10 mol%	TMG	0.5 equiv	**58**	44	0
ACN	4CzIPN	10 mol%	TMG	1 equiv	**77**	25	1
ACN	4CzIPN	10 mol%	TMG	1.25 equiv	**73**	27	1
ACN	4CzIPN	10 mol%	TMG	1.5 equiv	**62**	31	2
DMF	4CzIPN	10 mol%	Quinuclidine	0.5 equiv	**57**	34	1
DMF	4CzIPN	10 mol%	Quinuclidine	1 equiv	**75**	13	0
DMF	4CzIPN	10 mol%	TMG	0.5 equiv	**64**	27	0
DMF	4CzIPN	10 mol%	TMG	1 equiv	**74**	15	0
DMF	4CzIPN	10 mol%	TMG	1.25 equiv	**72**	18	1
DMF	4CzIPN	10 mol%	TMG	1.5 equiv	**61**	25	1
ACN	4CzIPN	20 mol%	Quinuclidine	0.5 equiv	**70**	31	0
ACN	4CzIPN	20 mol%	Quinuclidine	1 equiv	**106**	1	0
ACN	4CzIPN	20 mol%	TMG	0.5 equiv	**60**	46	0
ACN	4CzIPN	20 mol%	TMG	1 equiv	**48**	51	1
ACN	4CzIPN	20 mol%	TMG	1.25 equiv	**42**	53	1
ACN	4CzIPN	20 mol%	TMG	1.5 equiv	**74**	21	2
DMF	4CzIPN	20 mol%	Quinuclidine	0.5 equiv	**58**	27	1
DMF	4CzIPN	20 mol%	Quinuclidine	1 equiv	**78**	6	1
DMF	4CzIPN	20 mol%	TMG	0.5 equiv	**62**	20	0
DMF	4CzIPN	20 mol%	TMG	1 equiv	**84**	4	0
DMF	4CzIPN	20 mol%	TMG	1.25 equiv	**77**	8	0
DMF	4CzIPN	20 mol%	TMG	1.5 equiv	**66**	18	0

Data from Fig. S63. Base and base loading vs photocatalyst and photocatalyst loading.

Solvent	Base	Base loading	Quinuclidine loading	Photocatalyst	Photocatalyst loading	Product (%)	ArBr (%)	ArH (%)
ACN	Quinuclidine	1 equiv	10 mol%	$[Ir(dF(CF_3)ppy)_2dtbbpy]PF_6$	0.5 mol%	**87**	16	3
ACN	TMG	0.5 equiv	10 mol%	$[Ir(dF(CF_3)ppy)_2dtbbpy]PF_6$	0.5 mol%	**25**	78	1
ACN	TMG	1 equiv	10 mol%	$[Ir(dF(CF_3)ppy)_2dtbbpy]PF_6$	0.5 mol%	**31**	68	2

ACN	Quinuclidine	1 equiv	10 mol%	4CzIPN	0.5 mol%	**87**	14	0
ACN	TMG	0.5 equiv	10 mol%	4CzIPN	0.5 mol%	**45**	60	1
ACN	TMG	1 equiv	10 mol%	4CzIPN	0.5 mol%	**31**	70	2
ACN	Quinuclidine	1 equiv	10 mol%	$[Ir(dF(CF_3)ppy)_2dtbbpy]PF_6$	1 mol%	**86**	13	3
ACN	TMG	0.5 equiv	10 mol%	$[Ir(dF(CF_3)ppy)_2dtbbpy]PF_6$	1 mol%	**49**	56	2
ACN	TMG	1 equiv	10 mol%	$[Ir(dF(CF_3)ppy)_2dtbbpy]PF_6$	1 mol%	**35**	65	3
ACN	Quinuclidine	1 equiv	10 mol%	4CzIPN	1 mol%	**98**	4	0
ACN	TMG	0.5 equiv	10 mol%	4CzIPN	1 mol%	**16**	86	1
ACN	TMG	1 equiv	10 mol%	4CzIPN	1 mol%	**7**	90	1
ACN	Quinuclidine	1 equiv	20 mol%	$[Ir(dF(CF_3)ppy)_2dtbbpy]PF_6$	0.5 mol%	**92**	11	2
ACN	TMG	0.5 equiv	20 mol%	$[Ir(dF(CF_3)ppy)_2dtbbpy]PF_6$	0.5 mol%	**37**	69	1
ACN	TMG	1 equiv	20 mol%	$[Ir(dF(CF_3)ppy)_2dtbbpy]PF_6$	0.5 mol%	**39**	60	2
ACN	Quinuclidine	1 equiv	20 mol%	4CzIPN	0.5 mol%	**101**	3	0
ACN	TMG	0.5 equiv	20 mol%	4CzIPN	0.5 mol%	**70**	35	0
ACN	TMG	1 equiv	20 mol%	4CzIPN	0.5 mol%	**48**	53	1
ACN	Quinuclidine	1 equiv	20 mol%	$[Ir(dF(CF_3)ppy)_2dtbbpy]PF_6$	1 mol%	**97**	6	2
ACN	TMG	0.5 equiv	20 mol%	$[Ir(dF(CF_3)ppy)_2dtbbpy]PF_6$	1 mol%	**69**	37	1
ACN	TMG	1 equiv	20 mol%	$[Ir(dF(CF_3)ppy)_2dtbbpy]PF_6$	1 mol%	**47**	6	2
ACN	Quinuclidine	1 equiv	20 mol%	4CzIPN	1 mol%	**103**	3	0
ACN	TMG	0.5 equiv	20 mol%	4CzIPN	1 mol%	**39**	63	0
ACN	TMG	1 equiv	20 mol%	4CzIPN	1 mol%	**16**	84	1
DMF	Quinuclidine	1 equiv	10 mol%	$[Ir(dF(CF_3)ppy)_2dtbbpy]PF_6$	0.5 mol%	**75**	12	2
DMF	TMG	0.5 equiv	10 mol%	$[Ir(dF(CF_3)ppy)_2dtbbpy]PF_6$	0.5 mol%	**53**	36	0
DMF	TMG	1 equiv	10 mol%	$[Ir(dF(CF_3)ppy)_2dtbbpy]PF_6$	0.5 mol%	**68**	22	0
DMF	Quinuclidine	1 equiv	10 mol%	4CzIPN	0.5 mol%	**72**	18	2
DMF	TMG	0.5 equiv	10 mol%	4CzIPN	0.5 mol%	**52**	28	0
DMF	TMG	1 equiv	10 mol%	4CzIPN	0.5 mol%	**87**	3	0
DMF	Quinuclidine	1 equiv	10 mol%	$[Ir(dF(CF_3)ppy)_2dtbbpy]PF_6$	1 mol%	**85**	6	6
DMF	TMG	0.5 equiv	10 mol%	$[Ir(dF(CF_3)ppy)_2dtbbpy]PF_6$	1 mol%	**57**	32	0
DMF	TMG	1 equiv	10 mol%	$[Ir(dF(CF_3)ppy)_2dtbbpy]PF_6$	1 mol%	**77**	12	0
DMF	Quinuclidine	1 equiv	10 mol%	4CzIPN	1 mol%	**77**	12	1
DMF	TMG	0.5 equiv	10 mol%	4CzIPN	1 mol%	**59**	29	0
DMF	TMG	1 equiv	10 mol%	4CzIPN	1 mol%	**77**	12	0
DMF	Quinuclidine	1 equiv	20 mol%	$[Ir(dF(CF_3)ppy)_2dtbbpy]PF_6$	0.5 mol%	**87**	6	2
DMF	TMG	0.5 equiv	20 mol%	$[Ir(dF(CF_3)ppy)_2dtbbpy]PF_6$	0.5 mol%	**58**	33	0
DMF	TMG	1 equiv	20 mol%	$[Ir(dF(CF_3)ppy)_2dtbbpy]PF_6$	0.5 mol%	**66**	28	1
DMF	Quinuclidine	1 equiv	20 mol%	4CzIPN	0.5 mol%	**81**	9	1
DMF	TMG	0.5 equiv	20 mol%	4CzIPN	0.5 mol%	**63**	25	1
DMF	TMG	1 equiv	20 mol%	4CzIPN	0.5 mol%	**76**	12	1
DMF	Quinuclidine	1 equiv	20 mol%	$[Ir(dF(CF_3)ppy)_2dtbbpy]PF_6$	1 mol%	**86**	6	2

DMF	TMG	0.5 equiv	20 mol%	$[Ir(dF(CF_3)ppy)_2dtbbpy]PF_6$	1 mol%	**59**	32	0
DMF	TMG	1 equiv	20 mol%	$[Ir(dF(CF_3)ppy)_2dtbbpy]PF_6$	1 mol%	**66**	28	0
DMF	Quinuclidine	1 equiv	20 mol%	4CzIPN	1 mol%	**84**	9	1
DMF	TMG	0.5 equiv	20 mol%	4CzIPN	1 mol%	**60**	25	1
DMF	TMG	1 equiv	20 mol%	4CzIPN	1 mol%	**71**	18	0

Data from Fig. S64. Nickel vs nickel catalyst loading.

Conditions	Nickel source	Nickel loading	Product (%)	ArBr (%)	ArH (%)
1	$NiCl_2$·dme	1 mol%	**97**	8	0
1	$NiCl_2$·dme	2.5 mol%	**107**	0	0
1	$NiCl_2$·dme	5 mol%	**92**	0	0
1	$NiCl_2$·dme	10 mol%	**78**	0	2
2	$NiCl_2$·dme	1 mol%	**89**	12	0
2	$NiCl_2$·dme	2.5 mol%	**87**	10	1
2	$NiCl_2$·dme	5 mol%	**79**	1	2
2	$NiCl_2$·dme	10 mol%	**80**	0	1
3	$NiCl_2$·dme	1 mol%	**59**	36	0
3	$NiCl_2$·dme	2.5 mol%	**77**	16	0
3	$NiCl_2$·dme	5 mol%	**80**	10	0
3	$NiCl_2$·dme	10 mol%	**74**	16	0
1	$NiCl_2$·$6H_2O$	1 mol%	**85**	6	3
1	$NiCl_2$·$6H_2O$	2.5 mol%	**87**	3	3
1	$NiCl_2$·$6H_2O$	5 mol%	**76**	2	2
1	$NiCl_2$·$6H_2O$	10 mol%	**74**	0	2
2	$NiCl_2$·$6H_2O$	1 mol%	**84**	10	3
2	$NiCl_2$·$6H_2O$	2.5 mol%	**83**	9	2
2	$NiCl_2$·$6H_2O$	5 mol%	**72**	5	2
2	$NiCl_2$·$6H_2O$	10 mol%	**67**	0	2
3	$NiCl_2$·$6H_2O$	1 mol%	**63**	26	1
3	$NiCl_2$·$6H_2O$	2.5 mol%	**78**	10	0
3	$NiCl_2$·$6H_2O$	5 mol%	**81**	6	0
3	$NiCl_2$·$6H_2O$	10 mol%	**79**	9	0
1	$NiBr_2$·$6H_2O$	1 mol%	**96**	8	3
1	$NiBr_2$·$6H_2O$	2.5 mol%	**92**	6	3
1	$NiBr_2$·$6H_2O$	5 mol%	**95**	6	3
1	$NiBr_2$·$6H_2O$	10 mol%	**88**	8	2
2	$NiBr_2$·$6H_2O$	1 mol%	**99**	13	2
2	$NiBr_2$·$6H_2O$	2.5 mol%	**85**	13	3
2	$NiBr_2$·$6H_2O$	5 mol%	**87**	12	3

2	$NiBr_2 \cdot 6H_2O$	10 mol%	**91**	12	2
3	$NiBr_2 \cdot 6H_2O$	1 mol%	**69**	20	0
3	$NiBr_2 \cdot 6H_2O$	2.5 mol%	**85**	11	0
3	$NiBr_2 \cdot 6H_2O$	5 mol%	**83**	10	0
3	$NiBr_2 \cdot 6H_2O$	10 mol%	**84**	14	0
1	$Ni(OAc)_2 \cdot 4H_2O$	1 mol%	**49**	39	4
1	$Ni(OAc)_2 \cdot 4H_2O$	2.5 mol%	**47**	42	10
1	$Ni(OAc)_2 \cdot 4H_2O$	5 mol%	**39**	45	10
1	$Ni(OAc)_2 \cdot 4H_2O$	10 mol%	**26**	46	14
2	$Ni(OAc)_2 \cdot 4H_2O$	1 mol%	**47**	54	4
2	$Ni(OAc)_2 \cdot 4H_2O$	2.5 mol%	**33**	60	5
2	$Ni(OAc)_2 \cdot 4H_2O$	5 mol%	**29**	62	8
2	$Ni(OAc)_2 \cdot 4H_2O$	10 mol%	**18**	65	11
3	$Ni(OAc)_2 \cdot 4H_2O$	1 mol%	**8**	73	2
3	$Ni(OAc)_2 \cdot 4H_2O$	2.5 mol%	**11**	70	1
3	$Ni(OAc)_2 \cdot 4H_2O$	5 mol%	**9**	66	1
3	$Ni(OAc)_2 \cdot 4H_2O$	10 mol%	**8**	64	2

Condition 1: 1.2 equiv. Quinuclidine, 1.75 equiv of alcohol. 0.5 mol% $[Ir(dF(CF_3)ppy)_2dtbbpy]PF_6$ in DMF. *Condition 2*: 1.2 equiv. Quinuclidine, 1.75 equiv of alcohol. 0.5 mol% 4CzIPN in DMF. *Condition 3*: 1 equiv. TMG as base, 10 mol% Quinuclidine. 1.75 equiv of alcohol. 0.5 mol% 4CzIPN in DMF.

Data from Fig. S65. Nickel vs nickel catalyst loading and time.

Conditions	Nickel source	Nickel loading	Time	Product (%)	ArBr (%)	ArH (%)
1	$NiCl_2 \cdot dme$	0.5 mol%	30 min	**11**	82	2
1	$NiCl_2 \cdot dme$	1 mol%	30 min	**27**	58	0
1	$NiCl_2 \cdot dme$	2 mol%	30 min	**73**	17	0
1	$NiCl_2 \cdot dme$	3 mol%	30 min	**85**	2	0
1	$NiCl_2 \cdot dme$	4 mol%	30 min	**82**	2	0
1	$NiCl_2 \cdot dme$	5 mol%	30 min	**84**	2	0
1	$NiCl_2 \cdot dme$	6 mol%	30 min	**81**	6	0
1	$NiCl_2 \cdot dme$	7 mol%	30 min	**78**	7	0
1	$NiCl_2 \cdot dme$	8 mol%	30 min	**74**	9	0
1	$NiCl_2 \cdot dme$	9 mol%	30 min	**76**	12	0
1	$NiCl_2 \cdot dme$	10 mol%	30 min	**76**	11	0
1	$NiCl_2 \cdot dme$	20 mol%	30 min	**69**	20	0
1	$NiCl_2 \cdot 6H_2O$	0.5 mol%	30 min	**11**	81	2
1	$NiCl_2 \cdot 6H_2O$	1 mol%	30 min	**32**	60	2
1	$NiCl_2 \cdot 6H_2O$	2 mol%	30 min	**77**	8	1

1	$NiCl_2·6H_2O$	3 mol%	30 min	**82**	0	0
1	$NiCl_2·6H_2O$	4 mol%	30 min	**79**	0	0
1	$NiCl_2·6H_2O$	5 mol%	30 min	**79**	0	0
1	$NiCl_2·6H_2O$	6 mol%	30 min	**78**	0	6
1	$NiCl_2·6H_2O$	7 mol%	30 min	**73**	1	0
1	$NiCl_2·6H_2O$	8 mol%	30 min	**79**	2	0
1	$NiCl_2·6H_2O$	9 mol%	30 min	**77**	2	0
1	$NiCl_2·6H_2O$	10 mol%	30 min	**78**	1	1
1	$NiCl_2·6H_2O$	20 mol%	30 min	**69**	1	4
1	$NiBr_2·6H_2O$	0.5 mol%	30 min	**12**	83	2
1	$NiBr_2·6H_2O$	1 mol%	30 min	**24**	66	2
1	$NiBr_2·6H_2O$	2 mol%	30 min	**72**	17	0
1	$NiBr_2·6H_2O$	3 mol%	30 min	**83**	5	0
1	$NiBr_2·6H_2O$	4 mol%	30 min	**83**	4	0
1	$NiBr_2·6H_2O$	5 mol%	30 min	**85**	4	0
1	$NiBr_2·6H_2O$	6 mol%	30 min	**82**	9	0
1	$NiBr_2·6H_2O$	7 mol%	30 min	**79**	8	0
1	$NiBr_2·6H_2O$	8 mol%	30 min	**80**	10	0
1	$NiBr_2·6H_2O$	9 mol%	30 min	**79**	11	13
1	$NiBr_2·6H_2O$	10 mol%	30 min	**78**	11	0
1	$NiBr_2·6H_2O$	20 mol%	30 min	**74**	15	1
2	$NiCl_2$·dme	0.5 mol%	30 min	**2**	91	2
2	$NiCl_2$·dme	1 mol%	30 min	**3**	87	2
2	$NiCl_2$·dme	2 mol%	30 min	**21**	65	2
2	$NiCl_2$·dme	3 mol%	30 min	**76**	7	0
2	$NiCl_2$·dme	4 mol%	30 min	**80**	3	0
2	$NiCl_2$·dme	5 mol%	30 min	**76**	3	0
2	$NiCl_2$·dme	6 mol%	30 min	**78**	4	0
2	$NiCl_2$·dme	7 mol%	30 min	**76**	5	0
2	$NiCl_2$·dme	8 mol%	30 min	**74**	6	0
2	$NiCl_2$·dme	9 mol%	30 min	**78**	8	0
2	$NiCl_2$·dme	10 mol%	30 min	**80**	7	0
2	$NiCl_2$·dme	20 mol%	30 min	**71**	15	0
2	$NiCl_2·6H_2O$	0.5 mol%	30 min	**1**	91	2
2	$NiCl_2·6H_2O$	1 mol%	30 min	**2**	87	2
2	$NiCl_2·6H_2O$	2 mol%	30 min	**33**	53	1
2	$NiCl_2·6H_2O$	3 mol%	30 min	**80**	4	1
2	$NiCl_2·6H_2O$	4 mol%	30 min	**77**	0	0
2	$NiCl_2·6H_2O$	5 mol%	30 min	**79**	1	0
2	$NiCl_2·6H_2O$	6 mol%	30 min	**80**	1	0

2	$NiCl_2·6H_2O$	7 mol%	30 min	**80**	1	0
2	$NiCl_2·6H_2O$	8 mol%	30 min	**79**	2	0
2	$NiCl_2·6H_2O$	9 mol%	30 min	**78**	2	0
2	$NiCl_2·6H_2O$	10 mol%	30 min	**77**	2	0
2	$NiCl_2·6H_2O$	20 mol%	30 min	**73**	2	5
2	$NiBr_2·6H_2O$	0.5 mol%	30 min	**3**	92	2
2	$NiBr_2·6H_2O$	1 mol%	30 min	**1**	89	2
2	$NiBr_2·6H_2O$	2 mol%	30 min	**32**	54	1
2	$NiBr_2·6H_2O$	3 mol%	30 min	**83**	6	1
2	$NiBr_2·6H_2O$	4 mol%	30 min	**83**	5	0
2	$NiBr_2·6H_2O$	5 mol%	30 min	**86**	5	0
2	$NiBr_2·6H_2O$	6 mol%	30 min	**83**	8	0
2	$NiBr_2·6H_2O$	7 mol%	30 min	**82**	10	0
2	$NiBr_2·6H_2O$	8 mol%	30 min	**80**	11	0
2	$NiBr_2·6H_2O$	9 mol%	30 min	**80**	11	0
2	$NiBr_2·6H_2O$	10 mol%	30 min	**74**	10	0
2	$NiBr_2·6H_2O$	20 mol%	30 min	**70**	17	0
1	$NiCl_2$·dme	0.5 mol%	45 min	**0**	88	3
1	$NiCl_2$·dme	1 mol%	45 min	**8**	78	3
1	$NiCl_2$·dme	2 mol%	45 min	**66**	25	0
1	$NiCl_2$·dme	3 mol%	45 min	**80**	0	0
1	$NiCl_2$·dme	4 mol%	45 min	**86**	0	0
1	$NiCl_2$·dme	5 mol%	45 min	**78**	0	0
1	$NiCl_2$·dme	6 mol%	45 min	**83**	1	0
1	$NiCl_2$·dme	7 mol%	45 min	**83**	2	0
1	$NiCl_2$·dme	8 mol%	45 min	**81**	4	0
1	$NiCl_2$·dme	9 mol%	45 min	**85**	5	0
1	$NiCl_2$·dme	10 mol%	45 min	**80**	0	0
1	$NiCl_2$·dme	20 mol%	45 min	**70**	18	0
1	$NiCl_2·6H_2O$	0.5 mol%	45 min	**0**	87	3
1	$NiCl_2·6H_2O$	1 mol%	45 min	**16**	70	2
1	$NiCl_2·6H_2O$	2 mol%	45 min	**77**	8	1
1	$NiCl_2·6H_2O$	3 mol%	45 min	**82**	0	1
1	$NiCl_2·6H_2O$	4 mol%	45 min	**75**	0	0
1	$NiCl_2·6H_2O$	5 mol%	45 min	**82**	1	0
1	$NiCl_2·6H_2O$	6 mol%	45 min	**79**	0	0
1	$NiCl_2·6H_2O$	7 mol%	45 min	**80**	0	0
1	$NiCl_2·6H_2O$	8 mol%	45 min	**85**	0	0
1	$NiCl_2·6H_2O$	9 mol%	45 min	**78**	0	0
1	$NiCl_2·6H_2O$	10 mol%	45 min	**73**	0	0

1	$NiCl_2{\cdot}6H_2O$	20 mol%	45 min	**68**	0	0
1	$NiBr_2{\cdot}6H_2O$	0.5 mol%	45 min	**0**	90	3
1	$NiBr_2{\cdot}6H_2O$	1 mol%	45 min	**13**	75	2
1	$NiBr_2{\cdot}6H_2O$	2 mol%	45 min	**86**	2	1
1	$NiBr_2{\cdot}6H_2O$	3 mol%	45 min	**85**	1	0
1	$NiBr_2{\cdot}6H_2O$	4 mol%	45 min	**87**	0	0
1	$NiBr_2{\cdot}6H_2O$	5 mol%	45 min	**86**	1	0
1	$NiBr_2{\cdot}6H_2O$	6 mol%	45 min	**82**	5	0
1	$NiBr_2{\cdot}6H_2O$	7 mol%	45 min	**79**	5	0
1	$NiBr_2{\cdot}6H_2O$	8 mol%	45 min	**81**	6	0
1	$NiBr_2{\cdot}6H_2O$	9 mol%	45 min	**83**	7	0
1	$NiBr_2{\cdot}6H_2O$	10 mol%	45 min	**80**	7	0
1	$NiBr_2{\cdot}6H_2O$	20 mol%	45 min	**75**	13	0

Condition 1: 1 equiv. TMG as base, 20 mol% Quinuclidine. 1.75 equiv of alcohol. 0.5 mol% 4CzIPN in DMF.
Condition 2: 1 equiv. TMG as base, 20 mol% Quinuclidine. 1.75 equiv of alcohol. 0.5 mol% $[Ir(dF(CF_3)ppy)_2dtbbpy]PF_6$ in DMF.

Data from Fig. S66. Photocatalyst loading vs nickel catalyst loading (*1 equiv. TMG, 20 mol% Quinuclidine, 1.75 equiv of alcohol, 0.5 mol% 4CzIPN in DMF, 30 minutes*).

Nickel loading	Photocatalyst loading	Product (%)	ArBr (%)	ArH (%)
2 mol%	0.05 mol%	**17**	85	0
2 mol%	0.1 mol%	**33**	63	1
2 mol%	0.2 mol%	**80**	23	1
2 mol%	0.25 mol%	**76**	13	0
2 mol%	0.3 mol%	**77**	12	0
2 mol%	0.35 mol%	**74**	14	0
2 mol%	0.4 mol%	**73**	15	0
2 mol%	0.45 mol%	**70**	20	1
2 mol%	0.5 mol%	**67**	23	0
2 mol%	0.55 mol%	**65**	24	0
2 mol%	0.6 mol%	**69**	24	1
2.5 mol%	0.05 mol%	**16**	78	1
2.5 mol%	0.1 mol%	**48**	43	0
2.5 mol%	0.2 mol%	**75**	10	1
2.5 mol%	0.25 mol%	**79**	5	0
2.5 mol%	0.3 mol%	**77**	6	0
2.5 mol%	0.35 mol%	**75**	9	0
2.5 mol%	0.4 mol%	**72**	13	1

2.5 mol%	0.45 mol%	**70**	17	0
2.5 mol%	0.5 mol%	**66**	21	1
2.5 mol%	0.55 mol%	**60**	27	1
2.5 mol%	0.6 mol%	**64**	23	1
3 mol%	0.05 mol%	**12**	79	2
3 mol%	0.1 mol%	**45**	45	1
3 mol%	0.2 mol%	**77**	8	0
3 mol%	0.25 mol%	**81**	3	0
3 mol%	0.3 mol%	**79**	4	1
3 mol%	0.35 mol%	**77**	6	0
3 mol%	0.4 mol%	**73**	8	0
3 mol%	0.45 mol%	**71**	13	1
3 mol%	0.5 mol%	**71**	15	1
3 mol%	0.55 mol%	**68**	18	1
3 mol%	0.6 mol%	**64**	20	1
3.5 mol%	0.05 mol%	**15**	79	2
3.5 mol%	0.1 mol%	**37**	50	1
3.5 mol%	0.2 mol%	**79**	8	0
3.5 mol%	0.25 mol%	**80**	3	0
3.5 mol%	0.3 mol%	**81**	4	1
3.5 mol%	0.35 mol%	**78**	5	0
3.5 mol%	0.4 mol%	**77**	6	1
3.5 mol%	0.45 mol%	**77**	8	1
3.5 mol%	0.5 mol%	**75**	11	1
3.5 mol%	0.55 mol%	**72**	12	0
3.5 mol%	0.6 mol%	**72**	15	1

Data from Fig. S67. Photocatalyst vs reagents ratio (*1 equiv. TMG as base, 20 mol% Quinuclidine, 0.5 mol% [Ir(dF(CF$_3$)ppy)$_2$dtbbpy]PF$_6$ or 0.25 mol% 4CzIPN, in DMF*).

Photocatalyst	Alcohol : ArBr ratio	Product (%)	ArBr (%)	ArH (%)
[Ir(dF(CF$_3$)ppy)$_2$dtbbpy]PF$_6$	2:1	**75**	4	0
[Ir(dF(CF$_3$)ppy)$_2$dtbbpy]PF$_6$	1.75:1	**30**	54	0
[Ir(dF(CF$_3$)ppy)$_2$dtbbpy]PF$_6$	1.5:1	**35**	45	0
[Ir(dF(CF$_3$)ppy)$_2$dtbbpy]PF$_6$	1.25:1	**41**	38	0
[Ir(dF(CF$_3$)ppy)$_2$dtbbpy]PF$_6$	1:1	**40**	38	0
[Ir(dF(CF$_3$)ppy)$_2$dtbbpy]PF$_6$	1:1.25	**45**	55	0
[Ir(dF(CF$_3$)ppy)$_2$dtbbpy]PF$_6$	1:1.5	**57**	62	0
[Ir(dF(CF$_3$)ppy)$_2$dtbbpy]PF$_6$	1:1.75	**70**	74	0
[Ir(dF(CF$_3$)ppy)$_2$dtbbpy]PF$_6$	1:2	**73**	84	0

4CzIPN	2:1	**60**	29	0
4CzIPN	1.75:1	**74**	12	0
4CzIPN	1.5:1	**77**	6	0
4CzIPN	1.25:1	**75**	4	0
4CzIPN	1:1	**68**	8	0
4CzIPN	1:1.25	**76**	24	0
4CzIPN	1:1.5	**81**	40	0
4CzIPN	1:1.75	**81**	55	0
4CzIPN	1:2	**82**	74	0
4CzPN	2:1	**25**	66	0
4CzPN	1.75:1	**36**	53	0
4CzPN	1.5:1	**40**	49	0
4CzPN	1.25:1	**41**	47	0
4CzPN	1:1	**36**	48	0
4CzPN	1:1.25	**43**	64	0
4CzPN	1:1.5	**47**	81	0
4CzPN	1:1.75	**55**	96	0
4CzPN	1:2	**55**	122	0

Data from Fig. S68. Optimal conditions using 4 lights with 50% of light intensity.

Row	Column	Product (%)	ArBr (%)	ArH (%)
A	1	**18**	82	0
A	2	**20**	80	0
A	3	**21**	79	0
A	4	**21**	79	0
A	5	**20**	80	0
A	6	**20**	81	0
A	7	**19**	82	0
A	8	**21**	79	0
A	9	**24**	80	0
A	10	**24**	80	0
A	11	**23**	81	0
A	12	**22**	81	0
B	1	**20**	79	0
B	2	**22**	76	0
B	3	**22**	75	0
B	4	**22**	77	0
B	5	**21**	78	0
B	6	**20**	79	0

B	7	**19**	80	0
B	8	**22**	78	0
B	9	**27**	75	0
B	10	**26**	77	0
B	11	**25**	78	0
B	12	**24**	79	0
C	1	**21**	78	0
C	2	**23**	75	0
C	3	**23**	76	0
C	4	**22**	77	0
C	5	**19**	80	0
C	6	**20**	81	0
C	7	**20**	79	0
C	8	**21**	78	0
C	9	**27**	77	0
C	10	**26**	77	0
C	11	**27**	77	0
C	12	**24**	80	0
D	1	**21**	80	0
D	2	**23**	76	0
D	3	**22**	76	0
D	4	**21**	79	0
D	5	**19**	82	0
D	6	**19**	81	0
D	7	**19**	80	0
D	8	**21**	80	0
D	9	**26**	78	0
D	10	**26**	78	0
D	11	**26**	78	0
D	12	**25**	80	0
E	1	**21**	80	0
E	2	**23**	76	0
E	3	**23**	77	0
E	4	**21**	80	0
E	5	**20**	81	0
E	6	**19**	82	0
E	7	**19**	82	0
E	8	**21**	81	0
E	9	**26**	80	0
E	10	**27**	78	0

E	11	**28**	77	0
E	12	**25**	81	0
F	1	**21**	81	0
F	2	**24**	77	0
F	3	**23**	77	0
F	4	**22**	79	0
F	5	**21**	81	0
F	6	**20**	81	0
F	7	**20**	81	0
F	8	**22**	79	0
F	9	**28**	78	0
F	10	**29**	78	0
F	11	**27**	79	0
F	12	**25**	81	0
G	1	**22**	84	0
G	2	**21**	83	0
G	3	**24**	79	0
G	4	**23**	80	0
G	5	**23**	82	0
G	6	**21**	84	0
G	7	**23**	81	0
G	8	**24**	80	0
G	9	**28**	79	0
G	10	**29**	80	0
G	11	**28**	80	0
G	12	**17**	91	0
H	1	**20**	85	0
H	2	**21**	82	0
H	3	**22**	81	0
H	4	**22**	81	0
H	5	**23**	81	0
H	6	**22**	82	0
H	7	**22**	81	0
H	8	**23**	82	0
H	9	**24**	84	0
H	10	**22**	87	0
H	11	**17**	91	0
H	12	**14**	94	0

Data from Fig. S68. Optimal conditions using 4 lights with 100% of light intensity.

Row	Column	Product (%)	ArBr (%)	ArH (%)
A	1	**22**	76	0
A	2	**50**	43	0
A	3	**51**	41	0
A	4	**52**	39	0
A	5	**54**	40	0
A	6	**52**	45	0
A	7	**50**	42	0
A	8	**51**	40	0
A	9	**62**	40	0
A	10	**31**	71	0
A	11	**59**	42	0
A	12	**58**	47	0
B	1	**52**	44	0
B	2	**55**	39	0
B	3	**55**	39	0
B	4	**54**	40	0
B	5	**54**	42	0
B	6	**50**	44	0
B	7	**50**	46	0
B	8	**51**	43	0
B	9	**64**	39	0
B	10	**65**	39	0
B	11	**63**	40	0
B	12	**61**	44	0
C	1	**52**	44	0
C	2	**56**	38	0
C	3	**55**	39	0
C	4	**52**	42	0
C	5	**49**	46	0
C	6	**47**	50	0
C	7	**46**	51	0
C	8	**48**	48	0
C	9	**60**	44	0
C	10	**63**	41	0
C	11	**63**	40	0
C	12	**61**	45	0
D	1	**51**	44	0
D	2	**55**	39	0

D	3	**54**	41	0
D	4	**51**	45	0
D	5	**47**	49	0
D	6	**44**	54	0
D	7	**43**	53	0
D	8	**44**	49	0
D	9	**56**	45	0
D	10	**60**	43	0
D	11	**62**	41	0
D	12	**60**	45	0
E	1	**54**	47	0
E	2	**59**	106	0
E	3	**58**	41	0
E	4	**54**	44	0
E	5	**50**	51	0
E	6	**47**	55	0
E	7	**46**	55	0
E	8	**48**	52	0
E	9	**60**	47	0
E	10	**65**	43	0
E	11	**68**	41	0
E	12	**64**	43	0
F	1	**47**	56	0
F	2	**59**	39	0
F	3	**61**	40	0
F	4	**59**	42	0
F	5	**54**	46	0
F	6	**51**	51	0
F	7	**49**	51	0
F	8	**52**	48	0
F	9	**66**	44	0
F	10	**66**	37	0
F	11	**70**	38	0
F	12	**65**	40	0
G	1	**56**	45	0
G	2	**61**	41	0
G	3	**61**	41	0
G	4	**62**	43	0
G	5	**61**	45	0
G	6	**59**	47	0

G	7	**57**	49	0
G	8	**61**	48	0
G	9	**71**	41	0
G	10	**77**	41	0
G	11	**74**	40	0
G	12	**71**	45	0
H	1	**7**	101	0
H	2	**56**	47	0
H	3	**55**	44	0
H	4	**57**	43	0
H	5	**61**	43	0
H	6	**68**	47	0
H	7	**58**	45	0
H	8	**59**	44	0
H	9	**70**	41	0
H	10	**64**	37	0
H	11	**64**	40	0
H	12	**60**	45	0

9. List of Acronyms & Abbreviations used for the Organic Bases Screening

2-Me, 6-Cy-Py	2-cyclohexyl-6-methylpyridine
2,6-dtBu-(4-Me)-Py	2,6-di-*tert*-butyl-4-methylpyridine
2,6-dtBuPy	2,6-di-*tert*-butylpyridine
BEMP	2-*tert*-butylimino-2-diethylamino-1,3-dimethylperhydro-1,3,2-diazaphosphorine
BTMG	2-*tert*-butyl-1,1,3,3-tetramethylguanidine
BTTP	*tert*-butylimino-tri(pyrrolidino)phosphorane
Collidine	2,4,6-trimethylpyridine
DBN	1,5-diazabicyclo[4.3.0]non-5-ene
DBU	1,8-diazabicyclo[5.4.0]undec-7-ene
DMAP	4-(dimethylamino)pyridine
dPh-Py	2,6-diphenylpyridine
Lutidine	2,6-dimethylpyridine
MTBD	7-methyl-1,5,7-triazabicyclo[4.4.0]dec-5-ene
N-Bu-Imidazole	1-butylimidazole
N-Me-Imidazole	1-methylimidazole
NBu_3	tributylamine
NEt_3	triethylamine
NMM	4-methylmorpholine
P1tOct	*tert*-octylimino-tris(dimethylamino)phosphorane
P2tBu	1-*tert*-butyl-2,2,4,4,4-pentakis(dimethylamino)-2λ5,4λ5-catenadi(phosphazene)
Quinuclidine	1-azabicyclo[2.2.2]octane
Tetrahydroquinoline	1,2,3,4-tetrahydroquinoline
TMG	*N,N,N′,N′*-tetramethylguanidine

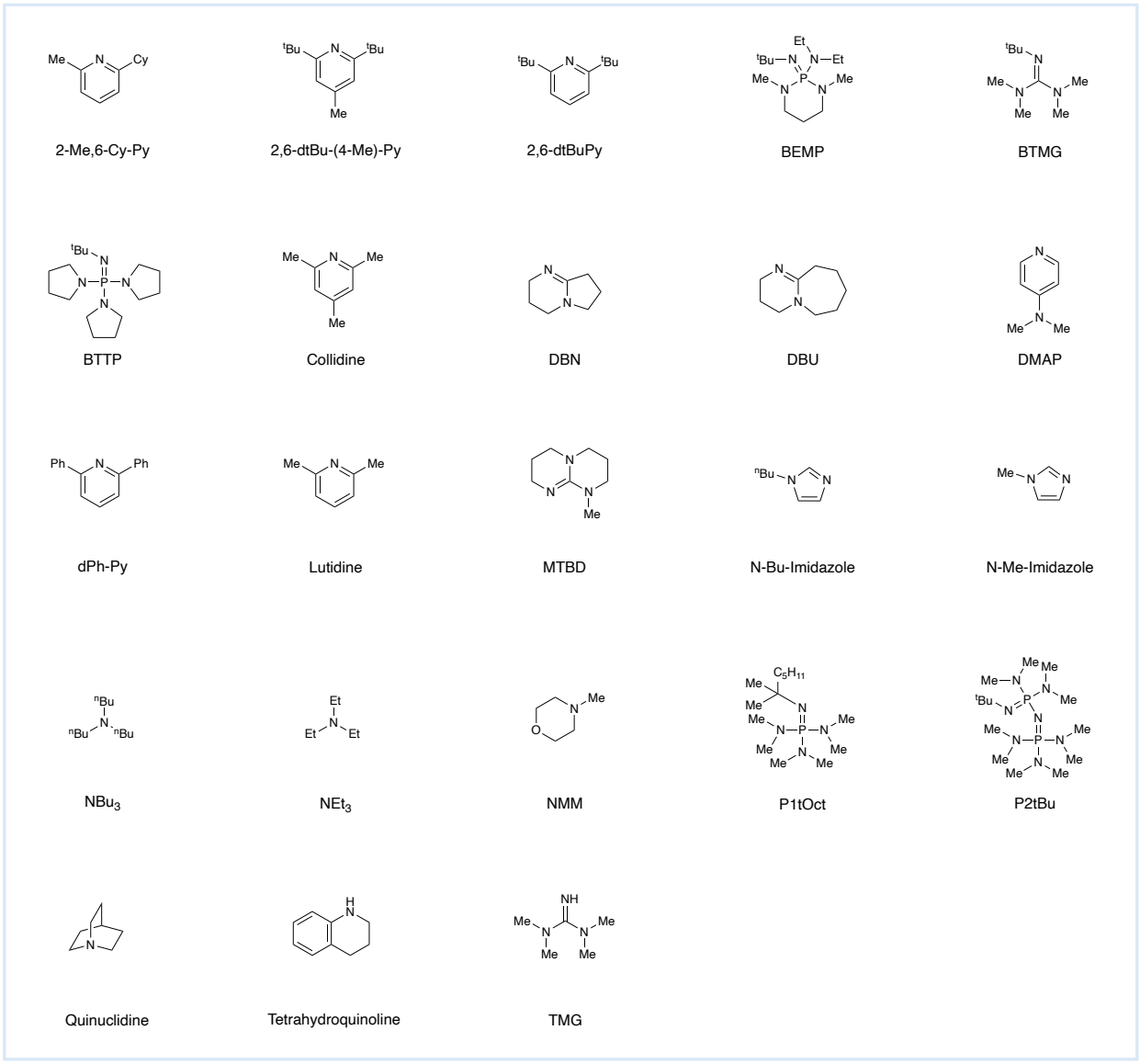

Fig. S75. Chemical structures of the organic bases used in the screening

10. References

1. Perrin, D. D.; Armarego, W. L. F. Purification of Laboratory Chemicals, 3rd ed. Pergamon Press: Oxford, (1988).

2. Pangborn, A. B.; Giardello, M. A.; Grubbs, R. H.; Rosen, R. K. & Timmers, F. J. Safe and Convenient Procedure for Solvent Purification. *Organometallics*, **15**, 1518–1520 (1996).

3. Still, W. C.; Kahn, M. A.; Mitra, J. Rapid Chromatographic Technique for Preparative Separations with Moderate Resolution. *J. Org. Chem.*, **43**, 2923–2925 (1978).

4. Kaljurand, I. et al. Extension of the Self-Consistent Spectrophotometric Basicity Scale in Acetonitrile to a Full Span of 28 pK_a Units: Unification of Different Basicity Scales. *J. Org. Chem.*, **70**, 1019−1028 (2005).

5. Kaupmees, K., Trummal, A., & Leito, I. Basicities of Strong Bases in Water: A Computational Study. Croatica Chemica Acta, **87**, 385–395 (2014).

6. Zuo, Z. et al. Merging Photoredox with Nickel Catalysis: Coupling of α-Carboxyl sp3-Carbons with Aryl Halides. *Science*, **345**, 437-440 (2014).

7. Liang, Y., Zhang, X. & MacMillan, D. W. C. Decarboxylative sp^3 C–N coupling via dual copper and photoredox catalysis. *Nature*, **559**, 83-88 (2018).

8. Le, C. et al. A General Small-Scale Reactor To Enable Standardization and Acceleration of Photocatalytic Reactions. *ACS Cent. Sci.* **3**, 647-653 (2017).

9. Zhang, P.; Le, C.& MacMillan, D. W. C. Silyl Radical Activation of Alkyl Halides in Metallaphotoredox Catalysis: A Unique Pathway for Cross-Electrophile Coupling. *J. Am. Chem. Soc.* **138**, 8084-8087 (2016).

10. Terrett, J. A., Cuthbertson, J. D., Shurtleff, V. W. & MacMillan, D. W. C. Switching on elusive organometallic mechanisms with photoredox catalysis. *Nature*, **524**, 330-334 (2015).